

DISSERTATION

DESIGN AND SYNTHESIS OF BIOLOGICALLY ACTIVE LARGAZOLE DERIVATIVES,
INCLUDING DEVELOPMENT OF IMPROVED SYNTHESSES OF LARGAZOLE ANALOGS

Submitted by

Christine E. Dunne

Department of Chemistry

In partial fulfillment of the requirements

For the Degree of Doctor of Philosophy

Colorado State University

Fort Collins, Colorado

Summer 2018

Doctoral Committee:

Advisor: Robert M. Williams

Yian Shi

Amy Prieto

Douglas Thamm

Copyright by Christine Elizabeth Dunne 2018

All Rights Reserved

ABSTRACT

DESIGN AND SYNTHESIS OF BIOLOGICALLY ACTIVE LARGAZOLE DERIVATIVES, INCLUDING DEVELOPMENT OF IMPROVED SYNTHESSES OF LARGAZOLE ANALOGS

Natural product histone deacetylase inhibitor, Largazole, has been developed into a streamlined synthetic pathway for the development of a complex library of analogs. The library developed within the Williams laboratory encompasses an array of derivatives, including but not limited to: thiazole modification and macrocycle substitutions. The cap group of Largazole, portion of the molecule extending outside of the enzyme binding pocket, was successfully modified to install new chemical handles for biologic and dual therapeutic conjugation.

Biological conjugates of Largazole, as well as its derivatives, aid in increasing selectivity and potency of the compound. Largazole has been conjugated to both biotin and folic acid for further studies. Additionally, a streamlined synthesis towards Wnt inhibitor 3289-5066 and a developed path for conjugation have been explored.

Modified procedures were developed to aid in scale up and improvement of synthetic pathways. Scale up is crucial for development of sufficient material for biological testing and further development of conjugative therapeutics. One main impediment in the synthesis of Largazole peptide isostere is towards the southern fragment, specifically the Grubbs olefin metathesis. Multiple routes were explored to combat this low yielding step. Further exploration of these synthetic routes are underway.

ACKNOWLEDGEMENTS

I want to start by thanking my advisor, Dr. Robert M. Williams. The opportunities given throughout my time at CSU would not have been possible without your support and guidance. I have had the ability to not only take ownership of my own ideas but also put them into action. Your motivation and mentorship has helped me to realize my true path in life and I could not be more grateful for your help in this process.

I would like to thank my mentors at CSU along the way. Dr. Tenaya Newkirk – you were so much more than a mentor, you've become a friend and I am honored to forever be a part of the Largazole team. Dr. Alan Kennan – thank you for always having an open door to listen and lend advice. Dr. Chris Rhitner and Dr. Karolien Deneff - thank you for the NMR and MS support academically (and emotionally). To the support staff within the Chemistry Department, thank you for answering questions along the way and being there as an ear to listen.

To the Williams Group – may you always Strive for Five in the years to come. I would like to specifically thank Kimberly Klas for being my voice of reality amidst the chaos (I'll be taking the mountains with me wherever I go) and Jonathan Thielman for being the Richard to my Bailey (maybe one day you'll understand). Nathan Bair, Vy Le and Le Zhao – your advice and guidance has been greatly appreciated over the years.

I truly believe I would not be here today having pursued my Ph.D. if it wasn't for Dr. Upendra Argikar and Jennifer Dumouchel. My time at Novartis showed me what it was like to question ideas, explore new (at times ocular) topics, and truly work as a team towards a common goal. From bromopride to ocular metabolism, I'm not sure what I would have done without your

support and friendship. Thank you to the Northeastern Chemistry Department for igniting my organic chemistry passion and the continued support.

To my mentors and friends within the Younger Chemists Committee, International Younger Chemists Network, ACS, and IUPAC – thank you! Specifically, Natalie LaFranzo for being an amazing leader, young chemists advocate, and travel buddy. To the far too many of you to name – the work we do together, your strong voices, and your reality check-ins have kept me grounded and motivated over the years. You all continue to inspire me on this journey while giving voices to the future generation of chemists.

Last, but certainly not least, I would like to thank my family. Danielle, Lindsay (and Hillary), and Richard – you have no idea how much the three of you have helped to mold me into who I am today. I am so excited to see your children grow up and can't wait to be the Aunt who instills the love of chemistry inside them for years to come. In this category of family, I would be amiss if I didn't include Levity. You have been my study partner, writing side kick, and reason to go outside three times a day (even in the negative temperatures). Thanks for the love.

And finally my mother, Dr. Kathleen Dunne. Where would I be without you? From day one you have always been there for me. I can truly say that you are my best friend. Whether it was in a small apartment in Shanghai playing cards and listening to James Blunt, driving cross country, or late night calls from lab to check in, I have never felt more supported and loved. I know the road was bumpy at times but look how far we've come! Words can't express how thankful I am to have you as a mother. I can't wait for our next adventure.

DEDICATION

This is dedicated to my mother, Dr. Kathleen Dunne.

TABLE OF CONTENTS

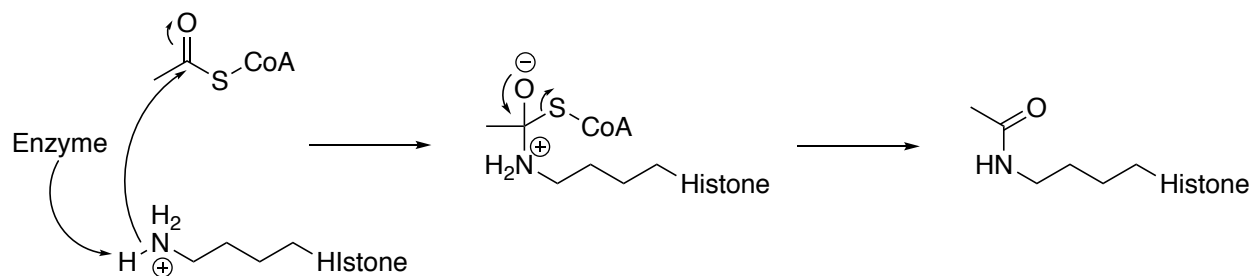
ABSTRACT.....	ii
ACKNOWLEDGEMENTS	iii
DEDICATION	v
Chapter 1. Introduction to Histone Deacetylase Inhibition and Largazole Total Synthesis	1
1.1. HDAC Inhibition and Importance	1
1.2. HDAC Inhibitors to Date	6
1.3. Largazole Isolation.....	10
1.4. Williams Group Total Synthesis	11
1.5. Additional Largazole Syntheses	19
CHAPTER 2. FULL SCOPE.....	32
2.1. Peptide Isostere	32
2.2. Pyridyl Derivatives	34
2.3. Oxazole Analogs	37
2.4. Derivatization at C12: New Chemical Space Analogs	39
2.5. Biological Lessons and Improvements	43
Chapter 3. Path to Complex Analogs.....	47
3.1. Biotin	47
3.2. Folic Acid/ Methotrexate	52
3.3. Wnt Inhibition: 3289-5066	62
Chapter 4. Peptide Base Route.....	77
4.1. Mitsunobu	77
4.2. Additional Olefination Routes	79
4.3. Asymmetric Synthesis	82
4.4. Additional Catalyst Metathesis	85
Chapter 5. Future Work	87
5.1. New Chemical Space of Oxazole Derivatives	87
5.2. Additional Conjugates	88
5.3. Further Scale-Up Development	89
5.4. Closing Remarks	90
References.....	91
Support Information.....	114

INTRODUCTION TO HISTONE DEACETYLASE INHIBITION AND LARGAZOLE TOTAL SYNTHESIS

1.1 HDAC inhibition and importance

Mechanism of Action

The chromosome can be broken down to its essential functions and properties, seen in Figure 1. The chromatin domain regulates gene expression and has been the major target for epigenetic drug development.¹ The condensed chromatin contains histones, which DNA is coiled around. The tightness of the coil depends on the acetylation or deacetylation nature of the lysine residues at the core of the histones, DNA methylation or other alterations affecting the charge state of the histones can also induce changes to the coiled nature around the histones. The histone deacetylase (HDAC) pathway is linked to the survival of many cancers.¹⁻³ The inhibition of the HDAC pathway has been seen to induce apoptosis of the diseased cell and lead to selective cancer cell death.^{4,5}



Scheme 1. Histone acetylation

Histones are first acetylated with histone acetyltransferase (HAT) to combat the negative phosphate interaction with the positive lysine residues on histone tails.⁶ This allows the DNA strands to expose areas for cell replication, transcription, and ultimately proliferation.⁷ It is through this pathway that diseased cells are replicated and continue to develop. The HDAC enzyme then

acts upon the lysine residues, which in turn returns the negative-positive DNA backbone interaction.⁸ When the histones return to their tightly coiled nature within the chromosome the gene is silenced from replication. In the case of disease cell replication, this allows the cancer to survive dormant within the body. However, hyperacetylation through inhibition of the HDAC functionality has been shown to induce apoptosis resulting in cell death or cell cycle arrest in either G1 or G2 phase.⁹⁻¹¹

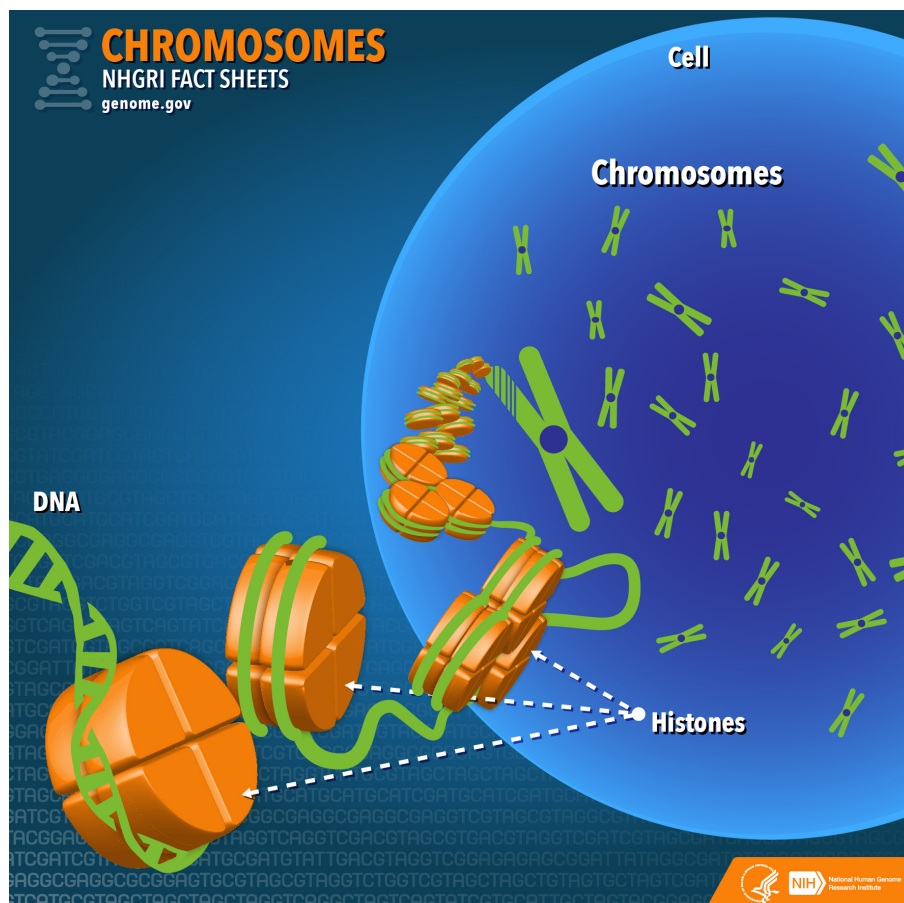


Figure 1. Chromosome to histone representation with DNA coil. (Figure adapted from the open source database for NIH at <https://www.flickr.com/photos/142595545@N03/26990475591/>)

The specific deacetylation either at H3 or H4 of the histones has been noted as an important pathway for the early development of tumor survival within the body.¹² It has been predicted that the transcription factor complex recruits the HDAC to a specific site on the genes' promoter region for further signaling leading to apoptosis.¹³ If the diseased cells can be targeted directly than cell death of normal, healthy cells could be avoided.¹⁴ With this revelation in mind, an explosion of research began towards the development of novel, selective, and potent HDAC inhibitors. It is important to note that both normal and diseased cells exhibit an accumulation of acetylated histones; yet, the normal cells are not induced to cell death.

Eighteen histone deacetylases in four classes have been identified to date, spearheaded by the Schreiber laboratory.⁶ Classes I, II, and IV HDACs contain zinc-binding domains within the active site of the enzyme. In contrast, class III HDACs, or sirtuins, do not contain a Zn²⁺ binding domain and have not been shown to affect the survival or proliferation of diseased cells. Class I HDACs (1, 2, 3, and 8) are smaller, primarily located in the nucleus, and contain an accessible Zn²⁺ binding domain. HDACs in Class II (4, 5, 6, 7, and 9) are larger domains, containing approximately 1000 amino acid residues.² The location of both Class II and Class IV are both in the cytoplasm and nucleus and have been hypothesized to act as shuttling systems. Table 1 outlines HDAC isoforms and their location, including size.

Pan-HDAC inhibitors will chelate to the Zn²⁺ domain unselectively across classes I, II and IV. HDACs in Class I and II have been the main focus of cancer therapeutic development.¹⁵ HDAC inhibition of both class I and II have been seen to upregulate apoptosis which leads to a stabilization in the p53 protein, often times increasing the rate of diseased cell death.¹⁶ The high HDAC isozyme expression seen in cancer cells prompted further investigation into the different pathways and isoforms that are relevant to specific cancers and in turn induce selective apoptosis.¹⁷

Table 1. HDAC Classes and isoforms with cellular localization.

HDAC with Zn²⁺ binding domain			
Class	Isoform	Length (aas)	Location
I	1	482	Nucleus
	2	488	Nucleus
	3	428	Nucleus/Cytoplasm
	8	377	Nucleus
2a	4	1084	Nucleus/Cytoplasm
	5	1122	Nucleus/Cytoplasm
	7	855	Nucleus/Cytoplasm
	9a	1011	Nucleus/Cytoplasm
	9b	879	Nucleus/Cytoplasm
2b	6	1215	Nucleus/Cytoplasm
	10	669	Nucleus/Cytoplasm
4	11	347	Nucleus

Disease States

Cancer therapy development is at the forefront for the development of HDAC inhibitors. Colon adenocarcinoma, breast cancer, and non-small cell lung cancer have been identified to overexpress HDACs 1 - 3, 1/3, and Class II, respectively.¹⁸⁻²⁷ HDAC 1 overexpression has also been seen in prostate cancer. It is important to note that HDAC inhibitors have been used to target a wide range of disease states, outside of cancer therapeutics, showing their breadth of therapeutic potential.²⁸⁻³⁵ Table 2 outlines which disease states overexpress HDAC isoforms and their activity. Epigenetic pathways are surmised to be the main targets for cancer therapy; however, further studies are needed in order to pinpoint the crucial protein-protein interactions and pathways for cancer cell replication and survival.³⁶ Many recent studies have shown that HDAC inhibitor therapeutics do not only act upon the deacetylase enzymes but also additional functionalities within the body that can be upregulated or repressed based on acetylation pathways. It also important to

note, the HDAC enzymes also deacetylate non-histone targets.³⁷ This factor is beyond the scope of this dissertation and has been discussed in an extensive review by Seto, as well as many others.³

Table 2. HDAC targeted disease states, including HDAC isoforms, therapeutics investigated, and activity; focused on Largazole testing across multiple disease states.

Disease State	HDAC isoform	Therapeutic	Activity
Rheumatoid Arthritis ^{38, 39}	1, 6	SAHA, Largazole	No significant SAHA activity Largazole may play a role in regulation
Colon adenocarcinoma ^{24, 25, 40}	1, 2, 3	All classes, Largazole	Inhibition of cell proliferation
Breast Cancer ^{26, 27}	1, 3	Vorinostat, Largazole	Suppress tumor growth
Non-small cell lung cancer ¹¹	Class II	Largazole	G1 phase cell cycle arrest
Prostate Cancer ⁴¹	1	All Classes	Transformed cells responsive to therapeutics
Neuroprotection ^{42, 43}	6	Chiral Mercaptoacetamides	Exhibited neuroprotection against stress-induced injury, nontoxic
Bone Disease ^{44, 45}	Not Identified	Largazole	Resulted in the stimulation of bone formation
Liver Fibrosis ⁴⁶	1, 2, 3	Largazole	Apoptosis induction of hepatic stellate cells

Varying hemoglobin diseases have been investigated with HDAC inhibitor treatment.³⁸ Both sickle cell anemia and thalassemia are regulated by an increase of fetal hemoglobin. Sickle cell anemia is the result of haemoglobin S protein irregular function. Low oxygen levels to the red blood cells decrease elasticity which results in abnormalities of blood flow, chronic pain, and additional complications. Fetal hemoglobin can inhibit the development of sickle cells and help combat the side effects. This may result from γ -globin expression induced by p38 signaling via H3

and H4 hyperacetylation, a resultant effect of HDAC inhibition. Both sodium butyrate and trichostatin A have been explored for therapeutic potential.

1.2 HDAC inhibitors to date

HDAC properties and current classes

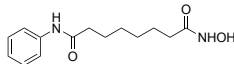
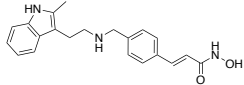
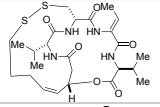
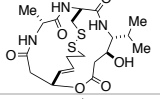
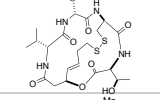
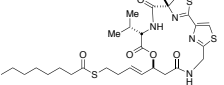
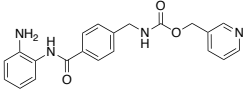
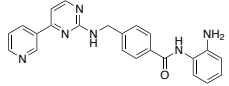
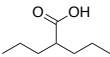
Three main properties that are imperative to HDAC inhibition are: 1) A metal binding domain to coordinate with the Zn^{2+} enzyme pocket; 2) A surface recognition unit (cap group) that interacts with the HDAC surface amino acids; and 3) A linker to connect the Zn^{2+} domain and surface recognition cap group.³⁹ Importantly, the natural product Largazole takes advantage of these three properties and will be discussed more in depth below in Chapter 1.3 and throughout this dissertation. In addition to Largazole, a wide range of HDAC inhibitors have been developed to date.^{40, 41}

There are over 15 HDAC inhibitors (HDACi's) that have reached either pre- or early clinical stages. SAHA and FK228, two FDA approved therapeutics, will be discussed more in-depth below. HDACi's of note fall under four main classes: hydroxamic acids, cyclic tetrapeptides, benzamides, and short-chain aliphatic acids.^{8, 42} Table 3 shows representative examples of each class.

The hydroxamic acid class of HDAC inhibitors have strong affinity for the Zn^{2+} binding site of the HDAC enzyme pocket. SAHA and panobinostat are all representative examples of hydroxamic acid containing inhibitors.^{43, 44} The strong binding affinity can be seen as both a positive property towards potency and a negative influence on selectivity of HDAC isoform specificity targeting.⁴⁵ SAHA, discussed more below, is a pan-HDAC inhibitor which leads to both

diseased and healthy cell targeting. Panobinostat, the pan-HDAC inhibitor LBH-589 developed by Novartis, has been approved for multiple myeloma combination therapy with bortezomib.⁴⁶

Table 3. Representative examples of HDACs across 4 classes and their marketed name and supplier where relevant

Class	Compound	Structure	Market Information
Hydroxamic Acid	SAHA		Vorinostat; Merck
	LBH-589		Panobinostat; Novartis
Cyclic Peptide	FK228		Romidepsin; Gloucester (Celgene)
	Spiruchostatin A		
	FR901375		
	Largazole		
Benzamide	MS-275		Entinostat; Syndax
	MGCD0103		Mocetinostat; Mirati
Short-Chain Aliphatic Acids	Valproic Acid		Depakene, Epival; Abbott (Brand name)

FK228, spiruchostatin A, FR901375, and Largazole (seen in Table 3) are all members of the cyclic peptide classification of HDAC inhibitors.⁴⁷⁻⁵² Spiruchostatin A shares the same heptanoic acid base structure seen in Table 3.^{53, 54} Many similar synthetic routes are implemented across the synthesis of this class of compounds.^{55, 56} FK228, an FDA approved therapeutic, will be discussed more in depth later. A more in-depth discussion of Largazole and its therapeutic potential will also be discussed in the continuing chapters. The half-life in plasma for depsipeptides is approximately 8 hours. This is higher than hydroxamic acids and lower than benzamides.^{57, 58}

Three notable representatives of the benzamide class of HDAC inhibitors are MS-275, MGCD0103, and entinostat.⁵⁹ These compounds have been investigated to target prostate cancer cells and various additional disease states. Mainly, their use has been in combination with other therapeutics. Short-chain aliphatic acids and electrophilic ketones are within an additional HDACi classification. Aliphatic acids, such as valproic acid, have reached phase III clinical trials for cancer treatment.⁶⁰ There has been limited research towards the structure activity relationships of valproic acid due to less expansive library development.

HDAC inhibitors have been recently explored for combination therapy. Combination therapy aids in not only increasing potency but also selectivity and overall effect of the therapeutic.⁶¹ Cancer cells find alternative ways to replicate and survive when therapeutics are introduced to the body. Targeting multiple gene replication routes through a combinatorial approach can combat some resistances that the diseased cells develop overtime. Dual dosed therapeutics aid in a variety of disease states, including but not limited to a variety of cancer treatments.⁶²

Platinum based chemotherapeutic agents, such as cisplatin, work to combat cancer through a variety of pathways for both positive and toxic effects. Dosage of both a traditional chemotherapeutic and epigenetic drug, such as Largazole, can work to combat resistances and decrease toxicity.⁶³ Since HDAC inhibitors control the access to DNA strands for transcription they can aid in the promotion of cisplatin access to form DNA adducts. This combination therapy has been investigated in both cancer cell lines and solid tumors.⁶⁴ One largely explored combination therapy is bortezomib, a proteasome inhibitor, with HDAC inhibitor, FK228.⁶⁵

FDA Approved Therapeutics

There are currently two Food and Drug Administration (FDA) approved HDAC inhibitors available, SAHA (Vorinostat, Merck) and FK228 (Romidepsin, Gloucester/ Celgene) seen in Figure 2. Both SAHA and FK228 are used for treatment in cutaneous T-cell lymphoma (CTCL).⁶⁶ CTCL cells have a higher affinity for the effects of HDACis in comparison to healthy cells. Further studies need to be performed to fully understand this reasoning but it has been surmised that tumor cells may be more attracted to these pathways. A table of activities in comparison to Largazole can be seen in Table 4.

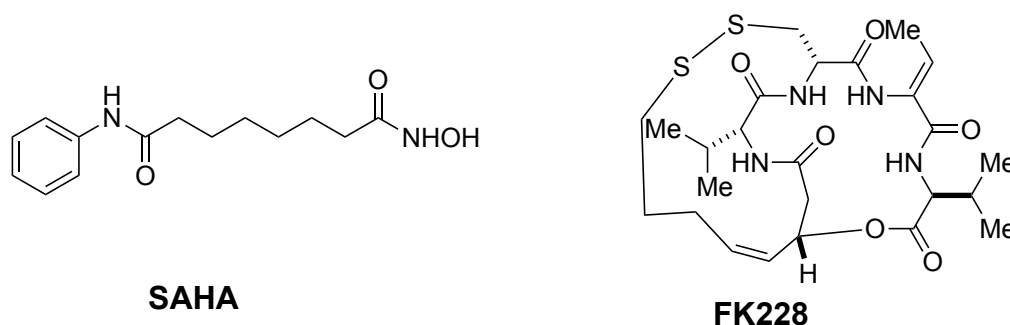


Figure 2. SAHA and FK228, two FDA approves and marketed HDAC inhibitors

The hydroxamic acid moiety of SAHA chelates to the Zn^{2+} active site of HDACs across multiple classes. The lack of functionality and bulk in SAHA decreases the selectivity towards HDAC isoforms to induce diseased cell apoptosis. SAHA is a potent HDAC inhibitor; however, the lack of selectivity can lead to undesired side effects, at μ M activity, such as fatigue, nausea, and diarrhea.⁶⁷

Table 4. HDAC IC₅₀ (nM) activities of FDA therapeutics vs natural product Largazole and its active free thiol.

Compound	HDAC1	HDAC2	HDAC3	HDAC8
FK228	0.12	0.14	0.28	35
SAHA	10	10	15	9
Largazole (1)	20	21	48	>1000
Largazole thiol (2)	0.07	0.07	0.17	25

FK228's structural complexity of the peptidic macrocycle aids in increasing selectivity towards specific HDAC binding sites. One site of improvement exists in FK228, the disulfide linkage that closes the bicycle. These bonds are easily cleaved via the glutathione S-transferase pathway.⁶⁸ Exposure of the Zn²⁺ binding site of the chelating free thiol too rapidly may provide unwanted competition or lack of permeability through the cell surface to reach the desired HDAC active site. Some undesired side effects include fatigue, nausea, vomiting, thrombocytopenia, and atrial fibrillation.⁶⁷

1.3 Largazole Isolation⁶⁹

Largazole (1), Figure 3, was first isolated by Luesch and coworkers in 2008 from the Floridian cyanobacterium *Symploca sp.* Upwards of six compounds have been isolated from the *Symploca* family.⁷⁰⁻⁷⁴ The secondary metabolite has a unique heptanoic acid base and cyclopeptidic macrocycle, previously seen in HDAC inhibitor FK228. This structural similarity was the first indicator of the potential targets of this natural product.

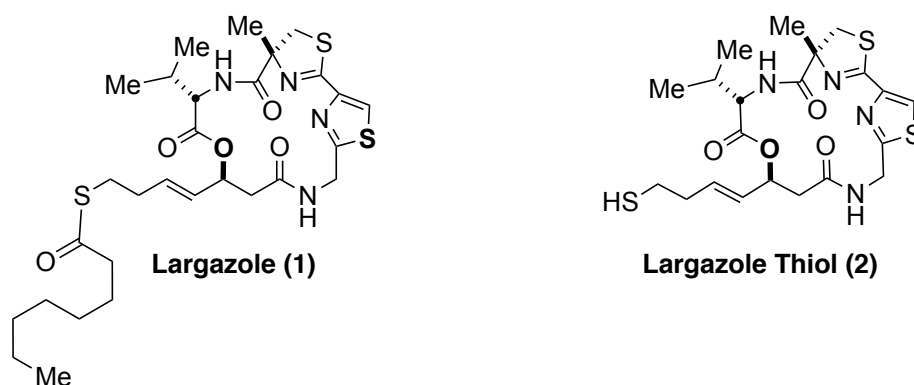


Figure 3. Parent natural product Largazole (1) and Largazole free thiol (2)

Luesch and coworkers tested Largazole across a variety of diseased cells. Selectivity and cytotoxicity was seen towards transformed human mammary epithelial cells, GI₅₀ 7.7 nM and LC₅₀ 117 nM. Largazole had reduced activity towards nontransformed cells. Additionally, transformed osteosarcoma cells showed potent sensitivity in comparison to the nontransformed. This

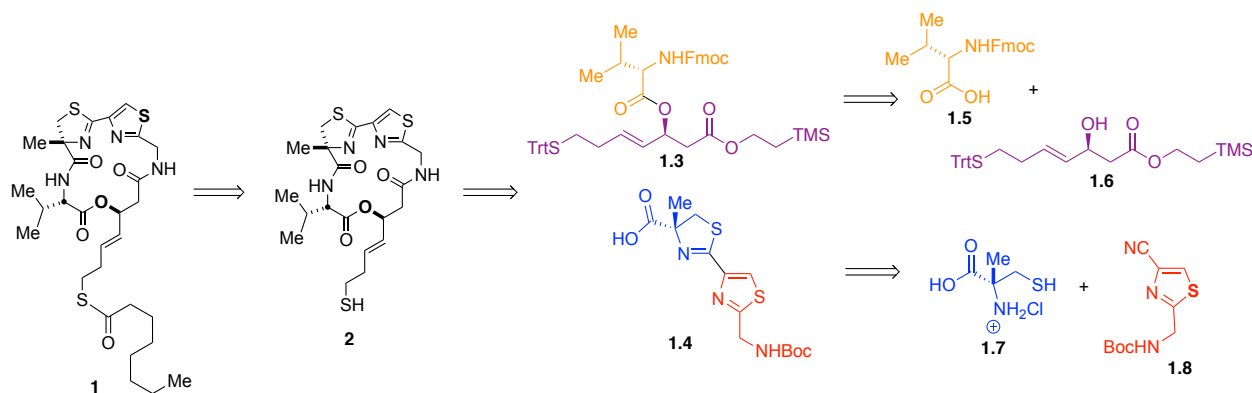
furthermore supports the prediction of selectively targeting cancer cells with the newly isolated natural product Largazole, including colon cancer and neuroblastoma cell lines. Studies across many laboratories further demonstrated the need for further studies of Largazole due to its immense therapeutic utility.^{75,76}

Naturally occurring Largazole is a prodrug that can be hydrolytically cleaved to reveal a free thiol that can chelate to the Zn²⁺ binding domain of the HDAC enzyme. Important structural motifs of Largazole include not only the thiol chelation site but also the linker length to macrocycle, macrocycle hydrogen bonding effects, and cap group functionalities.^{77,78}

1.4 Williams Group Total Synthesis⁷⁹

Retrosynthesis

A retrosynthetic analysis of Largazole was envisioned to develop from four key fragments (Scheme 2). The four fragments could be synthesized from readily available and affordable starting materials, including amino acid building blocks such as glycine and derivatized aspartic acid. The essential fragments: α -methyl cysteine (**1.7**), (*S*)-valine (**1.5**), 5-cyanothiazole (**1.8**), and protected (*S*)-3-hydroxy-7-mercaptohept-4-enoic acid (**1.6**), were envisioned to come together at a late stage to form the complex macrocycle.



Scheme 2. Retrosynthetic analysis developed by the Williams group of natural product Largazole (1)

Dr. Albert Bowers, a previous postdoctoral fellow within the Williams group, hypothesized these disconnects to provide the groundwork for further functionalization of Largazole after preliminary total synthesis.⁷⁹ These variations include, but are not limited to, thiazole replacement, amino acid substitution at the valine residue, and variations of other tail groups.⁸⁰ Development of the library of analogs will be further discussed in-depth later in this report.

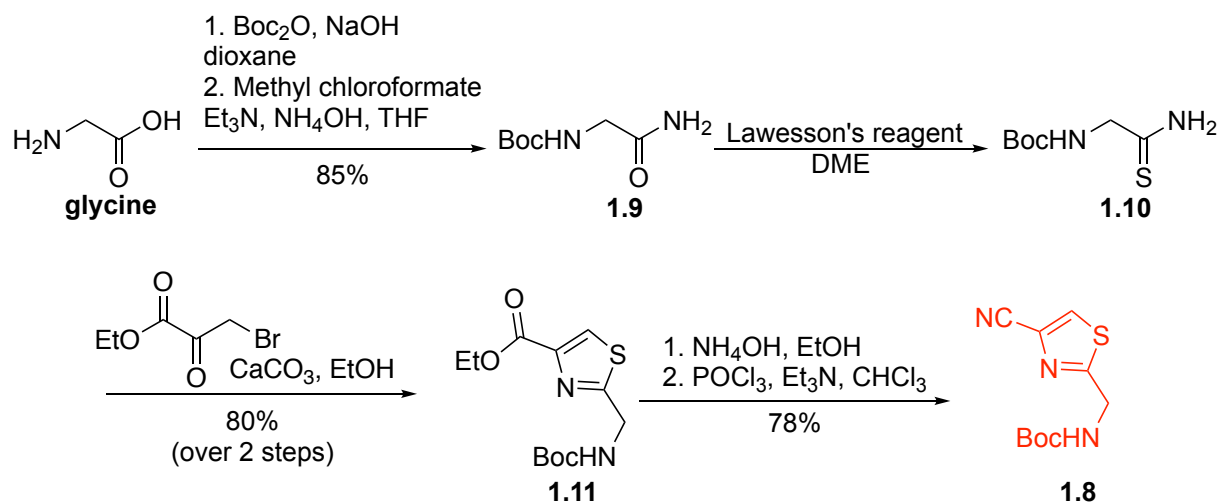
With only 1.2 mg isolable from 290 mg of the marine sponge, an opportunity for a total synthetic development towards this potential therapeutic was imminent.⁶⁹ Within three months of the isolation paper, both the Williams and Luesch groups published total syntheses of parent natural product Largazole. Over 11 total syntheses in 10 years of Largazole research have been published, not including derivatives and modifications of the core depsipeptide macrocycle. The Williams group total synthesis was envisioned from the four building blocks seen in the above retrosynthetic analysis, Scheme 2.

Total Synthesis

Dr. Bowers, along with former Williams group member Dr. Tenaya Newkirk, completed the most functionalizable total synthesis of Largazole to date.⁷⁹ The synthesis was completed in six linear steps with an overall yield of 37%. The aforementioned retrosynthetic analysis guided the synthesis of Largazole toward construction of the four main precursors (Scheme 2) for product development. Each crucial fragment was then coupled, providing Largazole's intricate macrocycle.

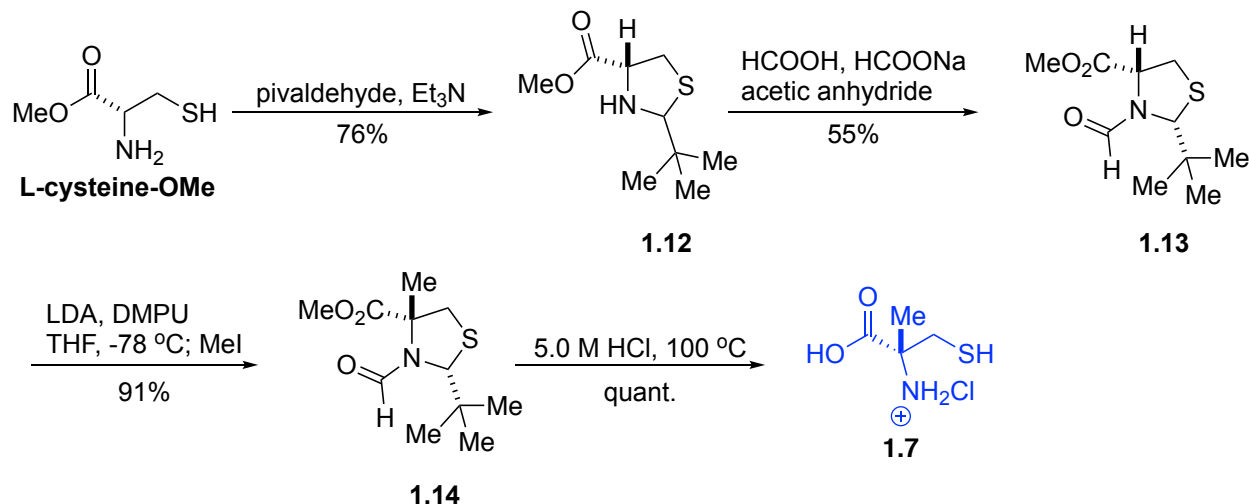
The thiazole, shown in red (**1.8**), was synthesized in six steps from readily available amino acid glycine (Scheme 3).⁸¹ Glycine was first protected with di-*tert*-butyl dicarbonate (Boc anhydride), which was then subjected to methyl chloroformate and ammonium hydroxide

providing intermediate **1.9**. Subsequent reaction with Lawesson's reagent and treatment with ethyl bromopyruvate allowed the transformation of amide **1.10** to the thioamide and formation of thiazole **1.11**. Subsequently, **1.11** was hydrolyzed with ammonium hydroxide followed by POCl₃ resulting in the key cyanothiazole fragment **1.8** in 46% yield over six steps.



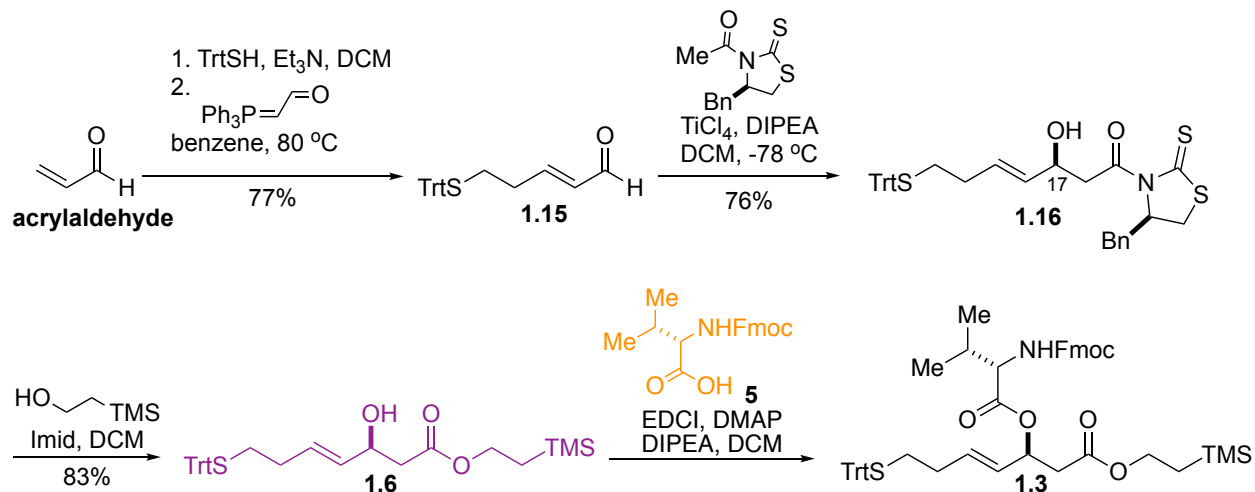
Scheme 3. Synthesis of thiazole fragment (8).

Amino acid derivative α -methylcysteine, **1.7**, was accessed from commercially available L-cysteine methylester by a modification of Seebach's method (Scheme 4).⁸² (R)-cysteine methylester reacts with pivaldehyde to produce **1.12**. Sodium formate in the presence of formic acid and acetic anhydride provides intermediate **1.13**. Thiazolidine **1.13** was methylated using LDA in THF at -78°C followed by addition of methyl iodide to provide methylated product **1.14**. Heating under acidic conditions yielded amino acid derivative **1.7** in an overall yield of 40%.



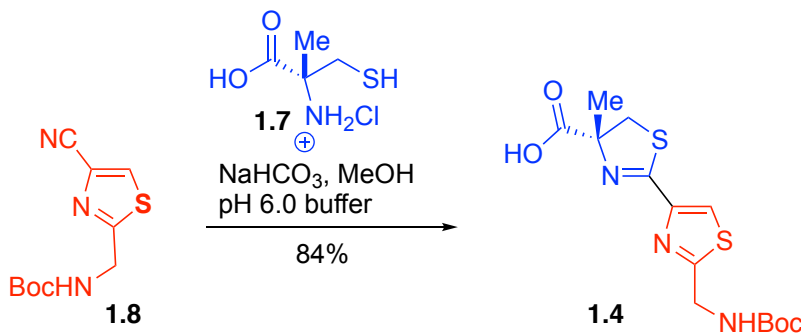
Scheme 4. Synthesis of α -methyl cysteine fragment (7).

The depsipeptide base fragment (*S*)-3-hydroxy-7-mercaptohept-4-enoic acid derivative **1.6** (Scheme 5) was obtained in four steps from acrylaldehyde. Hetero-Michael addition of trityl mercaptan to acrylaldehyde followed by Wittig olefination provided the conjugated aldehyde intermediate **1.15**. The use of Crimmins chiral auxiliary allowed for a stereoselective installation of the hydroxyl group at C17. Crimmins chiral auxiliary was synthesized from D-phenylalanine. The amino acid was reduced with lithium aluminum hydride to the alcohol. The alcohol was reacted with carbon disulfide in 1M potassium hydroxide to produce thiazolidinone thione. Acylation with acetyl chloride provided Crimmins chiral auxiliary to be utilized for the stereoselective installation of the alcohol at C17 for the depsipeptide base, needed for the transformation of compound **1.15** to **1.16**. Reaction with 2-(trimethylsilyl)ethanol cleaved the chiral auxiliary and produced protected ester **1.6**. Fmoc-protected valine (**1.5**) was coupled to **1.6** via Steglich esterification to yield compound **1.3** in 37% overall yield.



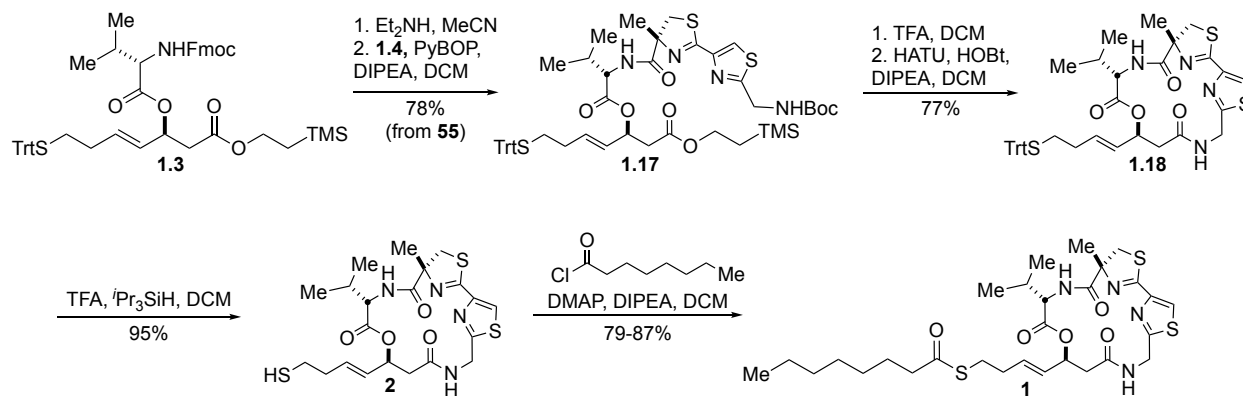
Scheme 5. Synthesis of depsipeptide base fragment (3).

α -Methyl cysteine, **1.7**, was reacted with thiazole **1.8** to obtain the cyclization product **1.4** in 84% yield. The thiazole-thiazoline fragment could then be coupled to the deprotected valine moiety of **1.3** of compound **1.3**. Macrocyclization presented itself as the most challenging step in the synthetic process due to dimerization, extensive purification, and low yields.



Scheme 6. Synthesis of thiazole-thiazoline fragment (4).

Deprotection of Fmoc protected amine **1.3**, followed by PyBOP coupling with free acid **1.4** provided compound **1.17**. Global deprotection provided the free carboxylic acid and amine of compound **1.17**. Amino acid coupling using HATU and HOBt gave the desired macrocycle. The S-trityl group was removed with TFA and triisopropylsilane. Acetylation of the free thiol with octanoyl chloride provided natural product Largazole, **1**.



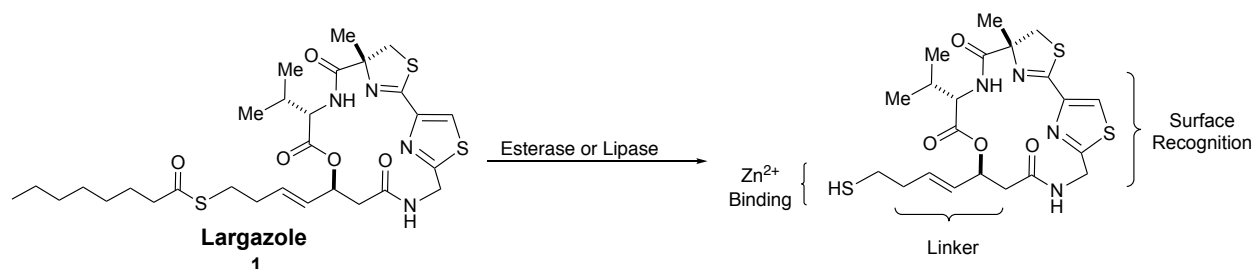
Scheme 7. Final steps towards the synthesis of natural product Largazole (**1**)

Successful synthesis of Largazole was thus accomplished in a convergent synthesis involving four main precursors. With this established synthetic route in hand, the Williams group began to develop Largazole derivatives. The total synthesis of Largazole was explored not only by the Williams group but also by eleven additional research groups, including the laboratories of Luesch, Cramer, Phillips, and Forsyth.^{79, 83-97}

Bioactivity

The octanoyl tail of the prodrug enhances cell-membrane permeability.⁹⁸ After cell wall penetration, an esterase or lipase can reveal the active free thiol for surface recognition, property

1. The active species for HDAC inhibition is the free thiol of parent Largazole, most likely due to its ability to fit within the enzyme pocket and coordinate with the Zn^{2+} domain present, seen in Scheme 8.



Scheme 8. Largazole properties and prodrug potential.

Additionally, the macrocyclic core is able to fit tightly within the active site of the HDAC pocket, forming conducive interactions between the cap group and enzyme surface, property 2. Studies have shown that the linker length is key for the promotion of activity as well. The Wiest group at Notre Dame performed the modeling studies (Figure 4) for probing structure activity relationships between Largazole and the HDAC binding site.^{99, 100}

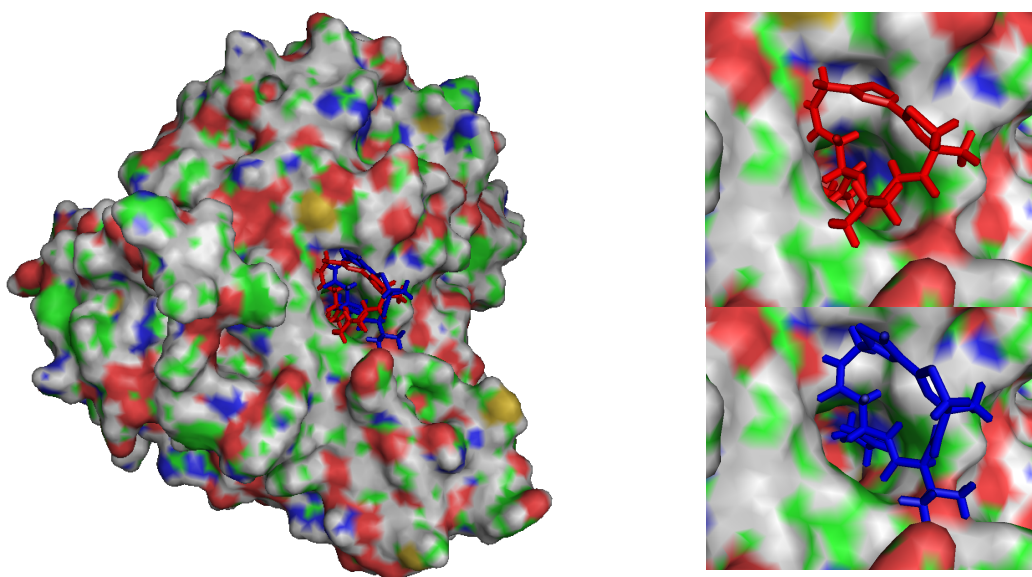


Figure 4. Modeling studies by the Wiest group to show the HDAC binding pocket and Largazole interactions.

Our group has provided the Bradner laboratory at the Dana Farber Cancer Research Institute with >50 synthetic Largazole analogs, prepared in the Williams laboratory, for biochemical and cellular activity profiling.^{39, 79, 80, 85, 101} HDAC inhibitory versus FDA approved therapeutics is seen in Table 4. Largazole shows IC₅₀ values below 20 nM for HDACs 1-3 and greater than 150 nM and 1000 nM for HDACs 6 and 8 respectively, showing selective inhibition towards isoforms 1-3. Largazole thiols potency rivals both FK228 and SAHA in isoform selectivity assays for HDAC 1-3 potency.

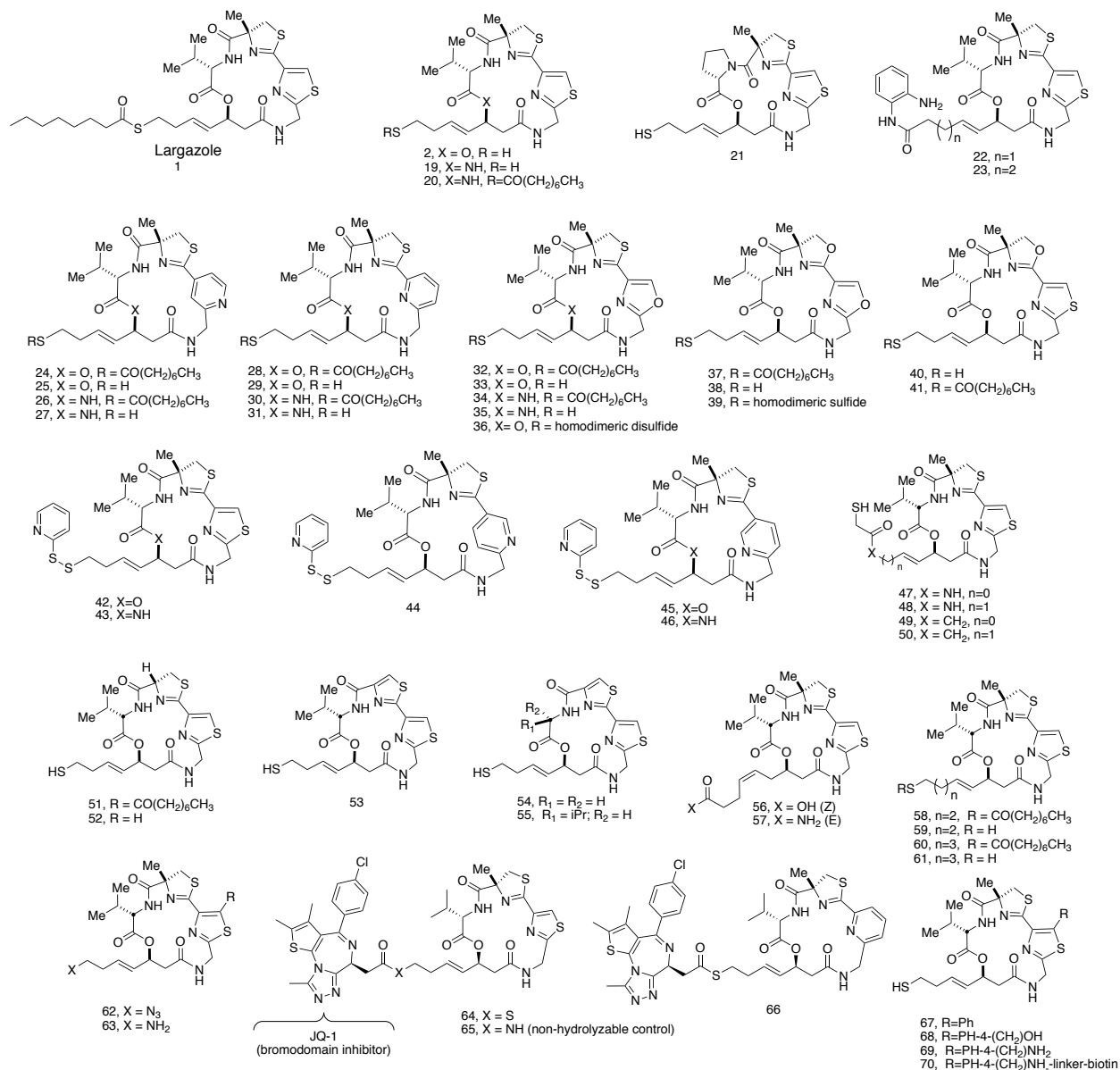


Figure 5. Williams library of Largazole derivatives.

Compounds **2**, **19**, **25**, **27**, **29**, and **42** display comparable or increased potency to parent Largazole, with IC₅₀ values below 25 nM for HDACs 1-3. It is important to note that half of these compounds are the pyridyl-containing species. The compounds developed from the new synthetic route for functionalization of the thiazole ring, **68** and **70**, display IC₅₀ values below 3 nM for HDACs 1-3. These low nM inhibitory constants provide further encouragement for continued

development of Largazole analogs for HDAC inhibition, a table of these results can be seen in Chapter 2. Largazole's activity across a large range of disease states provides a promising compound with a wide reaching therapeutic potential.¹⁰².

1.4 Additional Largazole Syntheses¹⁰³

*Luesch Total Synthesis*⁹⁵

During the same time period the iterative total synthesis came out from the Williams group, the Luesch group published a total synthesis, seen in Scheme 9. Two of the same building blocks, thiazole **1.8** and the methyl ester of α -methyl cysteine were employed in their total synthesis of Largazole. However, an olefin metathesis step was used to attach the linker and tail of the molecules.

Similar thiazole-thiazoline precursor, **1.71**, was reacted with Crimmins chiral auxiliary installed base **1.72**. The right hand side coupling was completed prior to conjugation with valine, and full macrocyclization. The alcohol is then coupled to Boc-protected valine. The methyl ester is hydrolyzed to allow for a final macrocyclization after TFA deprotection of the Boc group. Terminal alkene macrocycle **1.77** is accessed to allow for Grubbs II cross metathesis. The partnering terminal olefin with the thioester moiety, **1.78**, is accessed in two steps and 45% yield. Once both fragments are obtained and the cross metathesis is performed, parent Largazole is accessed. It is important to note that in this synthesis to access the free thiol, a divergent route from the macrocyclic terminal alkene is used.

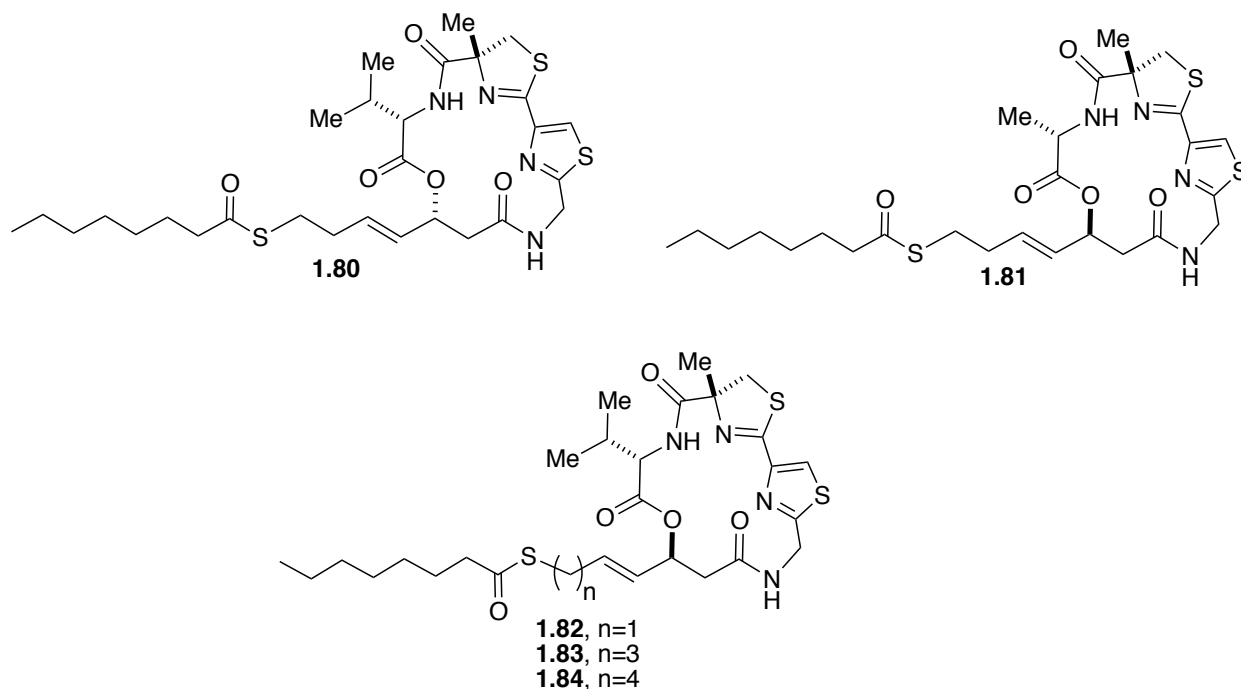


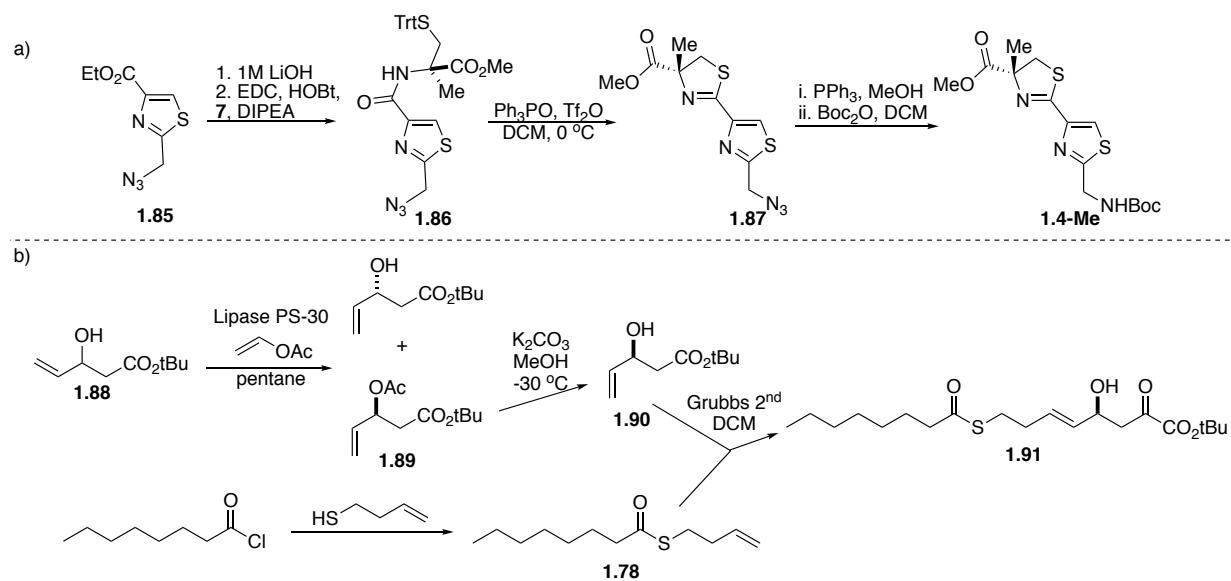
Figure 6. Luesch's developed Largazole derivatives: C17 epi (80), C2 substitution (81), and varied linker lengths (81-84)

Luesch and co-workers additionally synthesized the C17 epimer, and varied linker lengths of Largazole (Figure 6).¹⁰⁵ The linker of both Largazole and FK228 are 4 carbons in length which aid in the insertion of the thiol within the HDAC binding pocket for chelation with Zn^{2+} . In all cases, either the deletion or addition of methylenes to the linker length, the activity of Largazole was dramatically depleted. The C17 epimer also resulted in a considerable increase in GI_{50} towards HCT-116 cells.¹⁰⁶⁻¹⁰⁹

Ghosh, Phillips, and Cramer Total Syntheses

The Ghosh group's total synthesis of Largazole was completed in a similar fashion to both the Williams and Luesch syntheses, Scheme 10.^{35,110} An early stage Grubbs metathesis was utilized to complete the synthesis of the base depsipeptide fragment, **1.91**. The thiazole-thiazoline fragment derived from an intramolecular cyclization of α -methyl cysteine from EDC coupled thiazole moiety **1.85**. Valine was reacted to the acid chloride and the free alcohol of base fragment **1.91**

was added to the solution. Deprotection, coupling, and macrocyclization as seen in the Williams total synthesis resulted in the successful synthesis of the parent Largazole.



Scheme 10. Ghosh total synthesis of (a) thiazole-thiazoline fragment (4-Me), and (b) depsipeptide base derivative (91).

During this same time as the above three syntheses, the Phillips group complete an additional total synthesis of Largazole.⁸⁷ The late stage Grubbs II metathesis to install the thioester allowed a convenient route to synthesize both ester and ketone side chains. Biologically studies utilized the three metathesis products, including the terminal alkene and the pre-macrocycle product **1.92** seen in Figure 7. GI₅₀ of Largazole with MDA-MB231 cells showed a complete depletion of activity across the novel developed derivatives.

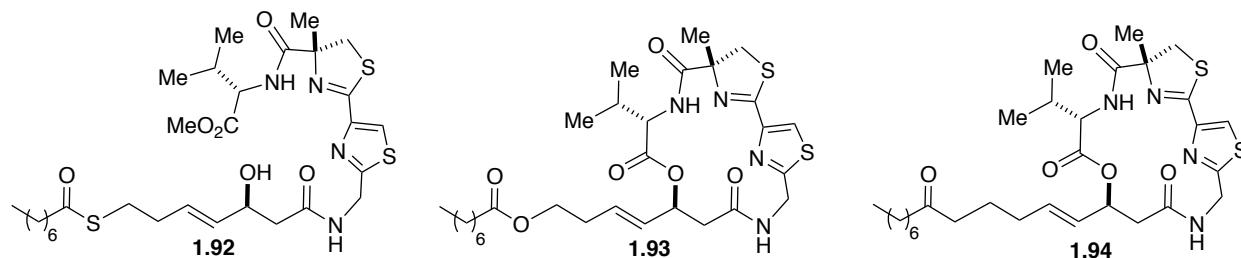
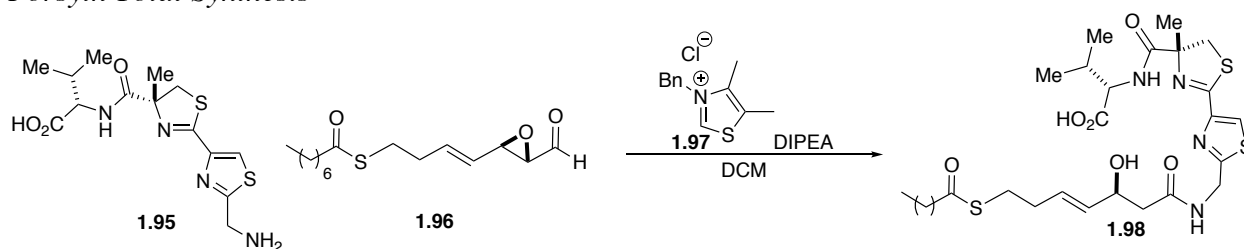


Figure 7. Phillips group developed derivatives of Largazole: pre-macrocyclization (92), ester replacement of thioester (93), and no Zn²⁺ binding affinity (94).

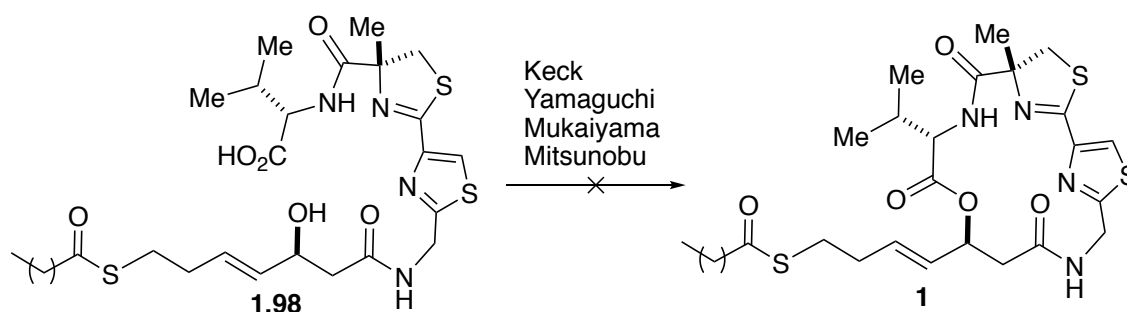
The Cramer laboratory approached an additional synthesis of Largazole in 2008.¹¹¹ This developed route installed the terminal alkene, followed by Grubbs metathesis prior to thiazole-thiazoline coupling and macrocyclization. The scope of this paper included an exploration of cross metathesis catalysts. Ultimately, the Grela catalyst resulted in a 92% yield with a favorable E/Z product formation.⁹⁰

Forsyth Total Synthesis



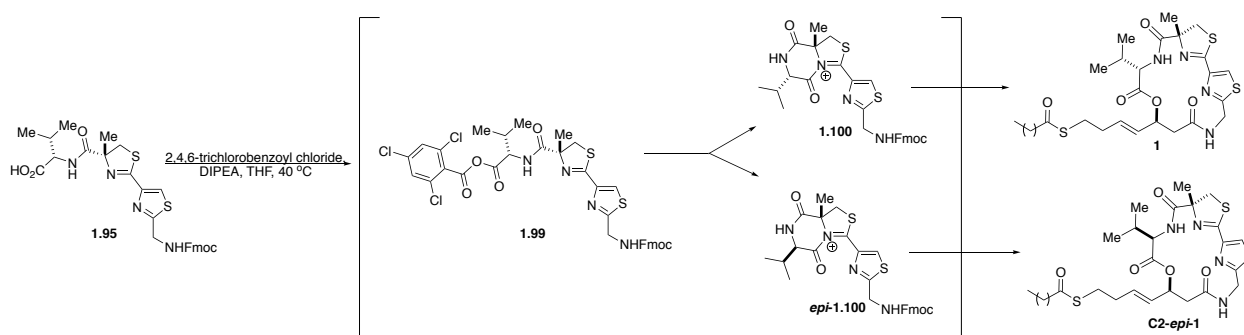
Scheme 11. Forsyth NHC route to intermediate 98.

Forsyth and coworkers completed a novel total synthesis of Largazole in 2009.¹¹² In their strategy, the final ring closure was envisioned to take place at the macrolactonization whereas prior strategies utilized amino acid coupling for a final amide bond formation. N-heterocyclic carbene chemistry developed by Bode and Rovis inspired this unforeseen pathway in the Largazole synthesis approach. Scheme 11 shows the NHC reaction used for formation the of the amide bond of the thiazole-thiazoline and base fragments, **1.98**, prior to macrocycliation.



Scheme 12. Failed attempts by Forsyth and coworkers to perform a late-stage macrocyclization at C17.

Synthetic differences of note to this point are the utilization of a Julia-Kocienski olefination and α,β -epoxy aldehyde to install the desired chemistry at C17 for the base fragment. The thiazole-thiazoline fragment were constructed via amino acid coupling, a Mitsunobu reaction, and microwave cyclization to yield the valine coupled thiazole-thiazoline derivative used for the NHC mediated amide bond formation. The advantages of this route would have provided an efficient way to avoid common protection and deprotection steps seen in amino acid coupling sequences. The β -hydroxy amide was obtained in moderate yield due to the competitive elimination reaction of the epoxy aldehyde, **1.96**, to the diene. The pre-macrocycle was further isolated to explore final lactonization conditions. This closure of the ring system proved to be unsuccessful due to ring strain and steric hindrance, conditions explored are seen in Scheme 12. Due to this road block, the synthetic route was altered to mimic those published by both the Williams and Luesch group.⁹²



Scheme 13. Undesired intermediate seen during the Forsyth synthesis towards LARGAZOLE, showing the C2 epimer pathway.

One important note in this synthesis, outside of the utilization of the NHC reaction, is the presence of the C2 epimer of parent LARGAZOLE (Scheme 13). This is predicted to result from an in situ ring closure from the thiazole to the valine carbonyl to form a diketopiperazine intermediate, **1.100**.^{113, 114} Biological activity of this compound showed to have lower inhibitory activity against HDAC class 1 isoforms but comparable activity towards prostate cancer cell lines. This is important to consider when routing the multiple amino acid couplings within the LARGAZOLE

scaffold; insuring that the valine is first coupled to the base depsipeptide, as seen in the Williams synthesis, can help to avoid this undesired epimer.¹¹⁵

Jiang Total Synthesis

Jiang et. al. completed an additional total synthesis of Largazole in 2010.^{116,117} This study investigated a new route, as well as modification of the valine portion of the macrocycle and *E* vs *Z* geometry of the sidechain alkene. The lysine substitution was predicted due to modeling studies that showed that portion of the molecule has hydrophobic interactions with tyrosine and leucine on the enzyme surface; inducing stronger hydrophobic effects could potentially increase the potency of the parent molecule.¹¹⁸

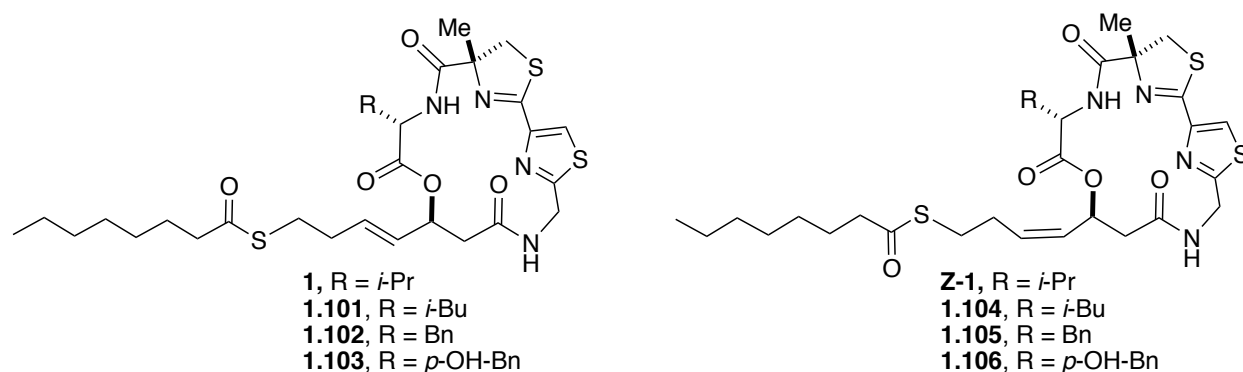
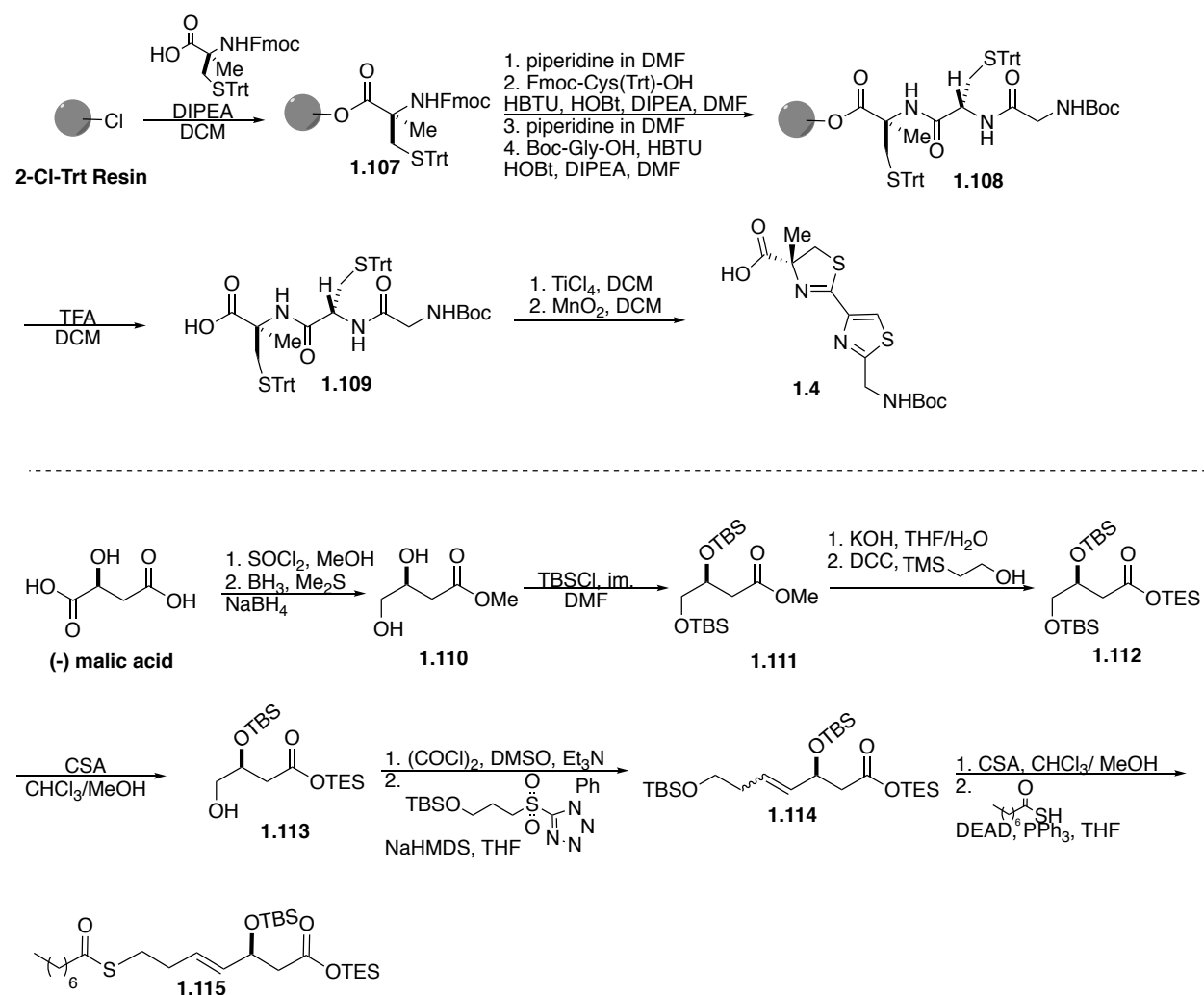


Figure 8. *E/Z* derivatives of Largazole developed by Jiang and coworkers.

Key differing steps of the Jiang group synthesis included the formation of the thiazole-thiazoline fragment and depsipeptide base fragment (Scheme 14). Solid phase peptide synthesis was utilized to construct the linear peptide which could undergo deprotection and cyclization resulting in common intermediate **1.4**. (-) Malic acid was used as starting material for the depsipeptide base fragment synthesis. Reduction using NaBH₄, followed by TBSCl protection, esterification, and selective deprotection provided compound **1.113** which could undergo a Julia-Kocienski olefination.¹¹⁹ This step proved to be unselective producing both *E* and *Z* isomers in an

8:1 ratio, respectively. A subsequent selective primary alcohol deprotection and Mitsunbo reaction provided the base thioester fragment which could then be linked to either valine or additional amino acids including: leucine, phenylalanine, and tyrosine. Amino acid coupling and macrocyclization under previously established conditions provided compounds **1.101-1.106**.¹²⁰ After further studies, a click chemistry route was developed for the synthesis of the thiazole-thiazoline fragment.¹²¹

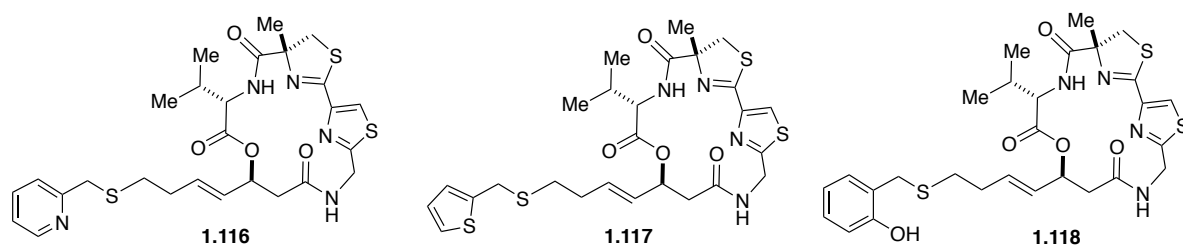


Scheme 14. Jiang total synthesis of Largazole fragments: (a) solid phase peptide synthesis route to thiazole-thiazoline (4-Me), (b) route to depsipeptide base derivative 114.

All Z alkene analogs resulted in a complete depletion of Largazole activity towards HCT-116 (colorectal carcinoma), A549 (human lung cancer), HEK293 (human embryonic kidney), and HLF (human embryonic lung fibroblast) cell lines. Across the valine substituted derivatives, leucine and phenylalanine retained selectivity but decreased in potency. The tyrosine substitution had a much stronger antiproliferative effect for the diseased cell lines, HCT-116 and A549 when compared to HEK293 and HLF. The outcome of this study strongly suggests that the *trans* geometry of the alkene is important for the selective and potent activity of Largazole.^{122, 123}

Additional Total Syntheses

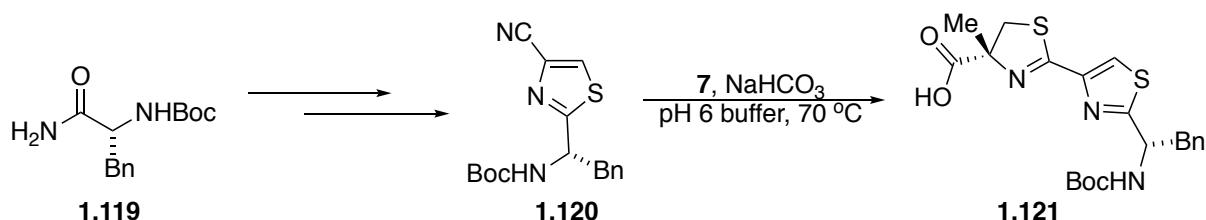
The Tillekeratne laboratory developed an additional synthesis of Largazole in 2011 to aid in their exploration of different tail groups on the free thiol of the active Largazole compound.¹²⁴ They envisioned adding additional Zn²⁺ chelating functionalities to the thiol protecting group in hopes of increasing the chelation effect and therefore increasing binding of the molecules. In their synthesis a similar, combined approach to the macrocyclization, as established by both the Williams and Luesch groups, was utilized. Their synthesis differed in implementing an enzymatic resolution for the synthesis of α -methyl cysteine. The base was synthesized with a t-butyl protection of the thiol versus a trityl protection; however, this route was unable to be deprotected and prior established routes were followed. In turn, the depsipeptide base was synthesized via the Williams route, while the macrocyclization utilized the Luesch synthesis of amidation followed by coupling to valine and subsequent macrocyclization.



Scheme 15. Tail group modifications developed by Tillekeratne during their total synthesis of Largazole

Final trityl deprotection of the thiol provided a nucleophile that could be utilized to synthesis pyridyl, thiophene, and phenol derivatives. All derivatives, as well as parent Largazole, were tested across HCT-116 cell lines. The three derivatives, Scheme 15, showed reduced activity in comparison to the parent Largazole, μM (of the most active) vs nM activity respectively.

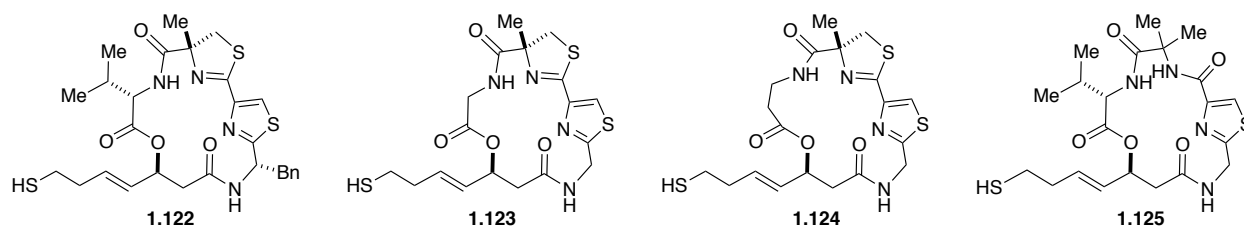
The Ganesan group additionally performed a total synthesis of Largazole in 2011, modifying substitutions around the macrocycle.⁸³ Deviations from the Williams group synthesis of note are: use of a phenylalanine in replace of glycine during thiazole synthesis to install a benzyl group, compound **1.119**, and coupling to glycine or alanine in replacement of valine to the depsi-peptide base fragment prior to macrocyclization.



Scheme 16. Phenylalanine derived starting material used by the Ganesan group for development of thiazole-thiazoline (**120**).

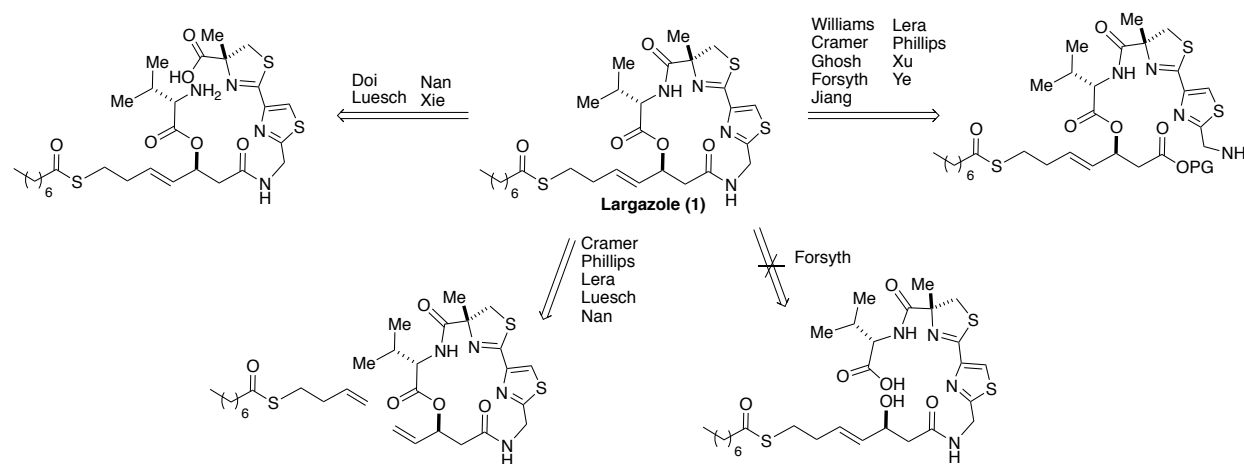
Additionally, a derivative with the deletion of the thiazoline group was synthesized with a gem dimethyl substitution. In all of the substituted cases, seen in Scheme 17, the alterations were tolerable and delivered HDAC inhibition. However, the parent Largazole thiol exhibited the highest potency in HDAC inhibition confirming the importance of the original macrocycle scaffold. One important property that was obtained through these studies was the half-life of ≤ 5 minutes of parent Largazole in mouse liver homogenate. This highlights the cleavable nature

of the thioester, prompting the need for further studies into different thiol masking groups which are currently being explored in our laboratory.



Scheme 17. Library derivatives developed by the Ganesan group, benzyl substitution at C14 (121), H substitution at C2 (122), one carbon homologation of the macrocycle (123), and gem dimethyl thiazoline substitution (124).

The Lera group investigated the synthesis of Largazole, as well as derivatives of the thiazoline fragment.⁹¹ These changes included substitution of the methyl to hydrogen, ethyl, and benzyl. Additionally, the thiazoline was replaced with a thiazole and oxazole for further studies. These scaffold modifications resulted in HDAC1 inhibition comparable or decreased in relation to parent Largazole. IC₅₀ values were obtained in across HDAC1-3, and 9 isoforms. Largazole continued to exhibit the highest potency in sub uM activity. This again confirms the importance of the functionalities of the parent natural product.



Scheme 18. Total representation of routes to obtain synthetic natural product, Largazole (1)

There are an additional 5 (Doi^{88, 125}, Ye¹²⁶, Breit¹²⁷, O'Doherty¹²⁸, Xie⁹⁴) total syntheses of Largazole for a combined 11 to date, not to mention the extensive development of analogs within

the literature.¹²⁹⁻¹³⁴ The importance of the Williams group convergent synthesis to provide routes to an elaborate library are highlighted below in the discussion of the continued library development of Largazole derivatives. An abbreviated representation of the total synthesis disconnects can be seen in Scheme 18. This high presence and investigation of Largazole in the literature further shows the true therapeutic potential of the complex macrocyclic scaffold.¹³⁵

FULL SCOPE

The extensive library of Largazole compounds within the Williams laboratory has been developed to probe the importance of these main functionalities of the parent compound: macrocycle stability, cap group bind effects, Zn²⁺ binding domain, and new chemical space exploration outside of the binding pocket.^{39, 80, 99, 136} Each of these syntheses utilize the convergent synthesis discussed in Chapter 1.3. Modifications can be synthetically utilized in both the depsipeptide and peptide isostere of Largazole.

While many analogs have been explored and further developed, discussion of the peptide isostere, pyridyl analogs, oxazole analogs, and development of novel chemical space off of the Largazole thiazole at C12 will be discussed herein. The derivatives that will not be discussed include, but are not limited to, alterations of the valine fragment with additional amino acid exchanges and tail group or linker length substitution (e.g. replacing the thioester with hydroxamic acid, depletion or addition of a methylene). In order to access the myriad of Largazole analogs the original and modified syntheses were repeated with improvements to scale up, yield, and functionality.

The ability to manipulate each fragment of the molecule to increase potency and improve the structure activity relationship of Largazole, or its derivative, with the HDAC binding pocket surface recognition units has been explored.¹⁰⁰ The surface recognition unit amino acids of importance are aspartic acid, tyrosine, and histidine.⁸ Increasing hydrogen bonding interactions with these amino acid residues could ultimately result in increased binding affinity. Additionally, stabilization of the macrocycle through installation of a more robust scaffold could increase potency and selectivity of the molecule.

The first analog developed of Largazole within the Williams laboratory were compounds **19** and **20**. The depsipeptide macrocyclic linkage of the parent compound was replaced with its peptide isostere at C17, Figure 9, Scheme 19.

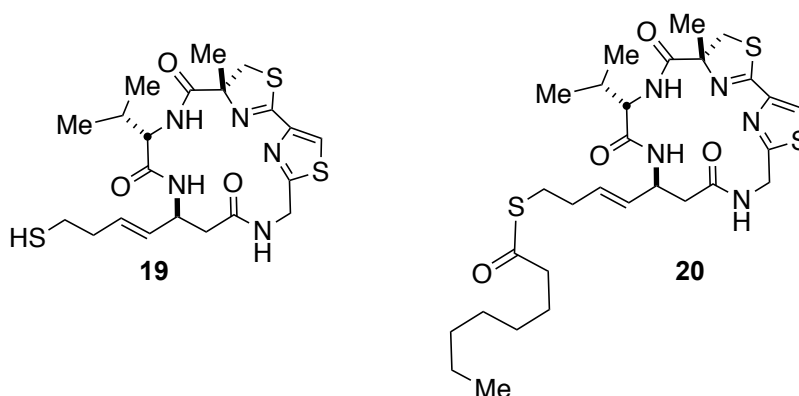
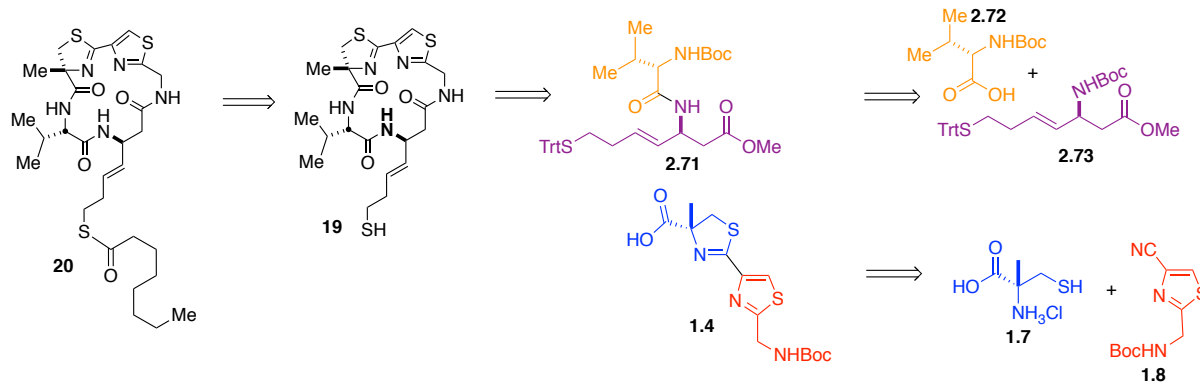


Figure 9. Largazole peptide isostere thiol (**2**) and peptide isostere (**20**).

Formation of a more rigid amide bond in place of the labile ester linkage in Largazole's original framework provides a more robust and stable macrocycle. This has led to both increased potency and cellular stability when tested across HDAC isoforms, biological activity will be discussed further in this chapter.⁸⁵

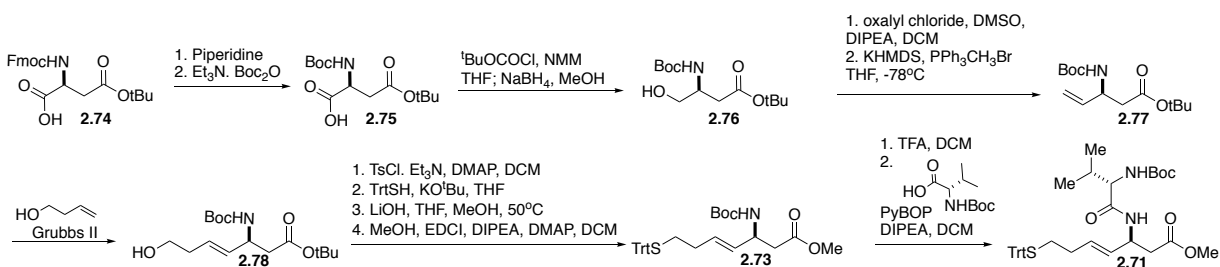


Scheme 19. Retrosynthetic analysis of Largazole peptide isostere

The original synthetic pathway to the peptide isostere base **2.71** can be seen in Scheme 20. Over 8 steps, the fragment is accessed in a 10% yield from commercially available t-butyl L-

aspartic acid. Additional methods for improvement of the overall synthesis of this fragment have been explored and are ongoing within our laboratory, further discussion can be found in Chapter 4.

Aspartic acid is Boc protected using Boc anhydride and triethylamine, due to the availability of Fmoc protected aspartic acid often times a protecting group swap is performed here. The carboxylic acid is activated with 4-methylmorpholine and isobutyl chloroformate in THF at -40 °C, then reduced with NaBH₄ in methanol at -20 °C to produce the free alcohol **2.76**. Following an oxidation with oxalyl chloride, DMSO and DIPEA in DCM at -65 °C and Wittig olefination with methyltriphenylphosphonium bromide and KHMDS in THF at -78 °C revealed the terminal olefin, **2.77**, for further functionalization.

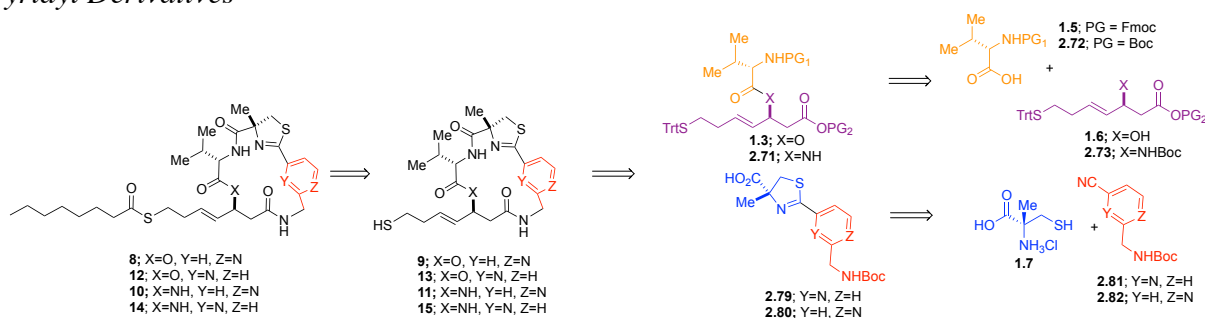


Scheme 20. Forward synthesis to peptide base fragment **125**.

Grubbs olefin metathesis with the 2nd generation catalyst and 3-buten-1-ol in DCM at 50 °C provides compound **2.78** in 25% yield. The free alcohol was then activated with TsCl, triethylamine and DMAP in DCM followed by nucleophilic substitution with trityl mercaptan and potassium tert-butoxide in THF. Hydrolysis using lithium hydroxide and methanol in THF at 50 °C provided the carboxylic acid, which then underwent a Steglich esterification using methanol and EDCI with diisopropylethylamine and DMAP in DCM to provide compound **2.73**. Compound **2.73** is then deprotected with trifluoroacetic acid in DCM and coupled to N-boc protected valine with PyBOP and DIPEA in DCM to yield compound **2.71**.

The thiazole-thiazoline synthesis in Scheme 3, 4, and 6 were used to provide compound **1.4** for amino acid coupling and macrocyclization with the peptide isostere base. TFA is utilized for the Boc deprotection of the protected valine fragment of the base followed by PyBOP coupling with thiazole-thiazoline. Hydrolysis of the methyl ester and deprotection of the Boc protected amine provide the free carboxylic acid and amine which can undergo amino acid coupling for final macrocyclization. HATU and HOBt with DIPEA provided macrocycle product. Trt deprotection with TFA and $i\text{Pr}_3\text{SiH}$ revealed the free thiol of the peptide isostere, **19**. Similar acylation conditions as with the parent Largazole compound with octanoyl chloride and DMAP provided Largazole peptide isostere from the four main building blocks. The synthetic development of the peptide isostere shows the original utility of a convergent developed route for structural modification.

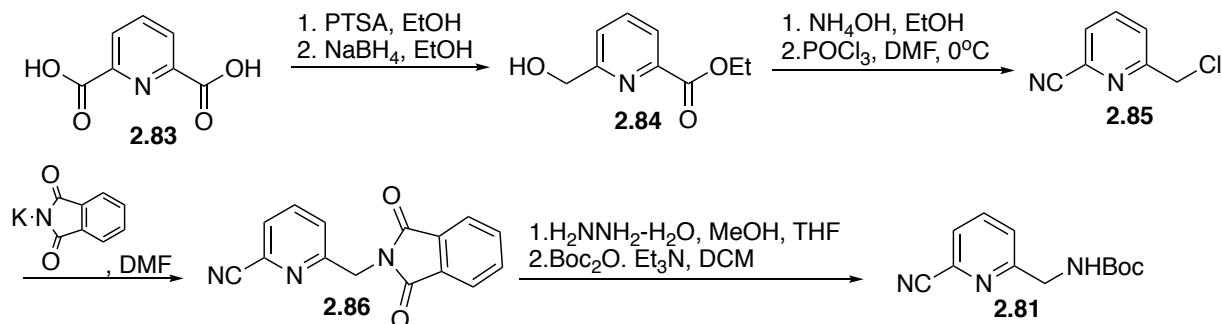
Pyridyl Derivatives¹⁰¹



Scheme 21. Retrosynthetic analysis of pyridyl substituted Largazole derivatives.

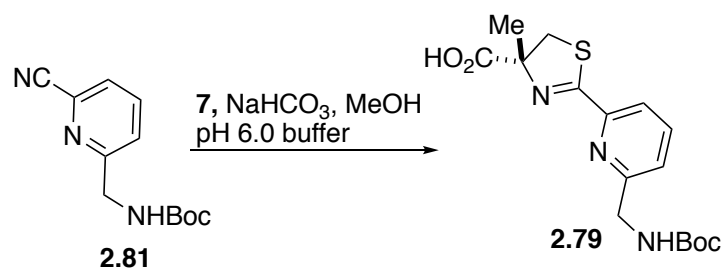
In order to probe the structure activity relationship of the macrocycle with the binding pocket of relevant HDACs, a series of pyridyl analogs were developed in collaboration with the Wiest laboratory.¹⁰¹ The thiazole ring (**1.8**) shown in Scheme 2 was replaced by a pyridine in either an “IN” or “OUT” configuration, giving compounds **2.81** and **2.82**, respectively (Scheme 21). The pyridine fragment was predicted to have conducive electrostatic interactions with the

native aspartic acid residue of the enzyme surface. Stronger hydrogen bonding enzyme interaction can lead to a more potent inhibition of the HDAC isoform.



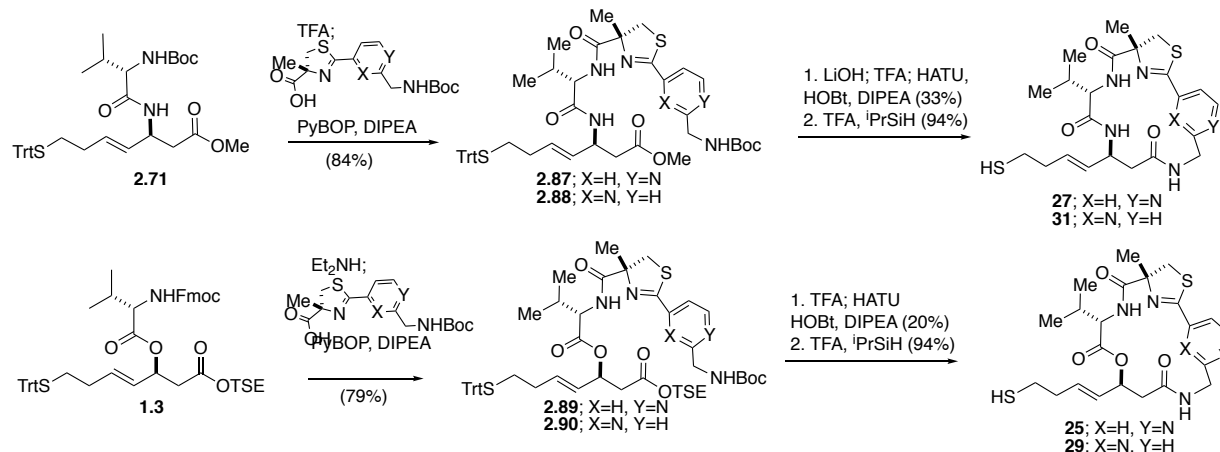
Scheme 22. Synthesis of cyano pyridine "IN" fragment 138.

2.81 and **2.82** were synthesized using the same route (Scheme 22). Pyridine "IN" cyano fragment **2.81** was synthesized in 7 steps with a 16% overall yield. Fischer esterification and selective reduction of 2,6-pyridinedicarboxylic acid provided intermediate **2.84** under mild conditions. **2.84** was converted to the amide followed by immediate cyano formation using POCl_3 and DMF providing intermediate **2.85**. Gabriel's synthesis was used to obtain phthalamide **2.86**, followed by free amine formation and Boc protection to provide precursor **2.81**.



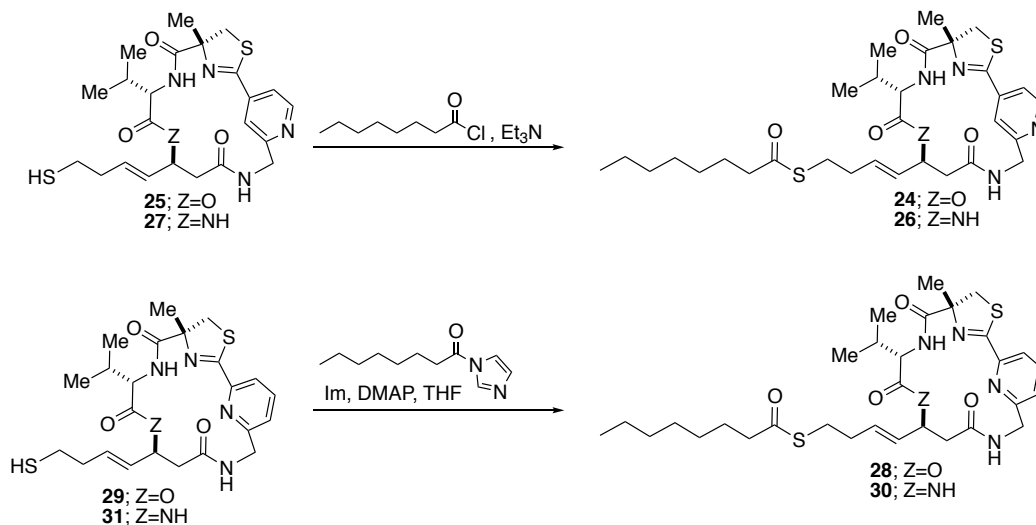
Scheme 23. Synthesis of thiazole-pyridine derivative 139.

The pyridine "OUT" fragment followed a similar pathway with 2,4-pyridinedicarboxylic acid as the starting material. Both pyridine "IN" and "OUT" cyano groups underwent cyclization with α -methylcysteine, Scheme 23.



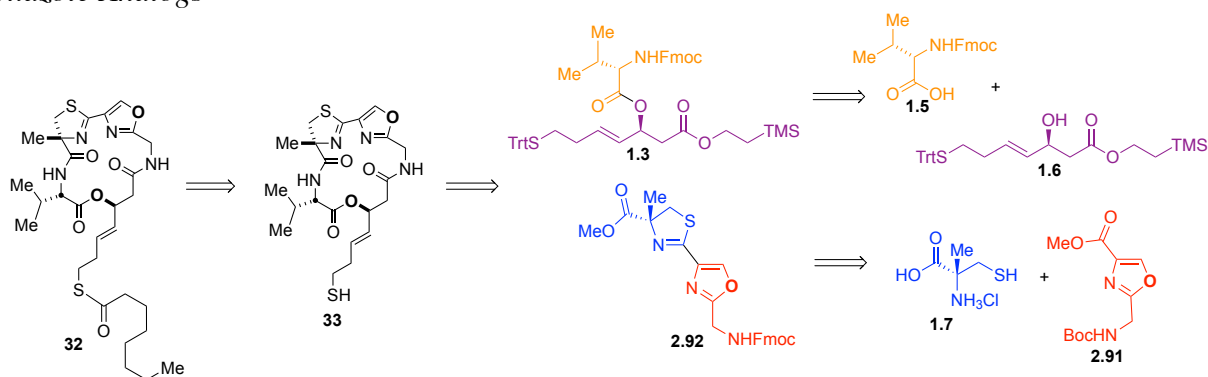
Scheme 24. Coupling and macrocyclization of Largazole depsipeptide and peptide derivatives (**27/31**, **25/29**).

Macrocyclization for “IN” (**29/31**) and “OUT” (**25/27**) derivatives mirrored the synthetic pathway for both Largazole (**1**) and its peptide isostere (**7**); pyridine macrocyclization is shown in Scheme 24. Addition of the octanoyl tail for pyridine “OUT” proceeded via the established route utilizing octanoyl chloride. Successful addition of the octanoyl tail for the pyridine “IN” compounds (**28/30**) proceeded through use of the imidazole octanoyl complex, due to di-octanoylation observed when octanoyl chloride was used. A comparison of the octanoyl tail addition routes can be seen in Scheme 25.



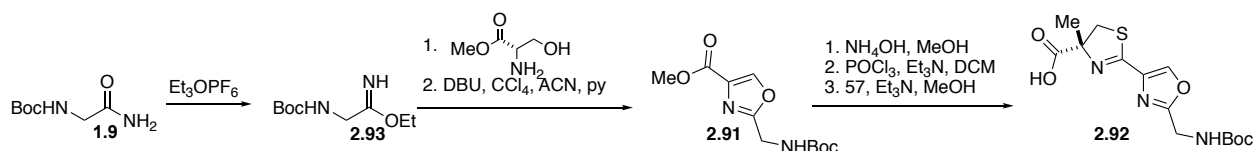
Scheme 25. Final acylation of pyridyl compounds, pyridine IN (**24/26**), pyridine OUT (**28/30**).

Oxazole Analogs³⁹



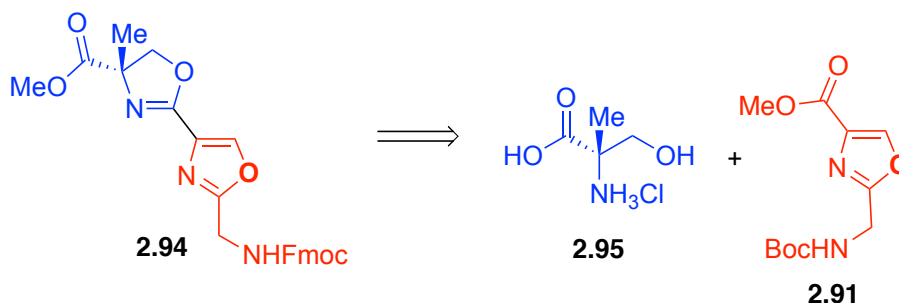
Scheme 26. Retrosynthetic analysis of oxazole derivatives.

Replacement of the thiazole ring with an oxazole was also explored for Largazole derivatization. Dr. Jennifer M. Guerra-Bubb and coworkers developed the synthetic route for oxazole-thiazoline depsipeptide analogs **32-36** (Figure 5).³⁹ Retrosynthetic analysis and disconnections can be seen in Scheme 26. As of more recently, scale up conditions and additional reactivity of this derivative is being explored.⁸¹ Carboxylic acid fragment **96** was obtained in three steps from oxazole **2.91** seen in Scheme 27.



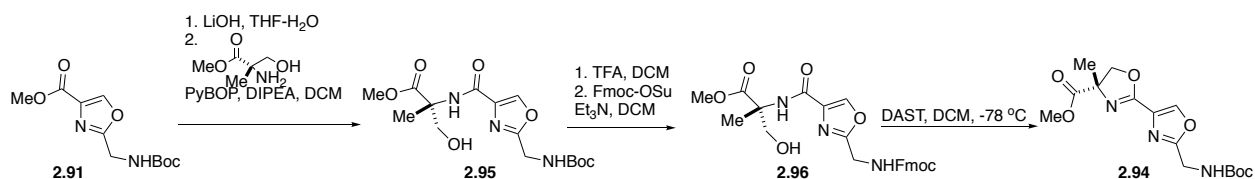
Scheme 27. Synthesis of oxazole fragment 146.

Boc protected ethyl acetimidate **2.93** was obtained from compound **1.9**. Reaction of **2.93** with L-serine methylester followed by oxidation provided oxazole **2.91**. The cyano-oxazole species was accessed through the route established for fragment **1.4**. Oxazole-thiazoline intermediate **2.92** was obtained via cyclization with α -methyl cysteine, **1.7**. Macrocyclization was performed similarly to parent complex, **1**, utilizing both PyBOP and HATU/HOBt coupling.



Scheme 28. Retrosynthetic analysis of oxazole-oxazoline fragment.

Oxazole-oxazoline analog fragment **2.94** was synthesized via an alternative route when compared to the previous conditions. Ester **2.91** was hydrolyzed and coupled to α -methyl serine using PyBOP and DIPEA. A protecting group swap from Boc-protected amine to Fmoc-protected amine was successful, utilizing TFA deprotection followed by Fmoc-OSu protection resulting in intermediate **2.94**. This protecting group swap was necessary due to the instability of oxazolines in acidic conditions, which would be necessary for final Boc removal.¹³⁷



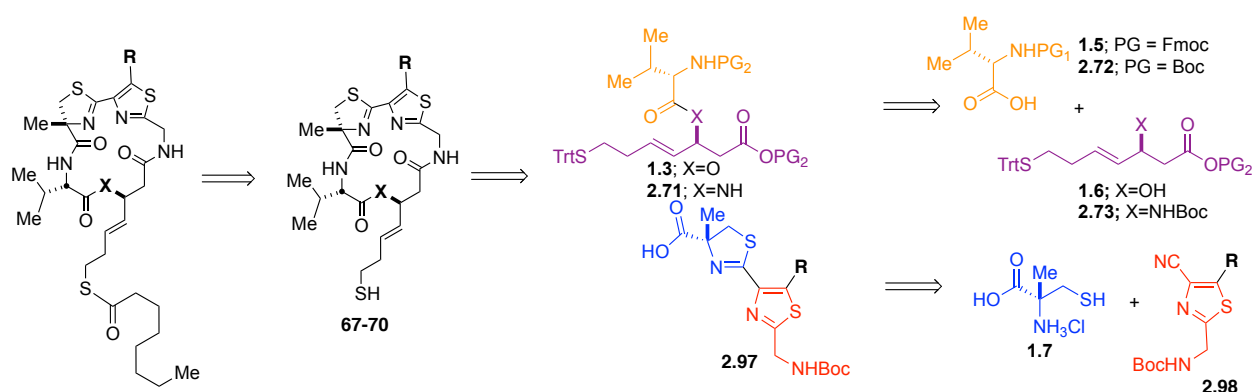
Scheme 29. Synthesis of oxazole-oxazoline fragment 150.

Diethylaminosulfur trifluoride (DAST) cyclocondensation was successfully accomplished to provide fragment **2.94**. Methyl ester **2.94** was coupled to the base depsipeptide fragment, followed by macrocyclization and addition of the octanoyl tail. This provided Largazole analogs **37** and **38**, as well as the homodimer **39** (Figure 2).

Derivatization at C12: New chemical space analogs¹³⁸

Alteration of the cap group of Largazole was the next focus of structure activity relationship development. We developed a new strategy for the conjugation of Largazole to

additional bioactive molecules, dual therapeutics, and additionally biologically relevant molecules. Further functionalization of the macrocycle was explored at the C12 position. Derivatization off of the thiazole allowed for a new chemical space to be probed in search of an enhanced structure activity relationships. Since, the thiazole ring is modeled outside of the binding pocket, it was envisioned that this new handle would interact with the protein surface and provide a cleavable handle for directed delivery while not interfering with Zn^{2+} coordination site. Retrosynthetic analysis can be seen in Scheme 30.

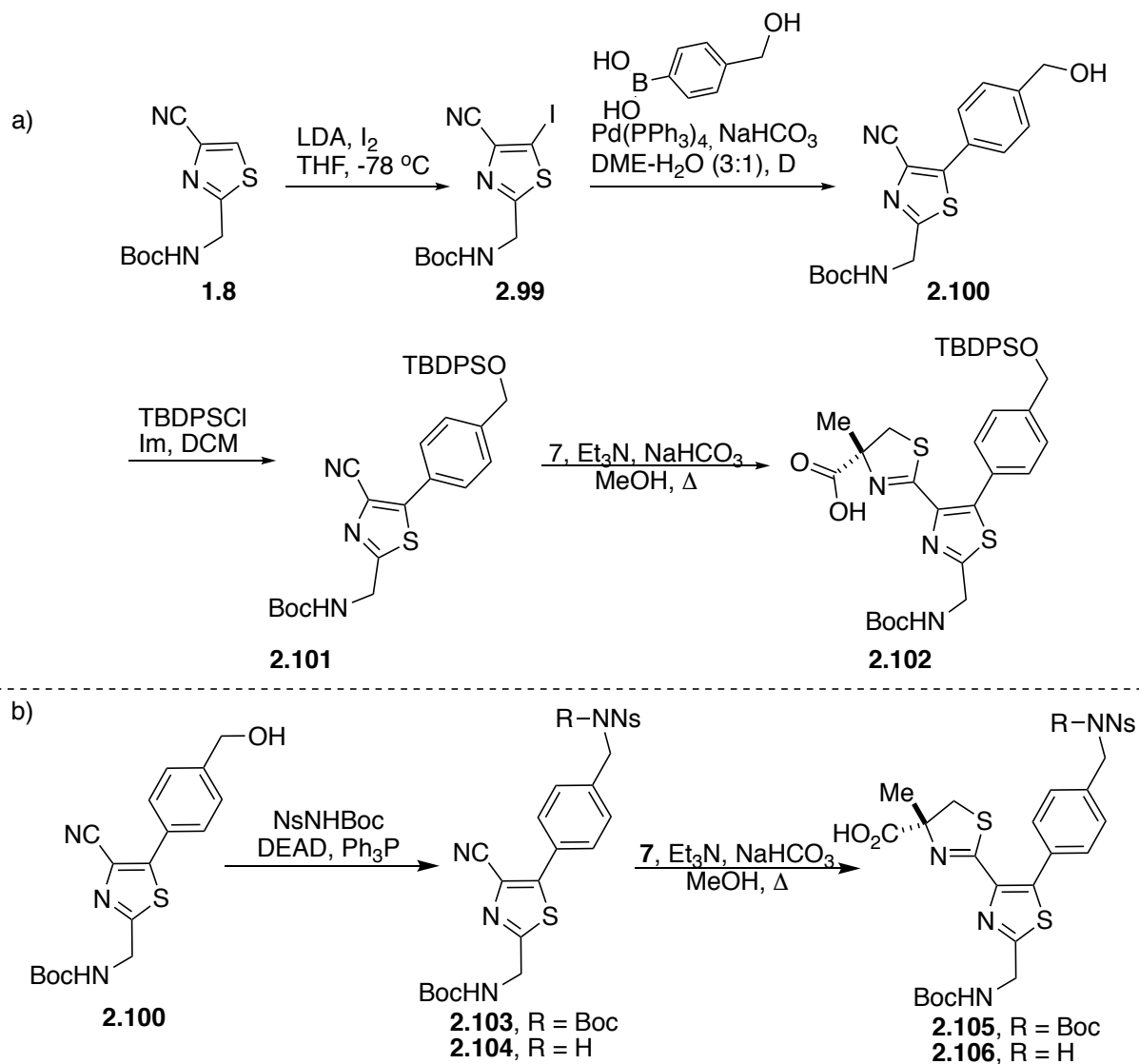


Scheme 30. Retrosynthetic analysis of new chemical space Largazole derivatives.

This is the first accessed derivative of Largazole that is absence of a hydrogen on the thiazole cap group. Thiazole intermediate **1.8** was iodinated with LDA and I_2 to provide **2.99**. Compound **2.99** underwent Suzuki coupling, $Pd(PPh_3)_4$ with $NaHCO_3$ in DCM- H_2O at reflux, with either phenyl- or 4-(hydroxymethylphenyl)-boronic acid, Scheme 31. In order to have both a cleavable and non-cleavable handle the hydroxymethyl moiety was either protected for later stage deprotection and coupling or converted to the protected amine, respectively. Protection of the free alcohol was achieved utilizing TBDPSCl to provide compound **2.101**.

Synthesis of the nitrogen handle resulted from further iterations on the hydroxyl methyl handle of compound **2.100**. Mitsunobu reaction with $NsNH\text{Boc}$ under standard DEAD conditions provided a mixture of Boc protected and deprotected products which were carried on

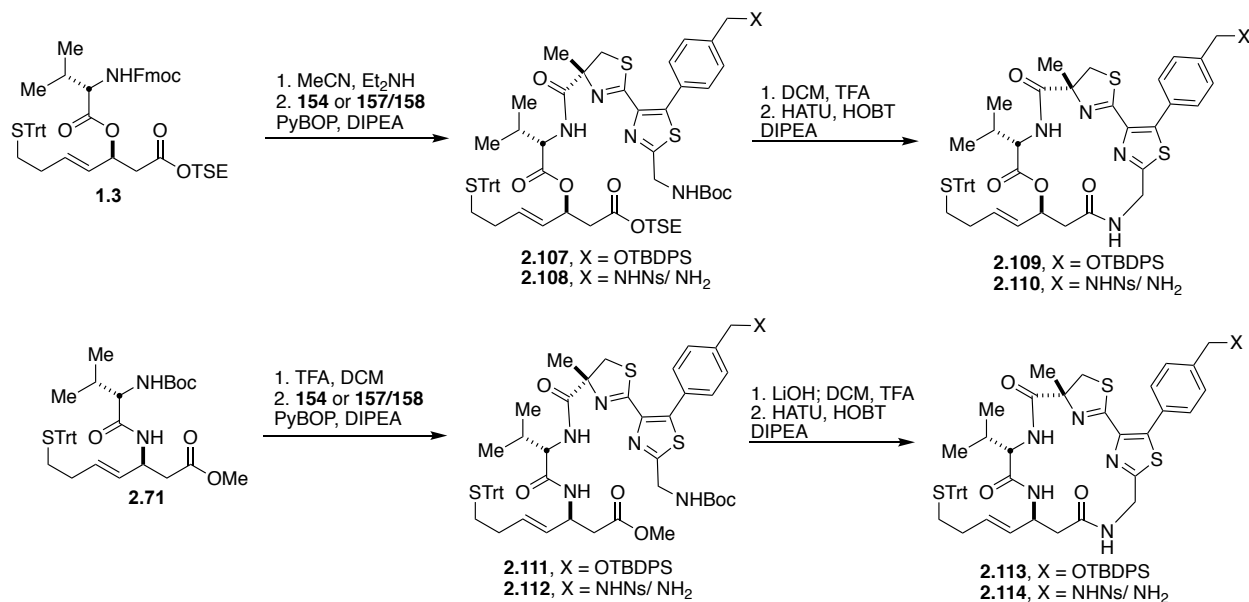
for the oxidative cyclization with α -methyl cysteine. The corresponding compound could then be used for coupling and macrocyclization to either the depsipeptide or peptide isostere base fragment.



Scheme 31. Synthesis of new chemical space thiazole-thiazoline analogs, (a) hydroxymethyl handle derivative, (b) amine handle.

The corresponding Largazole derivatives, **67**, **68** and **69**, were ultimately prepared in a similar fashion to the parent routes with both the depsipeptide parent and peptide isostere. following successful completion of premacrocycle fragments. Coupling and macrocyclization was

achieved using previously established conditions, Scheme 32. For the corresponding depsipeptide base the valine nitrogen was deprotected with Et₂NH in ACN, while the peptide base fragment was Boc deprotected using TFA in DCM. PyBOP coupling with the deprotected free amine of valine and the carboxylic acid provided pre-macrocyclization products. Either global deprotection or hydrolysis followed by Boc deprotection, compounds **2.109/2.110** or **2.113/2.114** respectively,



Scheme 32. Coupling and macrocyclization procedure for new chemical space derivatives

provided appropriate functionalities to undergo HATU/HOBt. Final trityl deprotection revealed the free thiols, **67**, **68**, and **69**. Deprotection to either the free alcohol or amine revealed a handle for further conjugation that will be discussed in Chapter 3. The free thiol can also be acylated pending on desired interest.

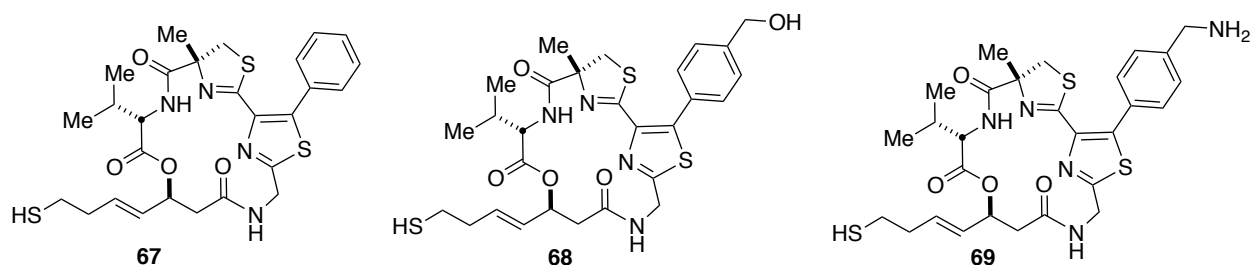


Figure 10. Depsipeptide Largazole analogs at the new chemical space, benzyl (**51**), hydroxy (**52**) and amine (**53**) handles.

All thiazole-thiazoline new chemical space derivatives can also be synthesized with the peptide base. The final sequence of deprotection steps is dependent on conjugation and desired product. Alcohol handle deprotection proceeds via TASF conditions and Ns deprotection with the use of thiophenol and 1M KOH. The trityl group is removed with iPr_3SiH and TFA to yield the free thiol that can be further reacted with octanoyl chloride. This successful synthesis allowed for further functionalization with biological probes and coupled therapeutics for dual targeted therapies.

Biological Lessons and Improvements

The peptide isostere derivative's amide linkage helps to maintain the macrocycle stability in a cellular medium. The isostere thiol, **19**, showed increased activity and selectivity when compared to parent thiol, **2**, towards HDAC1-3. IC_{50} values in nanomolar potencies are presented in Table 5 for a full comparison of analogs.

Cap group substitution for both pyridine and oxazole replacement of the thiazole moiety resulted in nanomolar potency and Class I selectivity. The electrostatic interactions on the surface of the HDAC binding pocket between aspartic acid and the protonated pyridine nitrogen are predicted to form a salt bridge. A stronger binding interaction may lead to the direct result of potent and selective enzyme pocket inhibition.⁸⁰

HDAC isoform panels were explored with derivatives of the new chemical space compounds. Both the hydroxyl handle and parent Largazole biotin derivative, compounds **68** and **70**, showed sub nanomolar activity for HDAC1. Improved potency across HDAC 2 and 3 were also seen, with a strong selectivity in comparison to HDAC 6 and 8.

Table 5. HDAC IC₅₀ (nM) values across HDAC 1-3, 6, and 8 for select compounds from the developed largazole library.

Compound	HDAC1	HDAC2	HDAC3	HDAC6	HDAC8
Largazole (1)	10.09	18.65	9.09	165.6	1068
2	2.51	4.19	2.78	28.11	228.4
19	1.95	3.38	2.59	102	255.3
20	544.1	825.2	1151	-	-
21	50	500	500	>10,000	2.8
24	340	655.4	319.5	-	-
25	2.2	4.42	2.31	35.16	101.8
26	816.9	1240	846.5	-	-
27	13.2	20.77	14.59	2849	1491
28	203.6	349.5	332.1	-	-
29	2.68	4.39	3.07	48.55	341.3
30	340.3	471.8	332.4	-	-
31	42	69.8	42.5	-	-
32	950	2100	1900	1100	-
33	4.4	20	72	98	1200
36	150	1300	550	50	-
42	0.01	0.3	0.1	8	400
68	0.166	2.61	0.734	14.9	94
70	0.2388	2.84	1.064	36.51	129.3

From this, we have identified lead compounds for further biological development. The peptide isostere lactam linkage has maintained and improved IC₅₀ values for selective HDAC inhibition. Studies not explored here but tested on analogs developed within our laboratory determined that depletion or addition of carbon atoms from the linker group result in an inactivation of enzyme binding effect. While cap group modifications have shown comparable activity to the thiazole-thiazoline, the parent structure fragment is easily accessible and the peptide isostere maintains superior potency across Class I HDAC isoforms. Additionally, lack of a chelation group results in no HDAC inhibition.⁷⁸

Alteration of the cap group has led to sub nanomolar IC₅₀ concentrations and increased the overall potency and selectivity towards Class I HDACs. Further discussion of this data will be addressed in relationship to the complex analog development in Chapter 3. It is important to note that the hydroxyl handle prior to conjugation remains active, further promoting the hypothesis of the cap group extending out of the Zn²⁺ binding pocket promotes an improved ability to interact with amino acids on the enzyme surface without interfering with chelation effects.

PATH TO COMPLEX ANALOGS

Dual targeted therapies have opened up opportunities to both increase potency and selectivity of developing therapies. In addition, dual therapeutics may target numerous disease states and increase the overall effect of developed compounds. In addition to increasing the therapeutic effect of Largazole, biological linkers can help to deduce protein-protein interactions and probe some of the still unclear biologic pathways. There are four specific, biologically relevant compounds linked to Largazole to date including: biotin, folic acid, methotrexate, and 5289-5066 (Figure 11).¹³⁹⁻¹⁴²

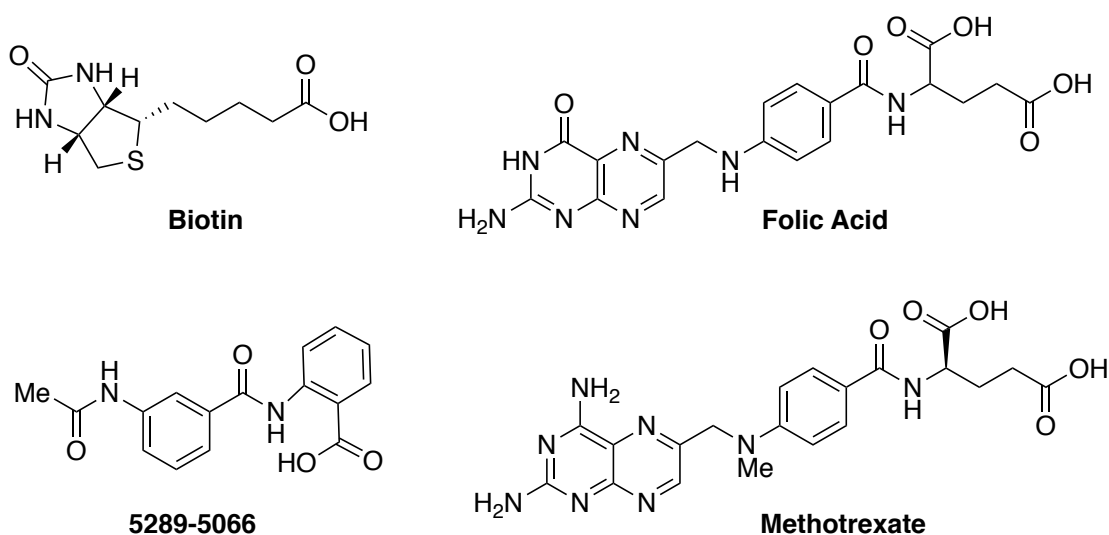


Figure 11. Biological conjugates of interest for conjugation to Largazole and Largazole peptide isostere.

In addition to the reasons stated above, bioconjugates can be employed to help selectively target specific pathways and carriers to diseased cells. This route has been widely used in cancer therapy investigations as the pathways, overexpressed proteins, and cell targets are further investigated.

In order to develop the dual targeted therapies and bioconjugates, it is important to identify linker space to the parent molecule that can be altered without depleting its original potency and

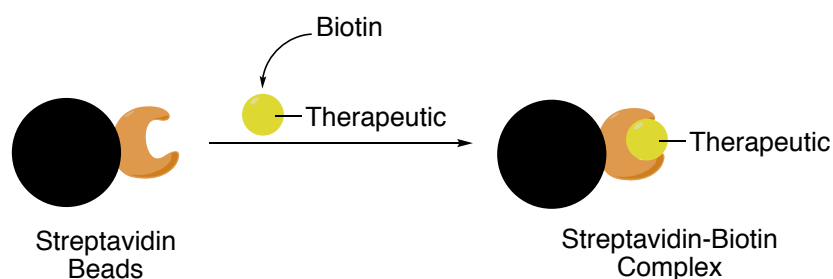
efficacy. Largazole contains two sites of conjugation on the parent macrocycle and will be discussed on a case by case basis below.

3.1 Biotin

Therapeutic Utility

Biotin, vitamin B7, seen in Figure 11 was the first biological Largazole conjugate synthesized in the Williams laboratory at the new chemical space handle of the thiazole, **70**.¹³⁸ Biotin has historically been implemented for multiple purposes. In our lab, two relevant function of biotin conjugates are for cancer targeting studies and pull-down biochemical assays. The biotin conjugate functionalization is at the thiazole carbon due to its ability to not interfere with parent compound activity by inhibiting the binding site.

Additionally, biotin has been seen to have strong affects towards both cell survival and protein synthesis. Studies have shown that in biotin deficient cells and animals, the cell proliferation and survival rate is dramatically reduced. The activity of biotin far surpasses the original hypothesis that it strictly acted upon carboxylases.¹⁴³ It is important to note that cell survival is not dependent on biotin but can be influenced via the concentration. Further studies on the mechanism of action of biotin and how it interacts with HDACs is important for the advancement and development of these Largazole analogs.¹²⁷



Scheme 33. Streptavidin-Biotin affinity for pull down assays

A pull-down biochemical assay was performed at Dana Farber Cancer Research Institute for the purpose of this study. In this case, pull-down assays were used to probe the interactions between the targeted drug and HDAC isoform. Streptavidin and biotin have a dissociation constant of 10^{-14} mol/L resulting in strong non-covalent interactions.¹⁴⁴ This complex can undergo several incubations and iterative purifications to probe the interaction between biotin linked complexes and potential enzymatic interactions.

The robust biotin and streptavidin interaction can contribute to many physical properties of both species. As we often look for in identifying selective drug targets, the binding pocket of streptavidin is complimentary for biotin. The snug fit furthermore introduces extensive hydrogen bonding from 8 different amino acid residues of the unbound biotin to the heteroatoms of biotin. In addition to the extensive hydrogen bonding channels, streptavidin contains a flexible loop which will encompass the biotin in a form of trap.¹³⁹

HDAC enzyme panels were run for both the parent Largazole, **68**, and Largazole-biotin conjugates. Little to no changes in potency and HDAC selectivity were seen after the structural modifications, which allowed further biochemical studies to be performed. Biotin's high affinity for streptavidin would allow for additional studies of protein-protein interactions. This route of synthesis and biochemical analysis can directly correlate to further developed biological conjugates.

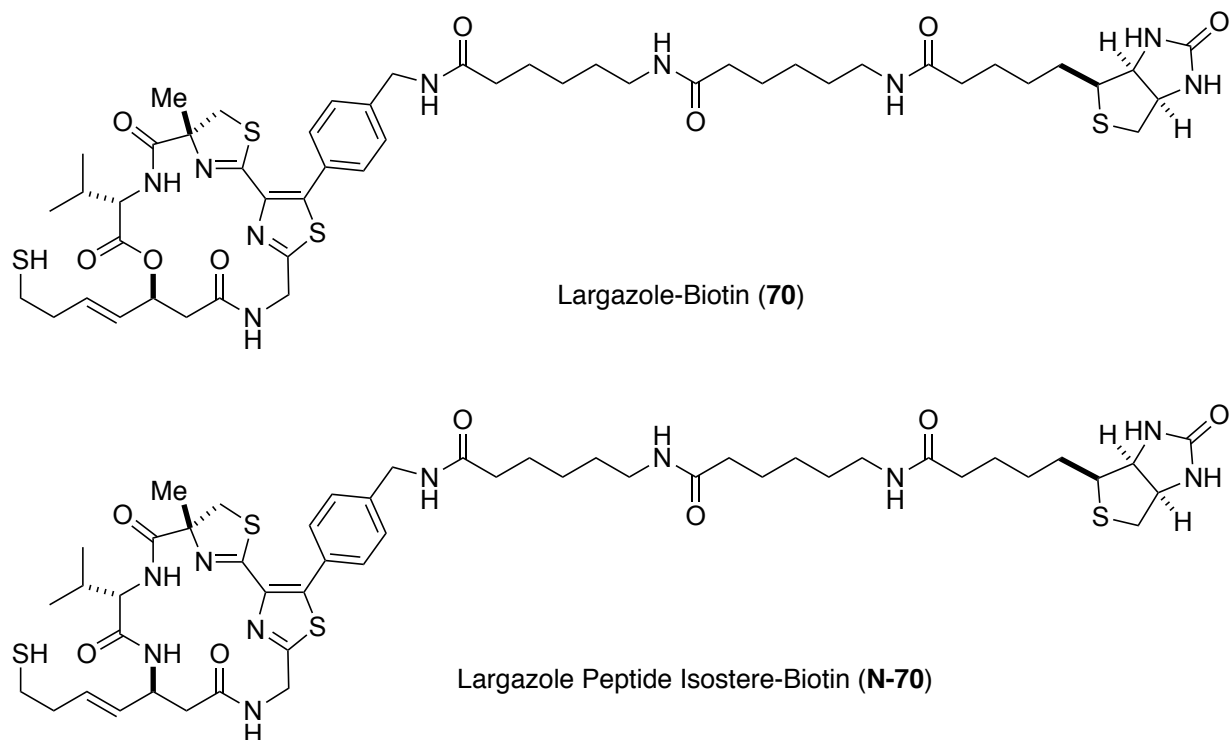


Figure 12. Largaazole thiol-biotin non-cleavable amide linked structures, depipeptide (54) and peptide isostere (167).

The carboxylic acid moiety that extends from the streptavidin biotin pocket allows for ease of conjugation to other function groups. Pending on which properties are being exploited in the newly conjugated molecule either a cleavable or non-cleavable bond could be introduced, in the case of Largazole the amide, non-cleavable bond was utilized for pull-down assays. The synthesis of **70** and **N-70**, Figure 12, is described in depth below.

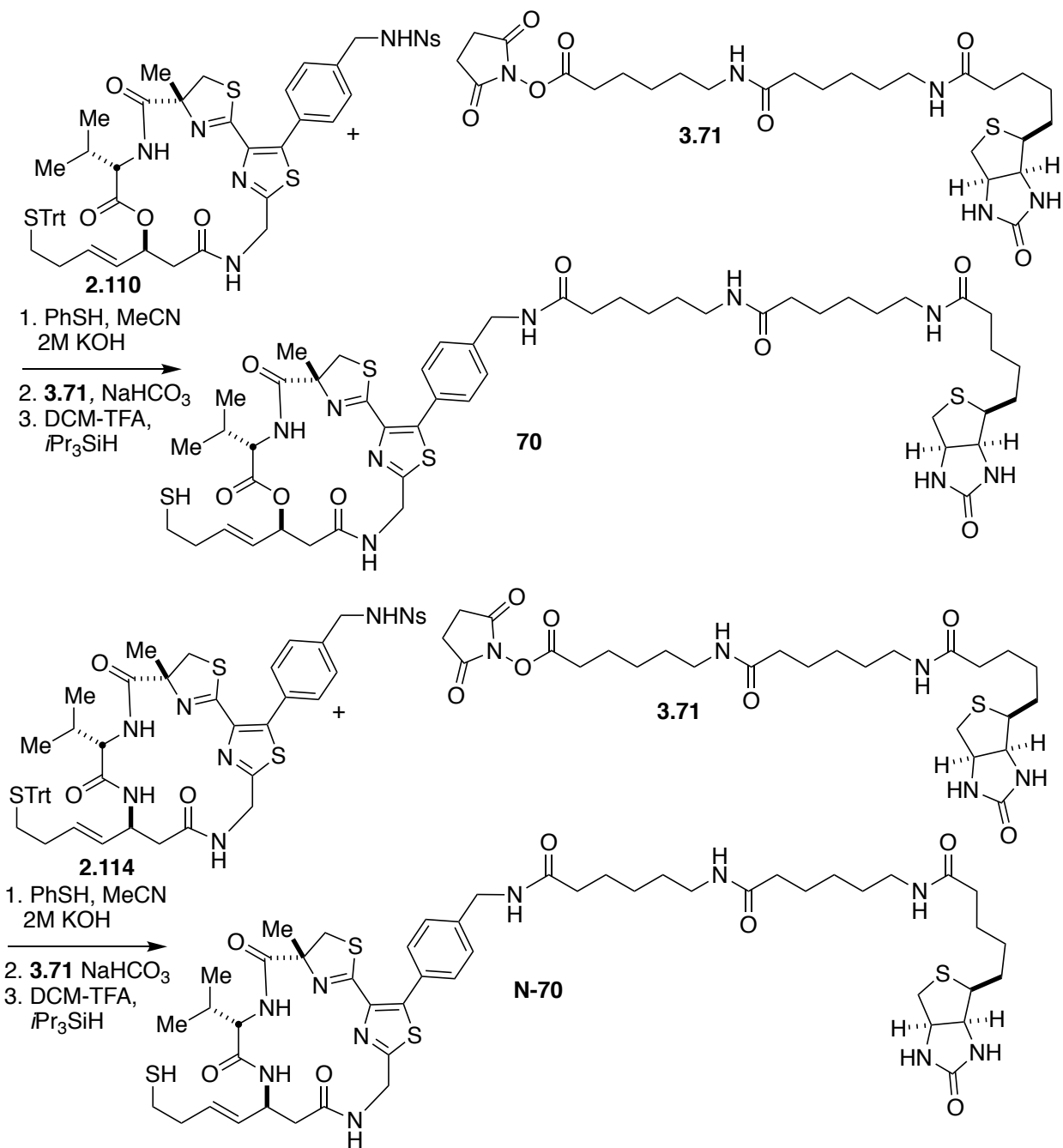
*Synthesis*¹³⁸

As discussed in Chapter 2.3, a new chemical space was developed on the thiazole of both Largazole and the peptide isostere. This cap group is easily accessible due to its distance from the complex macrocyclic core of Largazole. Prior modeling studies performed in collaboration with the Wiest group supported the prediction that further conjugation at that side would protrude outside of the HDAC enzyme pocket, without hindering the Zn^{2+} binding site.

Two syntheses of biotin linked Largazole were developed. Both a hydroxyl benzyl handle and amino benzyl handle were envisioned to produce both the cleavable ester and non-cleavable amide, respectively. A cleavable bond will be useful for drug delivery purposes in allowing Largazole thiol, the active HDAC inhibitor, to selectively target HDAC1-3 without interference, whereas the non-cleavable amide is a critical control and crucial for pull-down assays when analyzing the Largazole to HDAC site interactions. Scheme 34 shows the synthetic route to synthesis of the biotin non-cleavable compounds.

Early stage manipulation, four break-down units, and late stage macrocyclization has allowed an accessible route for further conjugation. The two halves, depsipeptide or peptide base and thiazole-thiazoline moiety are utilized to access the pre-macrocyclization products. Macrocyclization to trityl-protected precursors can be accessed through amide coupling technique previously established. The two halves can then be further dissected into the base amino or alcohol fragment, protected L-valine, α -methyl cysteine, and substituted thiazole cyano- precursor, previously discussed in Chapter 1. Retrosynthetically these molecules mirror **67-69**.

Compounds **2.110** and **2.114** were subjected to thiophenol and 2M KOH in acetonitrile to ensure the free amine was provided for coupling to biotin.¹⁴⁵ NaHCO_3 was used to promote the amide coupling of biotin for both the depsipeptide and peptide Largazole derivatives. Trityl deprotection using DCM-TFA and $i\text{Pr}_3\text{SiH}$ provide Largazole-biotin derivatives **70** and **N-70** in 41% and 36%, respectively, seen in Scheme 34. This convergent route can be utilized to access additional amide linked biological conjugates.



Scheme 34. Final deprotection and coupling steps for development of the biotin conjugates

Biochemical evaluation

Biotin-Largazole conjugate, **70**, exhibits extremely low change in IC₅₀ activity when compared to compound **68**. IC₅₀ values below 3 nM are maintained across HDACs 1-3 for **68** and

70. The small change in loss of activity confirms that further biomechanistic studies can be explored. Affinity chromatography assays were performed across HDACs 1-3 with the Largazole-biotin derivative, **5**. Streptavidin beads were added after a 16-hour incubation with compound **X** in 200 μ L of HeLa Nuclear Extract. Successful sustainable chelation of Largazole to the respective HDAC binding site was seen.¹³⁸

Table 6. HDAC isoform activity, IC50 (nM) across HDACs 1-3, 6, and 8

Compound	HDAC1	HDAC2	HDAC3	HDAC6	HDAC8
Largazole (1)	10.09	18.65	9.09	165.6	1068
Largazole thiol (2)	1.95	3.38	2.59	102	255.3
Hydroxy handle	0.166	2.61	0.734	14.9	94
Depsi-Biotin Conj	0.2388	2.84	1.064	36.51	129.3

In order to further probe the activity of the Largazole-biotin conjugates, an ester linkage could be explored. This would allow the biotin to be released in the cell for a more powerful effect. However, there are many biological compounds that show a higher affinity for cancer cells. With this in mind, we aimed to develop a route to synthesize both cleavable and non-cleavable derivatives of these compounds (discussed below).

3.2 Folic Acid/ Methotrexate

Folic acid, vitamin B9, is crucial for cell growth due to its role in producing tetrahydrofolate which partakes in the methylation of vital molecules in the cell replication pathway. Folic acid cannot be produced by the body but must be introduced through common dietary products such as lentils and spinach.¹⁴⁶ Cell division and replication would not be possible without folic acid. Because of this, cancer cells express higher levels of folic acid receptors on the cell surface due to their intrinsic properties of rapid DNA replication.¹⁴⁷ Once folic acid has reached

the folic acid receptor (FR), α -FR for the purpose of these developed compounds, the bound species will invaginate into the cell and metabolize via the pathway seen in Scheme 35.¹⁴⁸

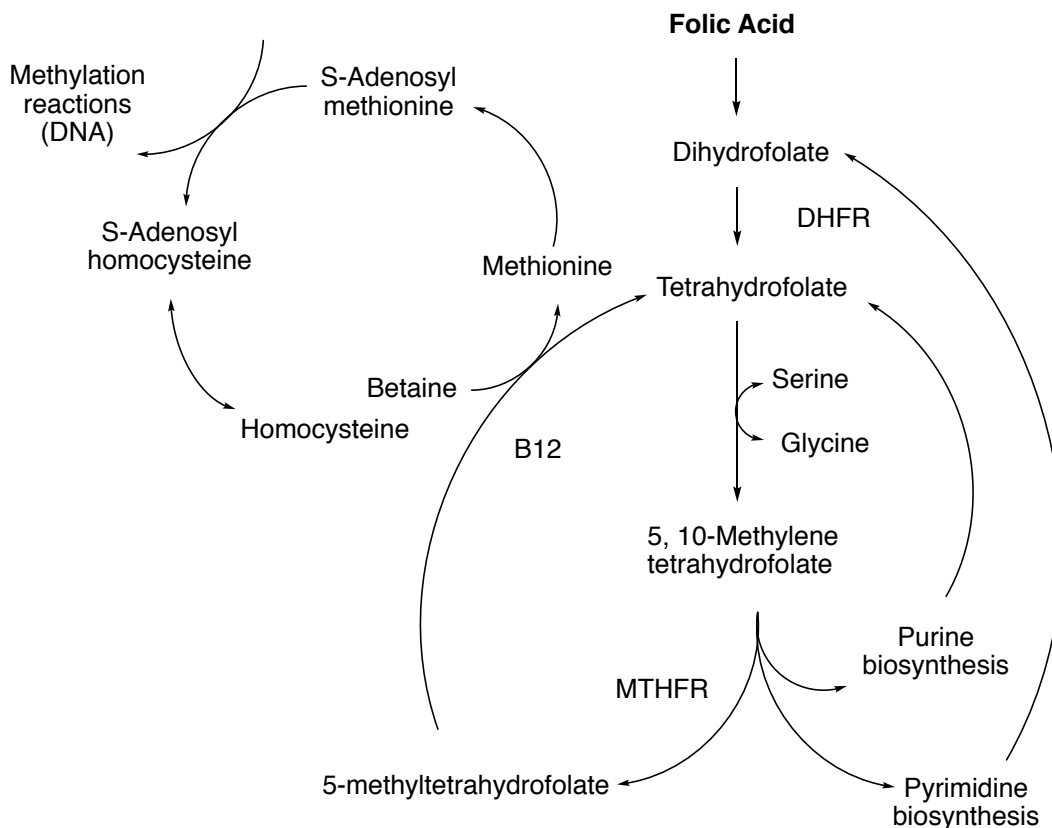
Another drug delivery route being explored within the Williams group is a pathway to direct Largazole derivatives to tumor cells selectively via folic acid conjugation. Folate is actively transported into cells via folate receptors, which are dramatically overexpressed on cancer cells, creating a site specific pathway for the Largazole-folic acid conjugate to follow to the cell surface.¹⁴⁰ There are two main sites on Largazole, as well as its derivatives, where folic acid conjugation can be explored: C12 and the terminal thiol. The first route to be explored conjugates Largazole at C12 (Figure 8). We have developed routes to the compounds using a linker for cleavage of the Largazole-methotrexate conjugate once inside the cell, as well as direct Largazole-folic acid, compounds **3.89** and **3.93**, respectively. Successful synthesis of C12 has been accomplished. However, further exploration of the thioester derivative with increased macrocycle for exploration still needs development.

Therapeutic Utility

Folic acid can be linked to molecules of therapeutic interest for more efficient cancer cell targeting, in some cases referred to as a 'Trojan horse' delivery system. Pre-clinical studies have shown this route to be effective.¹⁴⁹ Compounds of therapeutic interest can be linked either cleavable or non-cleavable routes, an ester or amide respectively. Both routes will be explored in the synthesis of Largazole bioconjugates.

A prior chemotherapeutic agent, desacetylvinblastine monohydrazone, has been linked to folic acid via a hydrophilic peptide linker bound to folic acid.¹⁵⁰ In this route, the conjugation is successfully accessed through a disulfide linkage. The Leamon group has synthesized both the

disulfide linkage and acylhydrazone, EC145 and EC140, respectively. Increased activity of the chemotherapeutic agent was seen in the case of EC145 with the disulfide linker.¹⁴⁰ With that in mind, our laboratory began investigation of different routes for folic acid linkage around the parent molecule, Largazole.



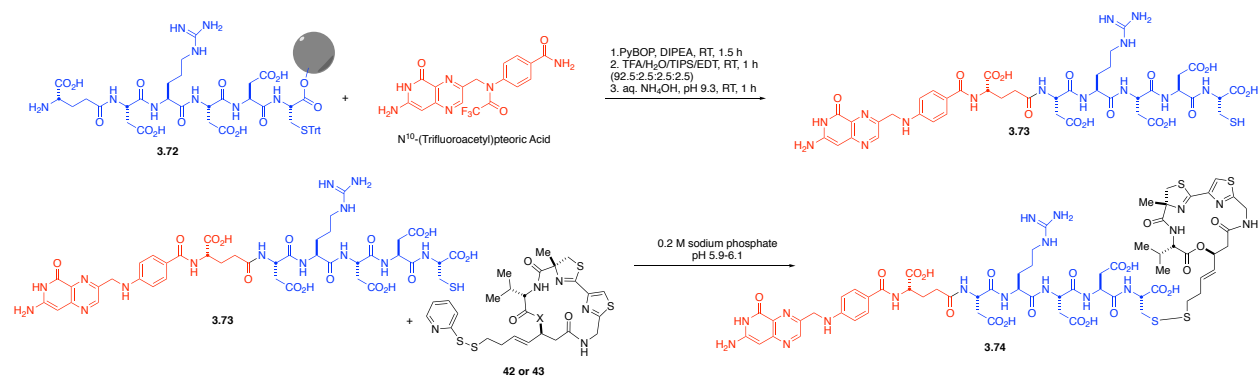
Scheme 35. Folic acid pathway and biologic importance for DNA methylation.

One drug that has been used to interact and inhibit the FR pathway in place of folic acid is methotrexate (MX). MX has been FDA approved for use as an antitumor drug and antirheumatic in the class of antimetabolites. The structure of methotrexate, Figure 11, is structurally similar to folic acid leading to its ability to inhibit the α -FR.

carboxylic acid exhibits for activity. A simple protection of the α -carboxylic acid could not be selectively performed leading to development of more complex pathways in the development of the folic acid and Largazole conjugate.

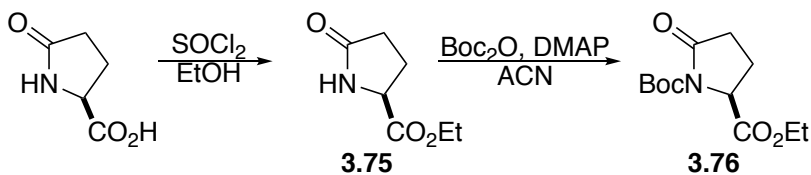
Additional routes to be explored include utilizing a disulfide folate-linked peptide EC119 at the free thiol unit (Scheme 37, compound **3.72**), or direct folic acid conjugation via formation of the model thioester (compound **2.78**).^{150, 151} The activated pyridyl disulfide derivatives **26 – 30** (Figure 2), have been successfully synthesized in the Williams laboratory and can be used for disulfide conjugation. A direct cross coupling would provide target compound **3.74** in one step.

Solid phase peptide synthesis has been explored for linker development in many drug conjugates. One advantage of this synthetic route is the linearity and prior art behind the development of the compound. However, a major disadvantage presents itself in the iterative deprotection steps and overall length of the linker. If possible, a direct conjugation of Largazole, or its peptide isostere, to either folic acid or methotrexate would be a more desirable pathway.¹⁵¹



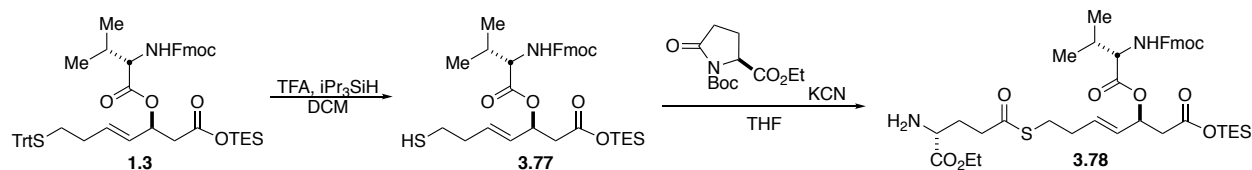
Scheme 37. Route to synthetic development of a peptide conjugated Largazole - folic acid derivative.

An overview of the predicted final conjugation can be seen in Scheme 37. This folic acid derivative could also be utilized for additional amino acid couplings to different linkers and functionalities. Ultimately, a disulfide linkage would be utilized to synthesize compound **3.74**. However, this route was not utilized due to an increased focus on a direct folic acid to Largazole conjugation.



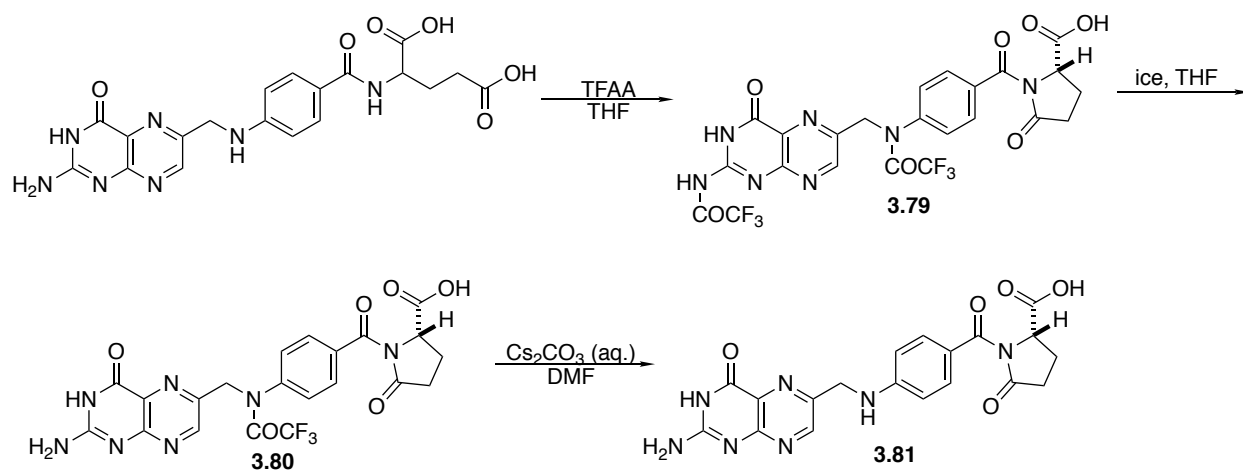
Scheme 38. Synthesis of lactam X.

In order to model this predicted pathway, lactone **3.76** was synthesized. L-Pyrroglutamic acid was first esterified using SOCl_2 and ethanol.¹⁵² Lactam **3.75** was further protected using Boc_2O and DMAP in ACN to provide compound **3.76**. Depsipeptide base **1.3** was chosen as a proper model for lactam opening due to the strong similarity with the parent Largazole. Tirtyl thiol **1.3** was deprotected with TFA and $i\text{Pr}_3\text{SiH}$. The free thiol was further reacted with lactam **3.76** and KCN in THF.



Scheme 39. Synthesis of base conjugated lactam X, as a model study for folic acid-Largazole thiol conjugation.

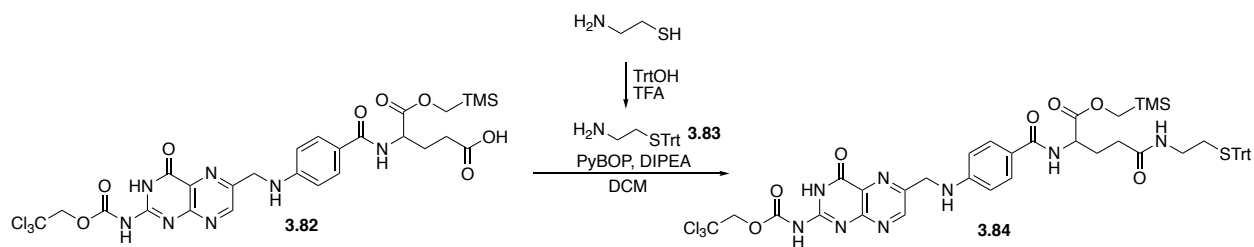
With this model study in mind, a route to form the intramolecular lactam of folic acid was investigated.¹⁵³ Trifluoroacetic anhydride was used to protect the internal amide. Under these conditions both the internal amide and pyridinone nitrogen were protected. This reaction also formed the anhydride of the γ -carboxylic acid inducing an intramolecular cyclization. Stirring the compound in THF with ice deprotected the external amine to produce compound **3.80**. Trifluoroacetate masking group was revealed with aqueous Cs_2CO_3 in DMF to yield the desired folic acid derivative, lactam **3.81**.



Scheme 40. Synthesis of folic acid derivative X.

Conjugation to parent Largazole could be assumed to arise from lactam **3.81** under similar conditions to Scheme 39. With both fragments in hand, the addition of **Largazole** and **3.81** did not afford the desired product. This pathway albeit promising on paper did not lead to the production of a Largazole-folic acid conjugate.

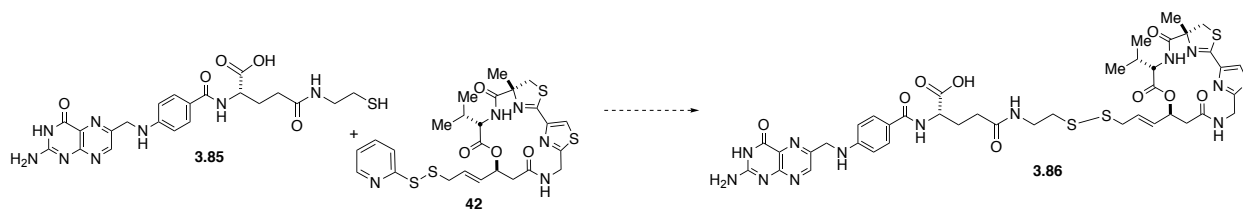
In an effort to bypass the thioesterification, a route to disulfide formation was next investigated. Cysteamine had both a nitrogen that could undergo amino acid coupling and a thiol that could be used for disulfide formation. Selective trityl protection of the sulfur resulted in compound **3.83**. The amine could then be coupled with diprotected folic acid **3.82**. EDC coupling with Et_3N and DMAP in DCM produced compound **3.84**.



Scheme 41. Synthetic route to coupled cysteamine and folic acid lactam for further disulfide conjugation.

During this time a synthetic route to folic acid conjugation at the new chemical space was additionally being developed within the Williams laboratory and yielded success. It was at this

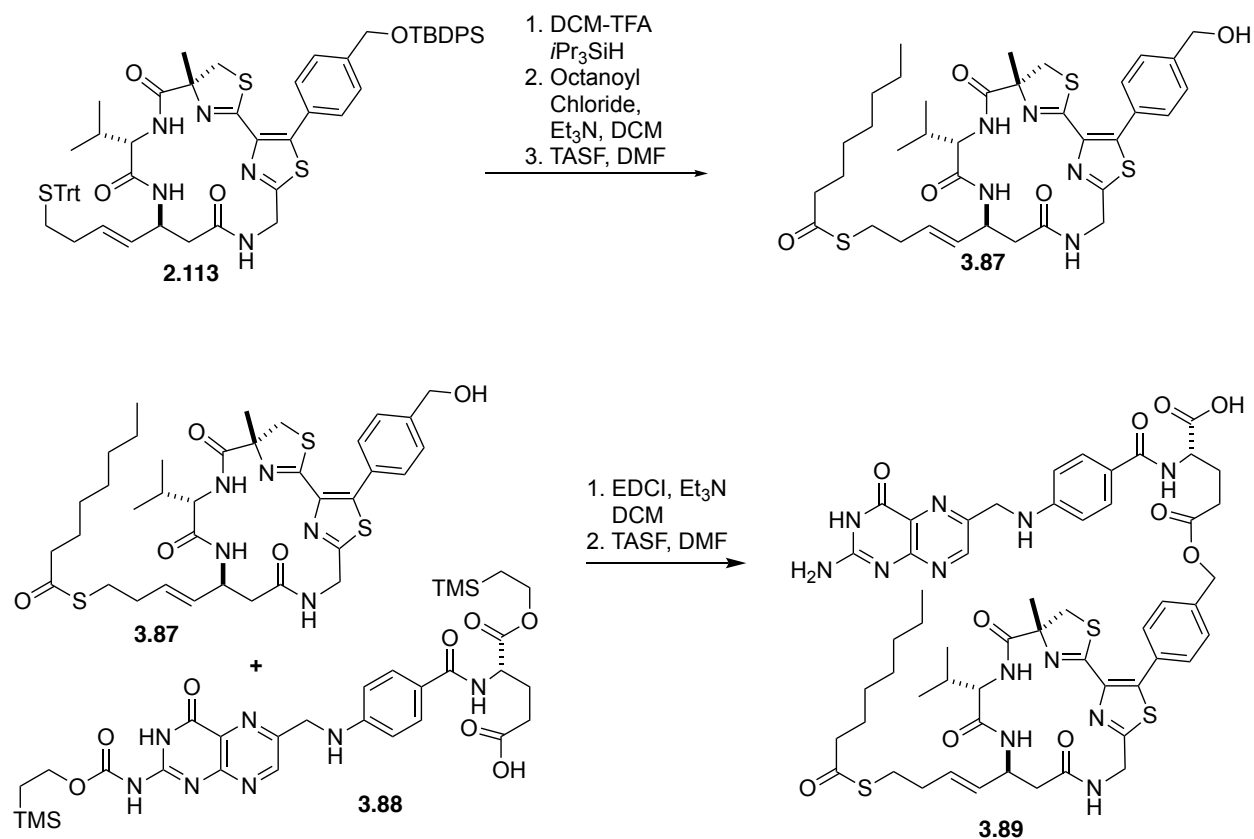
point our efforts were utilized towards the alternative route. However, global deprotection and reaction of the free thiol and a disulfide conjugate of Largazole or its derivative could yield a successful route to a disulfide linked Largazole – folic acid derivative (Scheme 42).



Scheme 42. Route to disulfide conjugation of folic acid and Largazole, or the variety of derivatives, thiol.

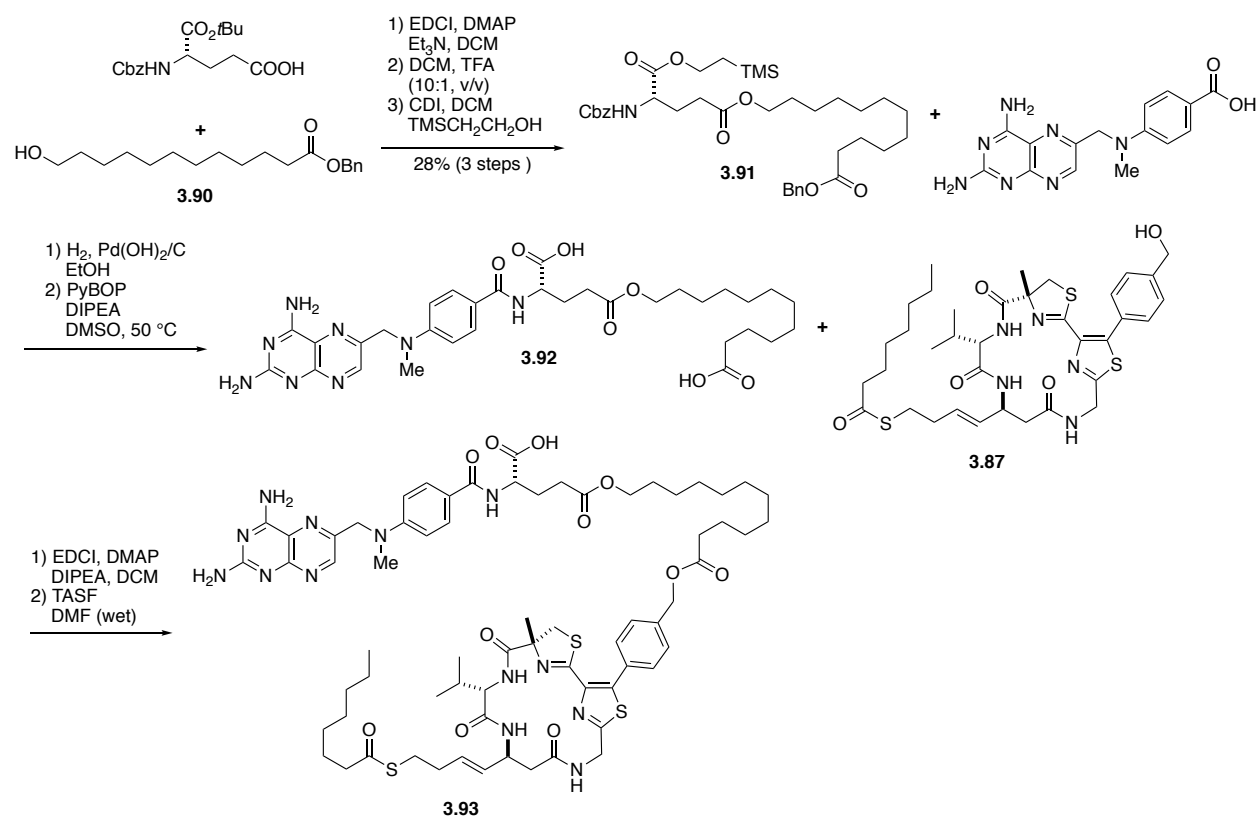
Synthetic Pathway Accomplished

The successfully developed route to Largazole, as well as its peptide isostere, derivatives with folic acid conjugation can be seen in Scheme 43. This compound can be ultimately linked to **3.87** via a Steglich esterification and global deprotection, EDCI and TASF respectively. The new chemical space derivatives were accessed via the route for synthesis with a hydroxyl methyl handle.



Scheme 43. Direct conjugation of folic acid and Largazole via a labile ester linkage at the new chemical space Largazole derivative, X.

To date the amino handle control derivatives have not been accessed but are being developed. The key difference in conjugation is the amino acid coupling utilized. PyBOP coupling conditions will be explored for the final amide bond formation between the free amine of the Largazole derivative and carboxylic acid of protected folic acid.



Scheme 44. Synthetic route to methotrexate-Largazole derivative via a carbon linker at the ester site of the new chemical space.

Utilizing pterotic acid as a starting precursor for folic acid conjugation shed light on the route to be developed for methotrexate conjugation. In a similar fashion, the benzoic acid to be coupled is methotrexate without the amide, as well as absent of the β/γ carboxylic acids. However, unlike folic acid, a direct conjugation of methotrexate to the hydroxyl methyl handle was not feasible due to solubility issues of methotrexate. Glutamic acid, alpha t-butyl Cbz protected amine, derivative was first coupled to free alcohol **3.90** via a Steglich esterification. A protecting group swap from t-butyl ester to TES provided compound **3.91** in 23% yield over three steps. Deprotection of the Cbz group, which also revealed the benzyl protected carboxylic acid for later stage conjugation, followed by PyBOP coupling provided compound **3.92**. Compound **3.92**, protected methotrexate with a saturated carbon linker, was isolated for conjugation to the peptide

isostere of Largazole. EDC coupling and TES deprotection with TASF provided compound X, the Largazole peptide isostere linked methotrexate compound for biological testing.

It is important to note that in both cases, compound **3.89** and **3.93**, the Largazole peptide isostere was utilized. In addition, the octanoyl tail was installed early stage. Both thiols can be derived via sustained thiol protection with trityl throughout the synthetic route with a final deprotection step. Additionally, a late stage thiol deprotection could provide a heteroatom, thiol, for conjugation to develop the thioester derivatives of these biological conjugates.

Biological Testing

Both the folic acid and methotrexate linked compounds were tested for activity against cancerous cell lines. Preliminary data showed submicromolar IC₅₀ values versus multiple cell lines. Further evaluation is needed and the data will be reported in due course.

3.3 Wnt Inhibitor: 3289-5066

The Wnt pathway has been extensively explored for the development and proliferation of cancer due to its extensive presence in developmental cell lines. There are three Wnt pathways that have been investigated: the canonical pathway, planar cell polarity pathway (non-canonical), and the Ca²⁺ pathway. The canonical pathway is β -catenin dependent whereas the non-canonical is β -catenin independent. When these pathways are mutated it may lead to a variety of diseases.¹⁵⁴

Therapeutic Utility

The Wnt family, 19 known members to date, has been extensively studied for cancer therapeutic potential. Wnt, name derived from *Drosophila* Wingless and Mouse int-1, contains

signaling sequences of approximately 350-400 amino acids. Wnt glycoproteins take part in a variety of developmental pathways through binding with the N-terminal of frizzled which in turn is bound and activates the Dishevelled (Dsh) protein. Presence of β -catenin is typically limited due to rapid turnover and utilization in encoding genes and developing complex tissues at adherens junctions. β -catenin accumulation in the cytoplasm can ultimately enter the nucleus.¹⁵⁴ Over expression of β -catenin has been linked to a variety of cancers and additional diseases. Therefore, hyperactivation via the Wnt signaling pathway is the start of this pathways domino effect. When the Wnt pathway is unactivated, β -catenin undergoes a series of transformations that result in its destruction, Scheme 45.¹⁵⁵

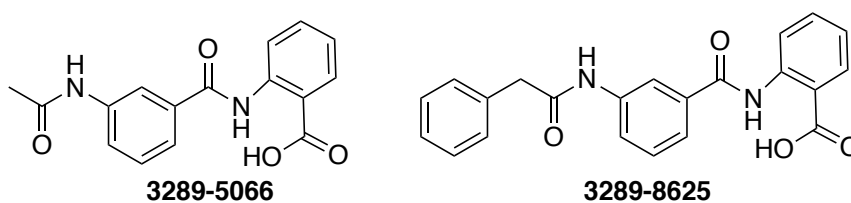
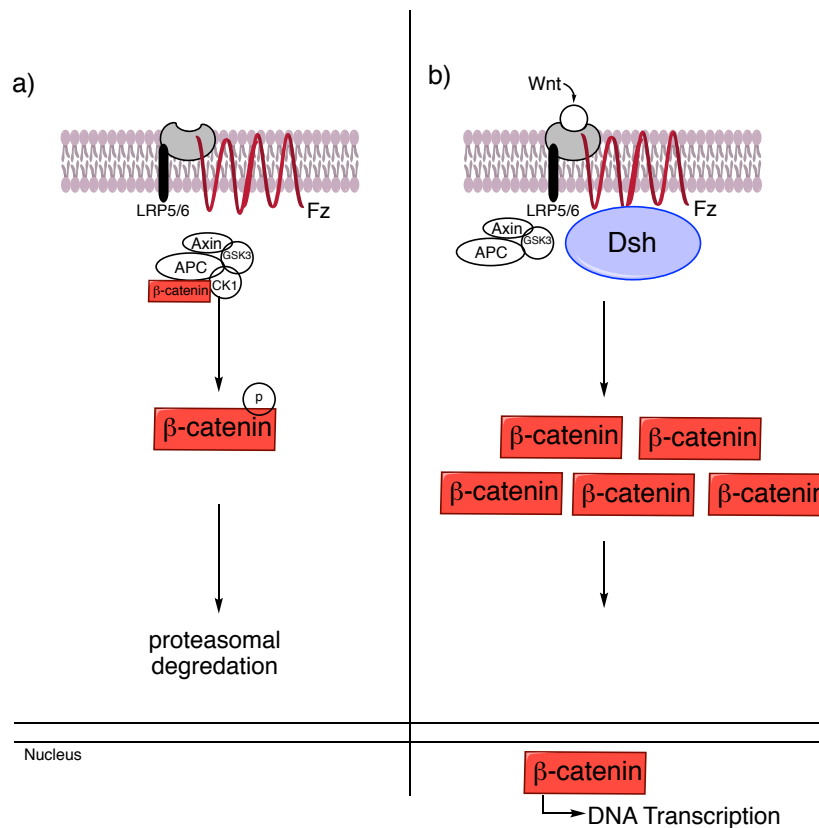


Figure 13. Compounds 3289-8625 and 3289-5066.

There are three Dsh domains which can be targeted to compete with the overexpression of Wnt signaling: Dix, PDZ, and DEP. One way to target the aforementioned complex protein interactions within the Wnt pathway is through targeting of the PDZ domain.¹⁵⁶ Many cancers have been targeted utilizing this pathway, including but not limited to prostate, colon, pancreatic, and breast cancers. Zheng and coworkers showed that compounds 3289-8625 and 3289-5066, seen in Figure 13, interact with the PDZ domain of Dsh at low micromolar affinity.¹⁴²



Scheme 45. Wnt therapeutic utility: (a) Wnt inhibition leads to a decrease in b-catenin development and proteasomal degradation, (b) Wnt activation of Fz leads to recruitment of Dsh leading to b-catenin upregulation and transport to the nucleus to aid in DNA transcription.

3289-8625 and -5066 were explored through computation analysis of the PDZ complex interactions.¹⁴² They were modeled in comparison to the Dpr peptide interactions with the PDZ complex. Ultimately, the focus of the Zheng labs study was on the β -B sheet and α B helix of PDZ and hydrogen interactions with 3289-8625. 3289-8625 showed comparable binding affinity to PDZ as exhibited with the Dpr protein due to the strong mimicking properties of the benzene moieties of -8625 to the Val or Met, pending on benzene ring, of Dpr. The compound exhibited Wnt3a inhibitory activity both *in vitro* and *in vivo*. For the purpose of our study Wnt inhibitor 3289-5066 will be further explored.

Synthetic Pathway

As stated in the above chapter regarding linkage to biotin, folic acid, and methotrexate – the Wnt inhibitor 3289-5066 (WntI), seen in Figure 13, can also be conjugated at the new chemical space position of the thiazole at position 5. WntI can be linked with via ester or amide to the peptide isostere, compounds **68-WntI** and **69-WntI** (Figure 14). Due to the robust nature of the amide linkage this compound will be more stable, yet less labile to reveal the dual therapeutic.

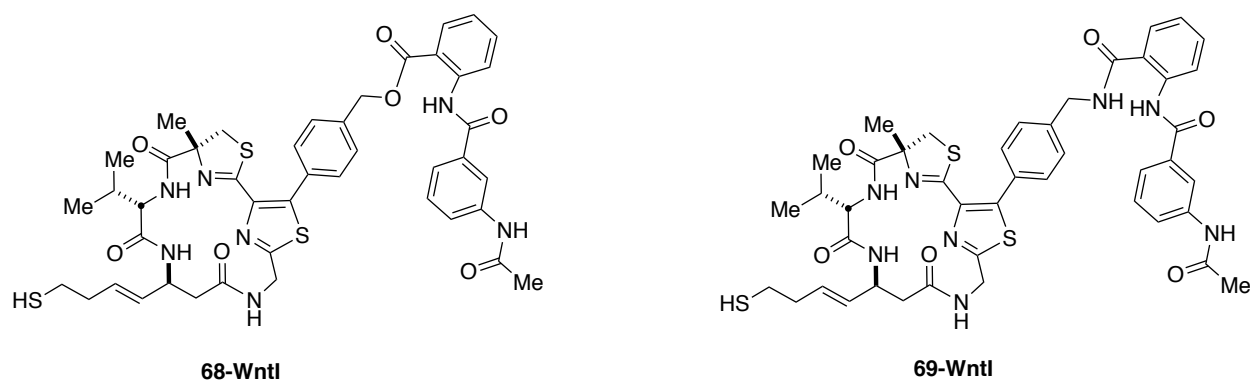


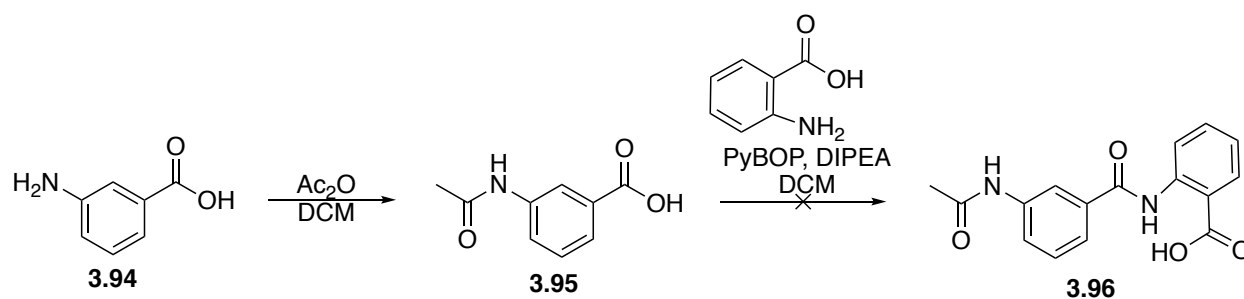
Figure 14. Wnt inhibitor targets at the new chemical space of Largazole peptide isostere.

Additionally, the free thiol of parent Largazole (or a comparable derivative from our library of 67+ compounds) and the carboxylic acid moiety of 3289-5066 can undergo reactivity to form either a thioester or disulfide bridge. This late stage conjugation would allow the entire library of Largazole derivatives to be tested as dual therapeutics for Wnt and HDAC targeting.

Wnt inhibitor synthesis of a variety of structurally similar compounds has previously been studied by Elofsson et al.¹⁵⁷ While the generalized synthesis was published, this specific compounds full procedural and data was not included. Due to this, a variety of synthetic pathways were explored for total synthesis of the compounds.

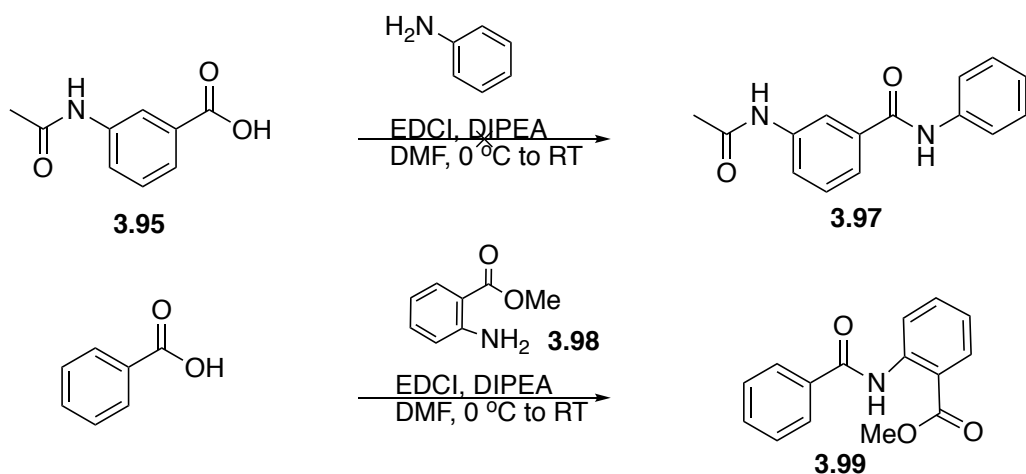
In the aim of accessing a streamlined synthesis of 3289-5066, we first explored eliminating the protection and deprotection steps, Scheme 46. 3-amino benzoic acid was reacted with acetic

anhydride to yield amide **3.95** in 75% yield. The meta substituted amide would further be reacted with anthranilic acid in an attempt to obtain the desired Wnt inhibitor in a two-step process.



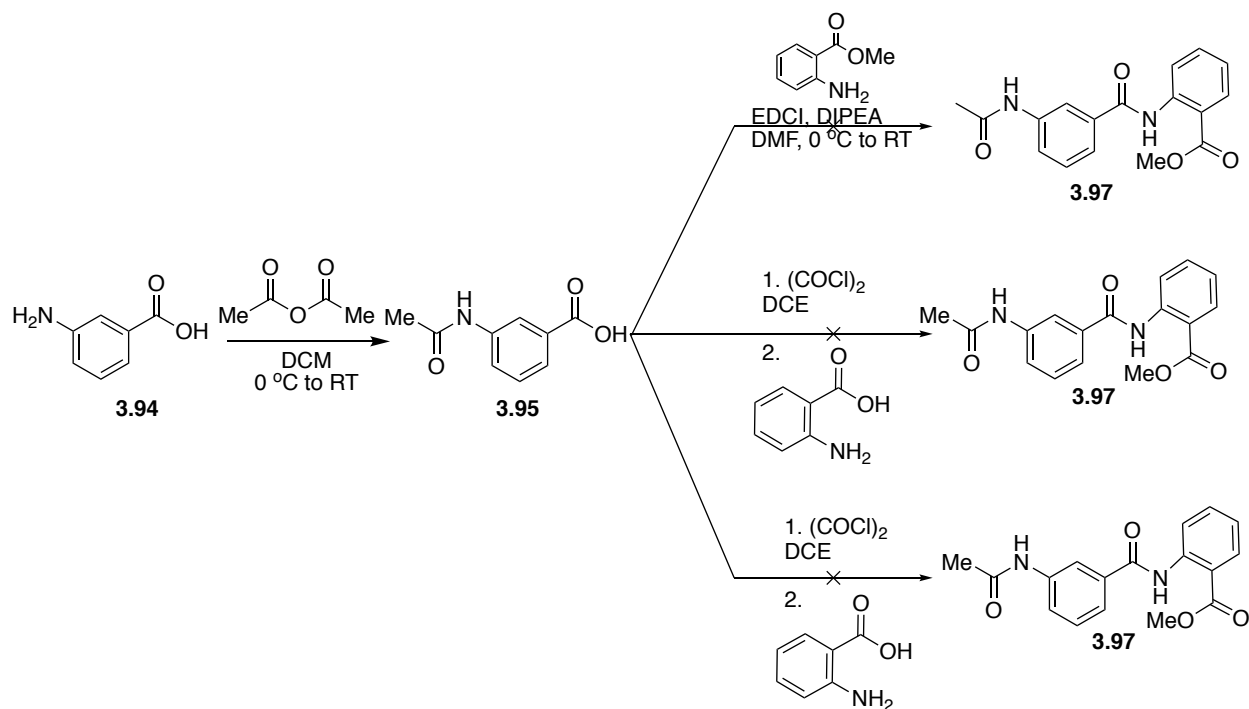
Scheme 46. Attempted coupling of carboxylic acid X and anthranilic acid to yield Wnt-OMe.

Many conditions were explored for the direct coupling of the free amine of anthranilic acid and meta amide substituted benzoic acid. First, direct PyBOP and EDCI coupling were explored. These conditions, seen in Scheme 48, resulted in multiple products and desired compound **3.96** was not produced. It can be surmised that the carboxylic acid of anthranilic acid could have been hindering direct amide coupling due to competing acylation and homodimerization.¹⁵⁸ In order to attempt at combatting this issue, the methyl ester instead of carboxylic acid was used from this point on, compound **3.98**. Following these same procedures with the methyl ester derivative, either undetectable amounts of the desired compound or no reaction took place.



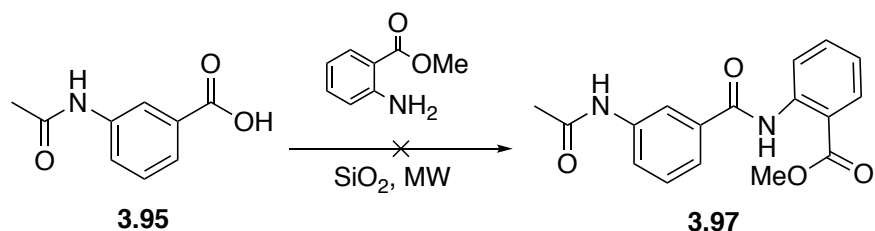
Scheme 47. Model studies to probe the reactivity of meta-substituted benzoic acids.

It was theorized that the meta amide substitution could be an issue in hindering a direct coupling to form the desired amide. Model studies performed included coupling of aniline to the meta substituted 3-acetyl amide benzoic acid with PyBOP. This was not seen to produce the desired product. In order to confirm that compound **3.95** was the issue, methyl ester anthranilic acid was coupled to benzoic acid, Scheme 47. This reaction proved successful and additional exploration into reactivity of the meta substituted 3-amide benzoic acid was explored.



Scheme 48. Synthetic coupling attempts towards compound X.

One possible route to avoid amino acid coupling techniques is to first form the acid chloride, followed by immediate treatment with an amine nucleophile. Compound **3.95** was treated with oxalyl chloride. After isolation and immediate treatment with the methyl ester of anthranilic acid the reaction was stirred for an additional four hours. Unexpectedly, the desired product was not observed. One possible explanation for this could be due to acylation of the meta amide with the acyl chloride formed *in situ*. This reaction would happen instantaneously and deplete the electrophilic site of the acyl chloride for reaction with the amine.



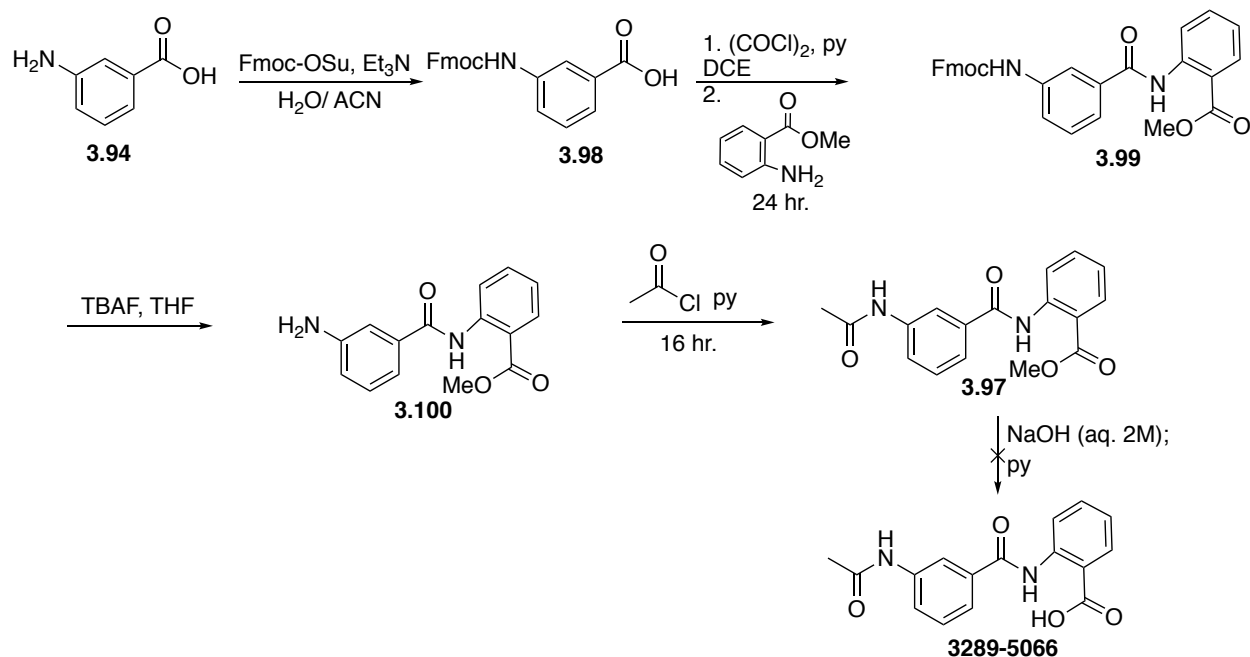
Scheme 49. Microwave, green chemistry synthetic attempt towards amide formation, X.

Microwave synthesis utilizing the methodology of the Gamba-Sanchez group for amide formation was explored.¹⁵⁹ Following green chemistry conditions for amide bond formation, the free carboxylic acid **3.95** and anthranilic methylester were absorbed to a SiO₂ support. The mixture was subjected to microwave conditions seen in Table 7. In the presence of the solid support, the solid support with solvent, and the solid support with both solvent and acid catalyst no product formation was observed. It was at this point that attempts to avoid initial protection steps of the 3-aminobenzoic acid were abandoned for the lengthier route established by Elofsson and coworkers.

Table 7. Microwave reaction conditions to probe amide formation.

Conditions	Time	Temperature	Yield
SiO ₂	80 min (20 x 4)	130	NR
SiO ₂ , solvent	60 min	130	NR
SiO ₂ , acid	60 min	130	NR

3- amino benzoic acid was protected with Fmoc-OSu on a 10-gram scale.¹⁶⁰ Fmoc protected 3-amino benzoic acid was subjected to acid chloride formation with oxalyl chloride and pyridine in DCE. After acid chloride formation was confirmed through absence of starting material on TLC, methyl ester anthranilic acid was added to produce compound **3.99**. TBAF deprotection provided free amine **3.100**. Reaction with acetyl chloride and pyridine in THF provided the methyl ester precursor to 3289-5066. Reported hydrolysis conditions NaOH reported by Elofsson and coworkers resulted in hydrolysis of not only the methyl ester but also the acyl amide producing an undesired product.



Scheme 50. Successful synthesis of Wnt-OMe, **3.97**.

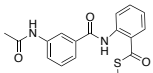
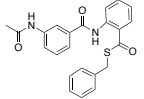
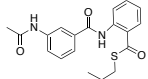
A myriad of hydrolysis conditions were explored to mildly hydrolyze the ester of compound **3.97** while maintaining the two amide bonds within the desired molecule, conditions in Table 8. TMSCl and NaI were added to a solution of methyl ester X in acetonitrile and brought to reflux. This route forms TMSI in solution via halogen exchange to promote a mild hydrolysis of esters. The reaction was tested at both 35 hours and five days with no observed isolable product. Me_3SnOH was tested next and monitored from 1-16 hours. In both cases, the desired product was observed in the crude NMR. Unfortunately, Purification techniques using preparatory TLC provided inseparable material from tin byproducts.

Table 8. Hydrolysis conditions explored for the total synthesis of 3289-5066.

Conditions	Time	Heat	Solvent	Result
TMSCl, NaI	5 days	80	Acetonitrile	SM recovered
TMSCl, NaI	~35 hr	80	Acetonitrile	SM recovered
Me ₃ SnOH	1-5 hr	80	DCM	Not isolable
Me ₃ SnOH	16 hr	80	DCE	Not isolable
NaOH, CaCl ₂	16 hr	RT	iPrOH:H ₂ O	Isolated
NaOH, CaCl ₂	4 hr	RT	iPrOH:H ₂ O	Isolated

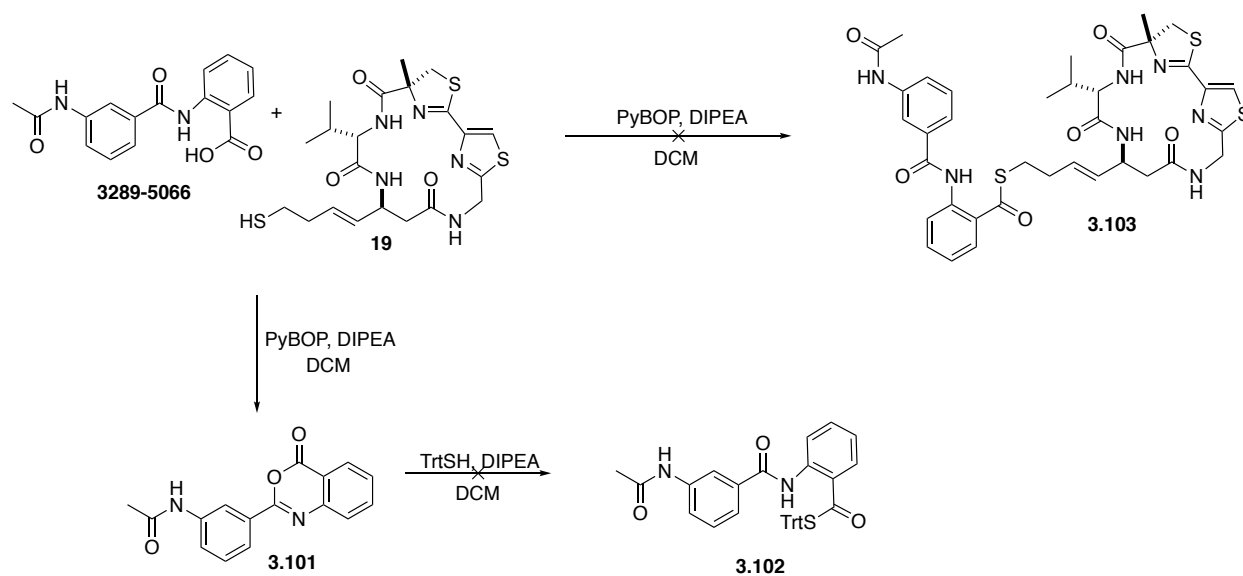
At this point, further investigation of the literature led to a milder NaOH hydrolysis developed by the Trauner group.¹⁶¹ These mild hydrolysis conditions in the presence of amide bonds using NaOH and 0.8 M CaCl₂ in *i*PrOH:H₂O (ratio) were next explored. This route proved successful and isolable on both small and large scale with a maximum yield of 41%. Further development of this method should be explored to increase the yield of the transformation. Successful synthesis of 3289-5066 was accessed in six steps.

Table 9. Thiol coupling to carboxylic acid conditions and coupling agents.

HSR	Coupling Agent	Desired Product	Result
	DCC, DMAP		Not Isolable
	EDCI-HCl, DIPEA		No product
	PyBOP, DIPEA		Product isolated

Many routes were explored to model the coupling conditions of the peptide isostere thiol to the free carboxylic acid of 3289-5066, Table 9. DCC and DMAP with ethanethiol was first explored. The urea byproduct was unable to be removed following work-up and preparatory TLC chromatography resulting in an unfeasible route. Next, Steglich-type thioesterification between benzyl thiol and 3289-5066 was explored with EDCI and DIPEA. No product was observed utilizing these conditions. Finally, a successful route utilizing PyBOP coupling between pentane thiol and the Wnt inhibitor provided desired thioester.

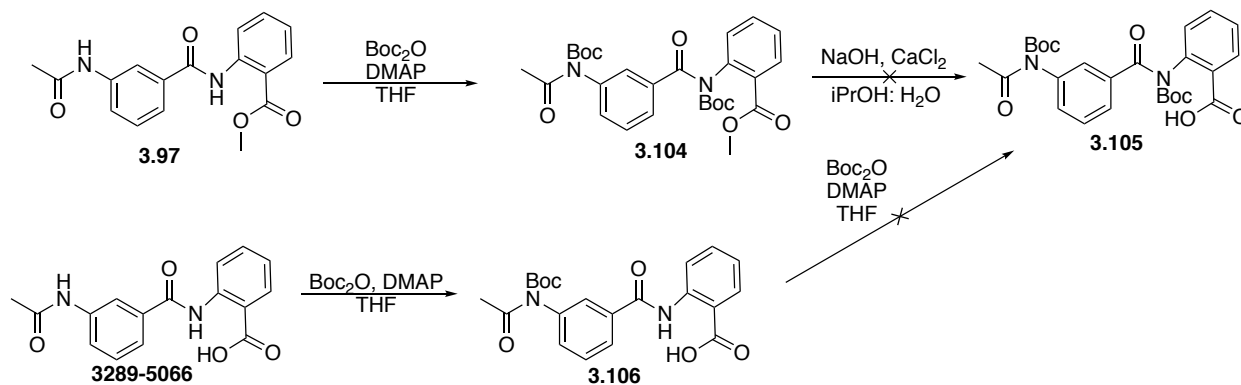
With this route in hand, protected Largazole peptide isostere was deprotected to the free thiol with TFA and $i\text{Pr}_3\text{SiH}$ in DCM. The free thiol was subjected to the developed PyBOP coupling conditions. However, this route proved unsuccessful with the peptide thiol. Intramolecular cyclization of 3289-5066 to compound **3.101** instead was produced, Scheme 51. The free thiol did not possess enough nucleophilicity to open the activated ester to synthesize **3.103**. In order to confirm the formation of the intramolecular product, **3.101**, the Wnt inhibitor was reacted with PyBOP and DIPEA in the absence of thiol. The intramolecular cyclization of 3289-5066 was further supported after the product was isolated from the reaction in absence of thiol.



Scheme 51. Largazole peptide isostere and 3289-5066 attempted PyBOP coupling and route to provide cyclization product.

Confirmation of this product provided a road block to coupling Largazole peptide isostere to the Wnt inhibitor, 3289-5066. In attempts to open the newly formed, reactive ring system, the cyclization product was reacted with TrtSH. Thioester **3.102** was a target in hopes of forming a protected thioester for late stage disulfide conjugation with the free thiol of Largazole peptide isostere. However, starting material carboxylic acid was instead the product of this reaction after work up. One route explored to bypass the intramolecular cyclization would be to block the cyclization and dehydration pathway through protection of the involved internal amide.

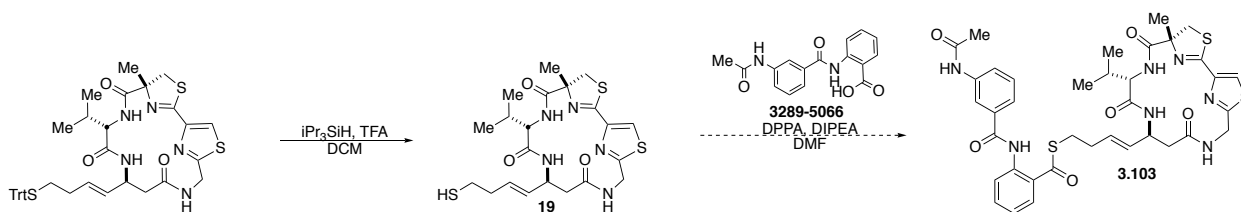
Due to the presence of two amides, 2.6 equivalent of Boc anhydride was used to protect the functionalities. The methyl ester, **3.97**, was first double Boc protected and then subjected to the developed hydrolysis conditions. While the Boc protected compound was isolable, the mild hydrolysis conditions resulted in no product formation. Next, the Boc protection was investigated on 3289-5066. After the addition of 2.6 equivalents of Boc₂O only one Boc protected amide was seen via NMR. The downfield shift of the acetyl methyl peak provided evidence that the external



Scheme 52. Amide protection routes to avoid undesired intramolecular cyclization products.

amide was the Boc protected functionality. The monoprotected Boc-3289-5066 was isolated and resubjected to the Boc protection conditions. The isolated product of this reaction was not the desired protected compound, **3.105**. At this point, protection conditions were abandoned for more robust thioesterification routes.

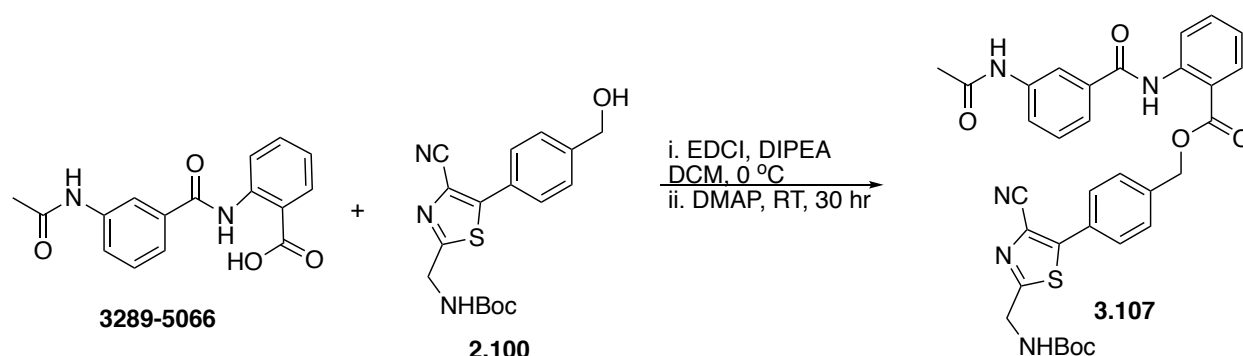
One drawback of many thioesterifications is that the thiol is utilized in excess. Due to the extensive route to synthesize the Largazole peptide isostere, it is often isolated in milligram quantities creating difficulty in testing across a variety of conditions. This was the main driving factor for developing a model system that would be sufficient to mimic the thiol nature of the parent compound. However, after failure of the PyBOP system on the parent compound succeeding successful model conditions it was clear a model system would not be feasible for these compounds.



Scheme 53. DPPA route towards thioesterification, Largazole peptide isostere and 3289-5066 conjugation.

In aim of developing an efficient route to the synthesis of thioester **3.103**, additional reactions were explored. Investigation of a Mitsunobu thioesterification conditions led to the

conclusion that multiple equivalents of precious thiol would be necessary for product formation. A route developed by Forsyth and coworkers on late stage material, provided a route utilizing DPPA and DIPEA for selective thioesterification between carboxylic acids and hindered thiols. This reaction was attempted and experimental results are pending.¹⁶²



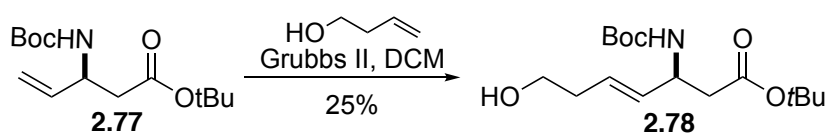
Scheme 54. Steglich esterification route towards coupling of the hydroxy methyl handle of thiazole, **X**, and **3289-5066**.

Synthesis of the hydroxyl and amine chemical handle are also being explored for Wnt inhibitor conjugation. In order to explore conditions for successful coupling, compound **2.100** was utilized to model hydroxyl methyl handle conjugation. Thiazole nitrile, **2.100**, with **WntI** underwent EDCI coupling successfully. With this route in hand, synthesis of the TBDPS protected Largazole peptide derivative was accessed for final conjugation. In regards to the amide bond formation, a PyBOP coupling method is predicted to be utilized to access the final product.

Late stage trityl deprotection of the macrocycle will provide a route to both thiol and octanoyl chloride derivatized conjugates. Further work will be explored to conjugate Wnt inhibitor **3289-5066** with additional Largazole derivatives. Extensively biological testing will be performed on this compounds to explore the utility of a dual Wnt and HDAC inhibitor towards relevant cancer cell lines.

PEPTIDE BASE ROUTE

The original synthesis of the peptide base was discussed in Chapter 2.1. The largest hindrance toward large-scale production via this route is the low yielding, 25%, cross metathesis step (Scheme 55). In an aim to improve this synthesis a variety of different pathways have been explored, including but not limited to: Mitsunobu, Julia-Kocienski olefination, asymmetric hydrogenation, utilization of Garners aldehyde, and cross coupling strategies. Detailed below are the explored routes towards an improved synthesis of the desired peptide base fragment. To date, none of the above attempts have yielded productive or successful routes for a myriad of reasons that will be discussed in detail below.



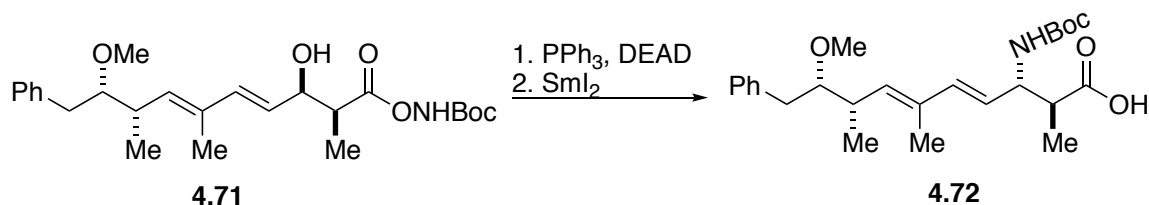
Scheme 55. Current Grubbs cross metathesis step towards the peptide isostere for method development.

The true complexity of this Largazole peptide isostere fragment comes from the conjugated stereocenter at C17. SAR studies have shown that inversion of that specific stereocenter in naturally isolated Largazole depsipeptide leads to full depletion of the molecules selective and potent activity across HDACS 1, 2, 3, and 6. Additionally, this olefin conjugated amine is susceptible to beta attack leading to elimination, undesired nucleophilic substitution, or epimerization of the stereocenter. The stereocenter and location of the nitrogen on the peptide base is important to maintain due to the reactivity of the molecule.

Mitsunobu

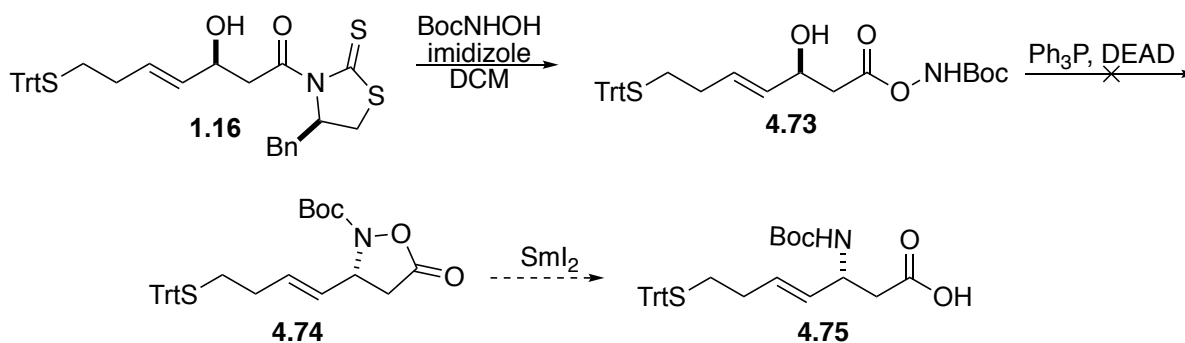
Rinehart and coworkers explored intramolecular Mitsunobu transformations with protected hydroxylamines for the synthesis of natural products containing unusual amino acid scaffolds.¹⁶³

The initial method can be seen in Scheme X. The marine derived natural products explored to originally utilize this methodology are nodularin, motuporin, and microcystins. Stereoselective installation of a carboxylic acid with an allylic beta amine has historically proven difficult due to nucleophilicity of the delta position, Scheme 56.



Scheme 56. Rinehart's method to Mitsunobu intramolecular cyclization.

The methodology was utilized to synthesize over six compounds with conjugated beta amines containing the (2*S*,3*S*,8*S*,9*S*)-3-amino-9-methoxy-2,6,8-trimethyl-10-phenyl-4,6-decadienoic acid. In the original synthesis Evans chiral auxiliary was displaced with tert-butyl-N-hydroxycarbamate utilizing NaH. The five membered intramolecular transition state was accessed under Mitsunobu conditions, DEAD and Ph₃P. Isoxazolidin-5-one, **4.74**, was cleaved with SmI₂ to provide final compound **4.75**. In order to test this hypothesis, the depsipeptide base was utilized, synthetic route seen in Scheme 57. For this model the Mitsunobu product would produce the undesired enantiomer of the peptide isostere base. However, the material was on hand and readily available for use to explore the feasibility of the predicted route.



Scheme 57. Application of the intramolecular Mitsunobu to Largazole building blocks.

We first desired to synthesis compound **4.73** to prove the reliability of the intramolecular cyclization and reduction with SmI_2 on the Largazole depsipeptide base. Amide **1.16** was reacted with hydroxycarbamate, HONHBoc, and NaH to produce compound **4.73**. The hydroxylamine provides the starting material which mimicked those explored by Rinehart and coworkers. The one pot reaction using DEAD and PPh_3 following the literature procedure was run at room temperature for 40 minutes. An aliquot of the reaction was removed and evaporated to provide a crude NMR sample to monitor the formation of the five-membered ring. This transition state, while able to be immediately subjected to SmI_2 in the same pot, is also able to be isolated for experimental analysis. Due to no NMR presence of the desired intramolecular cyclization the SmI_2 was not introduced into the reaction mixture for reduction.

In hopes of combatting the absence of reactivity of compound **4.73**, different conditions, times, and concentrations were tested. After an array of alterations were explored no reaction was observed with the predicted intramolecular outcome. This may be due in part to the conjugated alkene and nucleophilicity of the beta carbon.

If this route were to be further developed and optimized for product formation, the enantiomer of compound **4.73**, seen in Scheme 57, could be synthesized utilizing the R-phenylalanine in the synthesis of Crimmins chiral auxiliary. Then, with the enantiomer of the Crimmins chiral auxiliary used for Largazole depsipeptide, the enantiomer of the hydroxyl base fragment could be accessed. Following the developed pathway for intramolecular Mitsunobu cyclization and reduction, the desired stereospecific product could be accessed. However, further exploration of Mitsunobu conditions must be explored to combat the lack of reactivity seen.

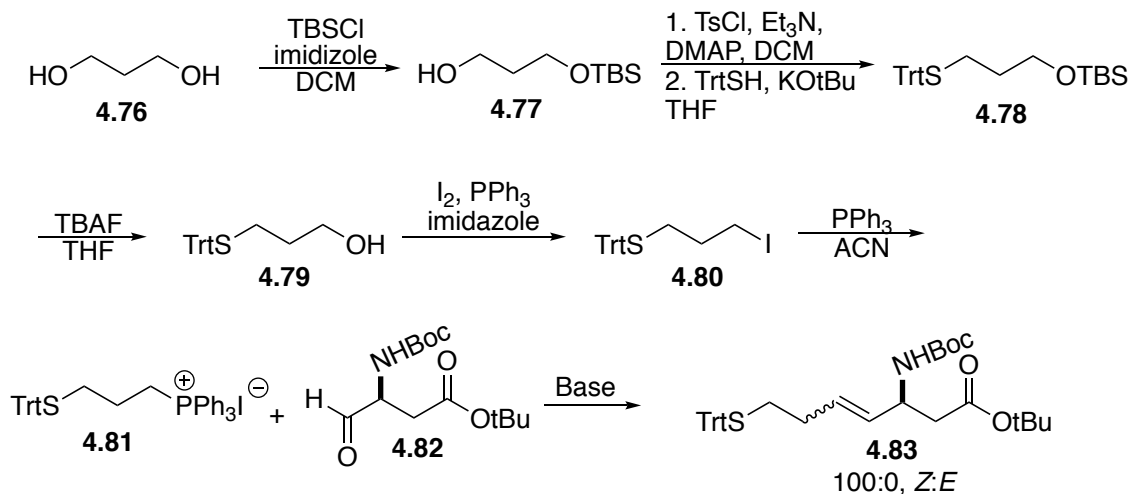
One main difference in the methodology tested natural products versus the desired peptide base is the double conjugation of the displaced alcohol. This causes a decrease in the electrophilic

nature of delta position. In the Largazole starting material, that double conjugation is not present creating a more accessible and undesired site of cyclization. Additionally, the trityl protected thiols steric bulk and interference with reactivity may impact the intramolecular cyclization and reactivity. Finally, intermolecular Mitsunobu may be outcompeting the intramolecular cyclization resulting in undesired dimerization products.

Additional Olefination Routes

There are many olefinations that can and have been utilized to install trans alkenes in synthetic scaffolds. Many traditional routes that come to mind are the Horner-Wadsworth Emmons (HWE), Grubbs, Peterson, Tebbe, and in these explored cases, the Wittig and Julia-Kocienski olefinations. Few have the capability of providing synthetically sound routes to retain stereochemistry of both the alkene and C17 amine stereochemistry in compound **2.71**.

Recently, a Wittig olefination route was explored by Dr. Anil Shelke following the pathway in Scheme 58. The desired Wittig salt was accessed in six steps from commercially available 1, 3 propane diol. Monoprotection with one equivalent of TBSCl and imidazole provided compound **4.77**. Tosylation and S_N2 displacement with TrtSH accessed the protected thiol **4.78**. TBS



Scheme 58. Wittig route development (Dr. Anil Shelke).

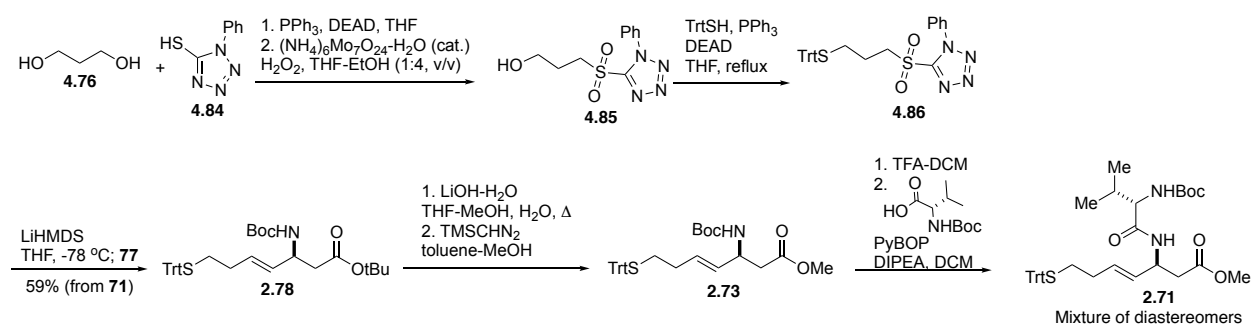
deprotection followed by iodination and reaction with PPh_3 in ACN yielded the desired Wittig salt. Synthesized Wittig salt was reacted with aldehyde **4.82**, a previous intermediate from the original peptide base route synthesis. Following analysis of the produced alkene, exclusively cis olefination of **4.83** was produced. As explored in past total syntheses of Largazole, the *Z* alkene confirmation depletes all HDAC activity.¹²⁰ Therefore, either a route to alkene isomerization or an exploration of modified Wittig conditions to provide the *E* alkene should be further explored.

An additional route explored was the Julia-Kocienski olefination. The Julia-Kocienski olefination utilizes a sulfone and aldehyde to undergo alkene formation. One strong proponent for the use of this synthetic route in development of the peptide base is that the Julia olefination can be modified to provide the *E* alkene in high selectivity based on the conditions used.

A classic Julia olefination is performed through the reaction of a sulfone and aldehyde to provide a compound which can be further eliminated to provide the desired alkenes. The sulfone is first treated with a base, such as *n*-BuLi at $-78\text{ }^\circ\text{C}$. The aldehyde is added followed by acetic anhydride. Finally, a metal that can act as a single electron donor is introduced to displace the sulfone and eliminate acetate. *E* selectivity is retained in the classic Julia olefination; however, the

modified Julia-Kocienski olefination has been developed to further increase selectivity and reactivity of the sulfone.

The modified Julia-Kocienski olefination utilizes activating groups on the sulfone, such as benzothiazole, benzotriazole, pyridine, or tetrazole.¹⁶⁴ The benzothiazole undergoes a Smiles rearrangement, to provides either an anti or syn intermediate which undergoes elimination to *E* or *Z* geometry, respectively. Through an open transition state, the *E* geometry can be selectively accessed. Large counterions and polar solvents aid in the transition of the sulfone and aldehyde through the open transition state.



Scheme 59. Attempted Julia-Kocienski route to Largazole peptide base development.

Recently, an improved synthetic route was explored by Dr. Le Zhao to establish a pathway that is both higher yielding and scalable (Scheme 59), utilizing the Julia-Kocienski Olefination. (*S*)-3-amino-7-mercaptohept-4-enoic acid derivative **2.73** was accessed. Sulphone **4.86** was accessed in 3 steps from tetrazole thiol **4.84** and 1,3-propanediol. Mitsunobu conditions, DEAD and PPh₃, displaced one of the alcohols for a thioether that could undergo oxidation with the molybdenum catalyst in THF-EtOH with H₂O₂, Scheme 59. The remaining free alcohol underwent an additional Mitsunobu to provide protected thiol **4.86**. Coupling of key fragments via a modified Julia-Kocienski olefination with LiHMDS in THF at -78 °C allowed for formation of

beta amino ester **2.78**. Saponification, followed by esterification, resulted in the desired peptide base intermediate **2.73**.

Preliminary studies and $^1\text{H-NMR}$ analysis of the peptide base showed promising results towards an improved synthesis of the peptide isostere. Upon further reaction with Fmoc-valine to produce the amino acid coupled base, **2.71**, a second stereocenter was installed in the molecule. This stereocenter revealed that the base, prior to valine coupling, was a mixture of enantiomers.

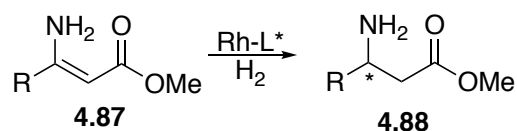
At this point the diastereomers could be separated for further conjugation in the path to Largazole peptide isostere, **19** and **20**. Macrocyclization was completed by the same route utilized for the parent depsipeptide compound on the chromatographically separable pure isomer. With this new finding, the Julia- Kocienski olefination route was proven to be lower yielding and less selective in comparison with the Grubbs metathesis route previously established within our laboratory for the peptide isostere synthesis. Additional metathesis reactions should be performed and developed to probe the true depth of this synthetic pathway.

Asymmetric Synthesis

Hydrogenations have been utilized for reduction of double bonds and various functionalities across a wide array of substrates in medicinal chemistry development. Hydrogenations are often performed with the use of H_2 and a catalyst support, such as Pd, Pt, Rh, Ni, etc. An alkene typically interacts with hydrogens that are interacting with the metal surface. The alkene then chelates to the surface and hydrogen can add across the double bond. Hydrogen is added in a syn, unselective manner to the alkene in the absence of catalyst. Utilization of a chiral catalysts to promote this addition can provide a stereoselective route for H_2 addition.

Asymmetric hydrogenation can introduce either one, or two, stereocenters in an efficient manner pending on the alkene being utilized. In 2001 Dr. Knowles and Noyori were awarded the Nobel Prize for asymmetric hydrogenation and its implementation in the field of asymmetric total synthesis.¹⁶⁵ The catalyst chelates to an electronegative atom and can selectively deliver H₂ to the desired site of hydrogenation. Hsiao and coworkers, with inspiration from a typical Noyori asymmetric hydrogenation, developed an efficient route towards the asymmetric hydrogenation of enamines.

A large scope of β-enamino esters and amides were synthesized from β-keto esters in one step. One of the first attempts seen in literature of this asymmetric hydrogenation of a conjugated enamine to synthesize and retain the stereocenter at C17 of the Largazole peptide base for large scale development. Hsiao and coworkers at Merck Pharmaceuticals developed a rhodium catalyst that was utilized across a range of enamines.¹⁶⁶

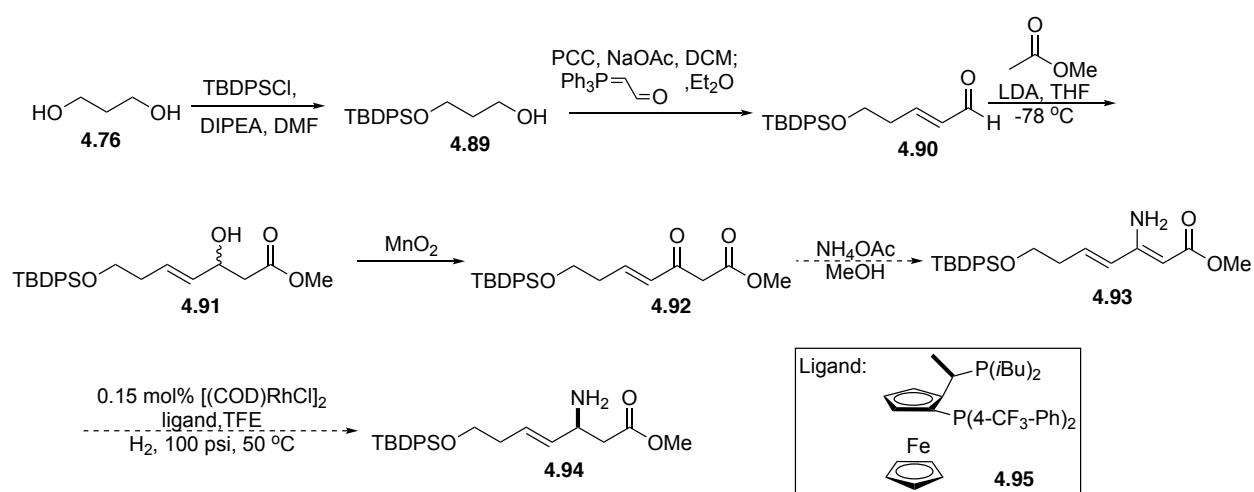


Scheme 60. Asymmetric hydrogenation route developed by Hsiao and coworkers.

Rh catalysis with a Josiphos style ligand in TFA provided an S configured stereocenter. The hydrogenation is predicted to go through a transition state of Rh chelated to both the ester oxygen and enamine nitrogen. After chelation, hydrogen is stereoselectively delivered to the back face of the molecule to produce an enantiopure compound in acceptable yield. The β-enamino esters are conjugated to aryl functionalities in the substrate scope. In the Largazole peptide base synthesis the β-enamino ester is conjugated to an alkene. This difference in reactivity may lead to lower yields and undesired side products. However, due to the predicted chelation transition state, the side reactions or further hydrolysis may be avoided for selectivity of the internal alkene.

The precursor to enamine formation is the conjugated beta keto ester. This can be accessed utilizing a similar route to that of the depsipeptide base. By intercepting intermediate the aldehyde the aldol reaction could now be performed in a non stereoselective manner with methyl acetate and LDA at -78 °C. The b-hydroxy methyl ester was stirred at room temperature with MnO₂ for three days to produce β-keto ester.

Attempts to access the b-amino ester via established protocol by Hsiao and coworkers did not yield compound **4.93** as predicted. Additional routes for successful synthesis are currently being explored. If compound **4.93** were to be accessed, the following steps in Scheme 61, this could be explored for successful synthesis of the desired peptide base in selective, large scale routes.



Scheme 61. Developed synthesis to probe the feasibility of asymmetric hydrogenation towards the development of the Largazole peptide isostere base.

B-amino ester would be subjected to Rh catalyst promoted, stereoselective hydrogenation with ligand **4.95** at 100 psi at 50 °C. The produced amine at C17 could be Boc protected to allow installation of the protected thiol tail. TBDPS deprotection with TASF, activation of the free alcohol with tosyl chloride, and final displacement with trityl thiol would provide desired peptide base intermediate. These synthetic transformations are highly reliable within our established routes

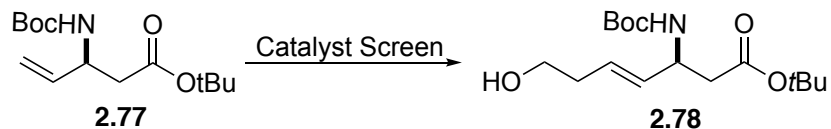
and would aid in the synthesis of the desired intermediate in reasonable yields. Further development and exploration of this route is needed for successful synthesis.

Additional Catalyst Metathesis

To date, over 5 derivatives of Grubbs 1st generation catalysts have been synthesized and used for the installation of alkenes for cross, ring closing, and ring opening metathesis. Within our laboratory we have explored using Grubbs 2nd generation and Hoveyda-Grubbs. Some studies have shown that the Grela catalyst increases yield for the cross metathesis.¹⁶⁷

Grubbs cross metathesis can produce multiple different products, including homodimerization and *E* vs *Z* isomers of the desired product. Because of the wide variety of products that can be accessed with Grubbs 2nd generation catalyst this typically leads to low yields and complex purification methods.

Developing a full screen of cross metathesis catalysts using compounds **2.77** and terminal alkene alcohol will provide a reasonable model for scale up and further development of the peptide base route.¹⁶⁸ Recent develops from Luesch and coworkers have shown a high yield of the desired alkene enantiomer when utilizing the Grela catalyst. The main differentiating factor between Grela's catalysts and Grubbs 2nd generation is the of the nitro group on the ligand.¹⁶⁹



Scheme 62. Catalyst development need for olefin metathesis route

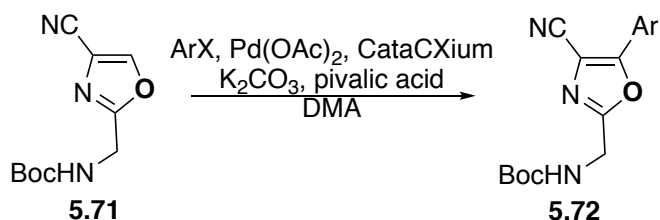
If this route could be utilized for peptide isostere synthesis in gram quantities it would allow for a wide array of medicinal chemistry testing to be performed on the molecule. One factor to keep in

mind is the difference in reactivity of the conjugated alcohol and amine. A full screen is needed for the highest yielding catalyst route to effectively and efficiently scale up the synthesis of the peptide isostere base fragment.^{170,171}

FUTURE WORK

5.1 New Chemical Space of Oxazole Derivatives

Interested in further expanding of the library of Largazole derivatives, the peptide derivatives of the thiazole-oxazoline analogs, compounds 32-35 in Figure 5 are being developed. The synthetic route for development is seen in Scheme 63. The base fragment used for macrocyclization will be accessed via a new developed base route or prior cross metathesis.



Scheme 63. Palladium catalyzed arylation route for direct functionalization.

In an attempt to utilize Pd-catalyzed direct arylation for development of compounds **5.73-5.76**, Wilson and coworkers' route for oxazole functionalization will be explored.¹⁷² This differs greatly from the functionalized route reliant on the iodination of thiazole **1.8**. In order to properly utilize this methodology, it will be important to conjugate to the oxazole at an early stage, prior to nitrile formation. Due to this, protecting group stability will be an important aspect to explore.

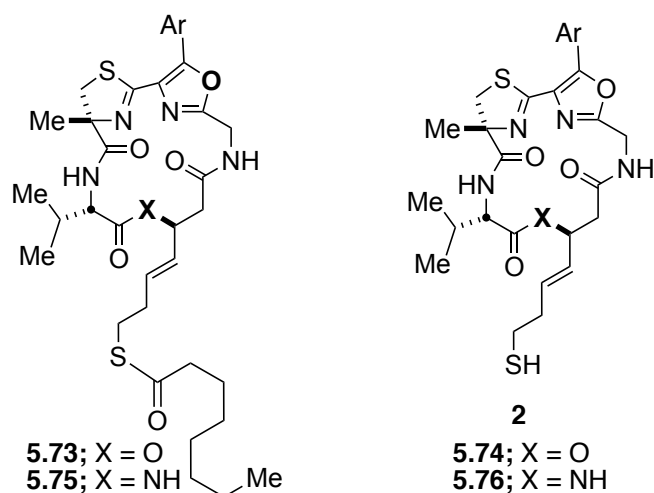


Figure 15. New chemical space oxazole derivatives.

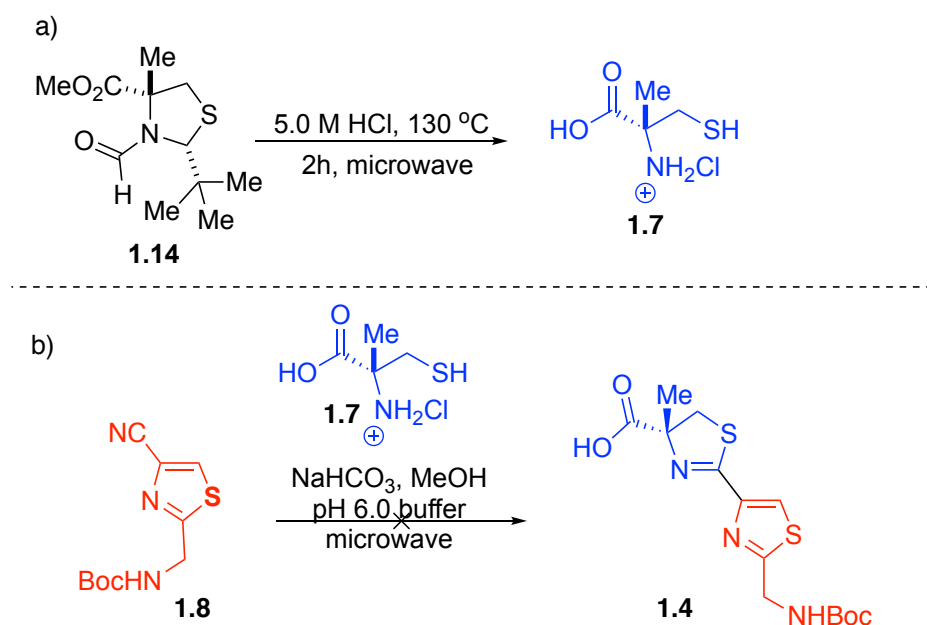
HDAC assays show impressive selectivity and potency for the Largazole derivatives containing the depsipeptide base and oxazole-thiazoline cap group. The more robust peptide isostere would aid in providing an even more potent and selective analog of this derivative. In addition, the increased functionalization at the hydroxyl handle of the oxazole compounds would increase the enzyme surface interactions. Following the increased potency seen with the hydroxyl handle of compound **68**, it is predicted the oxazole derivatives will follow in the same fashion.

5.2 Additional Conjugates

In developing therapeutics there are many biologic and drug conjugates to be explored. Due to the wide range of disease states HDAC inhibitors have been used to target, providing a direct route for functionalization to either Largazole peptide isostere or the new chemical space handle allows for a diverse library of compounds. This is especially highlighted by the fact compounds **68** and **69** have the opportunity to undergo esterification, thioesterification, amidation, and disulfide linkage at their respective sites of activity.

5.3 Further Scale-up Development

As the development of Largazole analogs progresses it is important to focus on the scalability of the reactions being performed. In continuing the development of decreased time and increased yield to aid in this efficiency, microwave reactions and alternate pathways should be explored. Synthetic byproducts and reagents being formed or utilized, respectively, should also be assessed to see if any additional greener techniques could be developed in scale-up.



Scheme 64. Previous microwave synthesis attempts to aid in compound accessibility; a) α -methyl cysteine synthesis, b) thiazole-thiazoline synthesis

α -methyl cysteine synthesis was decreased from a three-day reflux in 5M HCl to two hours utilizing microwave technology. However, this method will not work for all routes. Microwave technology was explored to decrease the 48-hour time frame needed for thiazole-thiazoline formation. This route led to decomposition of the starting material and ultimately no desired product. Additionally, a recent publication by Luesch and coworkers presented a scale-up development of the cyano thiazole that could be explored to bypass a large scale addition of POCl_3 .¹⁶⁹

5.4 Closing Remarks

An expansion of the library of Largazole compounds is an ongoing project within our laboratory. Recent advancements of interest include, but are not limited to, derivatization at a new chemical space unprecedented in Largazole analogs and extensive conjugation, biological conjugation, and methods towards the improved synthesis of the peptide isostere base fragment. It is envisioned that conjugation of Largazole to site specific bioactive molecules will provide a more direct pathway to the proposed therapeutic targets. This would both increase the selectivity and potency of Largazole towards HDAC active sites within cancer, as well as other diseased cells. Large scale development of key transformations within the total synthesis of the Largazole peptide isosteres, and in turn the conjugates synthesized, will aid in development and understanding of the natural product derivatives activity. Expansion of the Largazole library in conjunction with biological testing across a wide range of disease states will show the true impact of the synthesized compounds.

REFERENCES

1. Schnekenburger, M.; Dicato, M.; Diederich, M., Epigenetic modulators from "The Big Blue": A treasure to fight against cancer. *Cancer Lett* **2014**, *351*, 182-197.
2. Bradner, J. E.; West, N.; Grachan, M. L.; Greenberg, E. F.; Haggarty, S. J.; Warnow, T.; Mazitschek, R., Chemical phylogenetics of histone deacetylases. *Nat Chem Biol* **2010**, *6*, 238-243.
3. Seto, E.; Yoshida, M., Erasers of histone acetylation: the histone deacetylase enzymes. *Cold Spring Harb Perspect Biol* **2014**, *6*, a018713.
4. Bolden, J.; Shi, W.; Jankowski, K.; Kan, C.-Y.; Cluse, L.; Martin, B.; MacKenzie, K.; Smyth, G.; Johnston, R., HDAC inhibitors induce tumor-cell-selective pro-apoptotic transcriptional responses. *Cell Death and Disease* **2013**, *4*.
5. Hassig, C. A.; Fleischer, T. C.; Billin, A. N.; Schreiber, S. L.; Ayer, D. E., Histone deacetylase activity is required for full transcriptional repression by mSin3A. *Cell* **1997**, *89*, 341-7.
6. Hassig, C. A.; Schreiber, S. L., Nuclear histone acetylases and deacetylases and transcriptional regulation: HATs off to HDACs. *Current opinion in chemical biology* **1997**, *1*, 300-8.
7. Wittenberg, C., In search of a role in DNA replication: The enigmatic transcription factor Msa1. *Cell cycle* **2008**, *7*.
8. Salvador, L. A.; Luesch, H., Discovery and Mechanism of Natural Products as Modulators of Histone Acetylation. *Current Drug Targets* **2012**, *13*, 1029-1047.
9. Allfrey, V. G.; Faulkner, R.; Mirsky, A. E., Acetylation and Methylation of Histones and their Possible Role in the Regulation of RNA Synthesis. *Biochemistry* **1994**, *51*.

10. Tonelli, R.; Sartini, R.; Fronza, R.; Freccero, F.; Franzoni, M.; Dongiovanni, D.; Ballarini, M.; Ferrari, S.; D'Apolito, M.; Di Cola, G.; Capranico, G.; Khobta, A.; Campanini, R.; Paolucci, P.; Minucci, S.; Pession, A., G1 cell-cycle arrest and apoptosis by histone deacetylase inhibition in MLL-AF9 acute myeloid leukemia cells is p21 dependent and MLL-AF9 independent. *Leukemia* **2006**, *20*, 1307-1310.
11. Wu, L.-C.; Wei, M.-M.; Liu, Z.; Wen, Z.-S.; Chen, X.-Q.; Qiu, Y.-T.; Jiang, S.; Chen, H.-B.; Zhou, G.-B., Largazole Arrests Cell Cycle at G1 Phase and Triggers Proteasomal Degradation of E2F1 in Lung Cancer Cells. *ACS Med Chem Lett* **2013**, *4*, 921-6.
12. Hodawadekar, S. C.; Marmorstein, R., Chemistry of acetyl transfer by histone modifying enzymes: structure, mechanism and implications for effector design. *Oncogene* **2007**, *26*, 5528-5540.
13. Nagy, L.; Kao, H. Y.; Chakravarti, D.; Lin, R. J.; Hassig, C. A.; Ayer, D. E.; Schreiber, S. L.; Evans, R. M., Nuclear receptor repression mediated by a complex containing SMRT, mSin3A, and histone deacetylase. *Cell* **1997**, *89*, 373-80.
14. Minucci, S.; Pelicci, P. G., Histone deacetylase inhibitors and the promise of epigenetic (and more) treatments for cancer. *Nat Rev Cancer* **2006**, *6*, 38-51.
15. Ropero, S.; Esteller, M., The role of histone deacetylases (HDACs) in human cancer. *Mol Oncol* **2007**, *1*, 19-25.
16. Witt, O.; Deubzer, H. E.; Milde, T.; Oehme, I., HDAC family: What are the cancer relevant targets? *Cancer Lett* **2009**, *277*, 8-21.
17. Witt, O.; Lindemann, R., HDAC inhibitors: Magic bullets, dirty drugs or just another targeted therapy Foreword. *Cancer Letters* **2009**, *280*, 123-124.

18. Gabrielli, B. G.; Johnstone, R. W.; Saunders, N. A., Identifying Molecular Targets Mediating the Anticancer Activity of Histone Deacetylase Inhibitors: A Work in Progress. *Curr Cancer Drug Tar* **2002**, *2*, 337-353.
19. Lujambic, A.; Ropero, S.; Ballestar, E.; Fraga, M. F.; Cerrato, C.; Setien, F.; Casado, S.; Suarez-Gauthier, A.; Sanchez-Cespedes, M.; Git, A.; Spiteri, I.; Das, P. P.; Caldas, C.; Miska, E.; Esteller, M., Genetic unmasking of an epigenetically silenced microRNA in human cancer cells (vol 67, pg 1424, 2007). *Cancer Res* **2007**, *67*, 3492-3492.
20. Newman, D. J., Natural Products and Cancer Drug Discovery. *Future Oncol.* **2013**, *9*, 949-950.
21. West, A. C.; Johnston, R. W., New and emerging HDAC inhibitors for cancer treatment. *The Journal of Clinical Investigation* **2014**, *124*, 30-39.
22. Varshney, A.; Singh, V., Effects of algal compounds on cancer cell line. *J. Exp. Biol. Agric. Sci.* **2013**, *1*, 337-352, 16 pp.
23. Hassig, C. A.; Tong, J. K.; Schreiber, S. L., Fiber-derived butyrate and the prevention of colon cancer. *Chemistry & biology* **1997**, *4*, 783-9.
24. Liu, Y.; Salvador, L. A.; Byeon, S.; Ying, Y.; Kwan, J. C.; Law, B. K.; Hong, J.; Luesch, H., Anticolon cancer activity of largazole, a marine-derived tunable histone deacetylase inhibitor. *J. Pharmacol. Exp. Ther.* **2010**, *335*, 351-361.
25. Zhao, Y.; Fang, X.; Wang, Y.; Zhang, J.; Jiang, S.; Liu, Z.; Ma, Z.; Xu, L.; Li, E.; Zhang, K., Comprehensive Analysis for Histone Acetylation of Human Colon Cancer Cells Treated with a novel HDAC Inhibitor. *Curr. Pharm. Des.* **2014**, *20*, 1866-1873.
26. Law, M. E.; Corsino, P. E.; Jahn, S. C.; Davis, B. J.; Chen, S.; Patel, B.; Pham, K.; Lu, J.; Sheppard, B.; Norgaard, P.; Hong, J.; Higgins, P.; Kim, J. S.; Luesch, H.; Law, B. K.,

Glucocorticoids and histone deacetylase inhibitors cooperate to block the invasiveness of basal-like breast cancer cells through novel mechanisms. *Oncogene* **2013**, *32*, 1316-1329.

27. Sangeetha, S.; Ranjitha, S.; Murugan, K.; Kumar, G. R., Breast cancer specific histone deacetylase inhibitors and lead discovery using molecular docking and descriptor study. *Trends Bioinf.* **2013**, *6*, 25-44.

28. Calalb, M. B.; McKinsey, T. A.; Newkirk, S.; Huynh, K.; Sucharov, C. C.; Bristow, M. R., Increased Phosphorylation-Dependent Nuclear Export of Class II Histone Deacetylases in Failing Human Heart. *Cts-Clin Transl Sci* **2009**, *2*, 325-332.

29. Cao, H.; Fei, R. G.; Bowers, A. A.; Greshock, T. J.; Newkirt, T.; Miller, K. A.; Bradner, J. E.; West, N.; Williams, R. M.; Papayannopoulou, T.; Stamatoyannopoulos, G., Potent Induction of Human gamma Globin Gene Expression by Largazole, a New Histone Deacetylase Inhibitor. *Blood* **2009**, *114*, 798-798.

30. Carbone, R.; Botrugno, O. A.; Ronzoni, S.; Insinga, A.; Di Croce, L.; Pelicci, P. G.; Minucci, S., Recruitment of the histone methyltransferase SUV39H1 and its role in the oncogenic properties of the leukemia-associated PML-retinoic acid receptor fusion protein. *Mol Cell Biol* **2006**, *26*, 1288-1296.

31. Crazzolara, R.; Johrer, K.; Johnstone, R. W.; Greil, R.; Kofler, R.; Meister, B.; Bernhard, D.; Tcri, Histone deacetylase inhibitors potently repress CXCR4 chemokine receptor expression and function in acute lymphoblastic leukaemia. *Brit J Haematol* **2002**, *119*, 965-969.

32. Ellis, J.; Sayyed, F.; Inston, N.; Ready, A.; Jenkinson, E.; Drayson, M.; Shuttleworth, S.; Cobbold, M., Immunosuppressive effect of novel histone deacetylase inhibitors and their potential role in renal transplantation. *Brit J Surg* **2010**, *97*, S54-S55.

33. Ghosh, S. K.; Perrine, S. P.; Williams, R. M.; Faller, D. V., Histone deacetylase inhibitors are potent inducers of gene expression in latent EBV and sensitize lymphoma cells to nucleoside antiviral agents. *Blood* **2012**, *119*, 1008-1017.
34. Wang, Y. S.; Chen, T.; Yan, H. J.; Qi, H.; Deng, C. Y.; Ye, T.; Zhou, S. Y.; Li, F. R., Role of Histone Deacetylase Inhibitors in the Aging of Human Umbilical Cord Mesenchymal Stem Cells. *J Cell Biochem* **2013**, *114*, 2231-2239.
35. Ghosh, A. K., Harnessing Nature's Insight: Design of Aspartyl Protease Inhibitors from Treatment of Drug-Resistant HIV to Alzheimer's Disease. *J. Med. Chem.* **2009**, *52*, 2163-2176.
36. Methot, J. L.; Chakravarty, P. K.; Chenard, M.; Close, J.; Cruz, J. C.; Dahlberg, W. K.; Fleming, J.; Hamblett, C. L.; Hamill, J. E.; Harrington, P.; Harsch, A.; Heidebrecht, R.; Hughes, B.; Jung, J.; Kenific, C. M.; Kral, A. M.; Meinke, P. T.; Middleton, R. E.; Ozerova, N.; Sloman, D. L.; Stanton, M. G.; Szewczak, A. A.; Tyagarajan, S.; Witter, D. J.; Secrist, J. P.; Miller, T. A., Exploration of the internal cavity of histone deacetylase (HDAC) with selective HDAC1/HDAC2 inhibitors (SHI-1:2). *Bioorg Med Chem Lett* **2008**, *18*, 973-8.
37. Glozak, M. A.; Sengupta, N.; Zhang, X. H.; Seto, E., Acetylation and deacetylation of non-histone proteins. *Gene* **2005**, *363*, 15-23.
38. Williams, R. M.; Bradner, J. E.; Bowers, A.; Newkirk, T.; Youngman, A. E. Synthesis of Largazole analogs and their use in Cancer and Blood disorders therapy. WO2010009334A1, 2010.
39. Guerra-Bubb, J. M.; Bowers, A. A.; Smith, W. B.; Paranal, R.; Estiu, G.; Wiest, O.; Bradner, J. E.; Williams, R. M., Synthesis and HDAC inhibitory activity of isosteric thiazoline-oxazole largazole analogs. *Bioorg Med Chem Lett* **2013**, *23*, 6025-6028.
40. Johnstone, R. W., Histone-deacetylase inhibitors: Novel drugs for the treatment of cancer. *Nat Rev Drug Discov* **2002**, *1*, 287-299.

41. Silvestri, L.; Ballante, F.; Mai, A.; Marshall, G. R.; Ragno, R., Histone Deacetylase Inhibitors: Structure-Based Modeling and Isoform-Selectivity Prediction. *J. Chem. Inf. Model.* **2012**, *52*, 2215-2235.
42. Lombardi, P. M.; Cole, K. E.; Dowling, D. P.; Christianson, D. W., Structure, mechanism, and inhibition of histone deacetylases and related metalloenzymes. *Current Opinion in Structural Biology* **2011**, *21*, 735-743.
43. Butler, L. M.; Agus, D. B.; Scher, H. I.; Higgins, B.; Rose, A.; Cordon-Cardo, C.; Thaler, H. T.; Rifkind, R. A.; Marks, P. A.; Richon, V. M., Suberoylanilide hydroxamic acid, an inhibitor of histone deacetylase, suppresses the growth of prostate cancer cells in vitro and in vivo. *Cancer Res* **2000**, *60*, 5165-5170.
44. Fredenhagen, A.; Kittelmann, M.; Oberer, L.; Kuhn, A.; Kuhnol, J.; Delemonte, T.; Aichholz, R.; Wang, P.; Atadja, P.; Shultz, M. D., Biocatalytic Synthesis and Structure Elucidation of Cyclized Metabolites of the Deacetylase Inhibitor Panobinostat (LBH589). *Drug Metab Dispos* **2012**, *40*, 1041-1050.
45. Baud, M. G. J.; Leiser, T.; Haus, P.; Samlal, S.; Wong, A. C.; Wood, R. J.; Petrucci, V.; Gunaratnam, M.; Hughes, S. M.; Buluwela, L.; Turlais, F.; Neidle, S.; Meyer-Almes, F.-J.; White, A. J. P.; Fuchter, M. J., Defining the Mechanism of Action and Enzymatic Selectivity of Psammaplin A against Its Epigenetic Targets. *J. Med. Chem.* **2012**, *55*, 1731-1750.
46. Atadja, P., Development of the pan-DAC inhibitor panobinostat (LBH589): Successes and challenges. *Cancer Lett* **2009**, *280*, 233-241.
47. Conroy, T.; Guo, J. T.; Hunt, N. H.; Payne, R. J., Total Synthesis, and Antimalarial Activity of Symplostatin 4. *Organic Letters* **2010**, *12*, 5576-5579.

48. Hoque, M. A.; Islam, M. S.; Islam, M. N.; Kato, T.; Nishino, N.; Ito, A.; Yoshida, M., Design and synthesis of mono and bicyclic tetrapeptides thioester as potent inhibitor of histone deacetylases. *Amino Acids* **2014**, *46*, 2435-2444.
49. Narita, K.; Kikuchi, T.; Watanabe, K.; Takizawa, T.; Oguchi, T.; Kudo, K.; Matsuhara, K.; Abe, H.; Yamori, T.; Yoshida, M.; Katoh, T., Total Synthesis of the Bicyclic Depsipeptide HDAC Inhibitors Spiruchostatins A and B, 5''-epi-Spiruchostatin B, FK228 (FR901228) and Preliminary Evaluation of Their Biological Activity. *Chem-Eur J* **2009**, *15*, 11174-11186.
50. Newkirk, T. L.; Bowers, A. A.; Williams, R. M., Discovery, biological activity, synthesis and potential therapeutic utility of naturally occurring histone deacetylase inhibitors. *Nat Prod Rep* **2009**, *26*, 1293-1320.
51. Olsen, C. A.; Ghadiri, M. R., Discovery of Potent and Selective Histone Deacetylase Inhibitors via Focused Combinatorial Libraries of Cyclic alpha(3)beta-Tetrapeptides. *Journal of Medicinal Chemistry* **2009**, *52*, 7836-7846.
52. Stolze, S. C.; Kaiser, M., Challenges in the Syntheses of Peptidic Natural Products. *Synthesis-Stuttgart* **2012**, *44*, 1755-1777.
53. Fuse, S.; Okada, K.; Iijima, Y.; Munakata, A.; Machida, K.; Takahashi, T.; Takagi, M.; Shin-ya, K.; Doi, T., Total synthesis of spiruchostatin B aided by an automated synthesizer. *Organic & Biomolecular Chemistry* **2011**, *9*, 3825-3833.
54. Yurek-George, A.; Habens, F.; Brimmell, M.; Packham, G.; Ganesan, A., Total Synthesis of Spiruchostatin A, a Potent Histone Deacetylase Inhibitor. *J. Am. Chem. Soc.* **2004**, *126*, 1030-1031.

55. Iijima, Y.; Munakata, A.; Shin-ya, K.; Ganesan, A.; Doi, T.; Takahashi, T., A solid-phase total synthesis of the cyclic depsipeptide HDAC inhibitor spiruchostatin A. *Tetrahedron Letters* **2009**, *50*, 2970-2972.
56. Ishmuratov, G. Y.; Yakovleva, M. P.; Vydrina, V. A.; Shakhanova, O. O.; Ishmuratova, N. M.; Tolstikov, A. G., Synthesis of Macrocyclic Lactams and Lactones Containing Sulfur and Nitrogen. *Macroheterocycles* **2012**, *5*, 212-245.
57. Benelkebir, H.; Donlevy, A. M.; Packham, G.; Ganesan, A., Total Synthesis and Stereochemical Assignment of Burkholdac B, a Depsipeptide HDAC Inhibitor. *Org Lett* **2011**, *13*, 6334-6337.
58. Liu, X.; Phillips, A. J.; Ungermannova, D.; Nasveschuk, C. G.; Zhang, G. Macrocyclic compounds useful as inhibitors of histone deacetylases. WO2011150283A1, 2011.
59. Fournel, M.; Bonfils, C.; Hou, Y.; Yan, P. T.; Trachy-Bourget, M. C.; Kalita, A.; Liu, J.; Lu, A. H.; Zhou, N. Z.; Robert, M. F.; Gillespie, J.; Wang, J. J.; Ste-Croix, H.; Rahil, J.; Lefebvre, S.; Moradei, O.; Delorme, D.; MacLeod, A. R.; Besterman, J. M.; Li, Z. M., MGCD0103, a novel isotype-selective histone deacetylase inhibitor, has broad spectrum antitumor activity in vitro and in vivo. *Mol Cancer Ther* **2008**, *7*, 759-768.
60. Lane, A. A.; Chabner, B. A., Histone Deacetylase Inhibitors in Cancer Therapy. *J Clin Oncol* **2009**, *27* histone deacetylase inhibitors in cancer therapy, 5459-5468.
61. Taori, K.; Liu, Y.; Paul, V. J.; Luesch, H., Combinatorial Strategies by Marine Cyanobacteria: Symplostatin 4, an Antimitotic Natural Dolastatin 10/15 Hybrid that Synergizes with the Coproduced HDAC Inhibitor Largazole. *ChemBioChem* **2009**, *10*, 1634-1639.
62. Thurn, K. T.; Thomas, S.; Moore, A.; Munster, P. N., Rational therapeutic combinations with histone deacetylase inhibitors for the treatment of cancer. *Future Oncol* **2011**, *7*, 263-283.

63. Li, J. J.; Hao, D. P.; Wang, L.; Wang, H. T.; Wang, Y.; Zhao, Z. Q.; Li, P. P.; Deng, C. X.; Di, L. J., Epigenetic targeting drugs potentiate chemotherapeutic effects in solid tumor therapy. *Sci Rep-Uk* **2017**, *7*.
64. Diyabalanage, H. V. K.; Granda, M. L.; Hooker, J. M., Combination therapy: Histone deacetylase inhibitors and platinum-based chemotherapeutics for cancer. *Cancer Letters* **2013**, *329*, 1-8.
65. Lundqvist, A.; Abrams, S. I.; Schrump, D. S.; Alvarez, G.; Suffredini, D.; Berg, M.; Childs, R., Bortezomib and depsipeptide sensitize tumors to tumor necrosis factor-related apoptosis-inducing ligand: A novel method to potentiate natural killer cell tumor cytotoxicity. *Cancer Res* **2006**, *66*, 7317-7325.
66. Liu, L.; Witt, O.; Haefeli, W. E.; Burhenne, J., Selective and Sensitive Quantification of the Hdac-Inhibitor Vorinostat (Saha) in Plasma and Pbmcs by Hplc Coupled to Electrospray Tandem Mass Spectrometry (Lc/Ms/Ms). *Brit J Clin Pharmaco* **2009**, *68*, 35-35.
67. Subramanian, S.; Bates, S. E.; Wright, J. J.; Espinoza-Delgado, I.; Piekarz, R. L., Clinical Toxicities of Histone Deacetylase Inhibitors. *Pharmaceuticals* **2010**, *3*, 2751-2767.
68. Carlberg, I.; Mannervik, B., Glutathione-Reductase. *Methods in enzymology* **1985**, *113*, 484-490.
69. Taori, K.; Paul, V. J.; Luesch, H., Structure and activity of largazole, a potent anti-proliferative agent from the Floridian marine cyanobacterium *Symploca* sp. *J Am Chem Soc* **2008**, *130*, 1806-1807.
70. Luesch, H.; Liu, Y.; Taori, K.; Kwan, J.; Matthew, S.; Paul, V. J., Bioactive natural products from marine cyanobacteria: new structures and modes of action. *Planta Med* **2008**, *74*, 931-931.

71. Maruthanayagam, V.; Nagarajan, M.; Sundararaman, M., An insight into biological significance of marine cyanobacterial toxins in the recent decade. *Cahiers De Biologie Marine* **2013**, *54*, 221-238.
72. Morris, J. C.; Phillips, A. J., Marine natural products. Synthetic aspects. *Nat. Prod. Rep.* **2010**, *27*, 1186-1203.
73. Russo, P.; Cesario, A., New Anticancer Drugs from Marine Cyanobacteria. *Current Drug Targets* **2012**, *13*, 1048-1053.
74. Tan, L. T., Marine cyanobacteria: a treasure trove of bioactive secondary metabolites for drug discovery. *Stud. Nat. Prod. Chem.* **2012**, *36*, 67-110.
75. Ungermannova, D. P27 as a molecular target for cancer therapeutics: Discovering small molecule inhibitors of p27 proteolysis and structure-activity relationship and mechanistic studies of largazole, a potent inhibitor of histone deacetylase. 2010.
76. Ungermannova, D.; Parker, S. J.; Nasveschuk, C. G.; Wang, W.; Quade, B.; Zhan, G.; Kuchta, R. D.; Phillips, A. J.; Liu, X. D., Largazole and Its Derivatives Selectively Inhibit Ubiquitin Activating Enzyme (E1). *Plos One* **2012**, *7*.
77. Hong, J.; Luesch, H., Largazole: From discovery to broad-spectrum therapy. *Nat. Prod. Rep.* **2012**, *29*, 449-456.
78. Vickers, C. J.; Olsen, C. A.; Leman, L. J.; Ghadiri, M. R., Discovery of HDAC Inhibitors That Lack an Active Site Zn²⁺-Binding Functional Group. *Acs Medicinal Chemistry Letters* **2012**, *3*, 505-508.
79. Bowers, A.; West, N.; Taunton, J.; Schreiber, S. L.; Bradner, J. E.; Williams, R. M., Total synthesis and biological mode of action of largazole: A potent Class I histone deacetylase inhibitor. *J Am Chem Soc* **2008**, *130*, 11219-11222.

80. Bowers, A. A.; West, N.; Newkirk, T. L.; Troutman-Youngman, A. E.; Schreiber, S. L.; Wiest, O.; Bradner, J. E.; Williams, R. M., Synthesis and Histone Deacetylase Inhibitory Activity of Largazole Analogs: Alteration of the Zinc-Binding Domain and Macrocyclic Scaffold. *Org Lett* **2009**, *11*, 1301-1304.
81. Videnov, G.; Kaiser, D.; Kempter, C.; Jung, G., Synthesis of naturally occurring, conformationally restricted oxazole- and Thiazole-containing di- and tripeptide mimetics. *Angew Chem Int Edit* **1996**, *35*, 1503-1506.
82. Mulqueen, G. C.; Pattenden, G.; Whiting, D. A., Synthesis of the Thiazoline-Based Siderophore (S)-Desferrithiocin. *Tetrahedron* **1993**, *49*, 5359-5364.
83. Benelkebir, H.; Marie, S.; Hayden, A. L.; Lyle, J.; Loadman, P. M.; Crabb, S. J.; Packham, G.; Ganesan, A., Total synthesis of largazole and analogues: HDAC inhibition, antiproliferative activity and metabolic stability. *Bioorg Med Chem Lett* **2011**, *19*, 3650-3658.
84. Bhansali, P.; Hanigan, C. L.; Casero, R. A.; Tillekeratne, L. M. V., Largazole and Analogues with Modified Metal-Binding Motifs Targeting Histone Deacetylases: Synthesis and Biological Evaluation. *J Med Chem* **2011**, *54*, 7453-7463.
85. Bowers, A. A.; Greshock, T. J.; West, N.; Estiu, G.; Schreiber, S. L.; Wiest, O.; Williams, R. M.; Bradner, J. E., Synthesis and Conformation-Activity Relationships of the Peptide Isosteres of FK228 and Largazole. *J Am Chem Soc* **2009**, *131*, 2900-2905.
86. Ghosh, A. K.; Kulkarni, S., Enantioselective total synthesis of (+)-largazole, a potent inhibitor of histone deacetylase. *Org Lett* **2008**, *10*, 3907-3909.
87. Nasveschuk, C. G.; Ungermannova, D.; Liu, X. D.; Phillips, A. J., A concise total synthesis of largazole, solution structure, and some preliminary structure activity relationships. *Org Lett* **2008**, *10*, 3595-3598.

88. Numajiri, Y.; Takahashi, T.; Takagi, M.; Shin-Ya, K.; Doi, T., Total Synthesis of Largazole and Its Biological Evaluation. *Synlett* **2008**, 2483-2486.
89. Ren, Q.; Dai, L.; Zhang, H.; Tan, W. F.; Xu, Z. S.; Ye, T., Total synthesis of largazole. *Synlett* **2008**, 2379-2383.
90. Seiser, T.; Kamena, F.; Cramer, N., Synthesis and biological activity of largazole and derivatives. *Angew Chem Int Edit* **2008**, *47*, 6483-6485.
91. Souto, J. A.; Vaz, E.; Lepore, I.; Poppler, A. C.; Franci, G.; Alvarez, R.; Altucci, L.; de Lera, A. R., Synthesis and Biological Characterization of the Histone Deacetylase Inhibitor Largazole and C7-Modified Analogues. *J Med Chem* **2010**, *53*, 4654-4667.
92. Wang, B.; Forsyth, C. J., Total Synthesis of Largazole - Devolution of a Novel Synthetic Strategy. *Synthesis-Stuttgart* **2009**, 2873-2880.
93. Wang, B.; Huang, P. H.; Chen, C. S.; Forsyth, C. J., Total Syntheses of the Histone Deacetylase Inhibitors Largazole and 2-epi-Largazole: Application of N-Heterocyclic Carbene Mediated Acylations in Complex Molecule Synthesis. *J Org Chem* **2011**, *76*, 1140-1150.
94. Xiao, Q.; Wang, L. P.; Jiao, X. Z.; Liu, X. Y.; Wu, Q. A.; Xie, P., Concise total synthesis of largazole. *J Asian Nat Prod Res* **2010**, *12*, 940-949.
95. Ying, Y. C.; Taori, K.; Kim, H.; Hong, J. Y.; Luesch, H., Total synthesis and molecular target of largazole, a histone deacetylase inhibitor. *J Am Chem Soc* **2008**, *130*, 8455-8459.
96. Zeng, X.; Yin, B. L.; Hu, Z.; Liao, C. Z.; Liu, J. L.; Li, S.; Li, Z.; Nicklaus, M. C.; Zhou, G. B.; Jiang, S., Total Synthesis and Biological Evaluation of Largazole and Derivatives with Promising Selectivity for Cancers Cells. *Org Lett* **2010**, *12*, 1368-1371.
97. Cramer, N., Catalytic Asymmetric Functionalization of Inert Bonds and Synthesis of Bioactive Natural Products. *Chimia* **2011**, *65*, 656-658.

98. Arouri, A.; Lauritsen, K. E.; Nielsen, H. L.; Mouritsen, O. G., Effect of fatty acids on the permeability barrier of model and biological membranes. *Chem Phys Lipids* **2016**, *200*, 139-146.
99. Decroos, C.; Clausen, D. J.; Haines, B. E.; Wiest, O.; Williams, R. M.; Christianson, D. W., Variable Active Site Loop Conformations Accommodate the Binding of Macrocyclic Largazole Analogues to HDAC8. *Biochemistry* **2015**, *54*, 2126-2135.
100. Cole, K. E.; Dowling, D. P.; Boone, M. A.; Phillips, A. J.; Christianson, D. W., Structural Basis of the Antiproliferative Activity of Largazole, a Depsipeptide Inhibitor of the Histone Deacetylases. *J Am Chem Soc* **2011**, *133*, 12474-12477.
101. Clausen, D. J.; Smith, W. B.; Haines, B. E.; Wiest, O.; Bradner, J. E.; Williams, R. M., Modular synthesis and biological activity of pyridyl-based analogs of the potent Class I Histone Deacetylase Inhibitor Largazole. *Bioorgan Med Chem* **2015**, *23*, 5061-5074.
102. Pilon, J. L.; Clausen, D. J.; Hansen, R. J.; Lunghofer, P. J.; Charles, B.; Rose, B. J.; Thamm, D. H.; Gustafson, D. L.; Bradner, J. E.; Williams, R. M., Comparative pharmacokinetic properties and antitumor activity of the marine HDACi Largazole and Largazole peptide isostere. *Cancer Chemoth Pharm* **2015**, *75*, 671-682.
103. Szpilman, A. M.; Carreira, E. M., Probing the biology of natural products. Molecular editing by diverted total synthesis. *Angew. Chem., Int. Ed.* **2010**, *49*, 9592-9628.
104. Yu, X. L.; Zhang, B. B.; Shan, G. S.; Wu, Y.; Yang, F. L.; Lei, X. S., Synthesis of the molecular hybrid inspired by Largazole and Psammalin A. *Tetrahedron* **2018**, *74*, 549-555.
105. Kim, B.; Park, H.; Salvador, L. A.; Serrano, P. E.; Kwan, J. C.; Zeller, S. L.; Chen, Q. Y.; Ryu, S.; Liu, Y. X.; Byeon, S.; Luesch, H.; Hong, J. Y., Evaluation of class I HDAC isoform selectivity of largazole analogues. *Bioorg Med Chem Lett* **2014**, *24*, 3728-3731.

106. Salvador, L. A.; Park, H.; Al-Awadhi, F. H.; Liu, Y.; Kim, B.; Zeller, S. L.; Chen, Q.-Y.; Hong, J.; Luesch, H., Modulation of Activity Profiles for Largazole-Based HDAC Inhibitors through Alteration of Prodrug Properties. *ACS Med. Chem. Lett.* **2014**, *5*, 905-910.
107. Ying, Y.; Liu, Y.; Byeon, S. R.; Kim, H.; Luesch, H.; Hong, J., Synthesis and Activity of Largazole Analogues with Linker and Macrocyclic Modification. *Org. Lett.* **2008**, *10*, 4021-4024.
108. Ying, Y.; Taori, K.; Kim, H.; Hong, J.; Luesch, H., Total Synthesis and Molecular Target of Largazole, a Histone Deacetylase Inhibitor. *J. Am. Chem. Soc.* **2008**, *130*, 8455-8459.
109. Ying, Y. C.; Liu, Y. X.; Byeon, S. R.; Kim, H.; Luesch, H.; Hong, J. Y., Synthesis and activity of largazole analogues with linker and macrocyclic modification. *Organic Letters* **2008**, *10*, 4021-4024.
110. Ghosh, A. K.; Kulkarni, S., Enantioselective Total Synthesis of (+)-Largazole, a Potent Inhibitor of Histone Deacetylase. *Org. Lett.* **2008**, *10*, 3907-3909.
111. Seiser, T.; Cramer, N., Syntheses and Biological Activity of the HDAC Class I Inhibitor Largazole. *Chimia* **2009**, *63*, 19-22.
112. Wang, B.; Forsyth, C. In *Total Synthesis of Largazole and 2-Epi-Largazole, Potent Anticancer Agents* 2009 American Chemical Society; pp CRM-311.
113. Wang, B.; Forsyth, C. J. In *Total synthesis of largazole and 2-epi-largazole* 2010 American Chemical Society; pp ORGN-438.
114. Wang, B.; Huang, P.-H.; Chen, C.-S.; Forsyth, C. J., Total Syntheses of the Histone Deacetylase Inhibitors Largazole and 2-epi-Largazole: Application of N-Heterocyclic Carbene Mediated Acylations in Complex Molecule Synthesis. *J. Org. Chem.* **2011**, *76*, 1140-1150.
115. Forsyth, C. J. In *Novel Strategies for Complex Molecule Synthesis* 2009 American Chemical Society; pp CRM-260.

116. Jiang, S.; Zhou, G.; Yin, B.; Zeng, X.; Hu, Z. Method for synthesis of largazole and its analogs as antitumor agents. CN101781321A, 2010.
117. Zeng, X.; Yin, B. L.; Hu, Z.; Liao, C. Z.; Liu, J. L.; Li, S.; Li, Z.; Nicklaus, M. C.; Zhou, G. B.; Jiang, S., Total Synthesis and Biological Evaluation of Largazole and Derivatives with Promising Selectivity for Cancers Cells. *Organic Letters* **2010**, *12*, 1368-1371.
118. Li, S.; Yao, H.; Xu, J.; Jiang, S., Synthetic routes and biological evaluation of largazole and its analogues as potent histone deacetylase inhibitors. *Molecules* **2011**, *16*, 4681-94.
119. Yao, Z. Y.; Zeng, X.; Yi, W.; Jiang, S., Stereoselective Synthesis of (S,E)-2-(trimethylsilyl)ethyl 3-hydroxy-7-(tritylthio)hept-4-enoate. *Letters in Organic Chemistry* **2011**, *8*, 66-69.
120. Jiang, S.; Tu, Z.; Li, X.; Yao, Y.; Qiu, Y. Preparation of largazole analog compounds as antitumor agents. CN103601742A, 2014.
121. Sun, Q.; Yao, Y. W.; Liu, C. P.; Li, H.; Yao, H. Q.; Xue, X. W.; Liu, J. S.; Tu, Z. C.; Jiang, S., Design, synthesis, and biological evaluation of novel histone deacetylase 1 inhibitors through click chemistry. *Bioorganic & Medicinal Chemistry Letters* **2013**, *23*, 3295-3299.
122. Li, X.; Tu, Z.; Li, H.; Liu, C.; Li, Z.; Sun, Q.; Yao, Y.; Liu, J.; Jiang, S., Biological evaluation of new largazole analogues: Alteration of macrocyclic scaffold with Click chemistry. *ACS Med. Chem. Lett.* **2013**, *4*, 132-136.
123. Su, J.; Qiu, Y.; Ma, K.; Yao, Y.; Wang, Z.; Li, X.; Zhang, D.; Tu, Z.; Jiang, S., Design, synthesis, and biological evaluation of largazole derivatives: alteration of the zinc-binding domain. *Tetrahedron* **2014**, *70*, 7763-7769.

124. Bhansali, P.; Hanigan, C. L.; Casero, R. A., Jr.; Perera, L.; Tillekeratne, L. M. V., Synthesis and biological evaluation of largazole analogues with modified surface recognition cap groups. *Eur J Med Chem* **2014**, *86C*, 528-541.
125. Numajiri, Y.; Takahashi, T.; Takagi, M.; Shin-ya, K.; Doi, T., Total synthesis of largazole and its biological evaluation. *Pept. Sci.* **2009**, *45th*, 41-44.
126. Ren, Q.; Dai, L.; Zhang, H.; Tan, W.; Xu, Z.; Ye, T., Total synthesis of largazole. *Synlett* **2008**, 2379-2383.
127. Schotes, C.; Ostrovskiy, D.; Senger, J.; Schmidtkunz, K.; Jung, M.; Breit, B., Total Synthesis of (18S)- and (18R)-Homolargazole by Rhodium-Catalyzed Hydrocarboxylation. *Chemistry-a European Journal* **2014**, *20*, 2164-2168.
128. Yan, W.; O'Doherty, G. A., Total synthesis of (+)-largazole, a histone deacetylase inhibitor. *Chemtracts* **2009**, *22*, 50-58.
129. Chen, F.; Chai, H.; Su, M.-B.; Zhang, Y.-M.; Li, J.; Xie, X.; Nan, F.-J., Potent and Orally Efficacious Bisthiazole-Based Histone Deacetylase Inhibitors. *ACS Med. Chem. Lett.* **2014**, *5*, 628-633.
130. Chen, F.; Gao, A. H.; Li, J.; Nan, F. J., Synthesis and Biological Evaluation of C7-Demethyl Largazole Analogues (vol 4, pg 1269, 2009). *Chemmedchem* **2009**, *4*, 1217-1217.
131. Davyt, D.; Serra, G., Thiazole and Oxazole Alkaloids: Isolation and Synthesis. *Marine Drugs* **2010**, *8*, 2755-2780.
132. Diness, F.; Nielsen, D. S.; Fairlie, D. P., Synthesis of the Thiazole-Thiazoline Fragment of Largazole Analogues. *Journal of Organic Chemistry* **2011**, *76*, 9845-9851.
133. Lemerrier, B. C.; Pierce, J. G., Synthesis of Thiazolines by Copper Catalyzed Aminobromination of Thiohydroxamic Acids. *Organic Letters* **2014**, *16*, 2074-2076.

134. Montero, A.; Beierle, J. M.; Olsen, C. A.; Ghadiri, M. R., Design, Synthesis, Biological Evaluation, and Structural Characterization of Potent Histone Deacetylase Inhibitors Based on Cyclic alpha/beta-Tetrapeptide Architectures. *J Am Chem Soc* **2009**, *131*, 3033-3041.
135. Yu, M.; Salvador, L. A.; Sy, S. K. B.; Tang, Y.; Singh, R. S. P.; Chen, Q.-Y.; Liu, Y.; Hong, J.; Derendorf, H.; Luesch, H., Largazole pharmacokinetics in rats by LC-MS/MS. *Mar. Drugs* **2014**, *12*, 1623-1640, 18 pp.
136. Chen, K.; Xu, L. P.; Wiest, O., Computational Exploration of Zinc Binding Groups for HDAC Inhibition. *Journal of Organic Chemistry* **2013**, *78*, 5051-5055.
137. Meyers, A. I.; Temple, D. L.; Haidukew.D; Mihelich, E. D., Oxazolines .11. Synthesis of Functionalized Aromatic and Aliphatic-Acids - Useful Protecting Group for Carboxylic-Acids against Grignard and Hydride Reagents. *J Org Chem* **1974**, *39*, 2787-2793.
138. Zhao, L.; Dunne, C. E.; Clausen, D. J.; Roberts, J. M.; Paulk, J.; Liu, H. N.; Wiest, O. G.; Bradner, J. E.; Williams, R. M., Synthesis and Biochemical Evaluation of Biotinylated Conjugates of Largazole Analogues: Selective Class I Histone Deacetylase Inhibitors. *Isr J Chem* **2017**, *57*, 319-330.
139. Dakshinamurti, K., Biotin - a regulator of gene expression. *J Nutr Biochem* **2005**, *16*, 419-423.
140. Leamon, C. P.; Low, P. S., Folate-mediated targeting: from diagnostics to drug and gene delivery. *Drug Discov Today* **2001**, *6*, 44-51.
141. Kono, K.; Liu, M. J.; Frechet, J. M. J., Design of dendritic macromolecules containing folate or methotrexate residues. *Bioconjugate Chem* **1999**, *10*, 1115-1121.
142. Grandy, D.; Shan, J. F.; Zhang, X. X.; Rao, S.; Akunuru, S.; Li, H. Y.; Zhang, Y. H.; Alpatov, I.; Zhang, X. A.; Lang, R. A.; Shi, D. L.; Zheng, J. J., Discovery and Characterization of

- a Small Molecule Inhibitor of the PDZ Domain of Dishevelled. *J Biol Chem* **2009**, *284*, 16256-16263.
143. Lin, S.; Cronan, J. E., Closing in on complete pathways of biotin biosynthesis. *Mol Biosyst* **2011**, *7*, 1811-1821.
144. Bansal, N.; Zheng, Z.; Song, L. F.; Pei, J.; Merz, K. M., Jr., The Role of the Active Site Flap in Streptavidin/Biotin Complex Formation. *J Am Chem Soc* **2018**, *140*, 5434-5446.
145. Kan, T.; Fukuyama, T., New strategies: a highly versatile synthetic method for amines. *Chem Commun* **2004**, 353-359.
146. Crider, K. S.; Bailey, L. B.; Berry, R. J., Folic Acid Food Fortification-Its History, Effect, Concerns, and Future Directions. *Nutrients* **2011**, *3*, 370-384.
147. Ross, J. F.; Chaudhuri, P. K.; Ratnam, M., Differential Regulation of Folate Receptor Isoforms in Normal and Malignant-Tissues in-Vivo and in Established Cell-Lines - Physiological and Clinical Implications. *Cancer* **1994**, *73*, 2432-2443.
148. Elnakat, H.; Ratnam, M., Distribution, functionality and gene regulation of folate receptor isoforms: implications in targeted therapy. *Adv Drug Deliv Rev* **2004**, *56*, 1067-84.
149. Shi, H.; Guo, J.; Li, C.; Wang, Z., A current review of folate receptor alpha as a potential tumor target in non-small-cell lung cancer. *Drug Des Devel Ther* **2015**, *9*, 4989-96.
150. Leamon, C. P.; Reddy, J. A.; Vlahov, L. R.; Westrick, E.; Parker, N.; Nicoson, J. S.; Vetzal, M., Comparative preclinical activity of the folate-targeted Vinca alkaloid conjugates EC140 and EC145. *Int J Cancer* **2007**, *121*, 1585-1592.
151. Henne, W. A.; Doorneweerd, D. D.; Hilgenbrink, A. R.; Kularatne, S. A.; Low, P. S., Synthesis and activity of a folate peptide camptothecin prodrug. *Bioorg Med Chem Lett* **2006**, *16*, 5350-5.

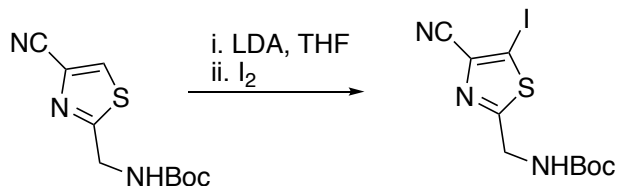
152. Molina, M. T.; Delvalle, C.; Escribano, A. M.; Ezquerra, J.; Pedregal, C., Regioselective Ring-Opening of Chiral N-Boc Protected Pyroglutamate and Pyroaminoadipate Ethyl-Esters with Heteronucleophiles. *Tetrahedron* **1993**, *49*, 3801-3808.
153. Luo, J.; Smith, M. D.; Lantrip, D. A.; Wang, S.; Fuchs, P. L., Efficient syntheses of pyrofolinic acid and pteroyl azide, reagents for the production of carboxyl-differentiated derivatives of folic acid. *J Am Chem Soc* **1997**, *119*, 10004-10013.
154. Tai, D.; Wells, K.; Arcaroli, J.; Vanderbilt, C.; Aisner, D. L.; Messersmith, W. A.; Lieu, C. H., Targeting the WNT Signaling Pathway in Cancer Therapeutics. *Oncologist* **2015**, *20*, 1189-98.
155. Masuda, M.; Sawa, M.; Yamada, T., Therapeutic targets in the Wnt signaling pathway: Feasibility of targeting TNK1 in colorectal cancer. *Pharmacol Ther* **2015**, *156*, 1-9.
156. Harris, B. Z.; Lim, W. A., Mechanism and role of PDZ domains in signaling complex assembly. *J Cell Sci* **2001**, *114*, 3219-31.
157. Oberg, C. T.; Strand, M.; Andersson, E. K.; Edlund, K.; Tran, N. P.; Mei, Y. F.; Wadell, G.; Elofsson, M., Synthesis, biological evaluation, and structure-activity relationships of 2-[2-(benzoylamino)benzoylamino]benzoic acid analogues as inhibitors of adenovirus replication. *J Med Chem* **2012**, *55*, 3170-81.
158. Weinstock, L. M.; Karady, S.; Roberts, F. E.; Hoinowski, A. M.; Brenner, G. S.; Lee, T. B. K.; Lumma, W. C.; Sletzing, M., Chemistry of Cephamycins .4. Acylation of Amides in Presence of Neutral Acid Scavengers. *Tetrahedron Letters* **1975**, 3979-3982.
159. Ojeda-Porras, A.; Hernandez-Santana, A.; Gamba-Sanchez, D., Direct amidation of carboxylic acids with amines under microwave irradiation using silica gel as a solid support. *Green Chem* **2015**, *17*, 3157-3163.

160. Dener, J. M.; Fantauzzi, P. P.; Kshirsagar, T. A.; Kelly, D. E.; Wolfe, A. B., Large-scale syntheses of Fmoc-protected non-proteogenic amino acids: Useful building blocks for combinatorial libraries. *Org Process Res Dev* **2001**, *5*, 445-449.
161. Bihelovic, F.; Stichnoth, D.; Surup, F.; Muller, R.; Trauner, D., Total Synthesis of Crocagin A. *Angew Chem Int Ed Engl* **2017**, *56*, 12848-12851.
162. Chen, J.; Forsyth, C. J., Total synthesis of the marine cyanobacterial cyclodepsipeptide apratoxin A. *Proc Natl Acad Sci U S A* **2004**, *101*, 12067-72.
163. Pearson, C.; Rinehart, K. L.; Sugano, M.; Costerison, J. R., Enantiospecific synthesis of N-Boc-Adda: A linear approach. *Organic Letters* **2000**, *2*, 2901-2903.
164. Kocienski, P. J.; Lythgoe, B.; Ruston, S., Scope and Stereochemistry of an Olefin Synthesis from Beta-Hydroxy-Sulfones. *J Chem Soc Perk T 1* **1978**, 829-834.
165. Noyori, R.; Hashiguchi, S., Asymmetric transfer hydrogenation catalyzed by chiral ruthenium complexes. *Accounts Chem Res* **1997**, *30*, 97-102.
166. Hsiao, Y.; Rivera, N. R.; Rosner, T.; Krska, S. W.; Njolito, E.; Wang, F.; Sun, Y. K.; Armstrong, J. D.; Grabowski, E. J. J.; Tillyer, R. D.; Spindler, F.; Malan, C., Highly efficient synthesis of beta-amino acid derivatives via asymmetric hydrogenation of unprotected enamines. *J Am Chem Soc* **2004**, *126*, 9918-9919.
167. Choluj, A.; Zielinski, A.; Grela, K.; Chmielewski, M. J., Metathesis@MOF: Simple and Robust Immobilization of Olefin Metathesis Catalysts inside (Al)MIL-101-NH₂. *Acs Catal* **2016**, *6*, 6343-6349.
168. Olszewski, T. K.; Bieniek, M.; Skowerski, K.; Grela, K., A new tool in the toolbox: electron-withdrawing group activated ruthenium catalysts for olefin metathesis. *Synlett* **2013**, *24*, 903-919.

169. Chen, Q. Y.; Chaturvedi, P. R.; Luesch, H., Process Development and Scale-up Total Synthesis of Largazole, a Potent Class I Histone Deacetylase Inhibitor. *Org Process Res Dev* **2018**, *22*, 190-199.
170. Samojlowicz, C.; Bieniek, M.; Zarecki, A.; Kadyrov, R.; Grela, K., The doping effect of fluorinated aromatic hydrocarbon solvents on the performance of common olefin metathesis catalysts: application in the preparation of biologically active compounds. *Chemical Communications* **2008**, 6282-6284.
171. Sawant, P.; Maier, M. E., Synthesis of the C1-C13 Fragment of Biselyngbyaside. *Synlett* **2011**, 3002-3004.
172. Strotman, N. A.; Chobanian, H. R.; Guo, Y.; He, J. F.; Wilson, J. E., Highly Regioselective Palladium-Catalyzed Direct Arylation of Oxazole at C-2 or C-5 with Aryl Bromides, Chlorides, and Triflates. *Organic Letters* **2010**, *12*, 3578-3581.

SUPPORTING INFORMATION

Unless otherwise noted, all reactions were performed under positive pressure of nitrogen or argon in oven/ flame dried glassware. Commercially available materials were used without further purification. Organic solvents were passed through J.C. Meyer of Glass Contour purifying solvent system under positive pressure of argon. The reactions were monitored by thin layer chromatography (TLC), visualized under UV light and a relevant stain. Standard silica gel for flash column chromatography was obtained from Sorbent Technologies. NMR spectra were recorded on Varian 400MHz spectrometer. ^1H - and ^{13}C -NMR were reported relative to CDCl_3 ($\delta = 7.26$ for ^1H -NMR spectra and $\delta = 77.16$ for ^{13}C -NMR spectra). All previously synthesized molecules matched literature spectra to the corresponding Williams paper.



Scheme 65. Reaction conditions

To a solution of thiazole (500 mg, 2.1 mmol) in 40 mL of THF at $-78\text{ }^{\circ}\text{C}$, 6.5 mL of LDA (synthesized *in situ* via DIPA and n-BuLi, 5.25 mmol, 0.8 M in THF) was cannulated slowly. The mixture was stirred at $-78\text{ }^{\circ}\text{C}$ for 15 min. I₂ (2.1 g, 8.4 mmol) was taken up in 4 mL of THF and the solution was added. After stirring at $-78\text{ }^{\circ}\text{C}$ for 5 min, the reaction was quenched with saturated aq. NH₄Cl and warmed to room temperature. The mixture was diluted with ethyl acetate and extracted 3 times with ethyl acetate. The organic layer was washed with brine and dried over Na₂SO₄ followed by filtration and concentrated under reduced pressure. The residue was purified by flash column chromatography on silica gel (0 to 9% ethyl acetate in DCM). The thiazole iodine was accessed in a 74 % yield.

¹H NMR (400 MHz, CDCl₃) δ 5.29 (s, 1H), 4.57 (d, J = 6.4 Hz, 2H), 1.46 (s, 9H);
¹³C NMR (100 MHz, CDCl₃) δ 176.5, 155.6, 134.6, 113.8, 85.0, 81.0, 42.6, 28.3; IR (neat) 3364, 2927, 1678, 1516; HRMS (ESI): m/z calcd. for C₁₀H₁₂IN₃NaO₂S⁺ (M + Na)⁺ 387.9587, found 387.9579.

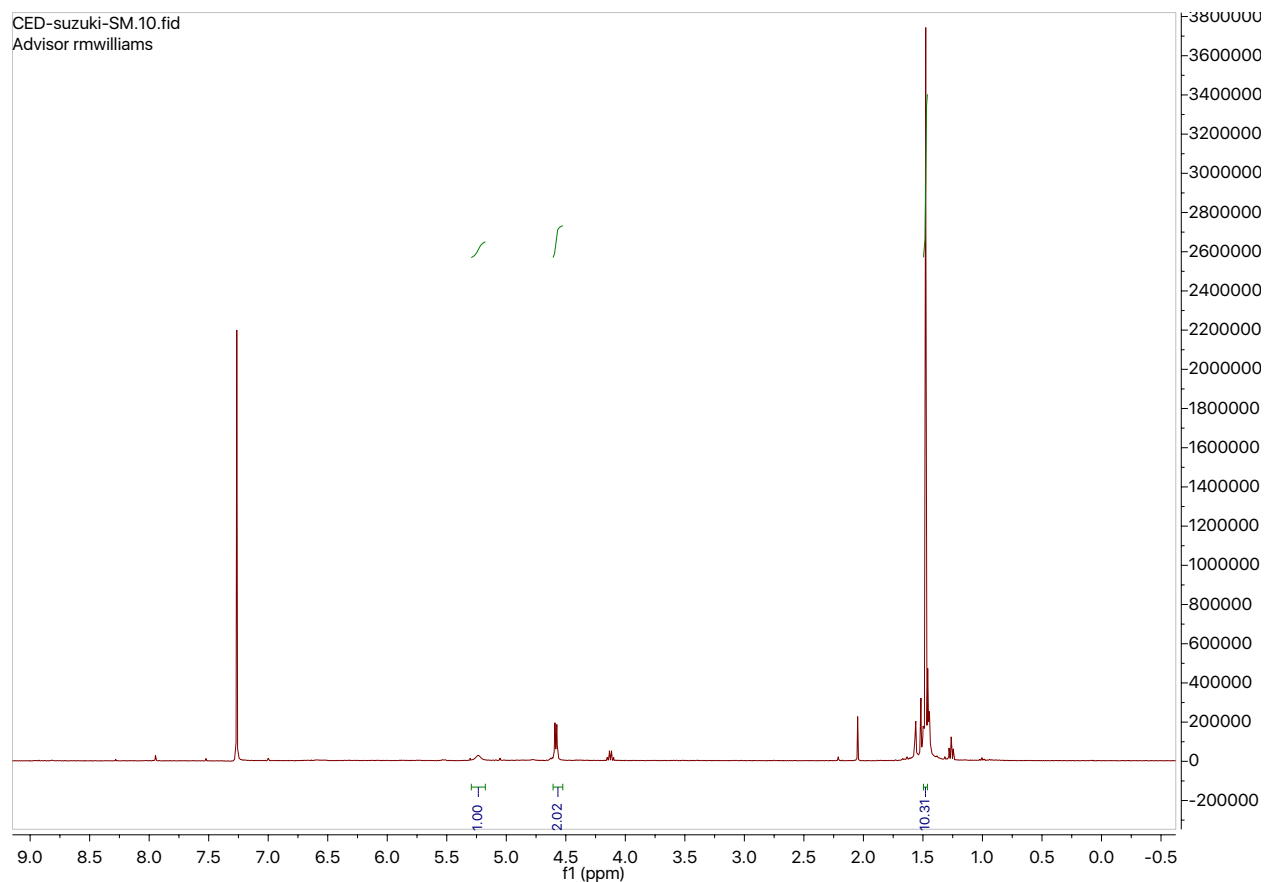
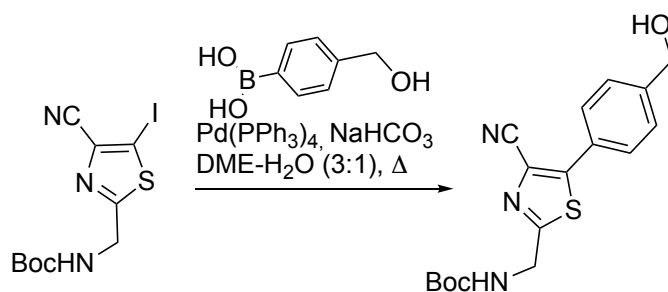


Figure 16. NMR of product



Scheme 66. Reaction conditions

Under inert atmosphere, thiazole iodide (500mg, 1.37 mmol), 4-(hydroxymethyl) phenylboronic acid (312.3 mg, 2.055 mmol), NaHCO_3 (345.24 mg, 4.11 mmol), and $\text{Pd}(\text{PPh}_3)_4$ (79.2 mg, 0.0685 mmol) were taken up in 16 mL DME:H₂O (3:1, v:v). The mixture was refluxed at 120 °C for 16 hours. The reaction was then cooled to room temperature and the reaction was

concentrated and diluted with equal parts H₂O and ethyl acetate. The organic layer was washed with brine and the aqueous layer was re-extracted with ethyl acetate. The ethyl acetate was dried over Na₂SO₄, filtered, and concentrated under reduced pressure. The crude residue was purified with silica gel column chromatography (0% to 10% methanol in DCM) to afford 220 mg of thiazole coupled product.

¹H NMR (400 MHz, CDCl₃): δ 7.68 (dd, *J* = 8.1, 1.5 Hz, 2H), 7.47 (d, *J* = 7.9 Hz, 2H), 5.41 (s, 1H), 4.74 (d, *J* = 7.7 Hz, 2H), 4.56 (d, *J* = 6.4 Hz, 2H), 1.47 (s, 9H).

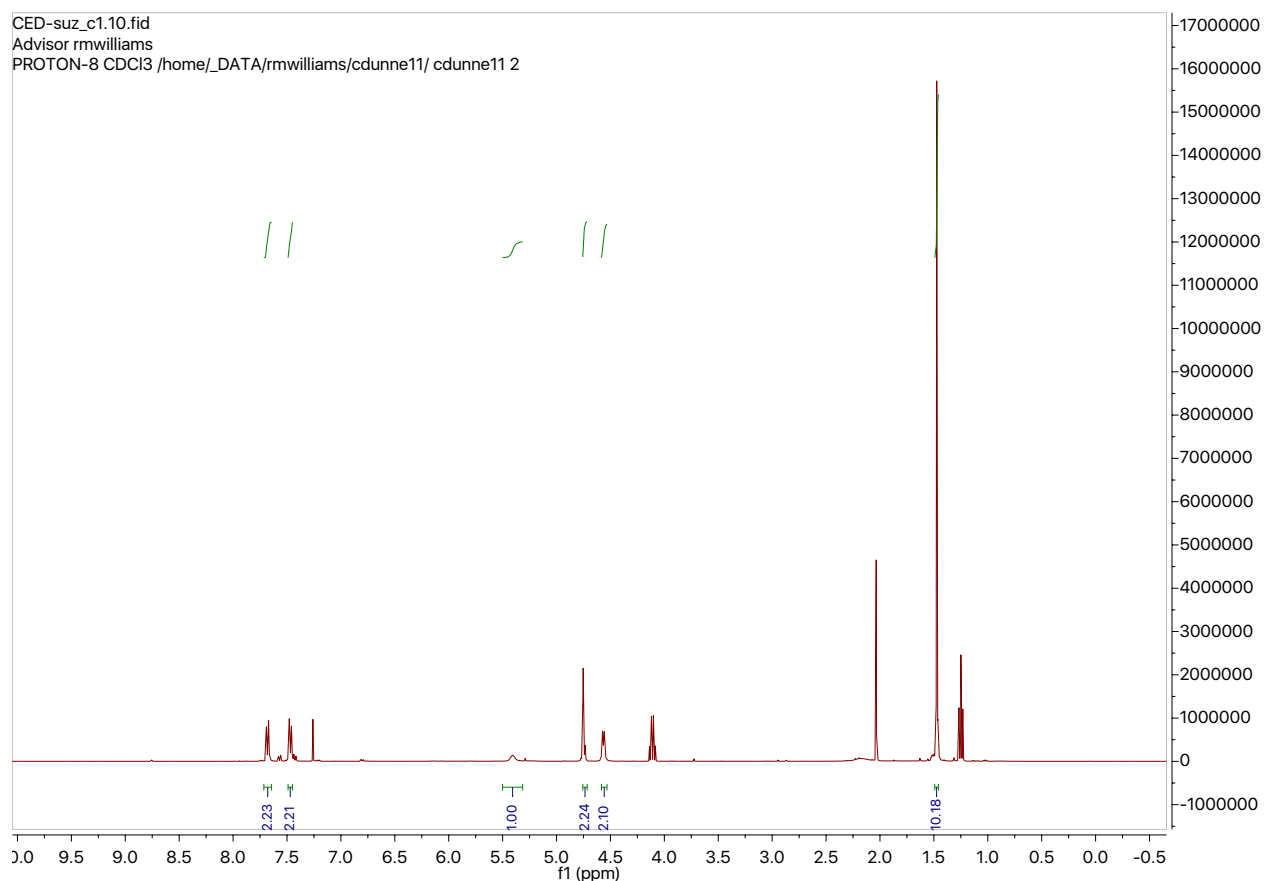
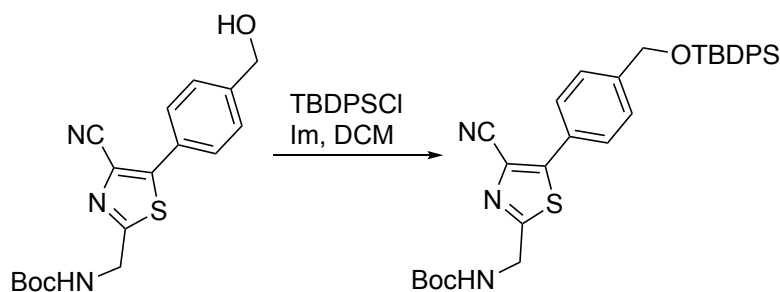


Figure 17. NMR of product



Scheme 67. Reaction conditions

Under inert atmosphere free alcohol (87.6 mg, 0.25 mmol) and imidazole (51.1 mg, 0.75 mmol) were taken up in 3 mL of DCM. 130 μ L of TBDPSCI (0.5 mmol) was added to the solution and the reaction was stirred overnight at room temperature. The reaction was quenched with 10% NH_4Cl in H_2O . The product was extracted three times with DCM and the organic was washed with brine. DCM was dried over Na_2SO_4 , filtered through a cotton plug, and evaporated under reduced pressure. The crude residue was purified with flash column chromatography on silica gel (12/1 to 5/1 hexane/ethyl acetate) to yield pure TBDPS protected alcohol (65 mg, 0.11 mmol) as a yellow solid.

$^1\text{H NMR}$ (400 MHz, CDCl_3) δ 7.71-7.69 (m, 6H), 7.48-7.37 (m, 8H), 5.38 (brs, 1H), 4.81 (s, 2H), 4.58 (d, $J = 8.2$ Hz, 2H), 7.41 (d, $J = 8.2$, 2H), 5.64 (brs, 1H), 4.70 (s, 2H), 4.52 (d, $J = 6.1$ Hz, 2H), 1.48 (s, 9H), 1.11 (s, 9H); **$^{13}\text{C NMR}$** (100 MHz, CDCl_3) δ 168.6, 155.7, 144.0, 135.6, 133.2, 129.9, 128.1, 127.9, 126.9, 120.6, 114.8, 80.8, 65.0, 42.5, 28.4 (X3), 26.9 (X3), 19.4; **IR** (neat) 3352, 2930, 2856, 2227, 1705, 1507, 1366, 1247, 1106, 823, 700; **HRMS** (ESI): m/z calcd. for $\text{C}_{33}\text{H}_{37}\text{N}_3\text{NaO}_3\text{SSi}^+$ ($\text{M} + \text{Na}$) $^+$ 606.2217, found 606.2211.

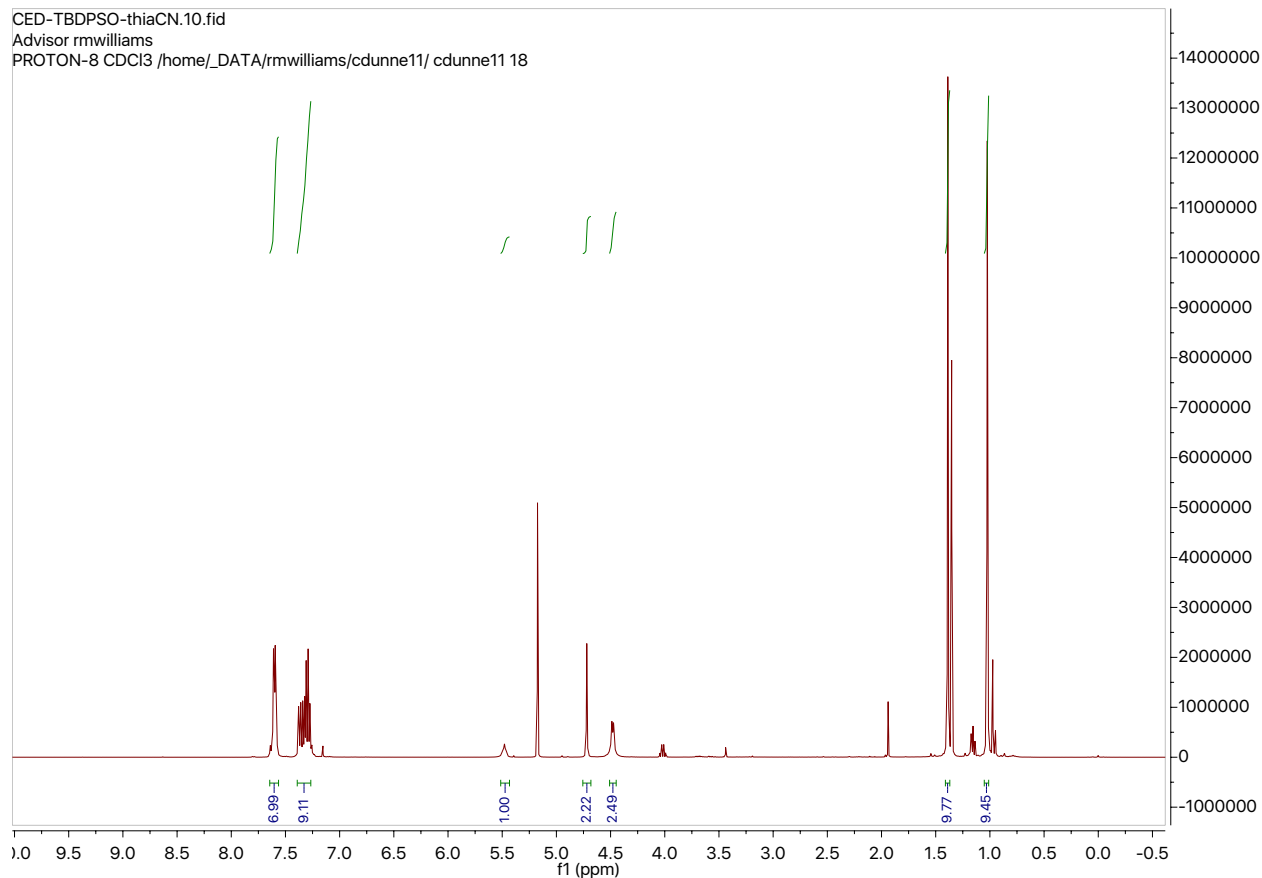
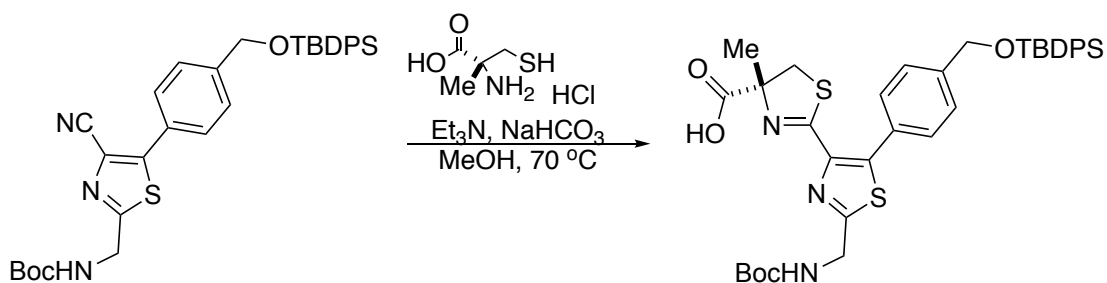


Figure 18. NMR of product

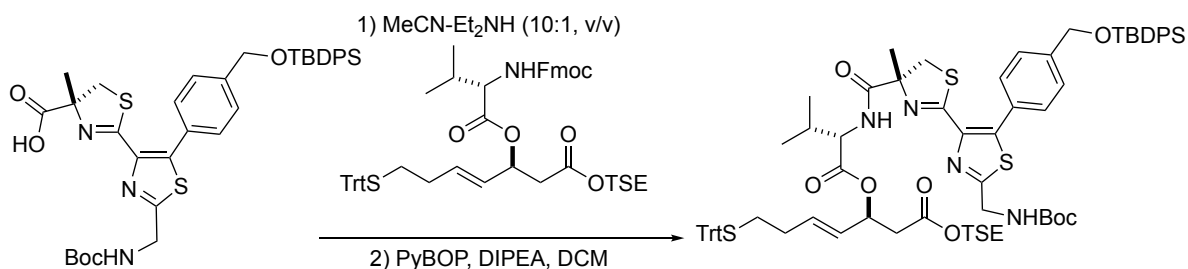


Scheme 68. Reaction conditions

Protected thiazole nitrile (154 mg, 0.26 mmol), *l*-methionine (66.92 mg, 0.39 mmol), and NaHCO_3 (32.76 mg, 0.39 mmol) were taken up in 3 mL methanol under an inert atmosphere. 72 μL of triethylamine (0.52 mmol) was added to the solution and the mixture was brought to 70

°C. The solution was refluxed for 15 hours. The mixture was cooled to room temperature and concentrated under reduced pressure. Crude oil was taken up in ethyl acetate and washed with 1M aqueous KHSO₄ and brine, prior to drying over Na₂SO₄. Ethyl acetate was filtered, concentrated under reduced pressure, and purified by flash column chromatography on silica gel (9% ethyl acetate in DCM followed by 9% methanol in DCM) to provide 110 mg of protected thiazole-thiazoline as a yellow oil.

¹H NMR (400 MHz, CDCl₃) δ 9.40 (brs, 1H), 7.73 (d, *J* = 7.7 Hz, 4H), 7.48-7.26 (m, 10H), 5.56 (brs, 1H), 4.83 (s, 2H), 4.63 (d, *J* = 5.7 Hz, 2H), 3.74 (d, *J* = 11.5 Hz, 1H), 3.25 (d, *J* = 11.5 Hz, 1H), 1.54 (s, 3H), 1.49 (s, 9H), 1.13 (s, 9H); ¹³C NMR (100 MHz, CDCl₃) δ 168.6, 155.7, 144.0, 135.6, 133.2, 129.9, 128.1, 127.9, 126.9, 120.6, 114.8, 80.8, 65.0, 42.5, 28.4 (X3), 26.9 (X3), 19.4; IR (neat) 3350, 2938, 2929, 2856, 1713, 1509, 1427, 1367, 1249, 1165, 1112, 744, 702; HRMS (ESI): *m/z* calcd. for C₃₇H₄₄N₃O₅S₂Si⁺ (M+ H)⁺ 702.2486, found 702.2484.



Scheme 69. Reaction conditions

Depsipeptide base fragment (67.2 mg, 0.08 mmol) was taken up in 10 mL acetonitrile under an inert atmosphere and brought to 0 °C. 1 mL of diethylamine was added to the solution and the mixture was stirred for two hours at room temperature. The solution was evaporated under reduced pressure and azeotroped three times with toluene (3 mL each). In a separate flask, thiazole-thiazoline (58.9 mg, 0.08 mmol) was dissolved in DCM. PyBOP (83.3 mg, 0.16 mmol) and 41 μ L DIPEA (0.24 mmoles) were added to the mixture and stirred at room temperature for 20 minutes.

Deprotected, crude amine was canulated into the thiazole-thiazoline solution with a total of 8 mL DCM. The reaction was stirred for three hours at room temperature, concentrated under reduced pressure and purified with column chromatography (6% to 25% ethyl acetate in hexane). Premacrocycle was accessed in 50% yield (0.04 mmol) as a yellow film.

$^1\text{H NMR}$ (400 MHz, CDCl_3) δ 7.72-7.70 (m, 4H), 7.52 (d, $J = 8.1$ Hz, 2H), 7.43-7.35 (m, 15H), 7.28-7.17 (m, 8H), 6.83 (d, $J = 8.8$ Hz, 1H), 5.60-5.52 (m, 2H), 5.41 (brs, 1H), 5.32 (dd, $J = 15.4, 7.3$ Hz, 2H), 4.86-4.78 (m, 2H), 4.63 (d, $J = 5.7$ Hz, 2H), 4.31 (dd, $J = 8.7, 5.2$ Hz, 2H), 4.14 (dd, $J = 9.0, 8.0$ Hz, 2H), 3.63 (d, $J = 11.5$ Hz, 1H), 3.23 (d, $J = 11.5$ Hz, 1H), 2.63 (dd, $J = 15.4, 7.3$ Hz, 1H) 2.50 (dd, $J = 15.6, 6.2$ Hz, 1H), 2.16-2.12 (m, 2H), 2.00-1.93 (m, 2H), 1.50 (s, 9H), 1.47 (s, 3H), 1.12 (s, 9H), 0.98-0.92 (m, 2H), 0.74 (d, $J = 6.8$ Hz, 3H), 0.60 (d, $J = 6.8$ Hz, 3H), 0.04 (s, 9H); $^{13}\text{C NMR}$ (100 MHz, CDCl_3) δ 1174.5, 170.0, 169.5, 162.7, 144.8, 142.4, 141.5, 135.5, 133.3, 130.1, 129.8, 129.5, 128.5, 127.9, 127.8, 126.6, 125.7, 80.4, 71.3, 66.6, 65.1, 63.0, 56.9, 42.3, 41.0, 39.7, 31.3, 31.1, 28.4, 26.9, 24.5, 19.3, 19.0, 17.5, 17.3, -1.4; **IR** (neat) 3379, 3054, 2959, 2930, 2857, 1737, 1675, 1507, 1444, 1366, 1249, 1166, 1111, 835, 752; **HRMS** (ESI): m/z calcd. for $\text{C}_{78}\text{H}_{88}\text{N}_4\text{NaO}_8\text{S}_3\text{Si}_2^+$ ($\text{M} + \text{Na}$) $^+$ 1323.5200, found 1323.5165.

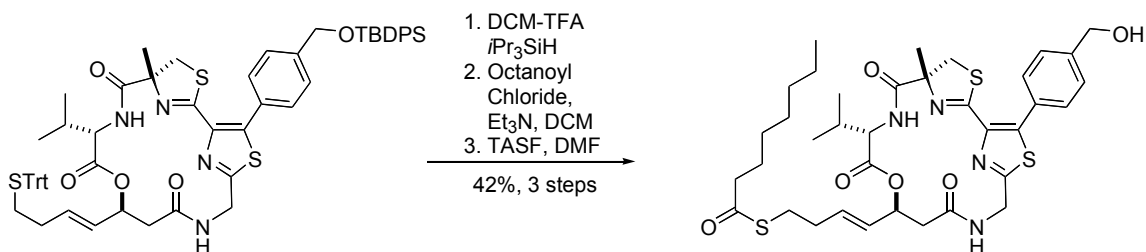


Scheme 70. Reaction conditions

Acyclic precursor (55 mg, 0.042 mmol) was dissolved in 5 mL of DCM, 1 mL of TFA was added to the solution at 0 °C. The reaction was allowed to warm to room temperature and stirred

for 16 hours. Solvents were evaporated and the crude amino acid was azeotroped with toluene (2x2 mL) to remove residual TFA. The crude amino acid was then taken up in 2 mL DCM and added to a stirred solution of DIPEA (50 μ L, 0.25 mmol) in 40 mL of CH₃CN (to ~0.001M). The resulting solution was allowed to stir for 10 minutes, before an acetonitrile (10 mL) solution of HATU (31 mg, 0.084 mmol) and HOBt (11 mg, 0.08 mmol) were added dropwise. The reaction was allowed to stir for 26 hours, then concentrated and redissolved in ethyl acetate. The solution was washed with saturated aqueous NH₄Cl, NaHCO₃ and brine, dried over Na₂SO₄, filtered, and concentrated under reduced pressure. The residue was purified by flash column chromatography on silica gel (9% methanol in DCM for the first column and 16% to 50% ethyl acetate in hexane for the second column) to afford 10.9 mg (24% yield) protected macrocycle.

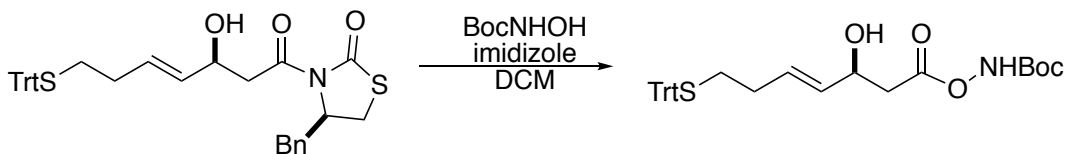
¹H NMR (400 MHz, CDCl₃) δ 7.67 (d, J = 7.0 Hz, 4H), 7.45-7.13 (m, 25H), 6.79 (brs, 1H), 5.74-5.64 (m, 2H), 5.41 (dd, J = 11.5, 6.0 Hz, 1H), 5.10 (dd, J = 17.6, 8.0 Hz, 1H), 4.81 (s, 2H), 4.61 (dd, J = 9.4, 3.7 Hz, 1H), 4.23 (dd, J = 17.4, 1.8 Hz, 1H), 3.86 (d, J = 11.4 Hz, 1H), 3.18 (d, J = 11.4 Hz, 1H), 2.70-2.69 (m, 2H), 2.25-2.01 (m, 5H), 1.80 (s, 3H), 1.23 (dd, J = 6.9, 6.4 Hz, 1H), 1.09 (s, 9H), 0.72 (d, J = 6.7 Hz, 3H), 0.61 (d, J = 6.8 Hz, 3H); 172.5, 169.1, 168.9, 165.6, 145.0, 135.7, 133.3, 130.2, 130.0, 129.7, 128.0, 127.9, 127.7, 126.8, 126.2, 71.7, 66.9, 65.2, 58.0, 44.1, 41.0, 40.8, 34.1, 31.7, 31.4, 27.0, 19.5, 19.2, 17.4; IR (neat) 3227, 2959, 2868, 103, 1484, 1250, 1195 1036, 738; HRMS (ESI): m/z calcd. for C₆₃H₆₇N₄O₅S₃Si (M+ H)⁺ 1083.4037, found 1083.4021.



Scheme 71. Reaction conditions

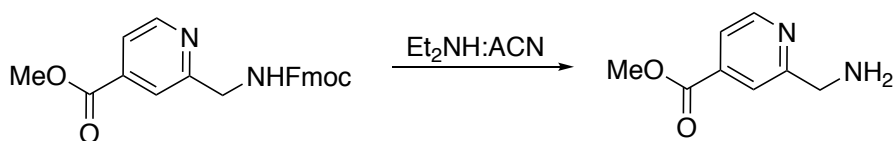
Trityl thiol 1 (58 mg, 53 μmol) was dissolved in 2.0 mL of DCM. 100 μL of TFA and $i\text{Pr}_3\text{SiH}$ (22 μL , 107 μmol) were added to the solution at 0 $^\circ\text{C}$. The reaction was allowed to warm to room temperature and stirred for 30 min. Solvents were evaporated and the residue was azeotroped with toluene (2 x 2 mL) to remove residual TFA. Crude thiol was dissolved in 2.0 mL of DCM and cooled to 0 $^\circ\text{C}$. The mixture was successively treated with Et_3N (70 μL , 0.53 mmol) and octanoyl chloride (18 μL , 0.11 mmol). The reaction was allowed to warm to room temperature and stirred for 2 hours. The reaction was cooled to 0 $^\circ\text{C}$ and quenched with 0.1 mL of 3N NH_4OH , before being concentrated and purified via column chromatography (11% AcOEt in DCM). TBDPS-protected thioester and TASF (21.5 mg, 78 μmol) were combined and 1.0 mL of DMF was added at room temperature. The reaction was allowed to warm to room temperature and stirred for 6 hours. Solvent was evaporated and the residue was purified by flash column chromatography on silica gel (11% to 33% AcOEt in DCM) to afford the product as a 42% yield over 3 steps (16.2 mg).

^1H NMR (400 MHz, CDCl_3) δ 7.44 (m, 4H), 6.94 (br, 1H), 5.85 (ddd, $J = 15.3, 7.3, 7.1$ Hz, 1H), 5.72 (br, 1H), 5.57-5.46 (m, 3H), 5.14 (dd, $J = 17.8, 8.1$ Hz, 1H), 4.77 (s, 2H), 4.68 (dd, $J = 9.8, 3.9$ Hz, 1H), 4.39 (dd, $J = 18.0, 2.3$ Hz, 1H), 3.85 (dd, $J = 11.4, 2.3$ Hz, 1H), 3.16 (dd, $J = 11.5, 1.4$ Hz, 1H), 2.93-2.69 (m, 4H), 2.51 (dd, $J = 7.5, 7.5$ Hz, 1H), 2.31 (dd, $J = 7.5, 0.5$ Hz, 1H), 2.21 (dd, $J = 7.5, 7.5$ Hz, 1H), 2.10 (m, 1H), 1.85 (s, 3H), 1.63 (m, 2H), 1.27 (m, 10H), 0.87 (m, 3H), 0.74 (d, $J = 6.8$ Hz, 1H), 0.62 (d, $J = 6.8$ Hz, 1H); **^{13}C NMR** (100 MHz, CDCl_3) 199.5, 175.9, 173.8, 169.2, 165.4, 143.3, 142.0, 132.7, 131.0, 129.8, 127.9, 127.6, 126.4, 83.3, 64.6, 44.2, 40.9, 36.2, 31.7, 29.0, 25.6, 22.6, 17.6, 13.6, 13.2 δ ; **IR** (neat) 3356, 2922, 2850, 1679, 1510, 1463, 1249, 1170, 1112; **HRMS** (ESI): m/z calcd. for $\text{C}_{36}\text{H}_{48}\text{N}_4\text{NaO}_6\text{S}_3^+$ ($\text{M}^+ \text{Na}^+$) 751.2628, found 751.2635.



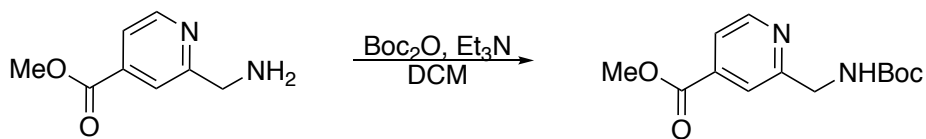
Scheme 72. Reaction conditions

Crimmins chiral auxiliary amide (0.16 mmoles, 100 mg) was dissolved in 8 mL DCM. BocNHOH (0.48 mmoles, 63.94 mg) and imidazole (0.24 mmoles, 16.34 mg) was added to the solution. The reaction was run for 16 hours. The crude mixture was evaporated and taken up in ether. Aqueous NH_4Cl was added and the organic layer was washed with sat. NaHCO_3 and brine. The organic was dried over Na_2SO_4 . The residue was purified by column chromatography on silica gel (8/1 to 4/1: Hexane/EtOAc). Due to the close R_f value of the starting material and additional column was run with a slower gradient. Product was obtained in a 45% yield.



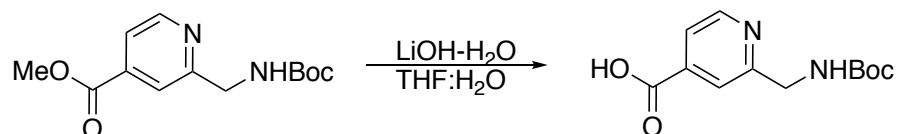
Scheme 73. Reaction conditions

Fmoc protected amine (0.51 mmoles, 200mg) was taken up in 5 mL ACN. The solution was brought to 0 °C. 500 μL of Et_2NH was added and the solution was brought to room temperature. The reaction was stirred for 2 hours and deprotection was confirmed by TLC and crude $^1\text{H-NMR}$.



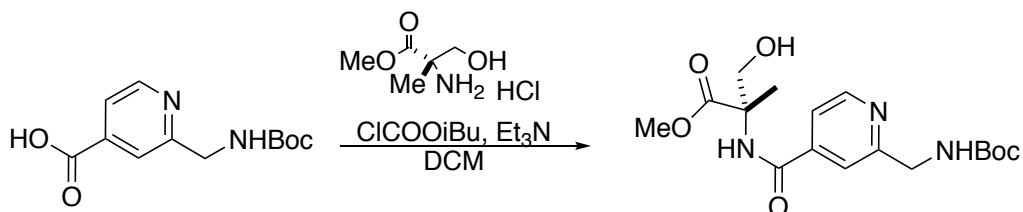
Scheme 74. Reaction conditions

Crude amine was taken up in 5 mL DCM. Boc₂O (0.56 mmoles, 122.22 mg) and Et₃N (1.53 mmoles, 213 μL) were added and the solution was stirred overnight. The reaction was quenched with aqueous NaHCO₃ and extracted with DCM (3x). The organic solution was dried over MgSO₄ and concentrated. The residue was purified by column chromatography on silica gel (6/1 to 2/1: Hexane/EtOAc). 0.45 mmoles of Boc protect amine was obtained in an 88.2% yield.



Scheme 75. Reaction conditions

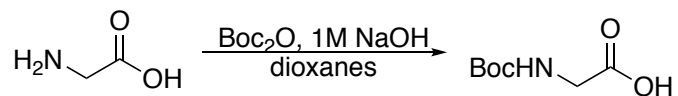
Methyl ester (0.45 mmoles, 120 mg) was taken up in a 2:1 THF:H₂O (15mL). Add LiOH-H₂O (0.9 mmoles, 37.8 mg) and stir for one hour at room temperature. The reaction was quenched with 1M NaOH and washed with EtOAc (2x). The aqueous layer was acidified to a pH of 2 with 1M HCl. Product was extracted with EtOAc (3x) and washed with brine. The organic layer was dried over Na₂SO₄ and concentrated. 0.32 mmoles of carboxylic acid was isolated in a 71% yield.



Scheme 76. Reaction conditions

At 0 °C carboxylic acid (0.12 mmoles, 30 mg) was taken up in 5 mL DCM. Et₃N (0.12 mmoles, 17 uL) was added and followed by isobutyl chloroformate (0.12 mmoles, 16.39 mg) and the reaction (solution A) was stirred for 30 minutes. In a separate flask, the amino alcohol (0.12 mmoles, 20.35 mg) was taken up in 3 mL of DCM. Et₃N (0.12 mmoles, 17 uL) was added (solution B). Solution A was cannulated into solution B at 0 °C. The flask containing Solution A was washed

1 mL of DCM (3x). The reaction was brought to room temperature and stirred overnight. The reaction was quenched with H₂O and 1M NaOH was added. The aqueous layer was washed with EtOAc (2x) and concentrated to provide product.



Scheme 77. Reaction conditions

To a solution of glycine (133.2 mmol, 10g) in 225 mL 1M NaOH at 0 °C, Boc₂O (159.9 mmoles, 34.8 g) via 150 mL of dioxanes was added over one hour. The mixture was warmed to room temperature and stirred for 3.5 hours. The solution was brought to half volume and cooled to 0 °C. 1M KHSO₄ was added until the solution reached a pH of ~3 (~100mL). The Boc protected amine was extracted with EtOAc (3x) and dried over Na₂SO₄. The mixture was concentrated. Quantitative yield was carried on to the next step.

¹H NMR (300 MHz, Chloroform-*d*) δ 5.02 (s, 1H), 3.97 (d, *J* = 5.6 Hz, 3H), 1.46 (s, 9H).

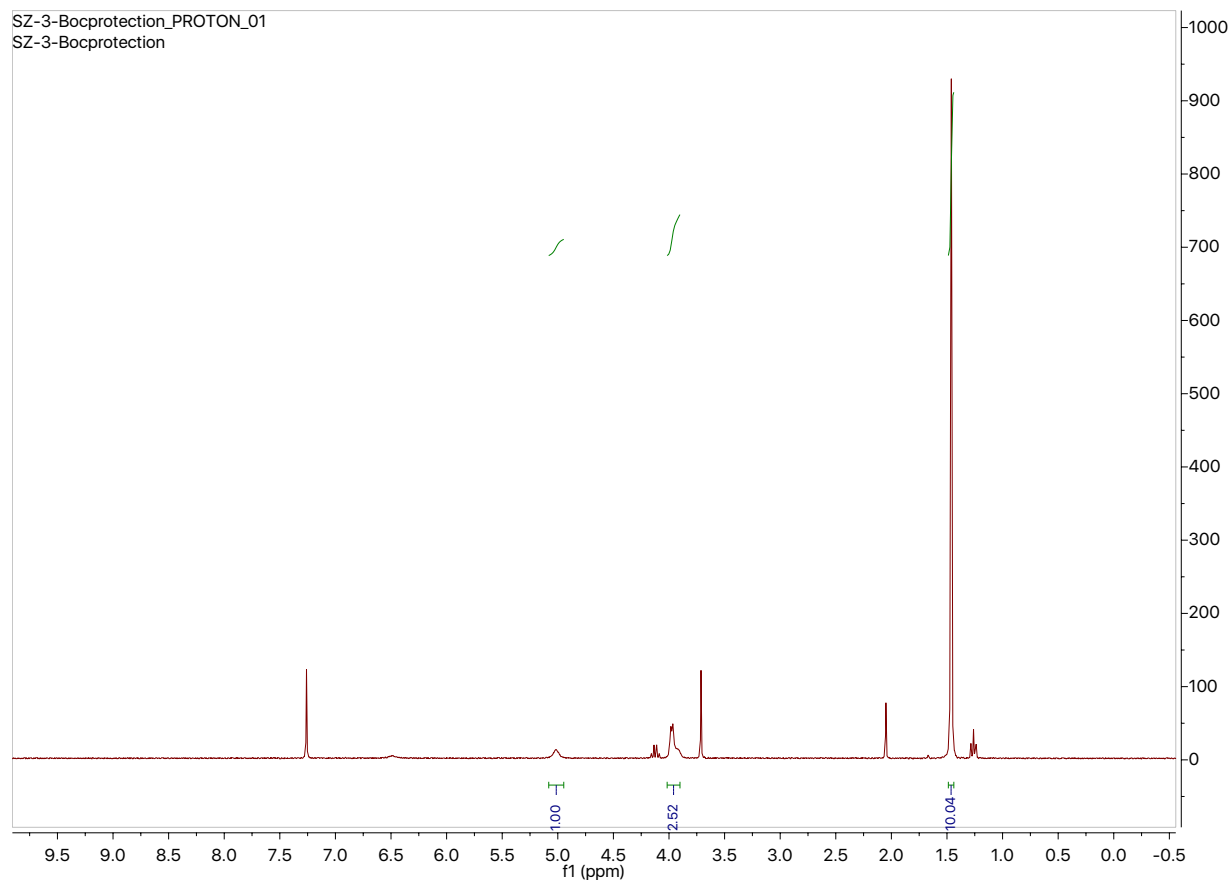
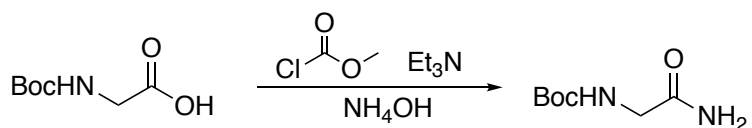


Figure 19. NMR of product



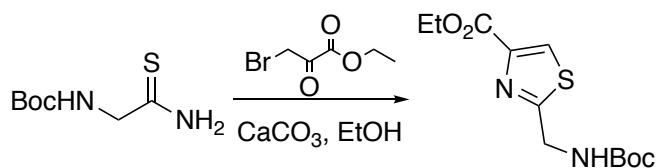
Scheme 78. Reaction conditions

N-Boc glycine (131.5 mmoles, 23.04 mg) was taken up in 250 mL THF and brought to -10 °C (ethylene glycol with dry ice bath). Et_3N (144.65 mmoles, 20.2 mL) was added followed by the dropwise addition of methylchloroformate (144.65 mmoles, 11.2 mL) over 30 minutes. 50 mL of 10% NH_4OH was added and the solution was warmed to room temperature. The mixture was stirred for two hours. The organic solution was evaporated and crude amide was carried on to the next reaction.



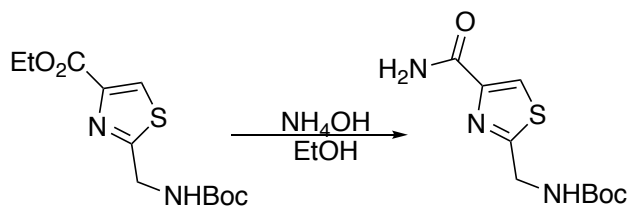
Scheme 79. Reaction conditions

To a stirred solution of crude amide (132 mmoles, 23 g) in DME at room temperature, Lawesson's reagent (66 mmoles, 26.7 g) was added. The solution was stirred for 16 hours. DME was evaporated and the crude product was taken up in EtOAc. Organic was washed with 10% NaHCO₃. The aqueous layer was washed with EtOAc (2x) and dried over Na₂SO₄. Crude was carried on to the next reaction.



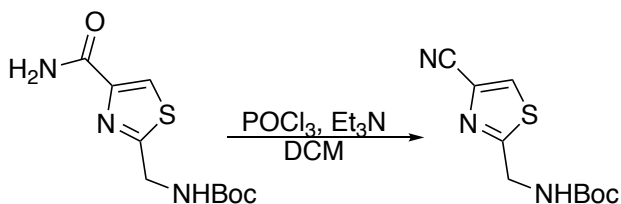
Scheme 80. Reaction conditions

A solution of crude thioamide (132 mmoles, 25 g) in 300 mL EtOH was prepared at room temperature. CaCO₃ (67.32 mmoles, 6.74 g) and ethyl bromo pyruvate (145.2 mmol, 18mL) was added to the solution and stirred at room temperature for 18 hours. The reaction was passed through a celite plug and the crude was taken up in CHCl₃. The organic was washed with NaHCO₃, H₂O, and brine. CHCl₃ solution was dried over Na₂SO₄ and concentrated. The residue was purified by column chromatography on silica gel (20% to 60% EtOAc in Hexanes).



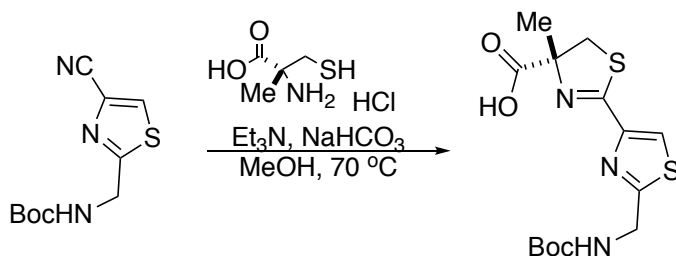
Scheme 81. Reaction conditions

Ester (6.89 mmoles, 2 g) was taken up in 30 mL EtOH at room temperature. 35 mL of NH_4OH was added and the reaction was stirred for 16 hours. The solvent was removed and crude amide was carried on to the next step.



Scheme 82. Reaction conditions

Amide (6.89 mmoles, 1.8 g) was taken up in 50 mL DCM at $-10\text{ }^\circ\text{C}$. Et_3N (104.7 mmoles, 15 mL) was added and the solution was brought to room temperature. POCl_3 (17.45 mmoles, 1.6 mL) was slowly added to the solution and the reaction was stirred for one hour. The reaction was concentrated and taken up in DCM. The organic layer was washed with sat. K_2CO_3 , brine, and H_2O . The crude solution was dried over Na_2SO_4 and concentrated.



Scheme 83. Reaction conditions

Nitrile (1.09 mmoles, 260 mg) and NaHCO_3 (1.64 mmoles, 137.8 mg) were taken up in 5 mL of MeOH . α -methyl cysteine (1.64 mmoles, 281.4 mg) was taken up in an additional 5 mL MeOH and added to the nitrile solution. Et_3N (2.18 mmoles, 302 μL) was added and the mixture was refluxed at $70\text{ }^\circ\text{C}$ for 48 hours. The reaction was brought to room temperature, concentrated and dissolved in EtOAc . The organic was washed with KHSO_4 , brine (3x), and dried over Na_2SO_4 . The residue was purified by column chromatography on silica gel (20:1, $\text{DCM}:\text{EtOAc}$ followed by 10:1, $\text{DCM}:\text{MeOH}$).

^1H NMR (400 MHz, Chloroform-*d*) δ 7.96 (d, $J = 6.8$ Hz, 1H), 5.67 – 5.48 (m, 1H), 4.60 (d, $J = 6.1$ Hz, 2H), 3.88 (d, $J = 11.5$ Hz, 1H), 3.38 – 3.24 (m, 1H), 1.65 (s, 3H), 1.45 (s, 9H).

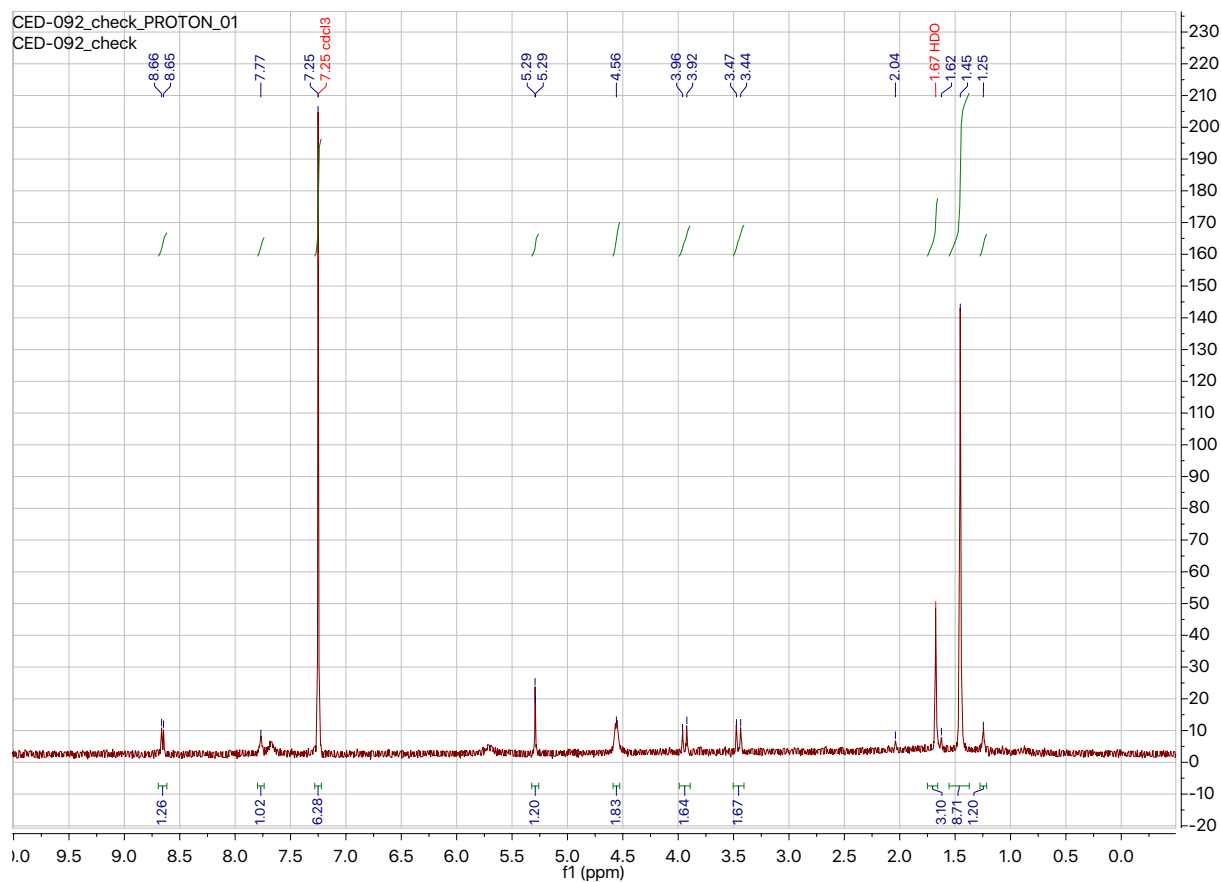
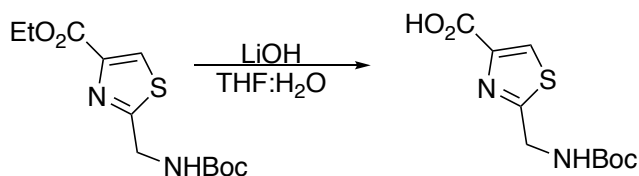
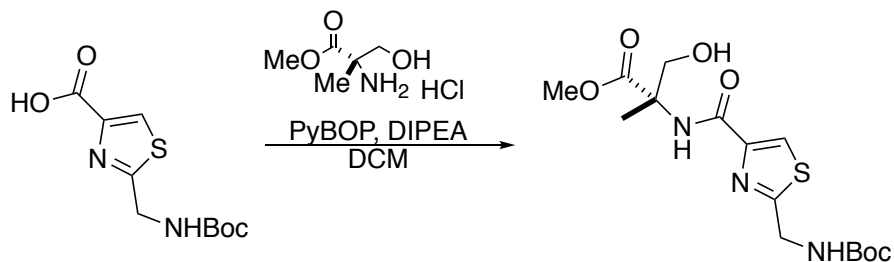


Figure 20. NMR of product



Scheme 84. Reaction conditions

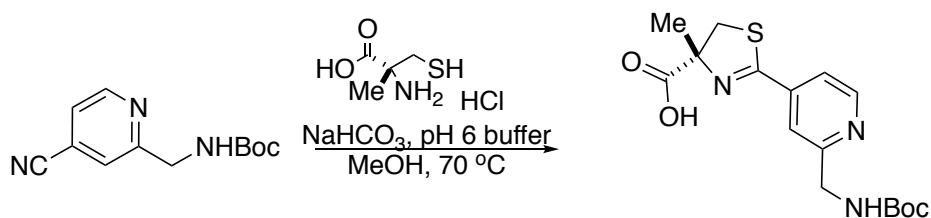
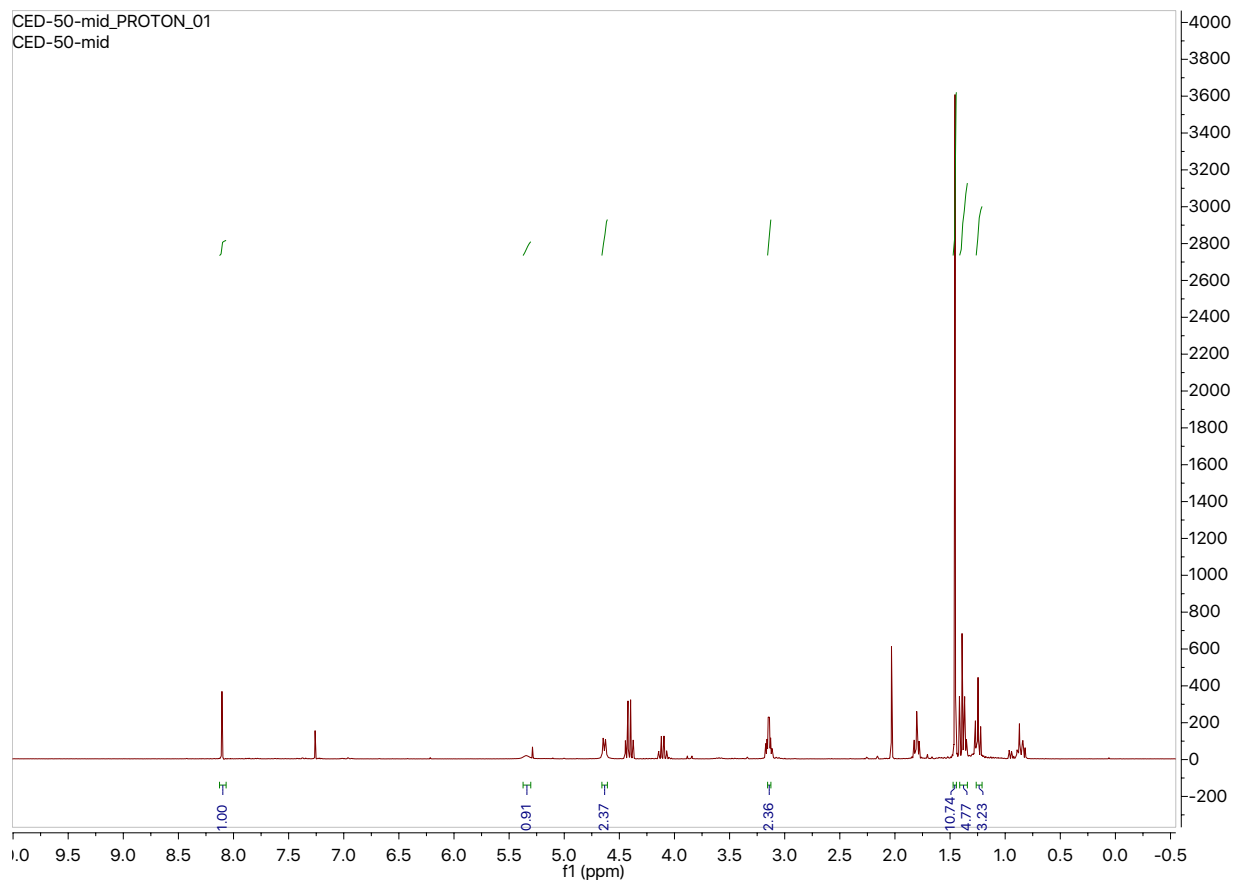
Thiazole (1.75 mmoles, 500 mg) was taken up in a 2:1 mixture of THF:H₂O (60mL). LiOH (3.5 mmoles, 83.8 mg) was added and the solution was stirred for 2 hours. The reaction was brought to a pH of 2 with 1M HCl. The carboxylic acid was extracted with EtOAc (3x) and dried over Na₂SO₄ followed by concentration. The crude carboxylic acid was carried on to the next step.



Scheme 85. Reaction conditions

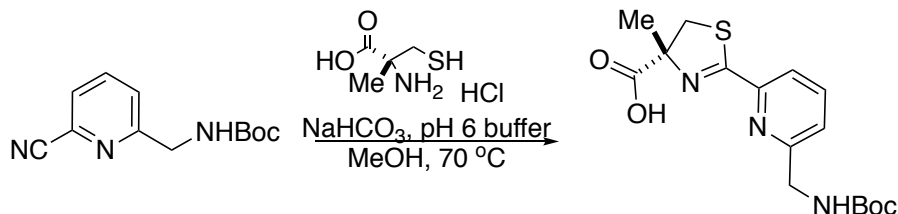
Crude acid was dissolved in 150 mL DCM. PyBOP (5.04 mmoles, 2.62 g), DIPEA (7.56 mmol, 1.32 mL), and L-methionine (3.02 mmoles, 512 mg) was added to the solution and stirred for 16 hours. The reaction was concentrated and purified by column chromatography on silica gel (20% to 80% EtOAc in hexanes). 0.94 mmoles of coupled amide was obtained in a 54% yield over two steps.

^1H NMR (300 MHz, Chloroform-*d*) δ 8.13 – 8.07 (m, 1H), 5.34 (s, 1H), 4.64 (d, $J = 6.4$ Hz, 2H), 3.16 – 3.13 (m, 2H), 1.47 – 1.44 (m, 11H), 1.41 – 1.34 (m, 5H), 1.26 – 1.21 (m, 3H).



Nitrile (0.86 mmoles, 200 mg) was taken up in 5.6 mL pH 6 phosphate buffer and 3.4 mL MeOH. α -methyl cysteine (1.028 mmoles, 176.5 mg) was added via 5 mL MeOH to the solution. NaHCO_3 (1.714 mmoles, 144 mg) was added and the reaction was brought to reflux at 70 °C for 48 hours. The reaction was cooled to room temperature and the organic layer was evaporated.

Byproducts were extracted with ether and the aqueous layer was acidified to pH of 2 with 1M HCl. The crude product was extracted with EtOAc (3x) and dried over MgSO₄. The crude product was concentrated and purified by column chromatography on silica gel.



Scheme 87. Reaction conditions

Nitrile (0.86 mmoles, 200 mg) was taken up in 5.6 mL pH 6 phosphate buffer and 3.4 mL MeOH. α -methyl cysteine (1.028 mmoles, 176.5 mg) was added via 5 mL MeOH to the solution. NaHCO₃ (1.714 mmoles, 144 mg) was added and the reaction was brought to reflux at 70 °C for 48 hours. The reaction was cooled to room temperature and the organic layer was evaporated. Byproducts were extracted with ether and the aqueous layer was acidified to pH of 2 with 1M HCl. The crude product was extracted with EtOAc (3x) and dried over MgSO₄. The crude product was concentrated and purified by column chromatography on silica gel.

¹H NMR (400 MHz, Chloroform-*d*) δ 7.79 (dt, $J = 11.2, 8.1$ Hz, 1H), 7.60 (d, $J = 7.6$ Hz, 1H), 7.52 (d, $J = 8.0$ Hz, 1H), 5.47 (s, 1H), 4.48 (d, $J = 5.0$ Hz, 2H), 1.46 (s, 9H).

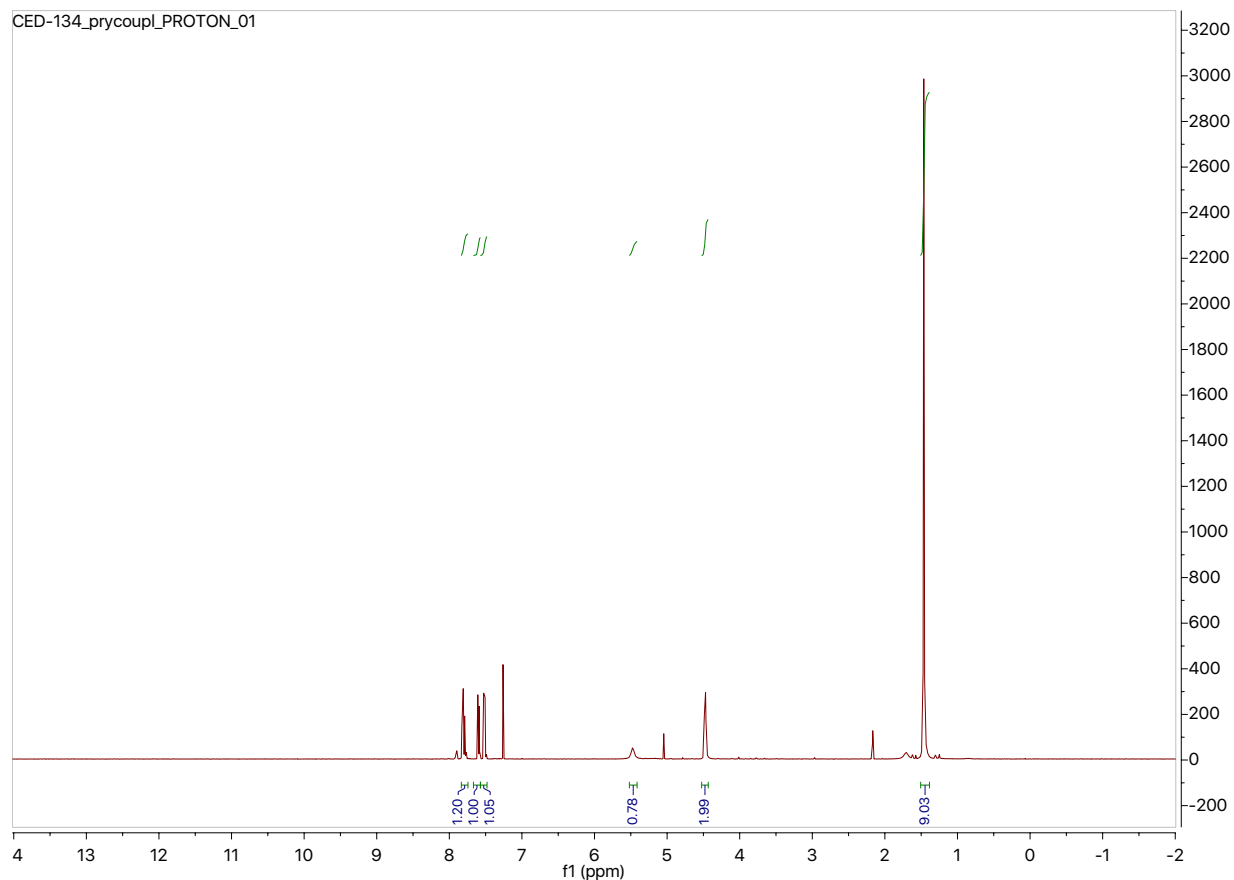
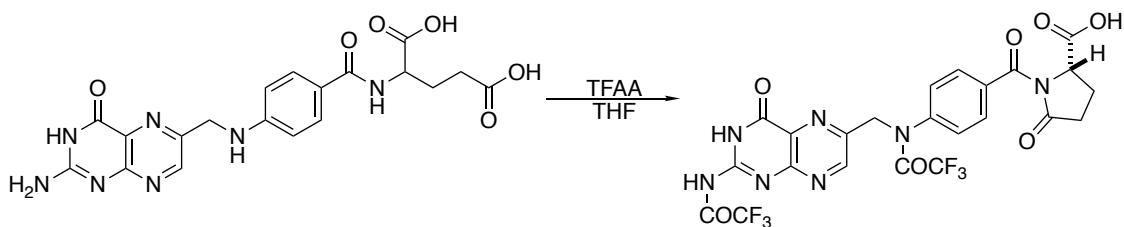
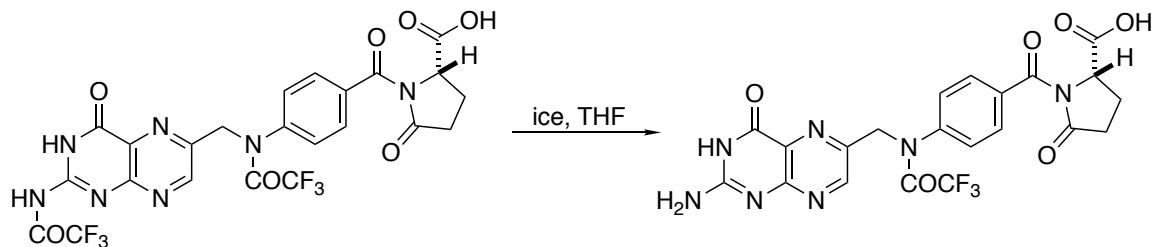


Figure 22. NMR of product



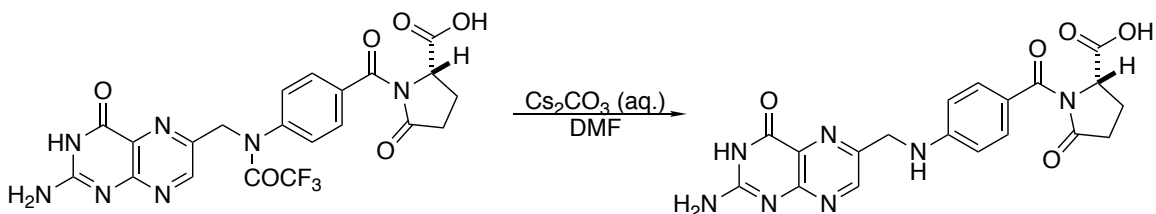
Scheme 88. Reaction conditions

Folic acid (6.7 mmol, 3 g) was taken up in 30 mL THF. The solution was brought to 0 °C. Trifluoroacetic anhydride (53.6 mmol, 7.5 mL) was added over 30 minutes. The mixture was warmed to room temperature and stirred for 10 hours. The solution went from a yellow cloudy consistency to a dark brown. The mixture was filtered through celite and evaporated. Crude was taken up in 35 mL benzene. A yellow precipitate formed rapidly and was isolated. Crude product was carried on after fluorine NMR confirmation.



Scheme 89. Reaction conditions

Crude lactam was taken up in 17 mL THF. Ice was added to the solution and was stirred at room temperature for three hours. The solution was sonicated in 10 minute intervals to bring into solution. 60 mL ether was added to precipitate the product out of solution. Crude product was isolated and carried on for final deprotection.



Scheme 90. Reaction conditions

Lactam was taken up in 63 mL DMF. 2.5 mL of aqueous Cs_2CO_3 was added and stirred at room temperature for five hours. The solution was filtered through celite and acidified to pH 4 with 1M HCl. Due to absence of precipitate formation, the mother liquor was concentrated to isolate the desired product.

^1H NMR (400 MHz, $\text{DMSO-}d_6$) δ 11.37 (s, 1H), 8.63 (s, 1H), 8.08 (d, $J = 7.6$ Hz, 1H), 7.63 (d, $J = 8.6$ Hz, 2H), 6.90 (t, $J = 6.1$ Hz, 2H), 6.83 (s, 1H), 6.62 (d, $J = 8.6$ Hz, 2H), 4.46 (d, $J = 6.0$ Hz, 2H), 4.32 (t, $J = 6.7$ Hz, 1H), 3.42 – 3.34 (m, 2H), 2.30 (t, $J = 7.4$ Hz, 3H), 2.02 (dd, $J = 13.8, 6.2$ Hz, 2H), 1.96 – 1.84 (m, 2H), 1.07 (t, $J = 7.0$ Hz, 1H).

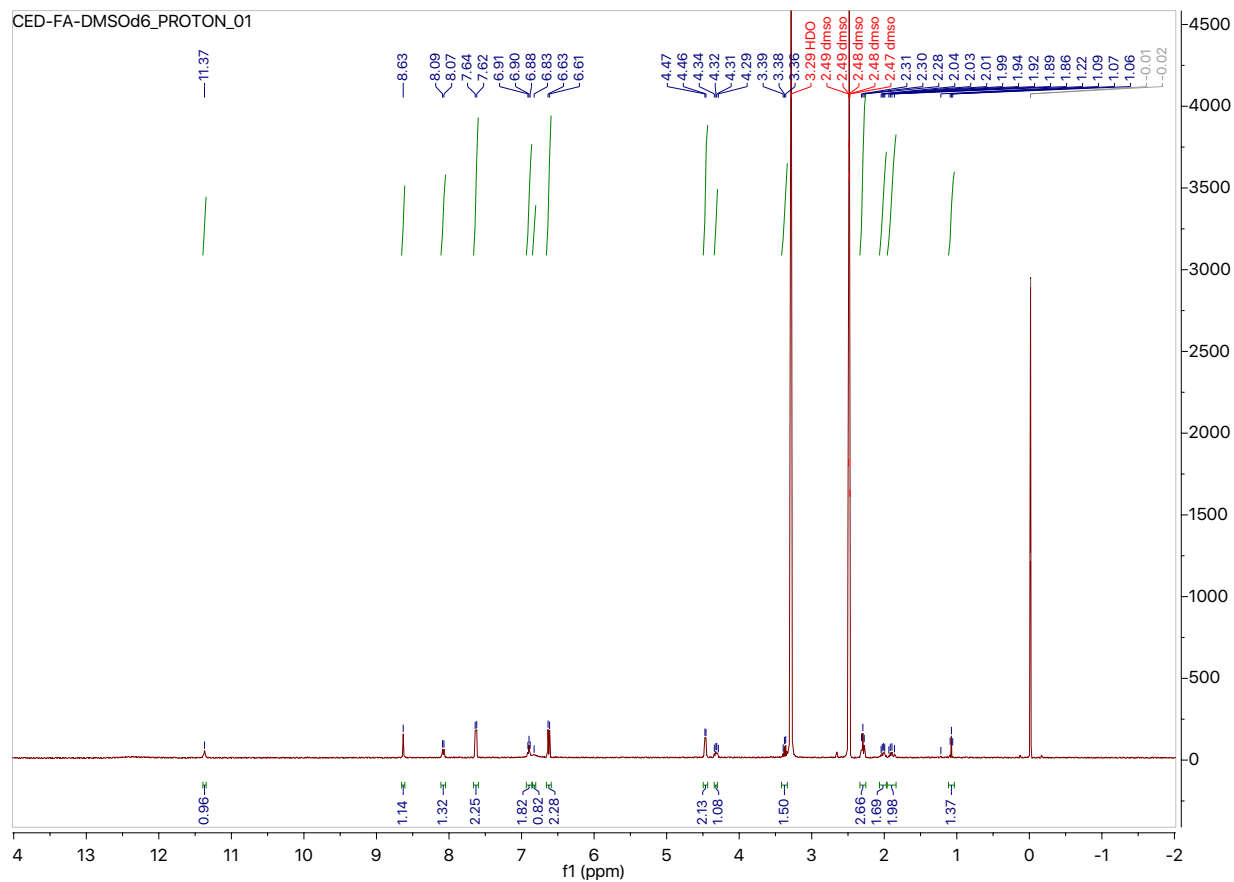
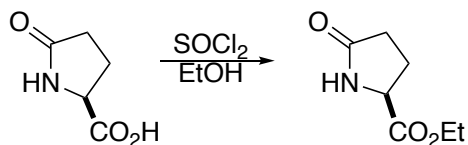
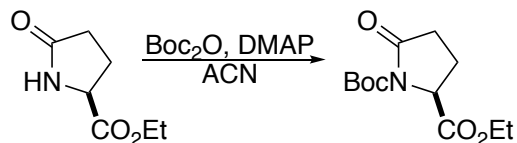


Figure 23. NMR of product



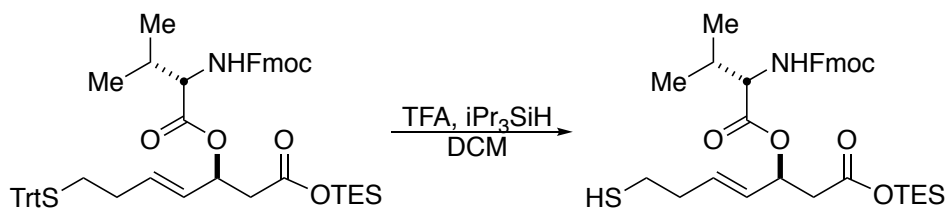
Scheme 91. Reaction conditions

Pyroglutamic acid (11.6 mmols, 1.5 g) was taken up in 20 mL of EtOH and cooled to 0 °C. Thionyl chloride (12.76 mmols, 927 uL) was added dropwise to the solution. The mixture was warmed to room temperature and stirred overnight. The reaction was cooled to 0 °C and neutralized with NaHCO₃. The product was extracted with DCM and dried over Na₂SO₄. Crude was evaporated and carried on to the next reaction.



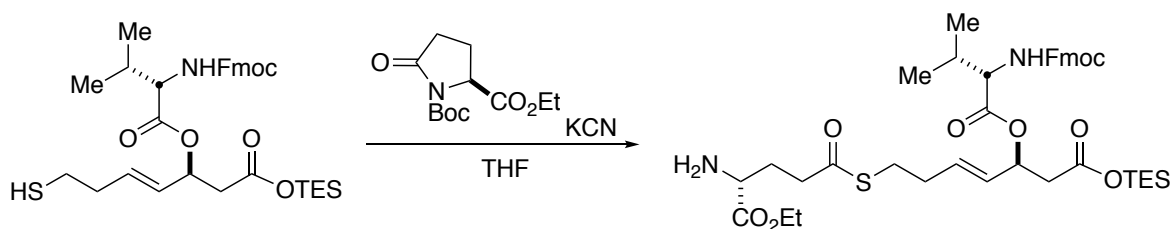
Scheme 92. Reaction conditions

Crude ester was taken up in 20 mL ACN. DMAP (1.16 mmoles, 141 mg) and Boc_2O (12.77 mmoles, 2.8 g) were added to the solution and stirred at room temperature for 18 hours. The reaction was concentrated and purified by column chromatography on silica gel (3:1 to 2:1, hexanes to EtOAc).



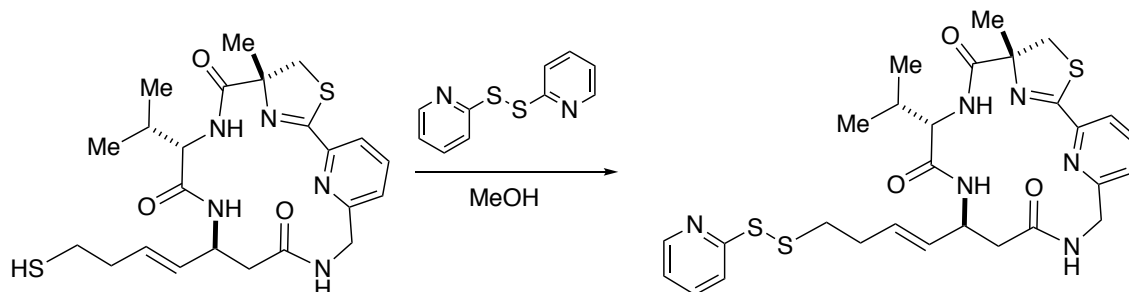
Scheme 93. Reaction conditions

Trityl protected thiol (0.23 mmoles, 200 mg) was taken up in 5 mL DCM at 0 °C. TFA (1.5 mL) and iPr_3SiH (0.46 mmoles, 94 μL) was added to the solution and stirred for two hours. The reaction was concentrated and purified by flash column chromatography on silica gel (3:1, hexane:EtOAc).



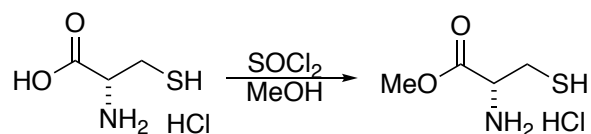
Scheme 94. Reaction conditions

Lactam (0.03 mmoles, 5mg) was taken up in THF. Free thiol (0.13 mmoles, 80 mg) was added followed by the addition of KCN (0.003 mmol, 0.2 mg). The reaction was sonicated for nine hours at room temperature.



Scheme 95. Reaction conditions

Free thiol (0.02 mmoles, 10 mg) was taken up in 0.5 mL MeOH at room temperature. Aldrithiol (0.1 mmoles, 22mg) was added and the reaction as stirred for two hours. The mixture was concentrated and the product was purified by preparatory TLC.



Scheme 96. Reaction conditions

To 70 mL MeOH at 0 °C was added 6 mL of SOCl₂ dropwise. After full addition the solution was brought to room temperature and stirred for one hour. L-cysteine (12.7 mmoles, 2 g) was added to the mixture and stirred for an additional three hours. Reaction was concentrated and the product was isolated for further reaction.

¹H NMR (300 MHz, Deuterium Oxide) δ 4.29 – 4.19 (m, 1H), 4.13 (td, *J* = 4.8, 2.4 Hz, 1H), 3.67 (q, *J* = 1.5, 1.1 Hz, 2H), 3.16 – 3.11 (m, 3H), 2.98 – 2.91 (m, 3H).

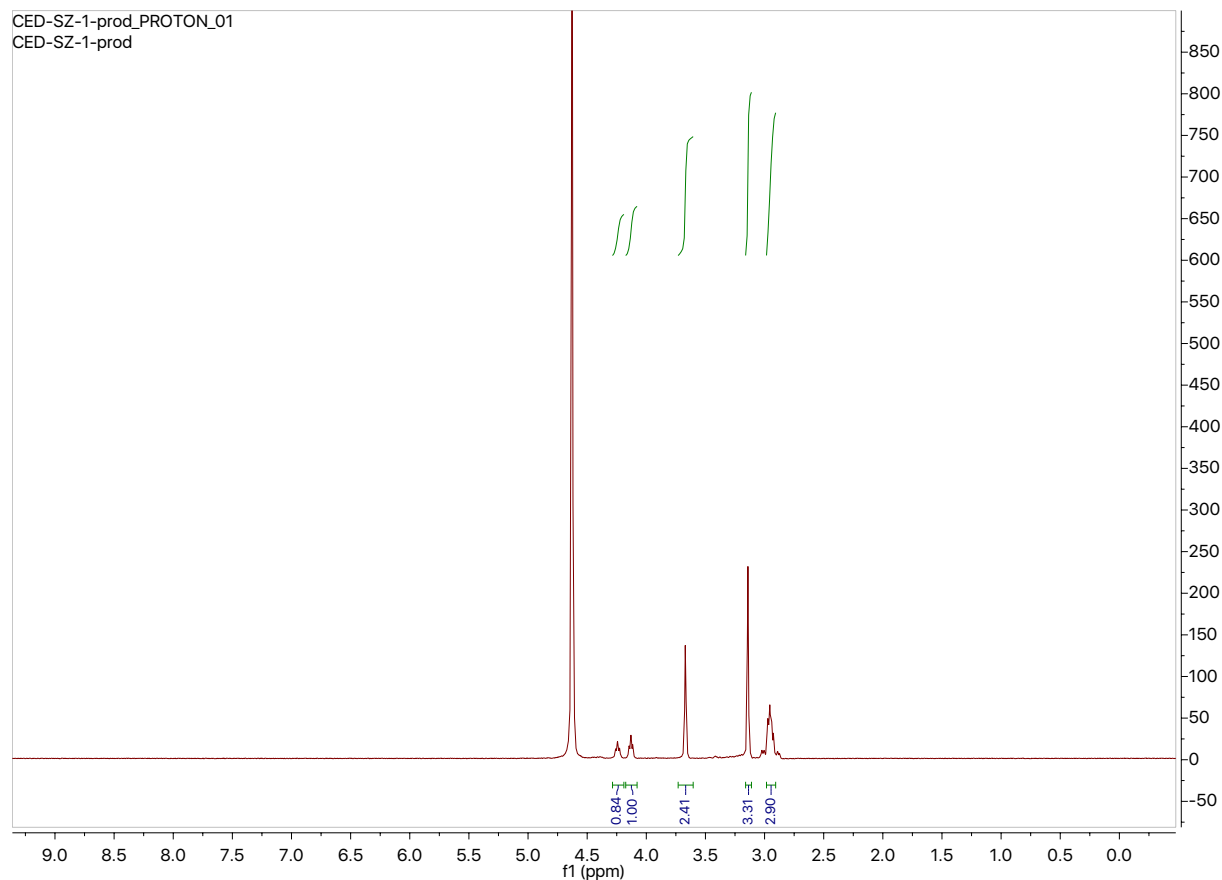
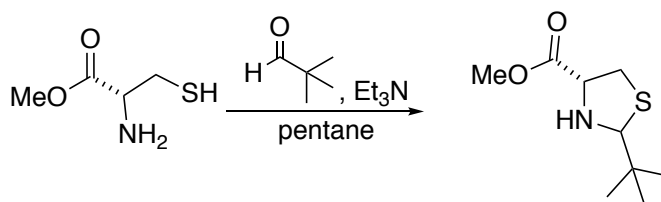


Figure 24. NMR of product



Scheme 97. Reaction conditions

Cysteine methyl ester hydrochloride (58.3 mmoles, 10 g) was taken up in 200 mL of pentane. Pivaldehyde (64.13 mmoles, 6.96 mL) and Et_3N (64.13 mmoles, 8.94 mL) were added to the solution at room temperature. The reaction was refluxed with a Dean Stark set up at 60 °C for 16 hours. The solution was cooled and filtered through celite. The celite cake was washed with ether and the organic extract was concentrated. Ester was isolated in quantitative yield to provide a light yellow oil.

^1H NMR (300 MHz, Chloroform-*d*) δ 4.47 (s, 1H), 3.86 – 3.79 (m, 1H), 3.80 – 3.76 (m, 3H), 3.27 (dd, $J = 10.2, 6.7$ Hz, 1H), 2.73 – 2.64 (m, 1H), 1.13 – 1.00 (m, 9H).

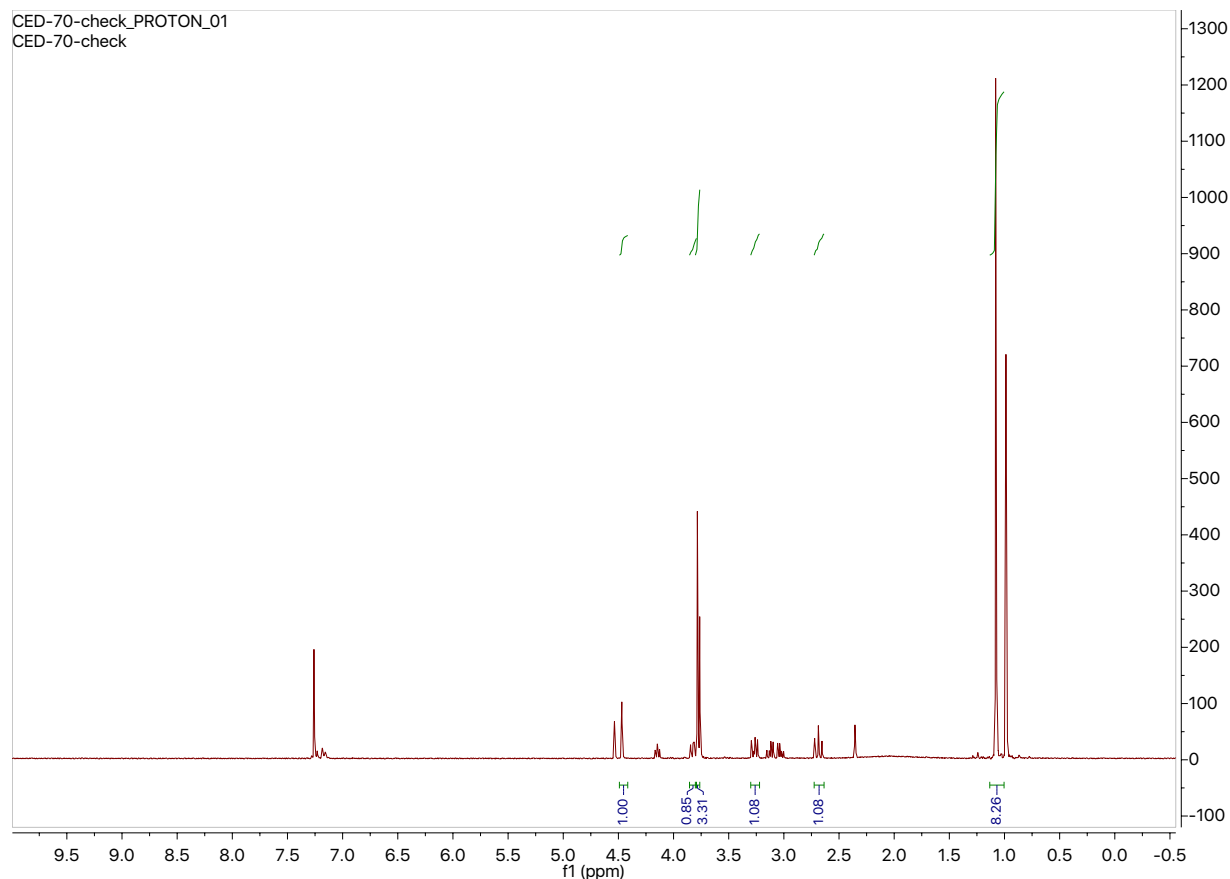
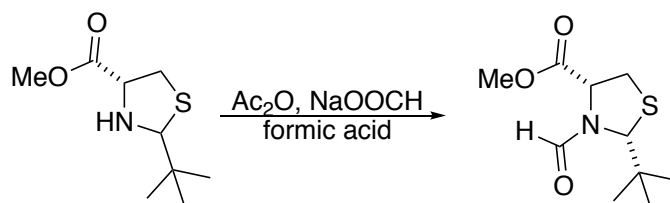


Figure 25. NMR of product



Scheme 98. Reaction conditions

Thiazolidine (49.2 mmol, 10 g) and sodium formate (54.12 mmol, 3.7 g) were taken up in 73 mL of formic acid at 0 °C. Acetic anhydride (148.1 mmol, 14 mL) was added dropwise over one hour. The reaction was warmed to room temperature and stirred overnight. The solvent

was removed and the compound was neutralized with NaHCO_3 . The product was extracted with ether and dried over Na_2SO_4 . The concentrated white solid yielded protected amine 78% yield.

^1H NMR (400 MHz, Chloroform-*d*) δ 8.36 (s, 1H), 4.90 (t, $J = 8.7$ Hz, 1H), 4.75 (s, 1H), 3.78 (d, $J = 0.9$ Hz, 3H), 3.52 – 3.43 (m, 1H), 3.34 – 3.25 (m, 2H), 1.04 (s, 9H).

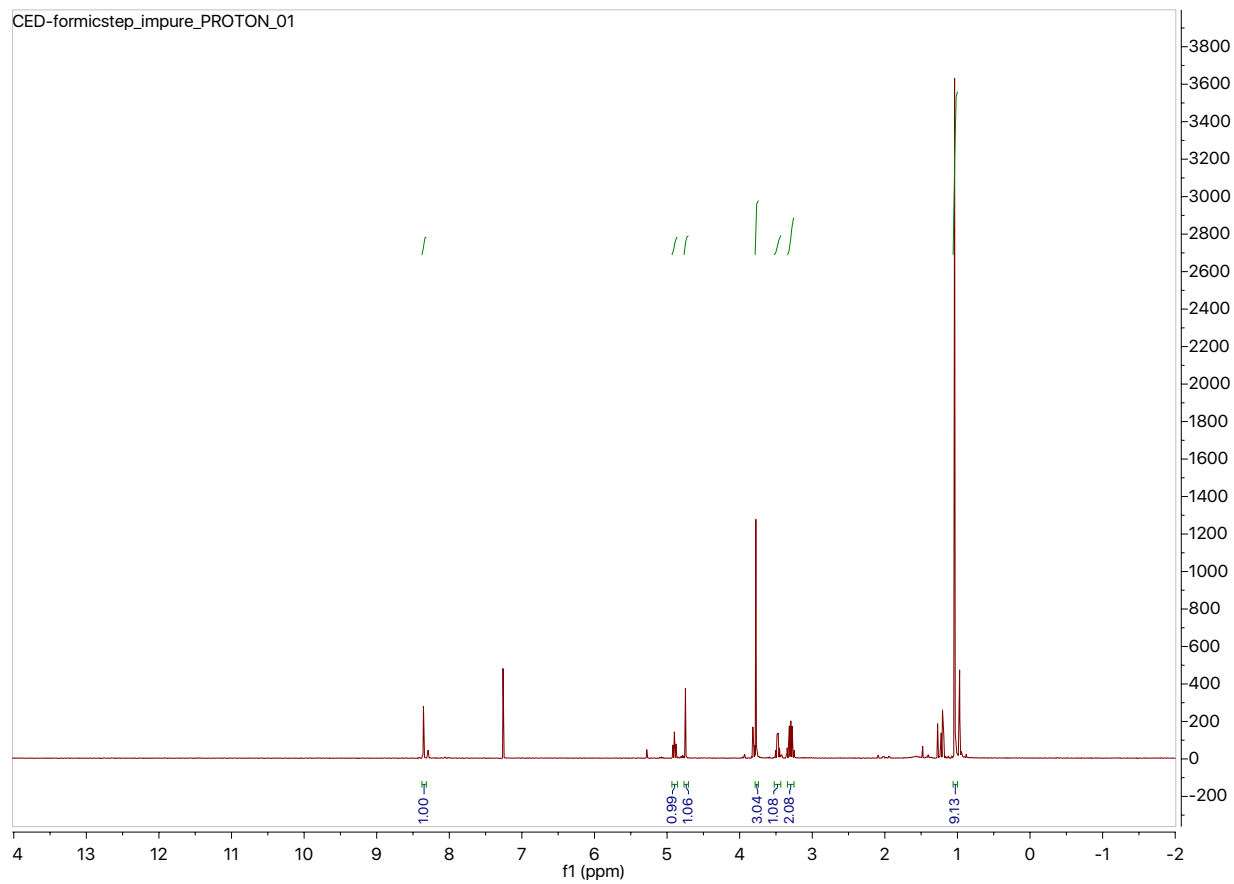
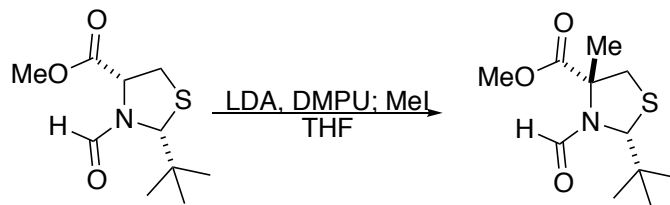


Figure 26. NMR of product



Scheme 99. Reaction conditions

To a solution of diisopropyl amine (64.8 mmoles, 9.08 mL) in 195 mL THF at $-78\text{ }^{\circ}\text{C}$ was added 1.6 M n-BuLi (45.36 mmoles, 28.4 mL). After 10 minutes 30 mL DMPU was added. The mixture was stirred for one hour at $-78\text{ }^{\circ}\text{C}$ and cooled to $-90\text{ }^{\circ}\text{C}$. Ester (43.2 mmoles, 10 g) was added via 10 mL THF over 15 minutes. The reaction was stirred for one hour. MeI (51.84 mmoles, 3.21 mL) was added and the reaction was stirred for two hours at $-90\text{ }^{\circ}\text{C}$. The solution was warmed to room temperature and the solvent was removed in vacuo. The crude methylated ester was taken up in 300 mL brine and extracted with 300 mL ether (3x). The organic layer was dried over Na_2SO_4 and concentrated. The crude product was purified by column chromatography on silica gel (10% to 40% EtOAc in hexanes). 21.56 mmoles of product was obtained in a 34% yield.

^1H NMR (400 MHz, Chloroform-*d*, major conformer) δ 8.26 (s, 1H), 4.64 (s, 1H), 3.74 (s, 3H), 3.30 (dd, $J = 11.6, 1.0$ Hz, 1H), 2.70 (dd, $J = 11.6, 0.9$ Hz, 1H), 1.73 (s, 3H), 1.05 (s, 9H).

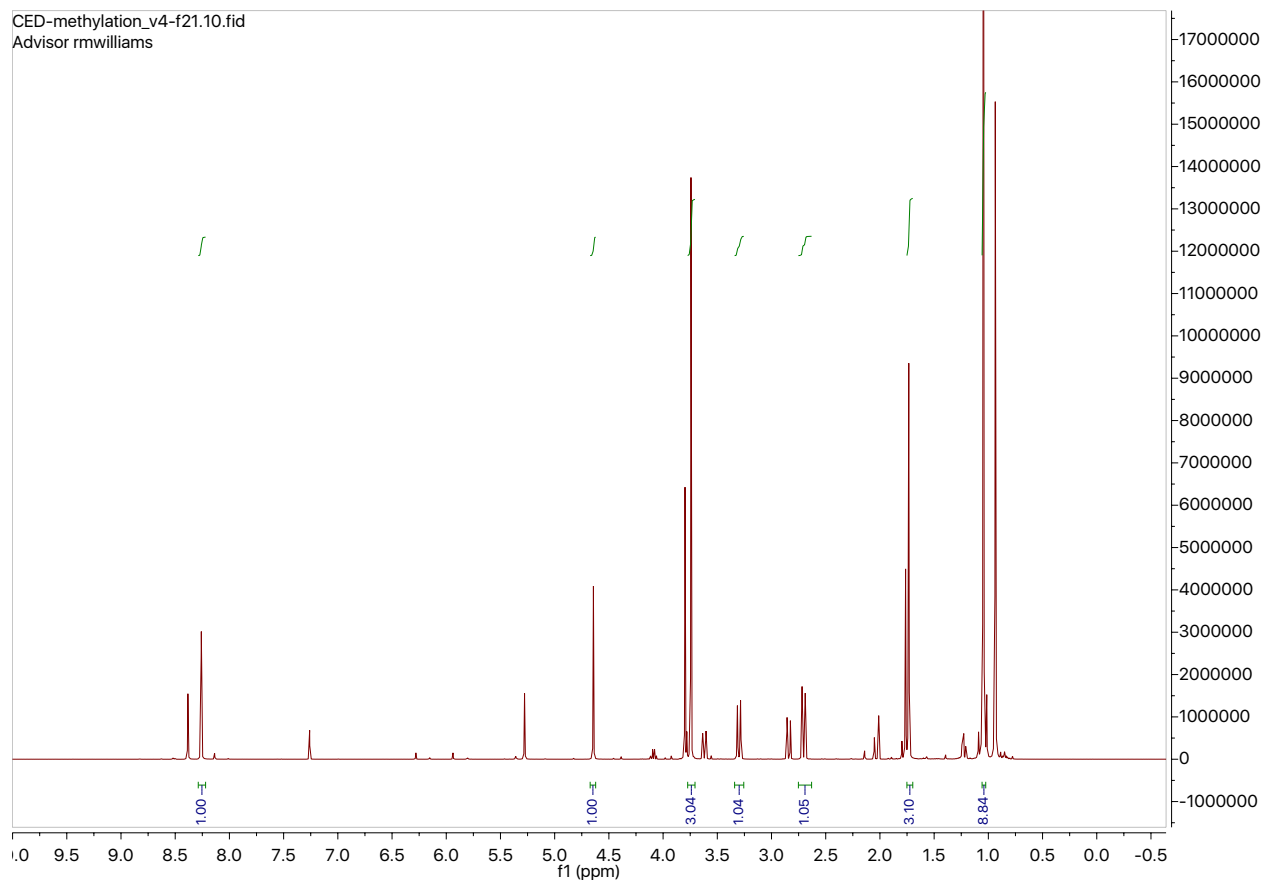
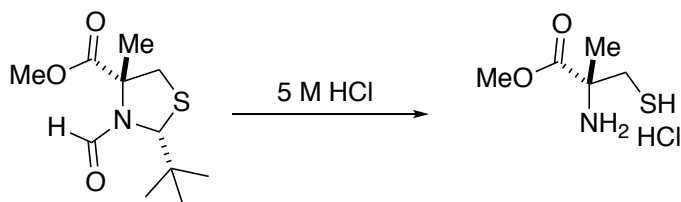


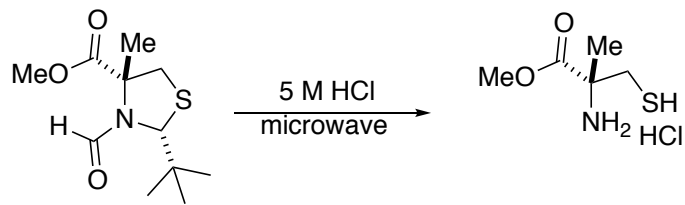
Figure 27. NMR of product



Scheme 100. Reaction conditions

Take up ester (20.4 mmol, 5g) in 130 mL 5M HCl. Reflux for 48 hours at 100 °C. The mixture was cooled to room temperature and extracted with EtOAc (3 x 100 mL). The aqueous layer was concentrated to yield a-methyl cysteine hydrochloride salt as a tan sticky solid in quantitative yield.

^1H NMR (400 MHz, Deuterium Oxide) δ 3.12 (d, $J = 15.1$ Hz, 1H), 2.84 (d, $J = 15.0$ Hz, 1H), 1.54 (s, 3H).



Scheme 101. Reaction conditions

Take up ester (103 mg) in 2 mL 5M HCl. The reaction was microwaved for one hour at 120 °C. The product was isolated with 3 mL EtOAc (3x). The aqueous layer was concentrated to yield α -methyl cysteine hydrochloride salt as a tan sticky solid in quantitative yield.

^1H NMR (400 MHz, Deuterium Oxide) δ 3.12 (d, $J = 15.1$ Hz, 1H), 2.84 (d, $J = 15.0$ Hz, 1H), 1.54 (s, 3H).

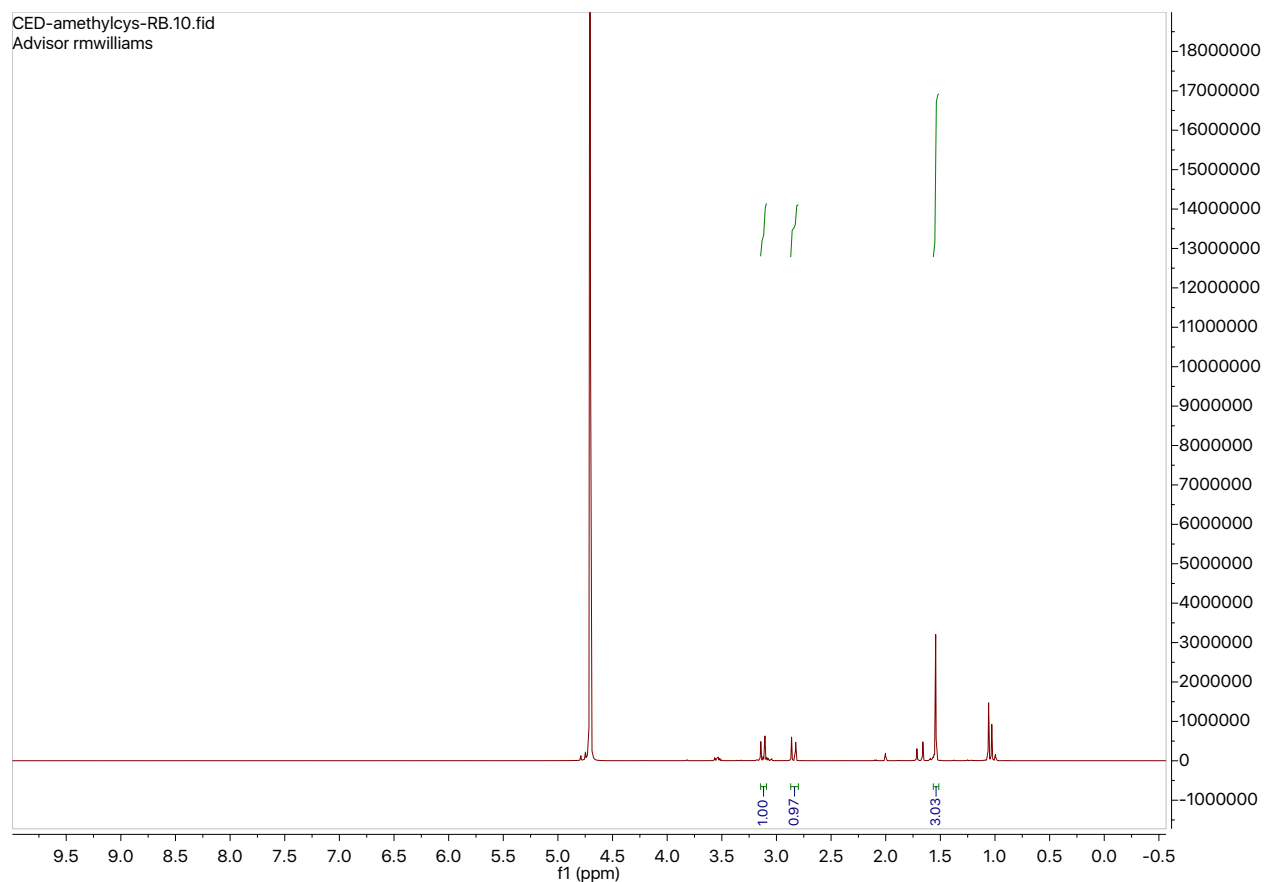
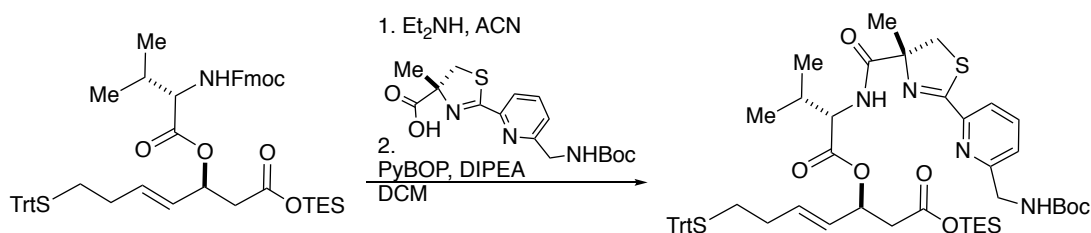
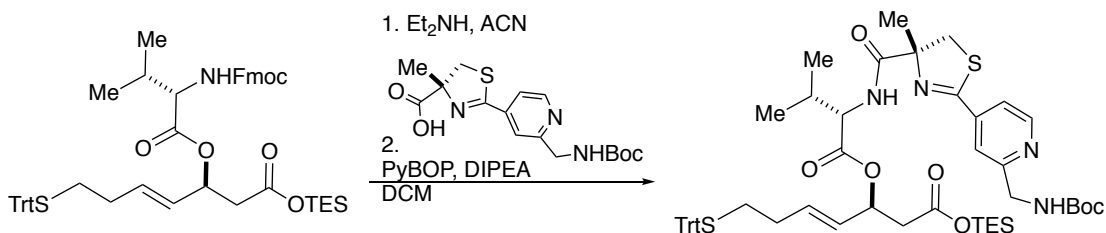


Figure 28. NMR of product



Scheme 102. Reaction conditions

Depsipeptide base fragment (0.71 mmol, 597 mg) was taken up in 50 mL acetonitrile under an inert atmosphere and brought to 0 °C. 3.86 mL of diethylamine was added to the solution and the mixture was stirred for two hours at room temperature. The solution was evaporated under reduced pressure and azeotroped three times with toluene (6 mL each). In a separate flask, pyridine-thiazoline (0.71 mmol, 250 mg) was dissolved in 35 mL DCM. PyBOP (1.42 mmol, 739 mg) and 370 uL DIPEA (2.13 mmoles) were added to the mixture and stirred at room temperature for 20 minutes. Deprotected, crude amine was canulated into the pyridine-thiazoline solution with a total of 15 mL DCM. The reaction was stirred for three hours at room temperature, concentrated under reduced pressure and purified with column chromatography (6% to 25% ethyl acetate in hexane).



Scheme 103. Reaction conditions

Depsipeptide base fragment (0.43 mmol, 361.3 mg) was taken up in 30 mL acetonitrile under an inert atmosphere and brought to 0 °C. 2.34 mL of diethylamine was added to the solution and the mixture was stirred for two hours at room temperature. The solution was evaporated under reduced pressure and azeotroped three times with toluene (6 mL each). In a separate flask, pyridine-thiazoline (0.43 mmol, 150 mg) was dissolved in 20 mL DCM. PyBOP (0.86 mmol, 448

mg) and 224 μ L DIPEA (1.29 mmol) were added to the mixture and stirred at room temperature for 20 minutes. Deprotected, crude amine was canulated into the pyridine-thiazoline solution with a total of 10 mL DCM. The reaction was stirred for three hours at room temperature, concentrated under reduced pressure and purified with column chromatography (6% to 25% ethyl acetate in hexane). Compound was accessed as a yellow film.

^1H NMR (300 MHz, Chloroform-*d*) δ 8.59 (d, $J = 5.1$ Hz, 1H), 7.63 (d, $J = 7.0$ Hz, 2H), 7.38 (d, $J = 7.4$ Hz, 4H), 7.32 – 7.08 (m, 8H), 5.67 (dq, $J = 20.6, 6.7$ Hz, 2H), 5.38 (dd, $J = 15.5, 7.5$ Hz, 1H), 4.53 – 4.34 (m, 2H), 4.15 (dd, $J = 11.3, 5.8$ Hz, 2H), 3.83 (d, $J = 11.6$ Hz, 1H), 3.40 (d, $J = 11.6$ Hz, 1H), 2.70 (dd, $J = 15.6, 7.8$ Hz, 1H), 2.56 (dd, $J = 15.8, 5.9$ Hz, 1H), 2.14 (dt, $J = 17.7, 10.0$ Hz, 3H), 2.05 (d, $J = 6.9$ Hz, 2H), 1.58 (d, $J = 16.5$ Hz, 2H), 1.47 (s, 6H), 0.97 (dd, $J = 11.2, 6.0$ Hz, 2H), 0.82 (d, $J = 6.9$ Hz, 2H), 0.76 (t, $J = 5.6$ Hz, 2H), 0.06 (s, 6H).

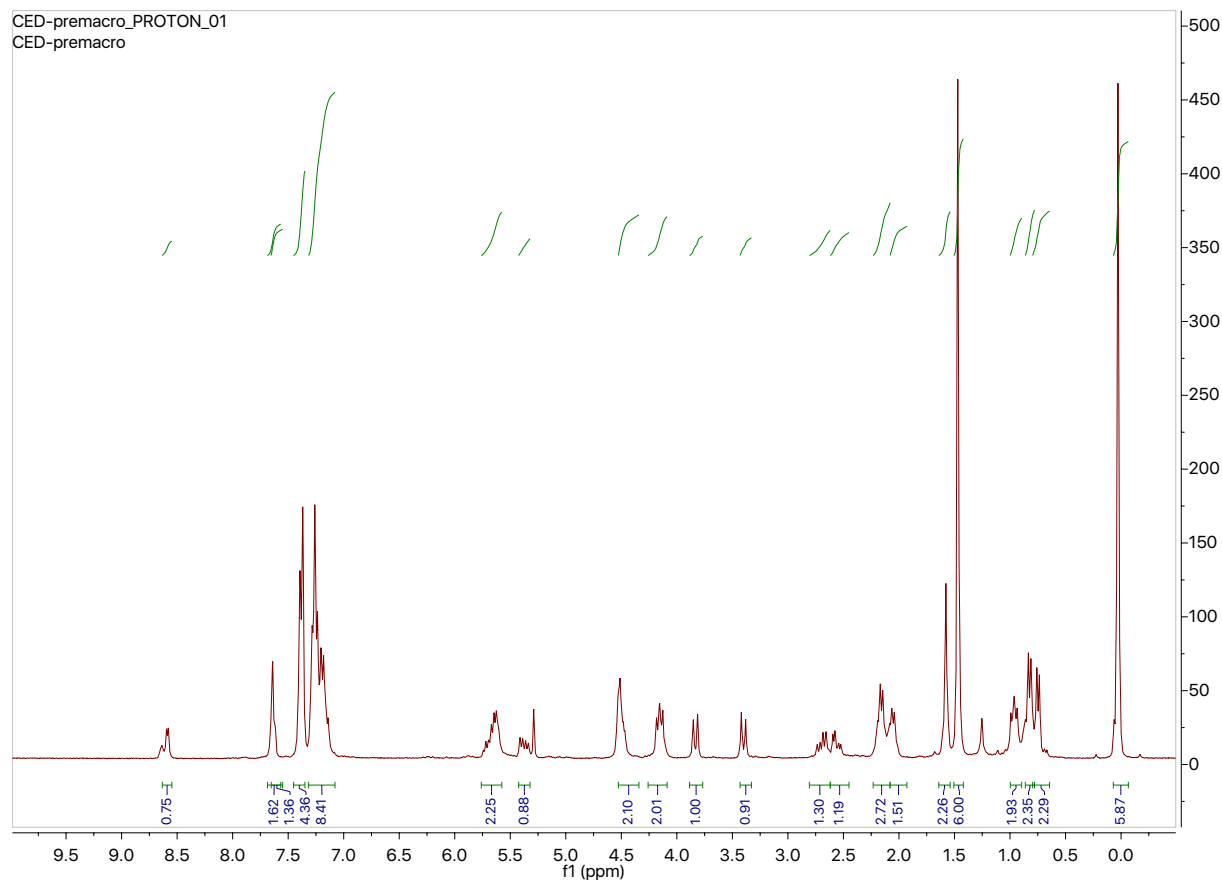
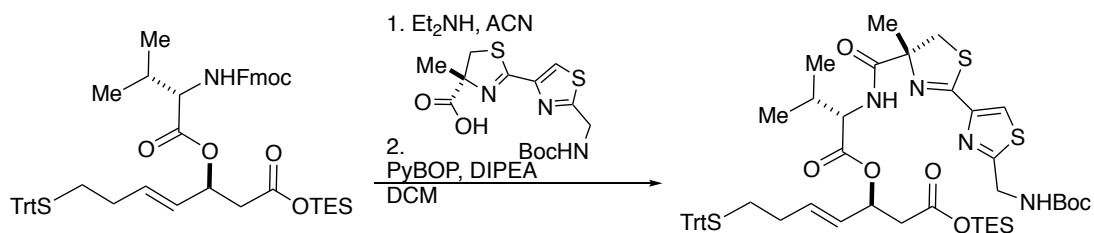


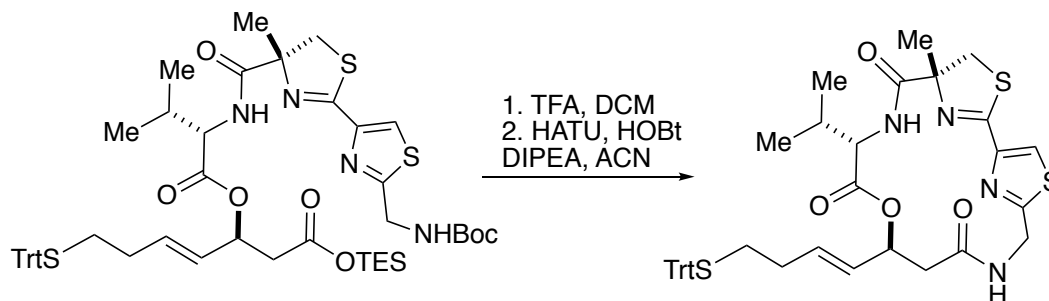
Figure 29. NMR of product



Scheme 104. Reaction conditions

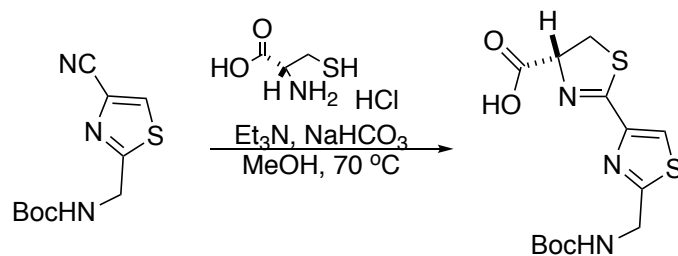
Depsipeptide base fragment (0.59 mmol, 496 mg) was taken up in 40 mL acetonitrile under an inert atmosphere and brought to 0 °C. 3.2 mL of diethylamine was added to the solution and the mixture was stirred for two hours at room temperature. The solution was evaporated under reduced pressure and azeotroped three times with toluene (10 mL each). In a separate flask, thiazole-thiazoline (0.59 mmol, 210 mg) was dissolved in 40 mL DCM. PyBOP (1.18 mmol, 614 mg) and 308 μ L DIPEA (1.77 mmoles) were added to the mixture and stirred at room temperature for 20

minutes. Deprotected, crude amine was cannulated into the pyridine-thiazoline solution with a total of 20 mL DCM. The reaction was stirred for three hours at room temperature, concentrated under reduced pressure and purified with column chromatography (6% to 25% ethyl acetate in hexane).



Scheme 105. Reaction conditions

Acyclic precursor (0.3 mmol, 284 mg) was dissolved in 12 mL of DCM. 2.5 mL of TFA was added to the solution at 0 °C. The reaction was allowed to warm to room temperature and stirred for 16 hours. Solvents were evaporated and the crude amino acid was azeotroped with 6 mL toluene (3x). The crude amino acid was then taken up in 20 mL ACN and added to a stirred solution of DIPEA (1.8 mmol, 313 μ L) in 130 mL of ACN. The solution was allowed to stir for 10 min., before a solution of 100 mL ACN and HATU (0.6 mmoles, 228 mg) and HOBT (0.6 mmoles, 82 mg) were added slowly. The reaction was allowed to stir overnight, then concentrated and redissolved in AcOEt. The solution was washed with saturated aqueous NH_4Cl , NaHCO_3 and brine, dried over Na_2SO_4 , filtered, and concentrated under reduced pressure. The residue was purified by flash column chromatography on silica gel (9% methanol in DCM for the first column and 16% to 50% ethyl acetate in hexane for the second column).



Scheme 106. Reaction conditions

Nitrile (2.09 mmoles, 500 mg) was taken up in 20 mL MeOH. Cysteine (2.51 mmoles, 396 mg) and Et₃N (3.2 mL) was added to the solution. The reaction was refluxed overnight at 70 °C. The mixture was cooled to room temperature and the solvent was evaporated. The crude was taken up in NaHCO₃ and washed with ether. The aqueous was acidified to pH 3 with 1M HCl and extracted with EtOAc (3x). The organic phase was dried over Na₂SO₄, filtered and concentrated. ¹H NMR (300 MHz, Chloroform-*d*) δ 10.09 (s, 1H), 8.01 (s, 1H), 5.59 (s, 1H), 4.60 (d, *J* = 6.5 Hz, 2H).

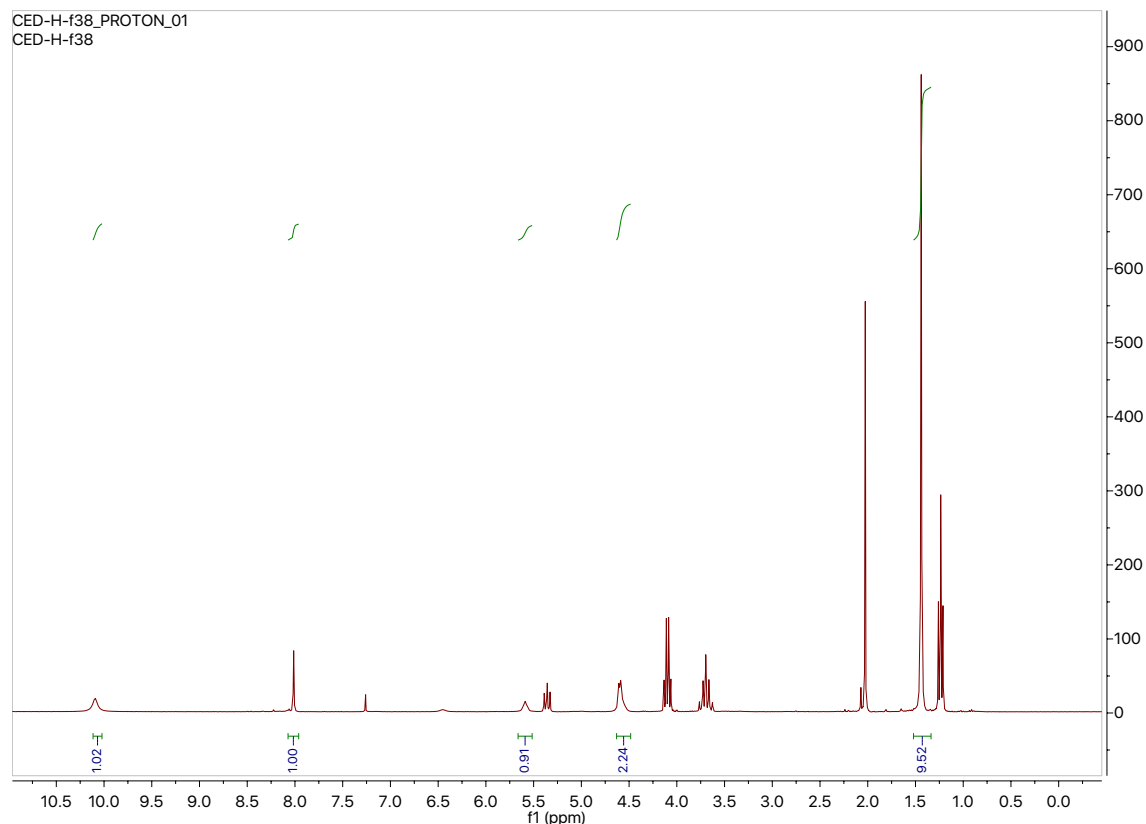
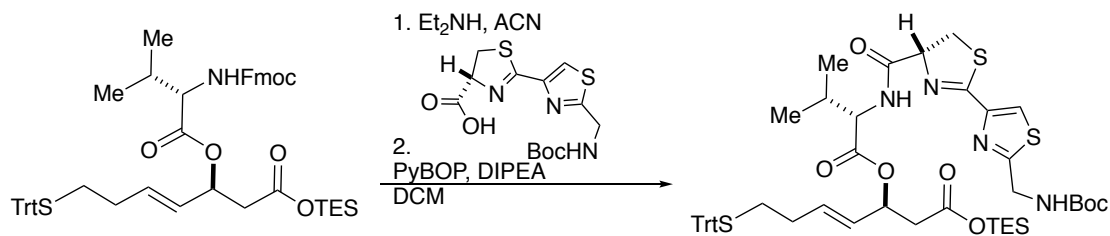


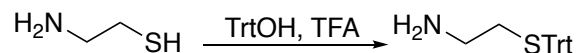
Figure 30. NMR of product



Scheme 107. Reaction conditions

Depsipeptide base fragment (1.34 mmol, 1.13 g) was taken up in 90 mL acetonitrile under an inert atmosphere and brought to 0 °C. 7.3 mL of diethylamine was added to the solution and the mixture was stirred for two hours at room temperature. The solution was evaporated under reduced pressure and azeotroped three times with toluene (30 mL each). In a separate flask, thiazole-thiazoline (1.34 mmol, 462 mg) was dissolved in 70 mL DCM. PyBOP (2.68 mmol, 1.4 g) and 700 μ L DIPEA (4.02 mmoles) were added to the mixture and stirred at room temperature for 20 minutes.

Deprotected, crude amine was canulated into the pyridine-thiazoline solution with a total of 30 mL DCM. The reaction was stirred for three hours at room temperature, concentrated under reduced pressure and purified with column chromatography (6% to 25% ethyl acetate in hexane).



Scheme 108. Reaction conditions

A solution of cysteamine (1.8 mmoles, 200 mg) and trityl alcohol (2.16 mmoles, 562 mg) in 2 mL TFA was stirred at room temperature for one hour. Toluene was added to the mixture and the solvent was evaporated under reduced pressure. Resultant crude mixture was dissolved in EtOAc and extracted with 1M NaOH, H₂O, and sat. NaCl. The organic layer was dried with MgSO₄, filtered, and concentrated.

¹H NMR (300 MHz, Chloroform-*d*) δ 7.41 (dd, *J* = 6.9, 1.5 Hz, 5H), 7.32 – 7.18 (m, 7H), 7.16 (dd, *J* = 3.4, 2.1 Hz, 1H), 2.57 (t, *J* = 6.5 Hz, 2H), 2.30 (t, *J* = 6.5 Hz, 2H), 1.30 (s, 1H).

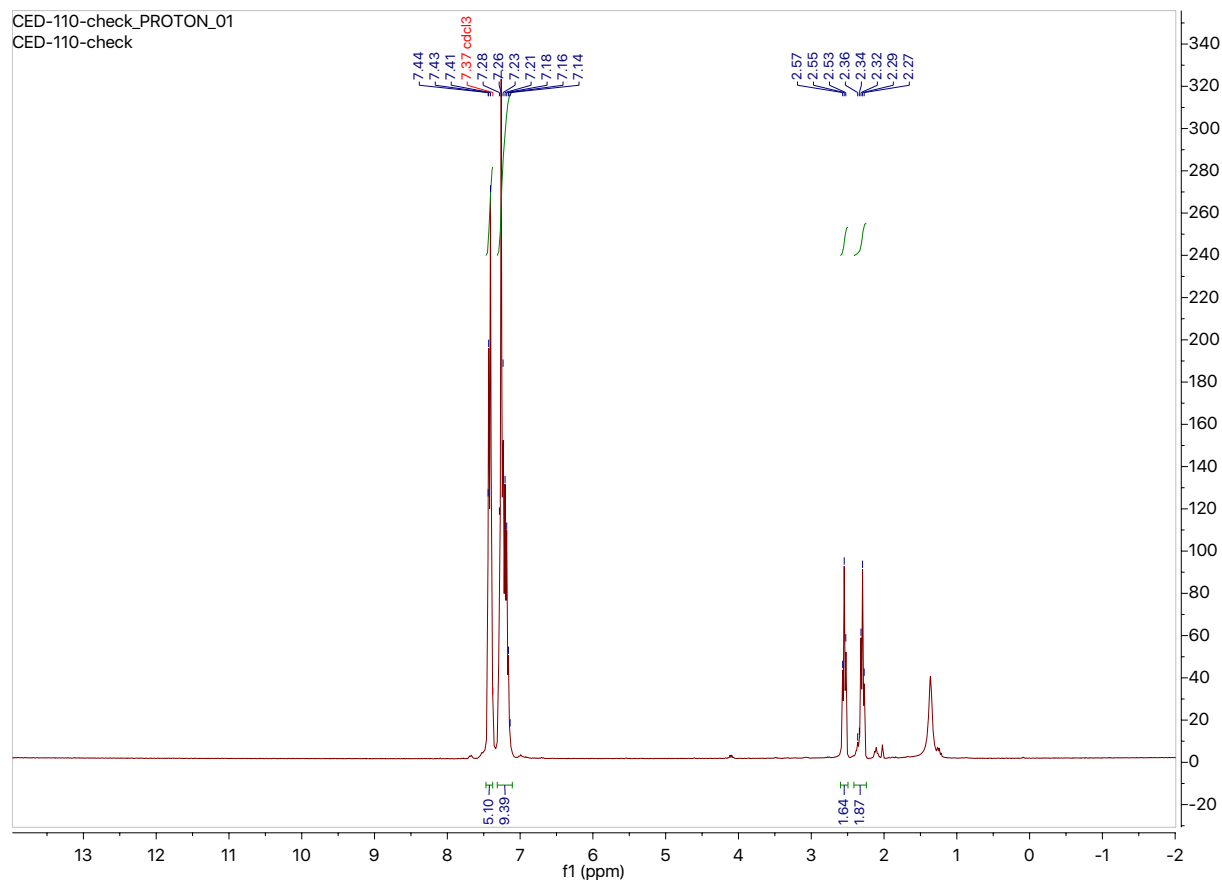
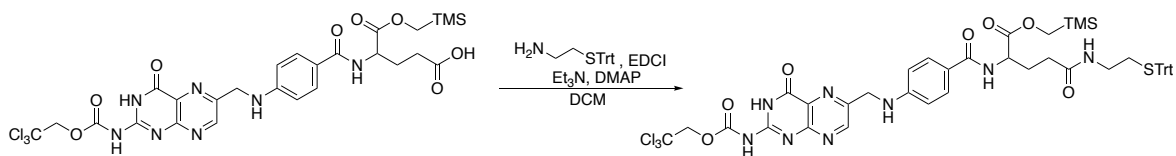
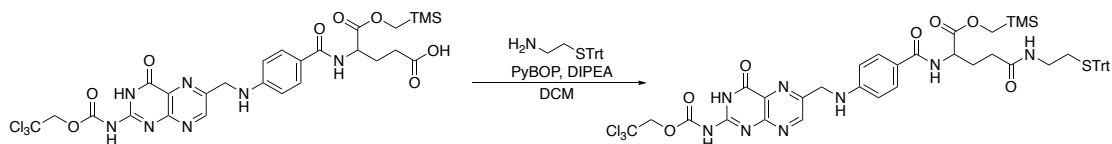


Figure 31. NMR of product



Scheme 109. Reaction conditions

Protected folic acid (0.007 mmoles, 5 mg) was taken up in 2 mL DCM. Protected cysteamine (0.005 mmoles, 1.8 mg) and cat. DMAP was added to the solution. EDCI (0.012 mmoles, 2.2 mg) and Et_3N (0.029 mmoles, 4 μL) were added and the solution was stirred overnight. Amide was purified with preparatory TLC in a 5:10:1, DCM:EtOAc:MeOH mobile phase.



Scheme 110. Reaction conditions

Acid (0.015 mmol, 10 mg) was taken up in 2 mL DCM. PyBOP (0.03 mmol, 15.6 mg) and DIPEA (0.045 mmol, 8 μ L) were added followed by the free amine of protected cysteamine (0.015 mmol, 4.8 mg). The reaction was stirred at room temperature for three hours.

^1H NMR (400 MHz, Methanol- d_4) δ 8.45 (s, 1H), 7.29 – 7.21 (m, 1H), 5.95 – 5.78 (m, 1H), 5.76 – 5.63 (m, 1H), 5.62 (s, 1H), 4.75 (d, $J = 17.5$ Hz, 1H), 4.43 (dt, $J = 9.0, 3.6$ Hz, 1H), 4.18 (dd, $J = 17.6, 1.0$ Hz, 1H), 3.91 (dd, $J = 11.6, 1.1$ Hz, 1H), 3.41 – 3.32 (m, 1H), 3.00 (ddd, $J = 16.6, 9.9, 1.3$ Hz, 1H), 2.80 – 2.69 (m, 2H), 2.56 (t, $J = 6.9$ Hz, 1H), 2.45 (q, $J = 7.1$ Hz, 1H), 2.41 – 2.31 (m, 1H), 2.22 (dt, $J = 21.4, 7.5$ Hz, 1H), 2.13 – 2.02 (m, 1H), 1.80 (d, $J = 1.1$ Hz, 4H), 1.60 (s, 2H), 1.72 – 1.54 (m, 1H), 1.39 – 1.22 (m, 19H), 1.04 – 0.83 (m, 3H), 0.88 (s, 4H), 0.77 – 0.69 (m, 4H), 0.66 (d, $J = 6.8$ Hz, 4H), 0.13 – 0.04 (m, 1H).

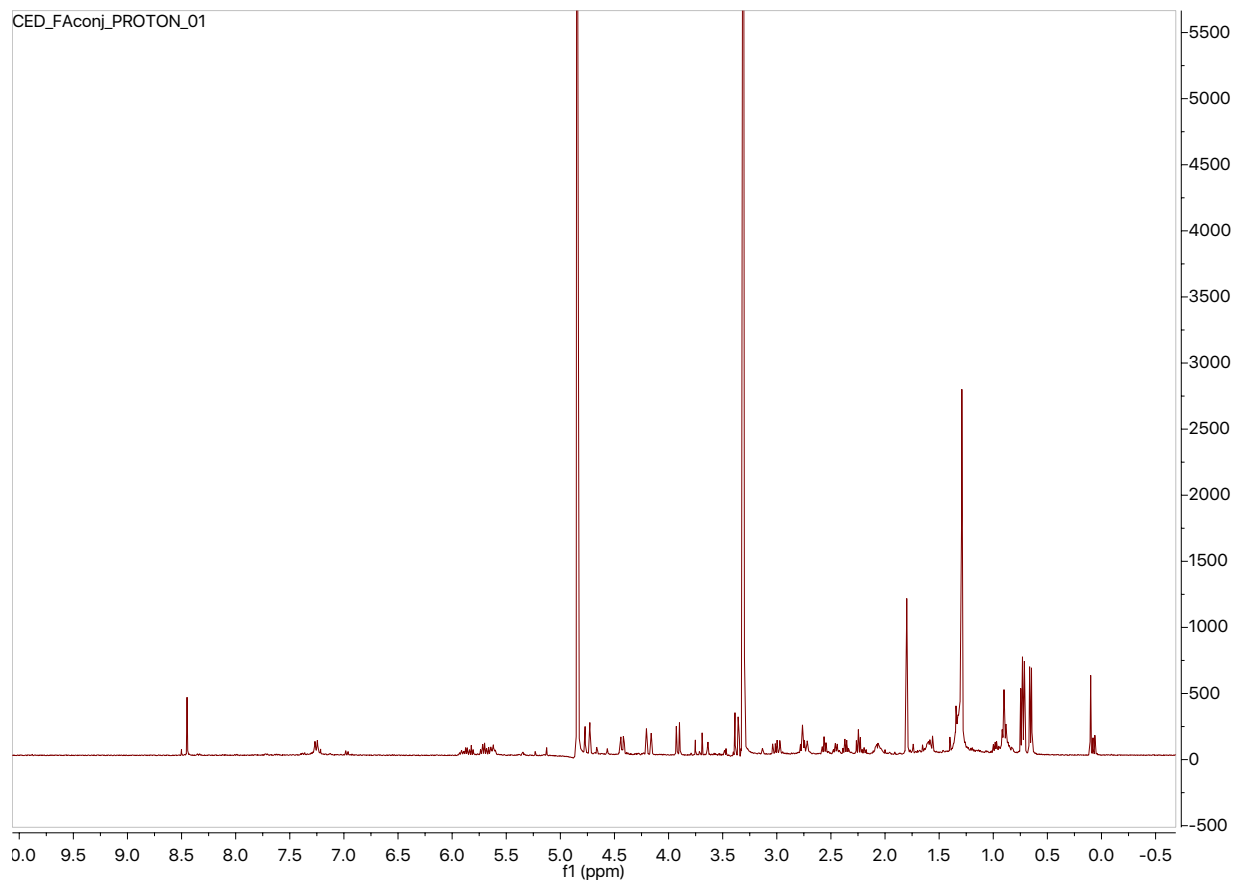
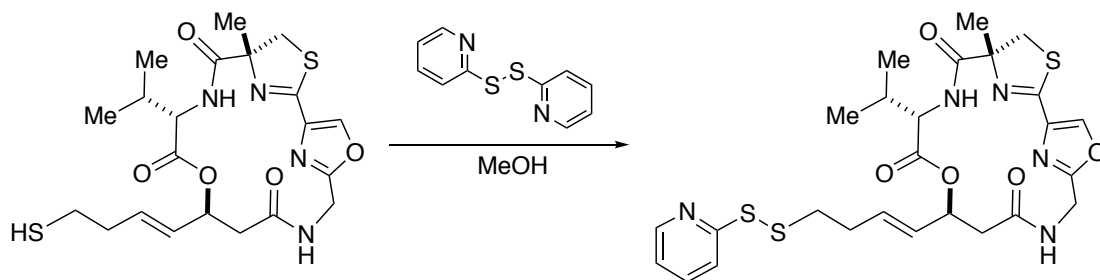
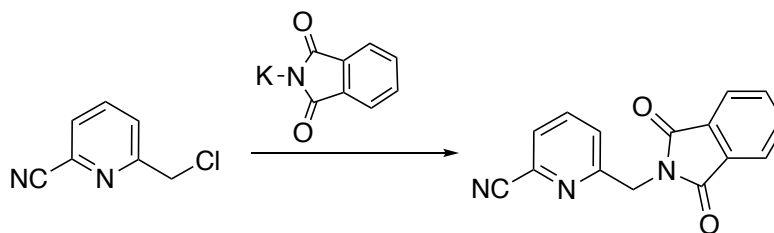


Figure 32. NMR of product



Scheme 111. Reaction conditions

Free thiol (0.02 mmoles, 10 mg) was taken up in 0.3 mL MeOH at room temperature. Aldrithiol (0.11 mmoles, 23mg) was added and the reaction as stirred for two hours. The mixture was concentrated and the product was purified by preparatory TLC.



Scheme 112. Reaction conditions

Pyridine chloride (6.6 mmoles, 1.007 g) was taken up in 40 mL DMF. K-phthalimide (6.6 mmoles, 1.22 g) was added and the reaction was stirred for five hours. The reaction was concentrated and 20 mL H₂O was added. The solid formed was filtered, collected, and washed with H₂O and THF.

¹H NMR (300 MHz, Chloroform-*d*) δ 7.91 (dd, *J* = 5.4, 3.1 Hz, 2H), 7.78 (dd, *J* = 8.1, 4.8 Hz, 3H), 7.58 (s, 1H), 7.50 (d, *J* = 7.9 Hz, 1H), 4.78 (s, 2H).

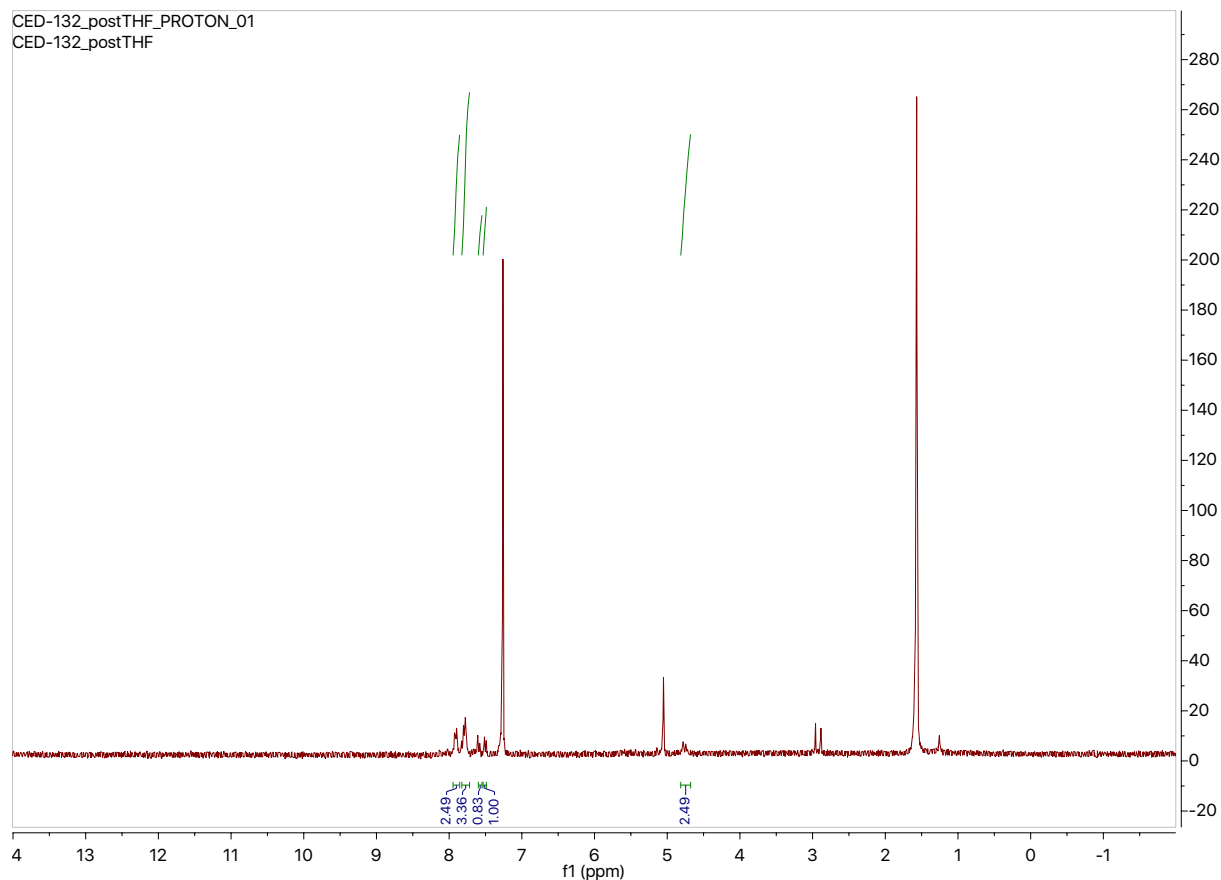
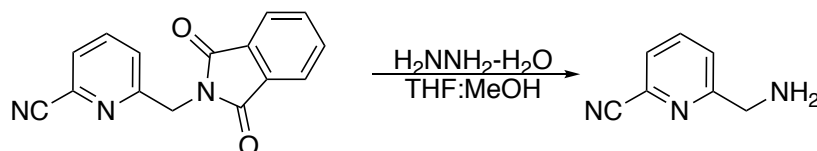
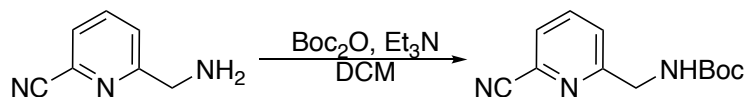


Figure 33. NMR of spectra



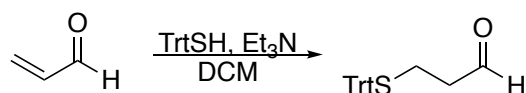
Scheme 113. Reaction conditions

To a solution of phthalimide (1.52 mmoles, 400 mg) in 10 mL THF and 10 mL MeOH was added hydrazine monohydrate (1.67 mmoles, 84 mg). The reaction was stirred for two hours followed by the addition of 20 mL 1M HCl. The solution was stirred for an additional three hours and concentrated. 20 mL of H₂O was added and the mixture was filtered. Filtrate was concentrated and the crude was carried on.



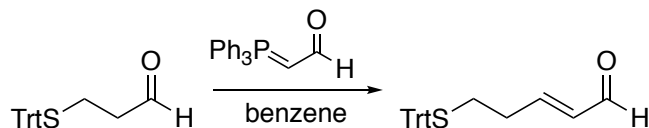
Scheme 114. Reaction conditions

Crude amine was taken up in 12 mL DCM. Et_3N (4.56 mmoles, 462 mg) and Boc_2O (1.67 mmoles, 365 mg) were added stirred for 12 hours. Reaction was quenched with 20 mL sat. NaHCO_3 and extracted with 20 mL DCM (3x). Organic layer was dried over MgSO_4 and concentrated. Boc protected amine was purified with column chromatography (10% to 40% ethyl acetate in hexane).



Scheme 115. Reaction conditions

Trityl thiol (3.6 mmoles, 1.0 g) was taken up in 30 mL DCM. Et_3N (5.04 mmoles, 702 μL) and acrolein (5.04 mmoles, 282 mg) were added to the solution. After one hour the DCM was evaporated and the crude was carried on for the Wittig olefination.



Scheme 116. Reaction conditions

30 mL benzene was added to crude aldehyde. The ylide (4.32 mmoles, 1.32 g) was added and the reaction was stirred at 80 $^\circ\text{C}$ for 16 hours. The reaction was cooled and concentrated for purification. Aldehyde was purified with column chromatography on silica gel (2.5% to 30% ethyl acetate in hexane). A yellow solid was isolated in 94% yield (3.4 mmoles, 1.2 g).

^1H NMR (300 MHz, Chloroform-*d*) δ 9.39 (d, $J = 7.9$ Hz, 1H), 7.43 – 7.18 (m, 18H), 6.59 (dt, $J = 16.0, 6.3$ Hz, 1H), 5.94 (dd, $J = 15.6, 7.9$ Hz, 1H), 2.50 – 2.18 (m, 5H).

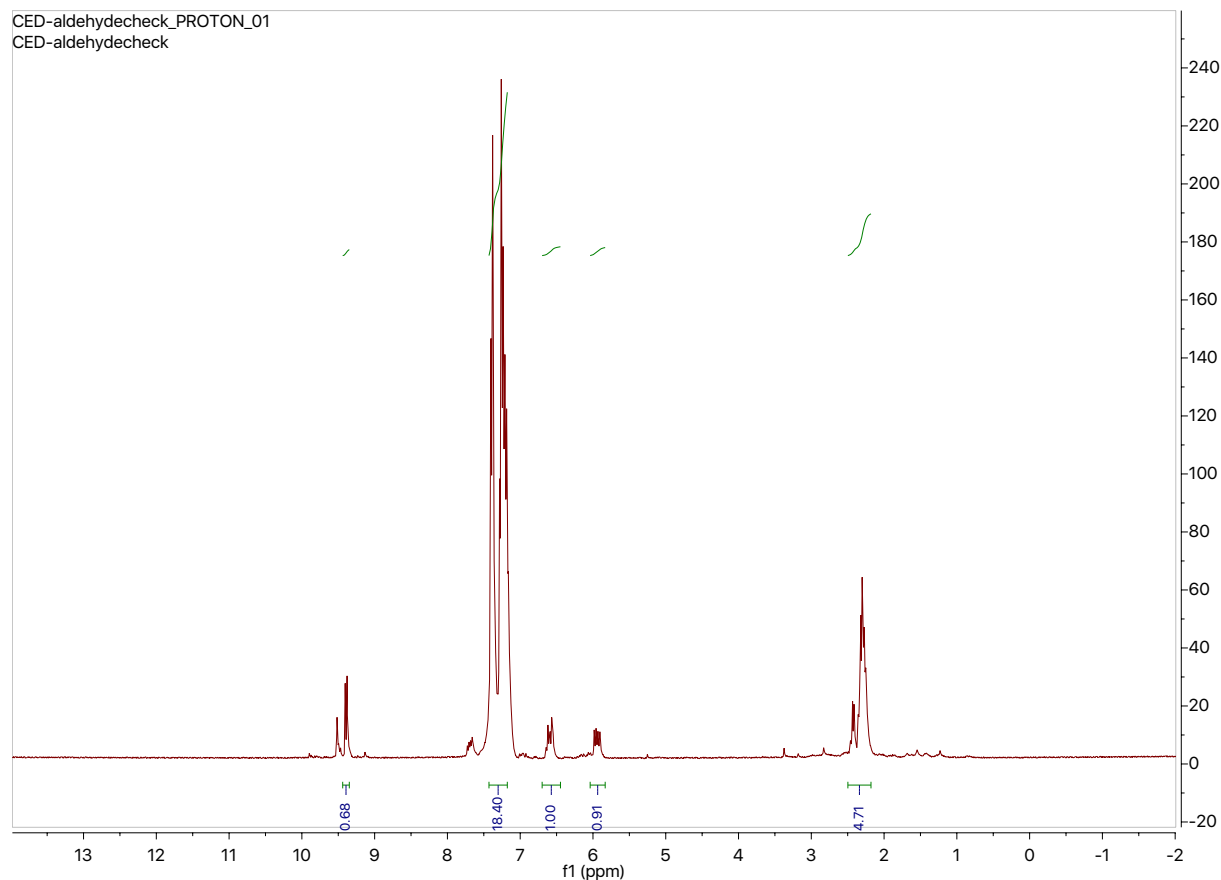
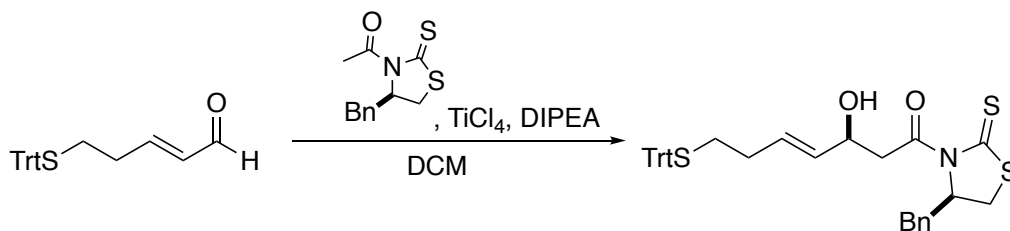


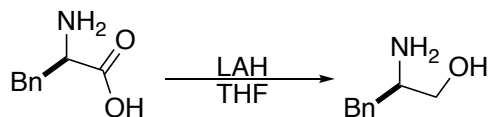
Figure 34. NMR of product



Scheme 117. Reaction conditions

To a solution of chiral auxiliary (4.08 mmoles, 1.03 g) in 30 mL DCM at 0 °C was added TiCl_4 (4.42 mmoles, 840 mg) dropwise. The reaction was stirred for five minutes and cooled to -78 °C. DIPEA (4.42 mmoles, 572 mg) was added dropwise and the reaction was stirred for two hours. Aldehyde (3.4 mmoles, 1.21 g) was added via 10 mL DCM to the solution at -78 °C and stirred for two hours. Sat. NH_4Cl (25 mL) was added to the reaction and the mixture was warmed to room temperature. Compound was extracted with DCM (3x) and dried over MgSO_4 . The organic

layer was concentrated and purified with column chromatography on silica gel (4% to 40% ethyl acetate in hexane).



Scheme 118. Reaction conditions

To a suspension of LAH (43.94 mmoles, 1.67 g) in 81 mL THF at 0 °C was added D-phenylalanine (30.3 mmoles, 5 g) over 30 minutes. The reaction was stirred at 0 °C for two hours and warmed to room temperature for an additional two hours. The reaction was then refluxed at 60 °C for 16 hours. The mixture was cooled and 50 mL of ether was added. 2.5 mL H₂O followed by 7.5 mL 15% NaOH and 7.5 mL H₂O was added to quench the reaction. The solution was filtered through celite and concentrated. The alcohol was carried on without further purification.

¹H NMR (400 MHz, Methanol-*d*₄) δ 7.36 – 7.15 (m, 5H), 3.52 (ddd, *J* = 10.8, 4.5, 1.0 Hz, 1H), 3.37 (ddd, *J* = 10.8, 6.9, 1.1 Hz, 1H), 3.04 (dtd, *J* = 7.8, 6.5, 4.5 Hz, 1H), 2.78 (dd, *J* = 13.4, 6.2 Hz, 1H), 2.57 (dd, *J* = 13.4, 7.7 Hz, 1H), 1.87 (tq, *J* = 4.9, 1.4 Hz, 2H).

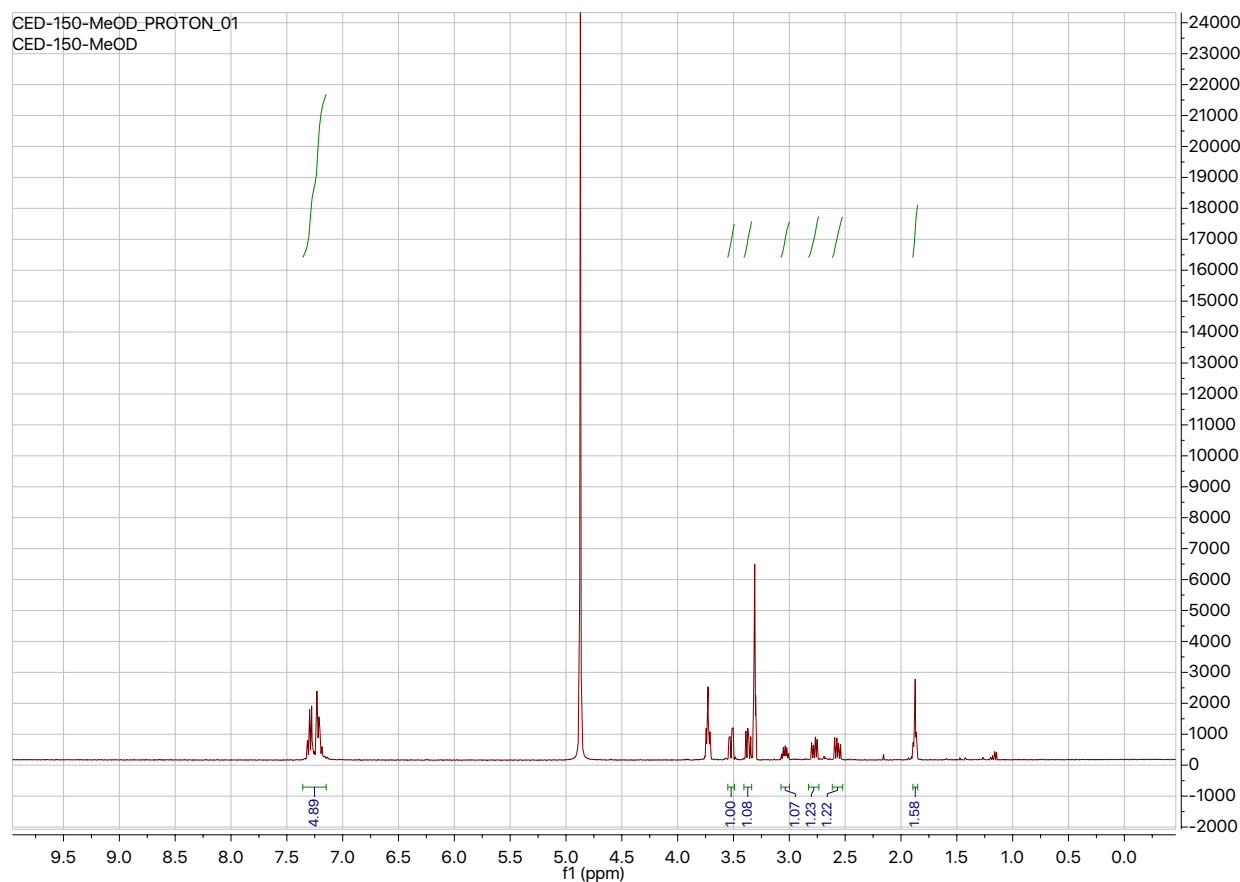
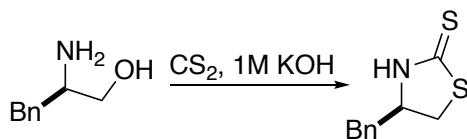


Figure 35. NMR of product



Scheme 119. Reaction conditions

To a mixture of aminol (30.3 mmol, 4.6 g) in 130 mL 1M KOH was added CS₂ (151.5 mmol, 11.5 g). After one hour the mixture was heated to 110 °C for 20 hours. The mixture was cooled to room temperature and extracted with 200 mL DCM (3x). The organic solution was dried over MgSO₄ and concentrated. Thione was purified with column chromatography on silica gel (10% to 40% ethyl acetate in hexane). Compound (28.9 mmol, 6.05 g) was isolated in a 95% yield over two steps.

^1H NMR (300 MHz, Chloroform-*d*) δ 7.47 – 7.08 (m, 5H), 4.52 (q, $J = 7.4$ Hz, 1H), 3.69 – 3.53 (m, 1H), 3.34 (ddt, $J = 9.8, 5.3, 2.4$ Hz, 1H), 3.14 – 2.94 (m, 2H).

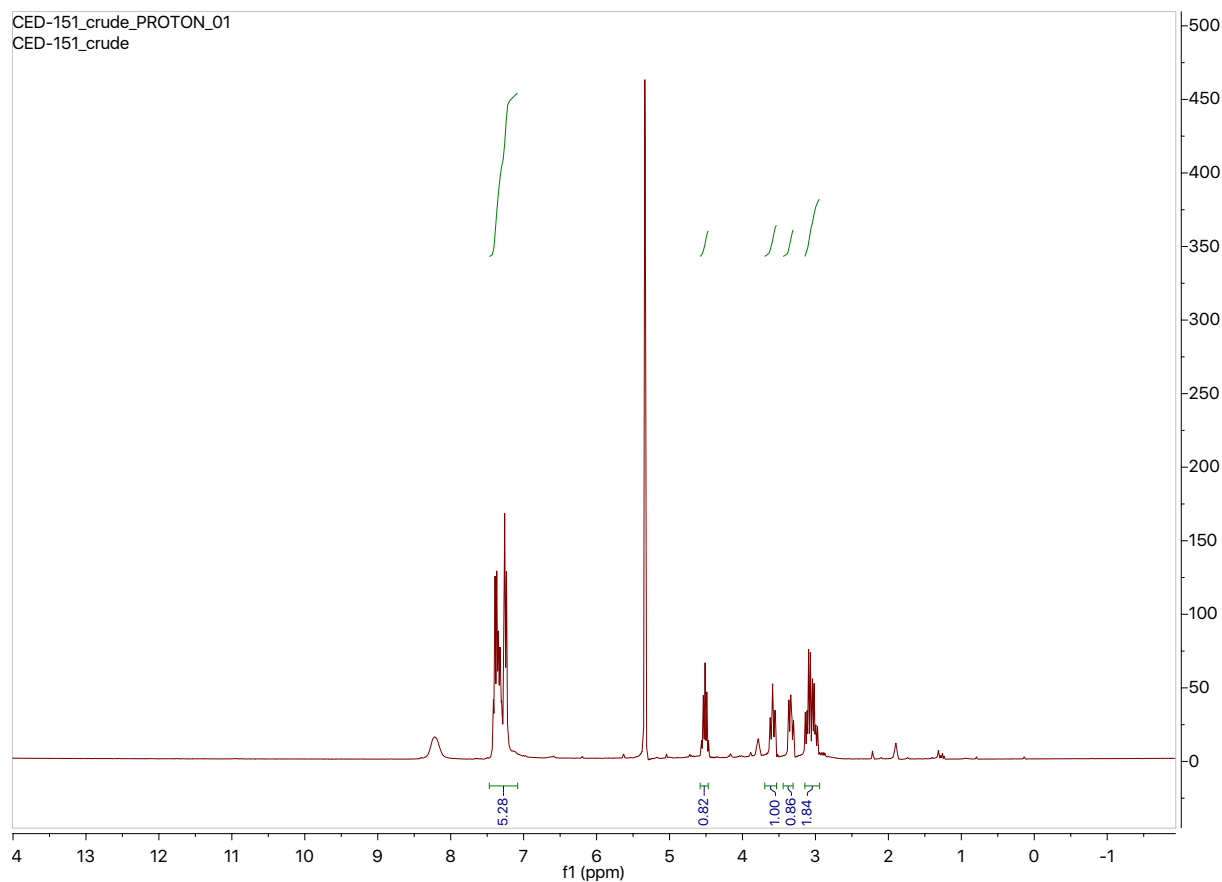
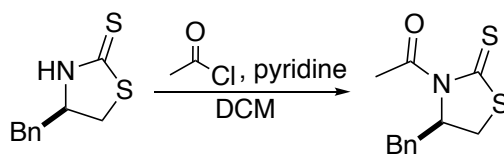


Figure 36. NMR of product



Scheme 120. Reaction conditions

To a mixture of thione (28.9 mmols, 6.05 g) and pyridine (43.55 mmols, 3.5 mL) in 130 mL DCM at 0 °C was added acetyl chloride (34.68 mmols, 2.5 mL) dropwise. After two hours the reaction was warmed to room temperature and stirred for 16 hours. The reaction was quenched with ~100 mL H₂O and extracted with 130 mL DCM (3x). The organic solution was dried over

MgSO₄ and concentrated. Thione was purified with column chromatography on silica gel (10% to 25% ethyl acetate in hexane). Compound (18.8 mmoles, 4.72 g) was isolated in a 65% yield.

¹H NMR (300 MHz, Chloroform-*d*) δ 7.34 – 7.22 (m, 7H), 3.37 (s, 1H), 3.19 (s, 1H), 3.03 (s, 1H), 2.88 (d, *J* = 11.3 Hz, 1H), 2.79 (s, 3H).

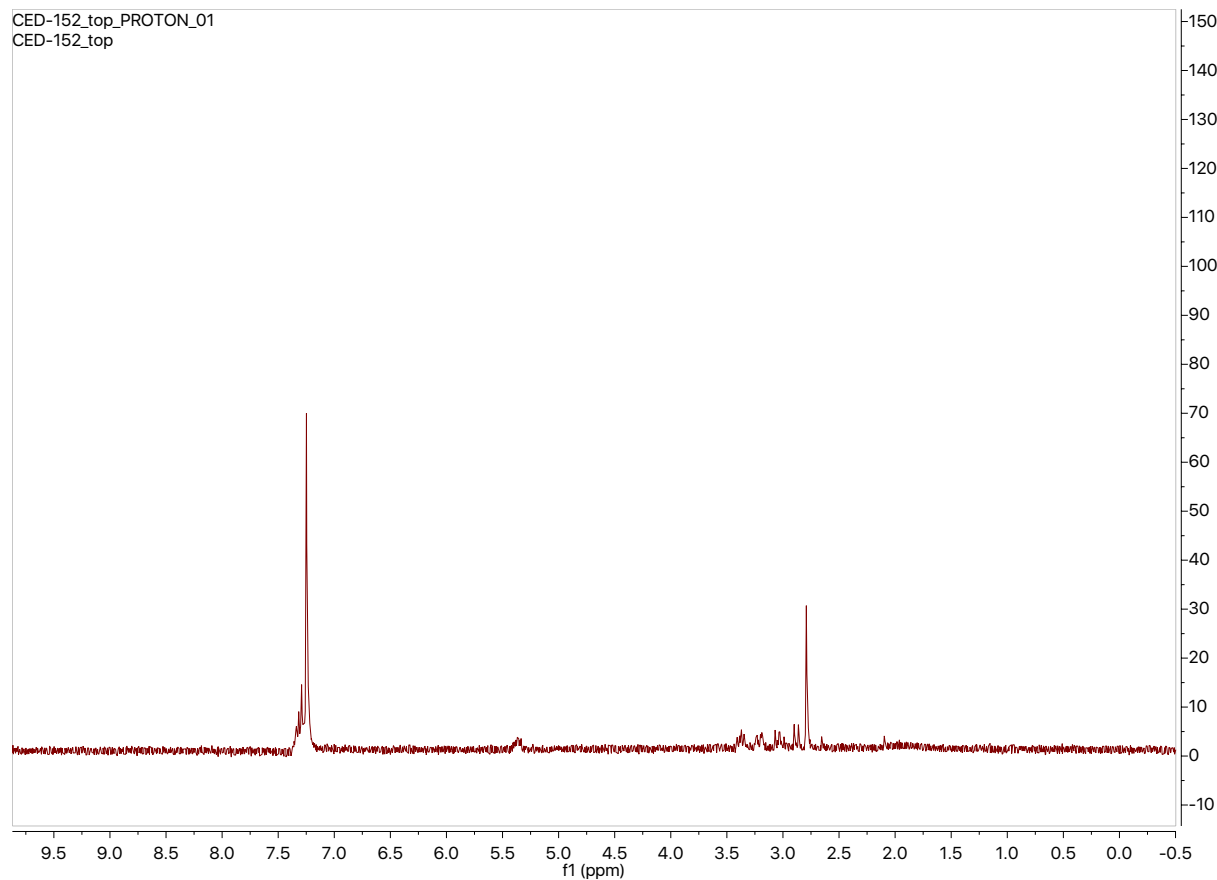
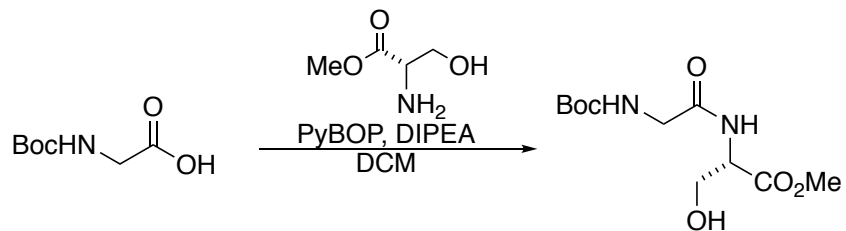
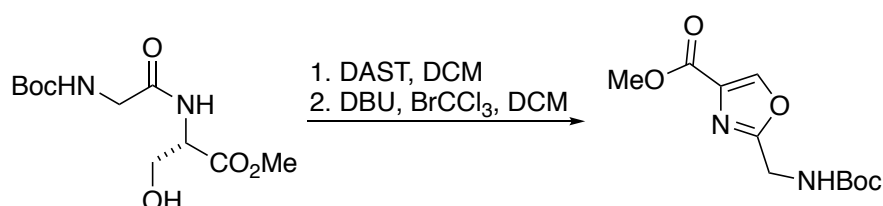


Figure 37. NMR of product



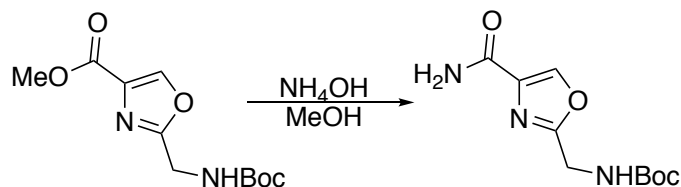
Scheme 121. Reaction conditions

Acid (5.71 mmoles, 1 g) was taken up in 215 mL of DCM. PyBOP (11.42 mmoles, 6 g) and DIPEA (17.13 mmoles, 3 mL) were added to the solution. L-serine (5.71 mmoles, 888 mg) was taken up in 215 mL DCM and added to the acid mixture. The reaction was stirred for three hours and concentrated.



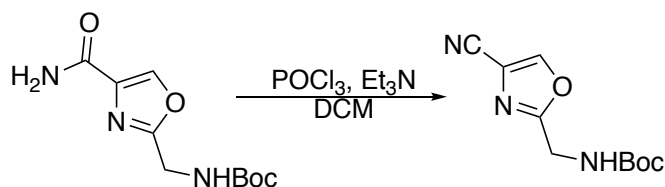
Scheme 122. Reaction conditions

Crude amide (33.9 mmoles) was taken up in 470 mL DCM and cooled to $-78\text{ }^{\circ}\text{C}$. DAST (40.68 mmoles, 5.38 mL) in 391 mL DCM was added dropwise via an addition funnel. After full addition, the reaction was stirred at $-78\text{ }^{\circ}\text{C}$ for 1.5 hours. Reaction solution was poured into sat. NaHCO_3 solution at $0\text{ }^{\circ}\text{C}$ and extracted with DCM (2x). The organic solution was dried over Na_2SO_4 and concentrated. Crude intermediate was taken up in 587 mL DCM. BrCCl_3 (169.5 mmoles, 16 mL) then DBU (169.5 mmoles, 25 mL) were added to the solution at room temperature. The reaction was stirred for three hours then concentrated. The crude mixture was taken up in EtOAc and washed with aq. NH_4Cl and brine. The organic layer was dried over Na_2SO_4 and filtered through celite with EtOAc.



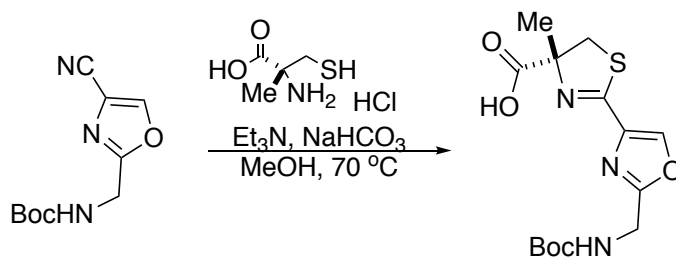
Scheme 123. Reaction conditions

Oxazole (0.52 mmoles, 133 mg) was taken up in 15 mL MeOH. NH_4OH (52 mmol, 2.1 mL) was added and the reaction was stirred overnight. The reaction was concentrated and after confirmation via NMR of the loss of methyl group the crude was carried on.



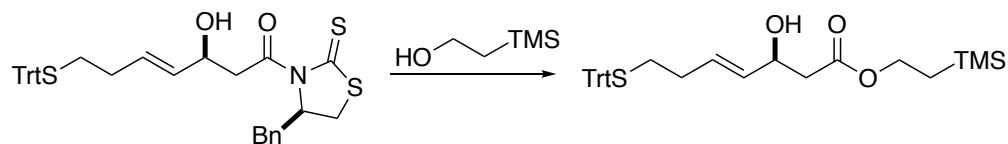
Scheme 124. Reaction conditions

Amide (0.52 mmoles crude) in 18 mL DCM was cooled to 0 °C. Et_3N (7.8 mmoles, 1.1 mL) was added followed by the dropwise addition of phosphorus oxychloride (1.3 mmoles, 121 μL). The reaction was warmed to room temperature and stirred for six hours. The mixture was concentrated and the crude was carried on to the next step.



Scheme 125. Reaction conditions

Crude oxazole (0.52 mmoles) was taken up in 20 mL MeOH. α -methyl cysteine (1.04 mmoles, 178 mg) and Et_3N (2.08 mmoles, 290 μL) was added and the reaction was stirred overnight.



Scheme 126. Reaction conditions

^1H NMR (400 MHz, Chloroform-*d*) δ 7.45 – 7.39 (m, 5H), 7.29 (t, $J = 7.6$ Hz, 6H), 7.24 – 7.18 (m, 3H), 6.69 (s, 1H), 5.53 – 5.44 (m, 1H), 5.39 (dd, $J = 15.4, 6.1$ Hz, 1H), 2.18 (td, $J = 7.3, 3.0$ Hz, 2H), 2.05 (q, $J = 7.1$ Hz, 2H), 1.46 (d, $J = 10.0$ Hz, 12H), 1.02 (d, $J = 6.8$ Hz, 2H), 0.94 (t, $J = 6.1$ Hz, 4H), 0.89 (d, $J = 6.8$ Hz, 2H).

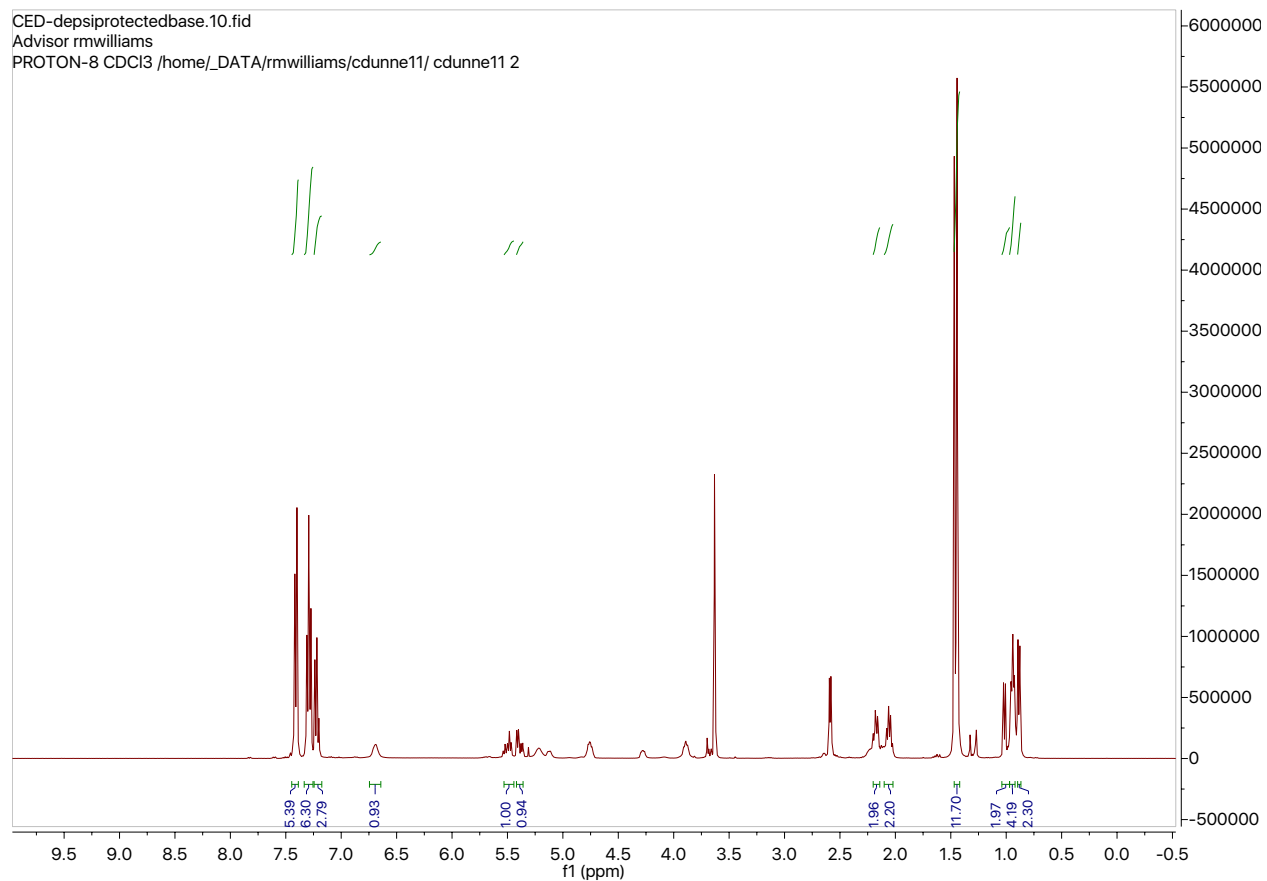
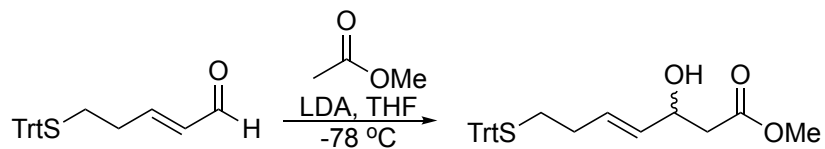


Figure 38. NMR of product



Scheme 127. Reaction conditions

LDA was prepared in situ by taking up DIPA (10.8 mmoles, 1.5 mL) in 45 mL THF. The mixture was brought to -78 °C and stirred for one minute. N-BuLi (1.6 M in hexanes, 7.6 mmoles,

5.4 mL) was added and stirred for three minutes. Methyl acetate (7.25 mmoles, 579 uL) was added at -78 °C and stirred for 30 minutes. Addition of aldehyde (8.7 mmoles, 3.12 g) via 20 mL THF was completed and stirred for two hours. The reaction was quenched with 5 mL acetic acid and 20 mL sat. aq. NH₄Cl. The solution was brought to room temperature and the product was extracted with EtOAc (3x). The organic layer was washed with brine, dried over Na₂SO₄ and concentrated. β -alcohol methyl ester was purified with column chromatography on silica gel (20% to 60% EtOAc in hexanes).

¹H NMR (400 MHz, Chloroform-*d*) δ 7.43 – 7.34 (m, 6H), 7.28 – 7.17 (m, 13H), 5.61 – 5.52 (m, 1H), 5.40 (dd, *J* = 15.6, 6.1 Hz, 1H), 3.68 (d, *J* = 10.2 Hz, 3H), 2.51 – 2.45 (m, 1H), 2.09 (s, 8H), 1.39 (d, *J* = 6.5 Hz, 1H), 1.27 – 1.22 (m, 1H).

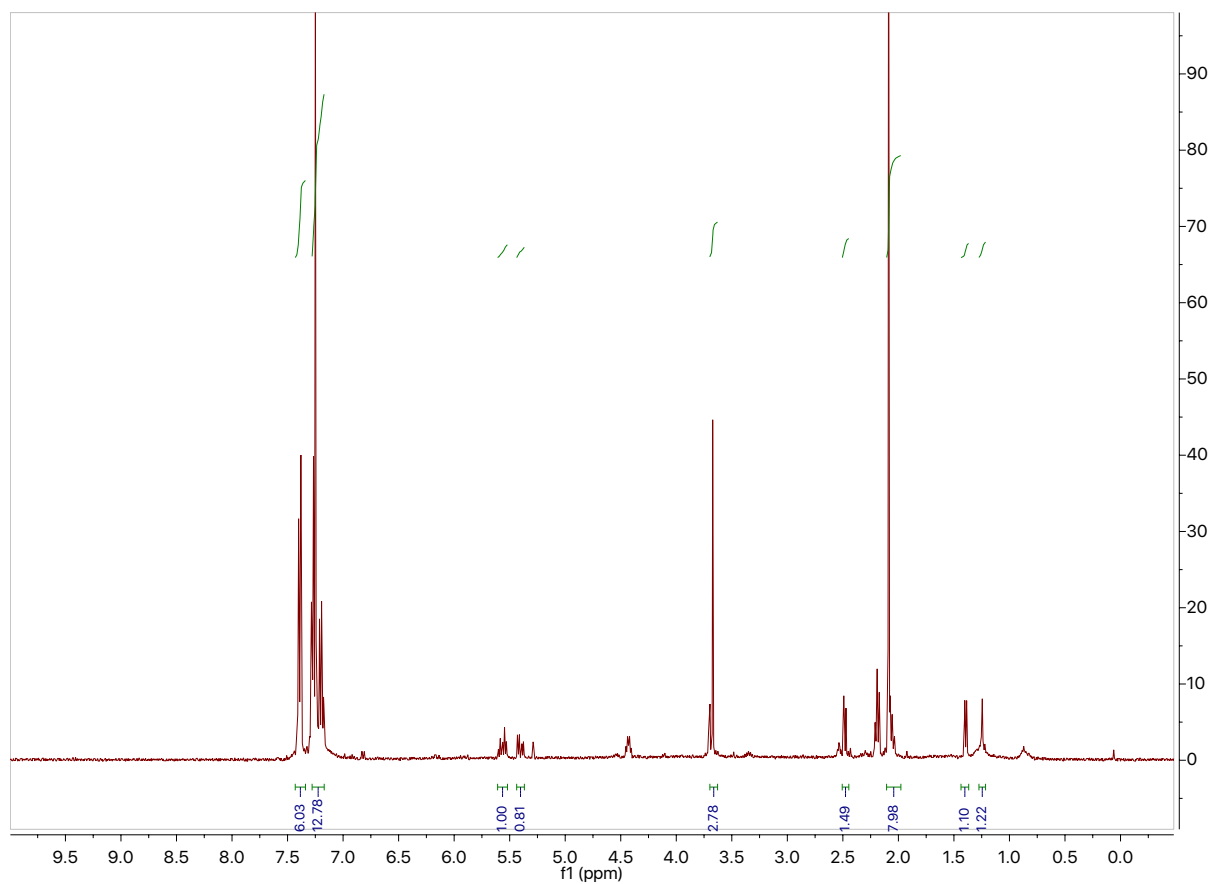
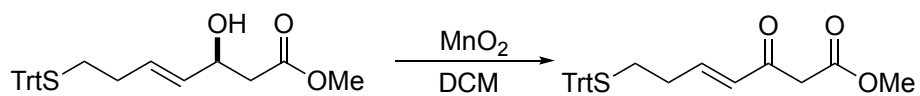
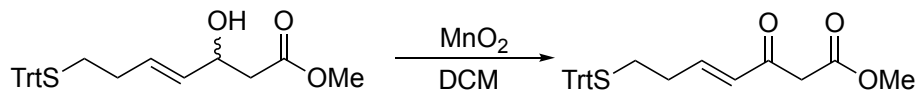


Figure 39. NMR of product



Scheme 128. Reaction conditions

A solution of alcohol (0.067 mmoles, 35 mg) in 2 mL DCM was added MnO_2 (1.34 mmoles, 116 mg). The reaction was stirred overnight and concentrated. B-keto ester was purified via column chromatography on silica gel (4/1 hexanes/EtOAc). Compound X (0.025 mmoles, 13 mg) was isolated in a 37% yield.



Scheme 129. Reaction conditions

A solution of alcohol (0.18 mmol, 77 mg) in 5 mL DCM was added MnO_2 (3.54 mmol, 308 mg). The reaction was stirred for 16 hours, filtered through celite, and concentrated. β -keto ester was purified via column chromatography on silica gel (4/1 hexanes/EtOAc). Ester (0.025 mmol, 13 mg) was isolated in a 37% yield.

^1H NMR (400 MHz, Chloroform-*d*) δ 7.45 – 7.37 (m, 4H), 7.32 – 7.26 (m, 11H), 7.24 – 7.19 (m, 2H), 5.62 – 5.50 (m, 1H), 5.45 – 5.37 (m, 1H), 3.69 (s, 3H), 2.54 – 2.44 (m, 2H), 2.21 (dd, $J = 7.7, 6.4$ Hz, 2H), 2.12 – 1.95 (m, 2H).

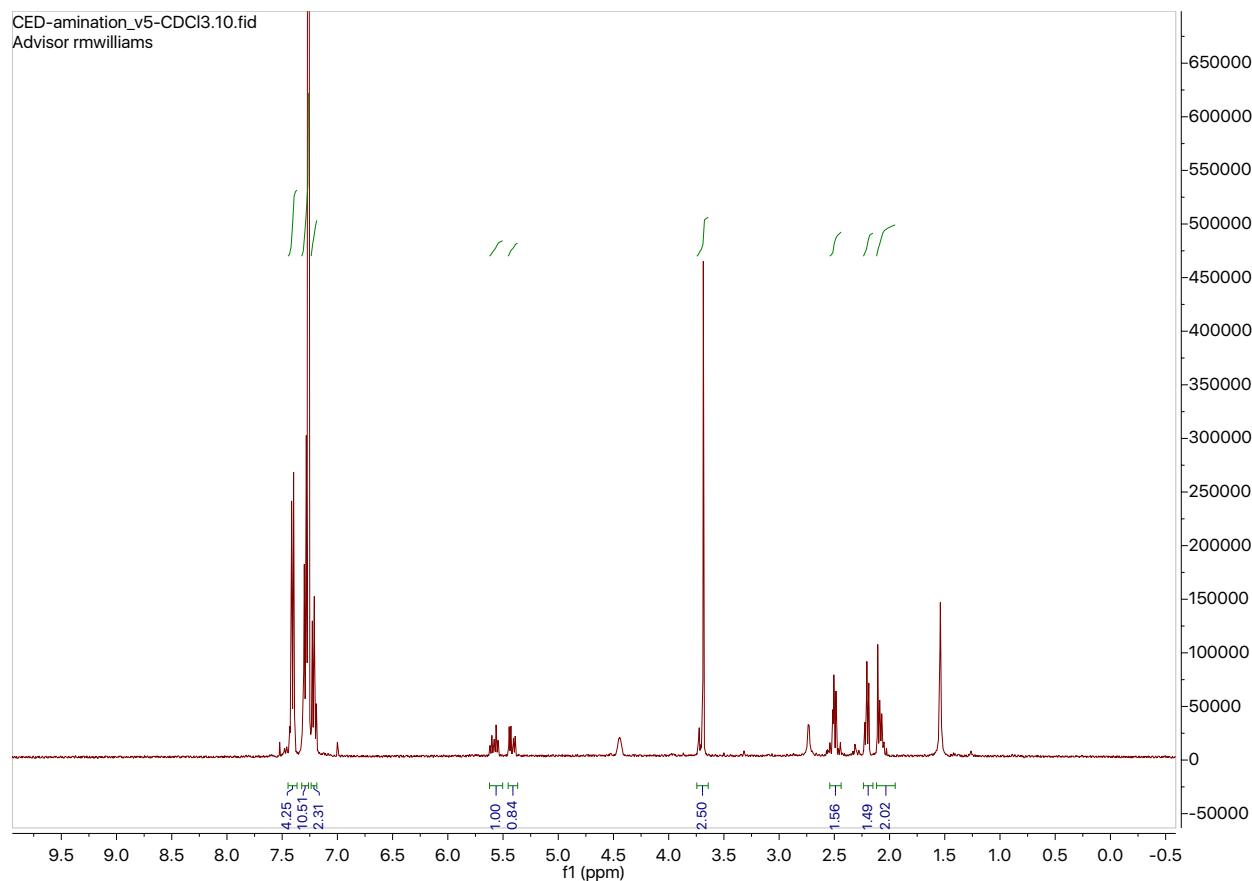


Figure 40. NMR of product



Scheme 130. Reaction conditions

To a solution of propanediol (105 mmol, 8 g) in 300 mL DMF was added DIPEA (1050 mmol, 182 mL). TBDPSCI (110.25 mmol, 28.7 mL) was added dropwise. The reaction was stirred at room temperature overnight. The reaction was quenched with cold H₂O and extracted with t-butyl methyl ether (3x). The organic was washed with 2N HCl (2x), saturated NaHCO₃, and brine. The organic later was dried over MgSO₄ and concentrated. Monoprotected alcohol was purified with flash column chromatography on silica gel (50:50, acetone:hexanes). Compound was isolated in a 33% yield.

¹H NMR (400 MHz, Chloroform-*d*) δ 7.75 – 7.67 (m, 4H), 7.42 (tdd, *J* = 8.4, 6.4, 4.6 Hz, 6H), 3.86 (dt, *J* = 8.9, 5.6 Hz, 4H), 2.49 (t, *J* = 5.4 Hz, 1H), 1.83 (h, *J* = 5.4 Hz, 2H), 1.08 (d, *J* = 0.8 Hz, 9H).

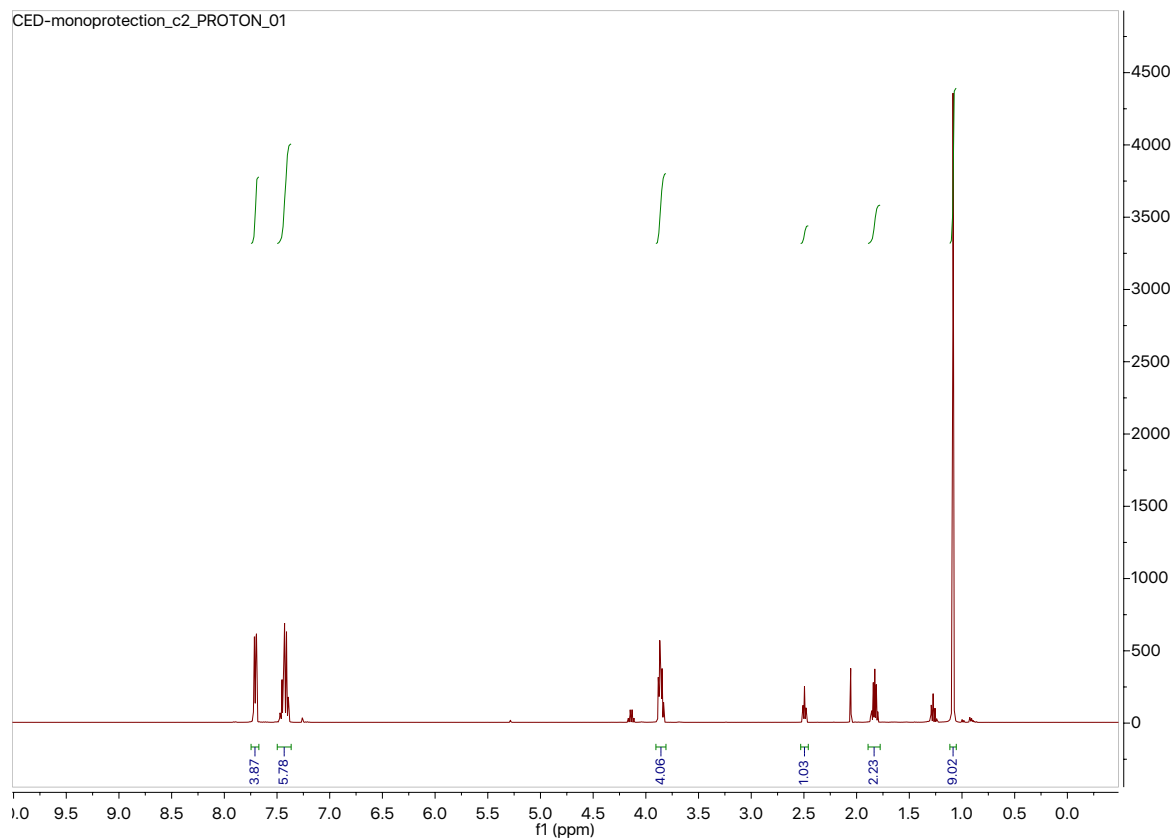
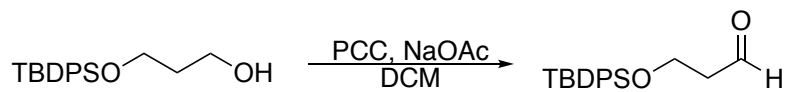
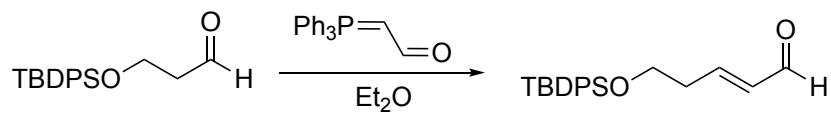


Figure 41. NMR of product



Scheme 131. Reaction conditions

PCC (14.25 mmol, 3.07 g) and NaOAc (14.25 mmol, 1.17 g) were taken up in 60 mL DCM. Alcohol (9.5 mmol, 3 g) was taken up in 30 mL DCM and added to the PCC mixture. The crude aldehyde was immediately carried onto the Wittig reaction.



Scheme 132. Reaction conditions

To the crude aldehyde (9.5 mmoles) in 90 mL DCM was added Wittig (9.5 mmoles, 2.89 g). After completion of reaction, monitored by TLC, 30 mL ether was added and the liquid was decanted. Combined organic solutions were filtered through celite and evaporated.

^1H NMR (400 MHz, Chloroform-*d*) δ 8.61 (d, $J = 4.7$ Hz, 1H), 7.65 (d, $J = 8.0$ Hz, 5H), 7.39 (q, $J = 7.1, 6.2$ Hz, 6H), 4.01 (t, $J = 6.0$ Hz, 1H), 3.83 (q, $J = 7.7, 6.7$ Hz, 2H), 3.49 – 3.40 (m, 1H), 1.20 (t, $J = 6.9$ Hz, 2H), 1.03 (t, $J = 6.8$ Hz, 11H).

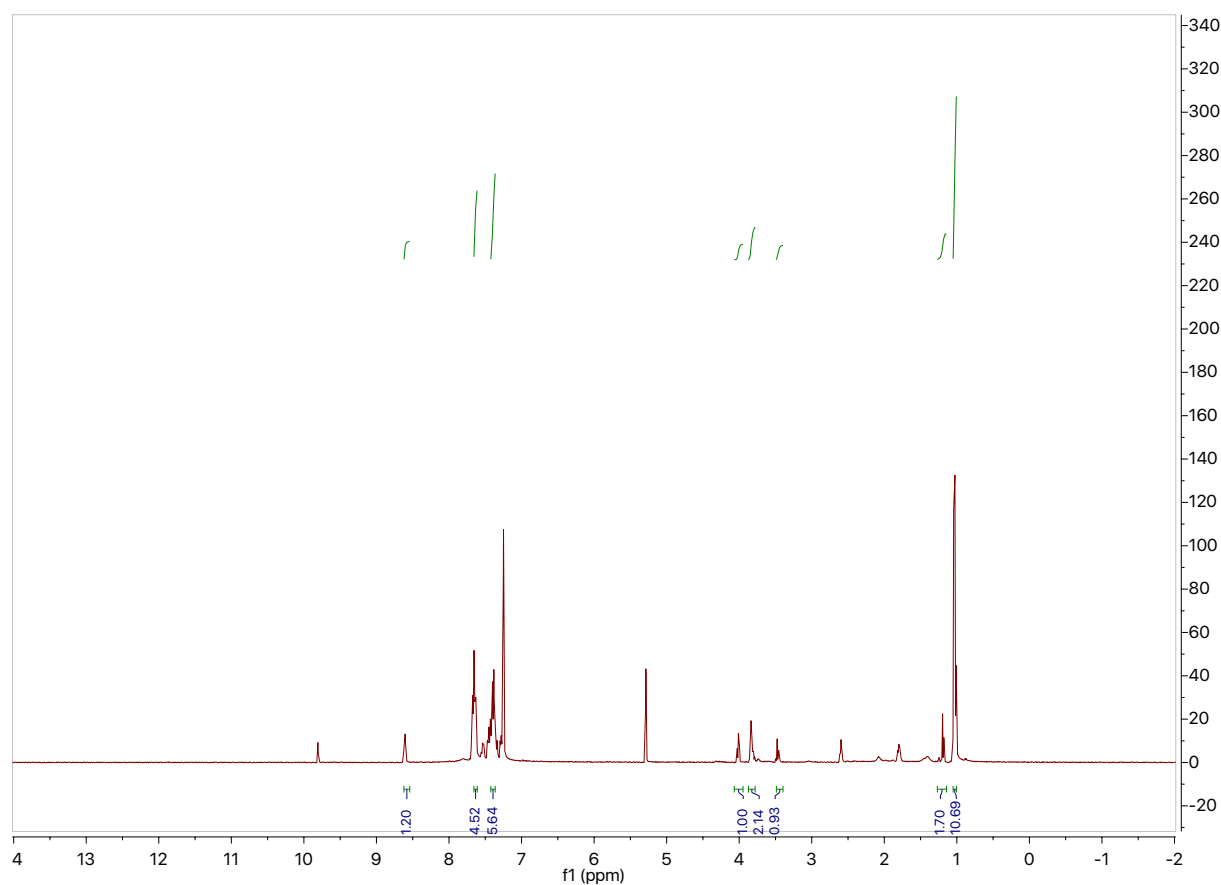
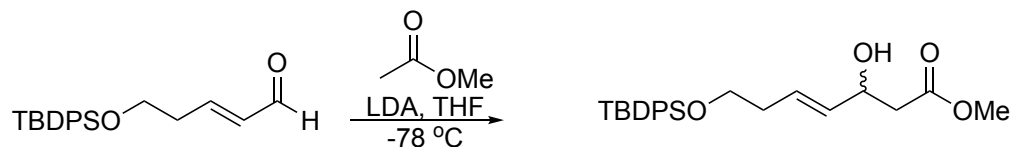


Figure 42. NMR of product



Scheme 133. Reaction conditions

LDA was prepared in situ by taking up DIPA (11.88 mmoles, 1.66 mL) in 38.5 mL THF. The mixture was brought to -78 °C and stirred for one minute. N-BuLi (1.6M in hexanes, 8.32 mmoles, 5.2 mL) was added and stirred for three minutes. Methyl acetate (7.92 mmoles, 630 uL) was added at -78 °C and stirred for 30 minutes. Addition of aldehyde (9.5 mmoles, 3.22 g) via 10 mL THF was completed and stirred for two hours. The reaction was quenches with 5 mL acetic acid and 20 mL sat. aq. NH₄Cl. The solution was brought to room temperature and the product was extracted with EtOAc (3x). The organic layer was washed with brine, dried over Na₂SO₄ and concentrated. β-alcohol methyl ester was purified with column chromatography on silica gel (20% to 60% EtoAC in hexanes).

¹H NMR (400 MHz, Chloroform-*d*) δ 7.70 – 7.64 (m, 6H), 7.56 (dd, *J* = 7.6, 1.7 Hz, 2H), 7.46 (td, *J* = 7.6, 2.8 Hz, 6H), 3.76 – 3.65 (m, 3H), 2.62 – 2.55 (m, 1H), 2.52 – 2.44 (m, 1H), 2.06 (d, *J* = 16.7 Hz, 7H), 1.08 – 1.00 (m, 2H), 0.87 (dt, *J* = 12.2, 7.4 Hz, 2H).

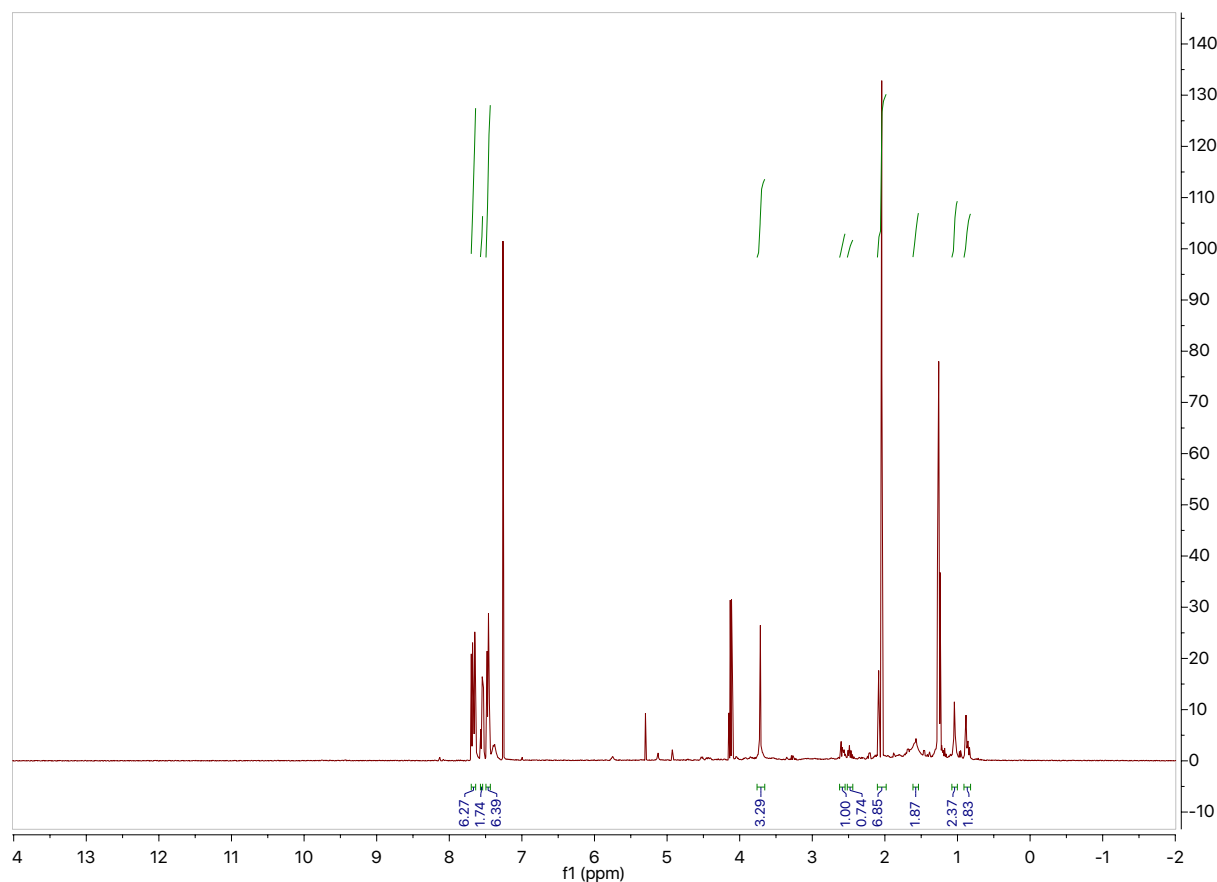
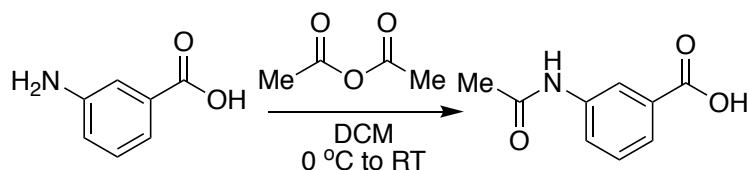


Figure 43. NMR of product



Scheme 134. Reaction conditions

3-amino benzoic acid (3.6 mmol, 500 mg) was taken up in 30 mL DCM at 0 °C. Acetic anhydride (3.6 mmol, 368 μ L) was slowly added to the solution. The mixture was warmed to room temperature and stirred for three hours. The precipitate was filtered and washed with H₂O to obtain a white powder (2.8 mmol) in 78% yield.

¹H NMR (400 MHz, DMSO-*d*₆) δ 12.92 (s, 1H), 10.10 (s, 1H), 8.19 (t, *J* = 1.9 Hz, 1H), 7.79 (dt, *J* = 8.3, 1.4 Hz, 1H), 7.59 (dd, *J* = 7.6, 1.4 Hz, 1H), 7.40 (t, *J* = 7.9 Hz, 1H), 2.05 (d, *J* = 1.0 Hz, 3H).

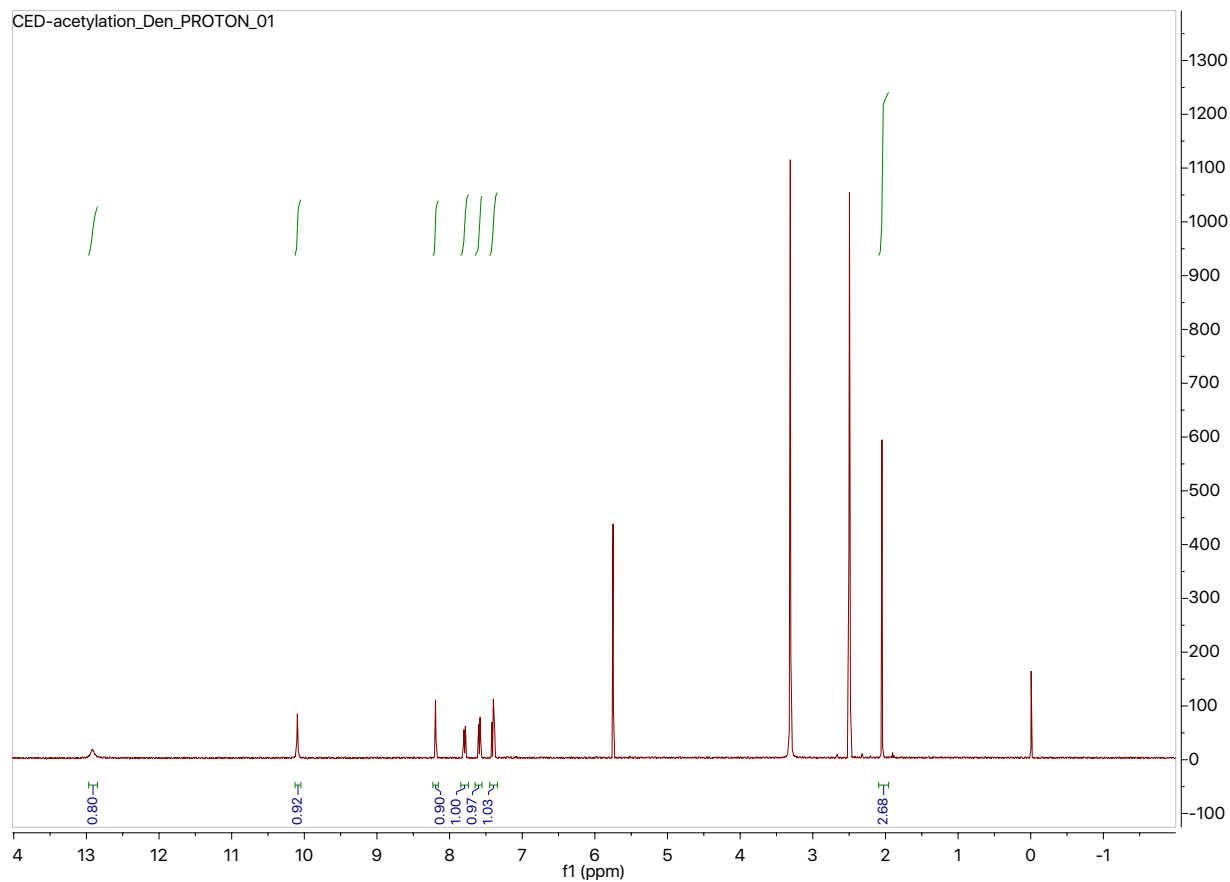
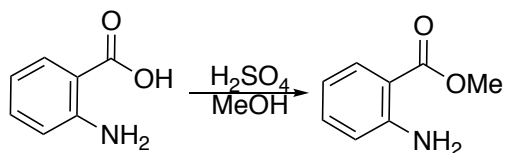
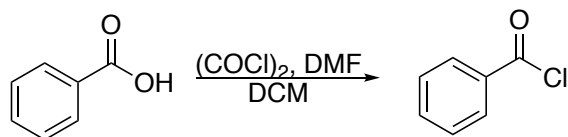


Figure 44. NMR of product



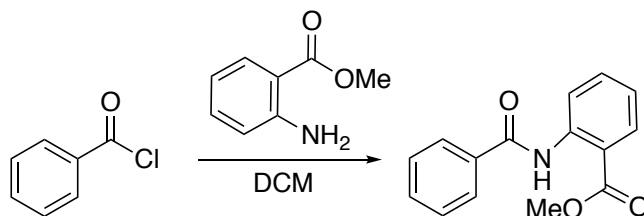
Scheme 135. Reaction conditions

Anthranilic acid (14.6 mmoles, 2 g) was taken up in 30 mL MeOH. H_2SO_4 (30 mmoles, 1.6 mL) was added dropwise and the reaction was heated at reflux for 8 hours. The solution was evaporated and taken up in 20 mL H_2O . The aqueous layer was taken to pH 3 with 2M NaOH. The precipitate was collected for further analysis.



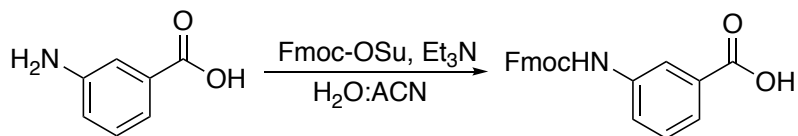
Scheme 136. Reaction conditions

Benzoic acid (0.82 mmoles, 100mg) was taken up in 20 mL DCM. Oxalyl chloride (1.64 mmoles, 140 uL) was slowly added. A few drops of DMF was added and the reaction was monitored for loss of starting material. The acid chloride solution was evaporated and immediately carried on to the next reaction.



Scheme 137. Reaction conditions

The crude was immediately dissolved in 20 mL DCE (DCM created slight solubility issues and DCE helped to combat those). Anthranilic methyl ester (1.64 mmoles, 248 mg) was added to the solution and monitored by TLC. Crude solution was evaporated and analyzed by NMR to confirm presence of amide.



Scheme 138. Reaction conditions

3-amino benzoic acid (7.29 mmoles, 1 g) was taken up in 10 mL H₂O. Et₃N (7.29 mmoles, 1.02 mL) was added and the mixture was stirred for 30 minutes. The mixture was diluted with 10 mL ACN and Fmoc-OSu (5.83 mmoles, 1.97 g) was added. The reaction was stirred overnight and identified to pH 2 with 6N HCl. The solution was stirred for an additional hour and filtered through a Buchner funnel. The cake was washed with H₂O (5x) and dried under vacuum.

^1H NMR (400 MHz, Chloroform-*d*) δ 9.89 (s, 1H), 8.11 (s, 1H), 7.95 – 7.86 (m, 2H), 7.75 (d, $J = 7.4$ Hz, 2H), 7.71 – 7.61 (m, 1H), 7.57 (t, $J = 1.4$ Hz, 1H), 7.48 – 7.27 (m, 6H), 4.48 (d, $J = 6.7$ Hz, 2H), 4.31 (t, $J = 6.6$ Hz, 1H).

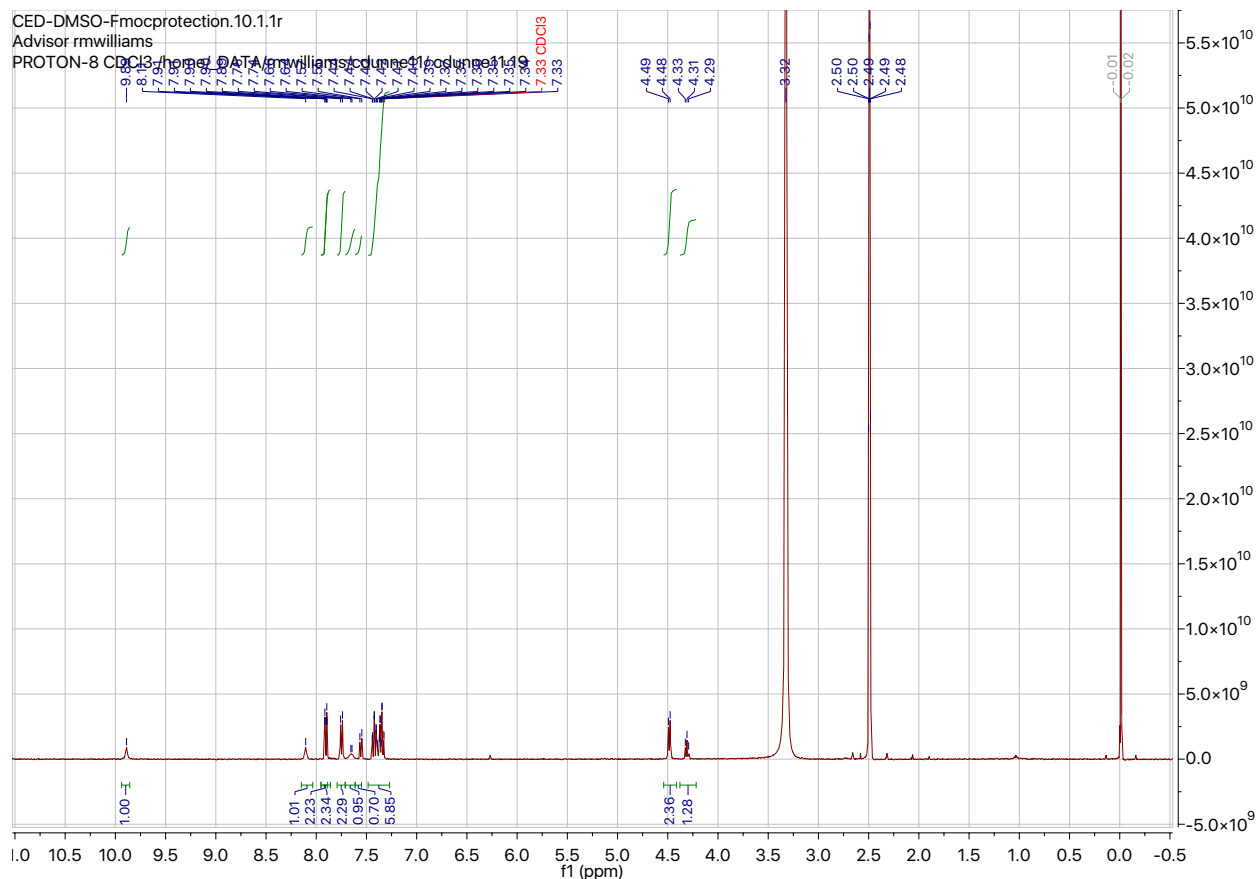
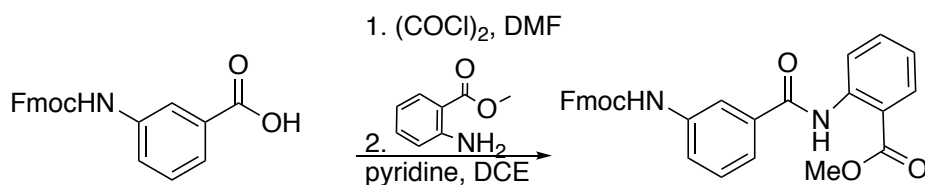


Figure 45. NMR of product



Scheme 139. Reaction conditions

Fmoc protected amino acid (0.47 mmol, 169 mg) was taken up in 6 mL DCE. Oxalyl chloride (9.4 mmol, 825 μL) and cat. DMF was added at room temperature. The reaction was stirred for 40 minutes and concentrated. The crude was taken up in DCE and concentrated a second time. The crude was immediately dissolved in 8 mL DCE. Pyridine (4.7 mmol, 379 μL) and

anthranilic methyl ester (1.88 mmol, 243 μ L) was added. The reaction was stirred overnight at room temperature. The mixture was diluted with DCM, washed with 1M HCl, sat. NaHCO₃, and brine. The organic layer was dried over MgSO₄ and concentrated.

¹H NMR (400 MHz, Chloroform-*d*) δ 12.01 (s, 1H), 8.91 (dd, $J = 8.5, 1.2$ Hz, 1H), 8.09 (dd, $J = 8.0, 1.7$ Hz, 1H), 7.88 (s, 1H), 7.83 – 7.72 (m, 4H), 7.67 – 7.55 (m, 3H), 7.45 (dt, $J = 21.6, 7.7$ Hz, 3H), 7.34 (td, $J = 7.4, 1.2$ Hz, 2H), 7.21 – 7.11 (m, 1H), 6.80 (s, 1H), 4.58 (d, $J = 6.6$ Hz, 2H), 4.31 (t, $J = 6.7$ Hz, 1H), 3.96 (s, 3H). ¹³C NMR (101 MHz, CDCl₃) δ 169.03, 165.20, 153.32, 143.67, 141.70, 141.36, 138.45, 135.84, 134.82, 130.96, 129.71, 127.81, 127.15, 124.95, 122.73, 121.98, 120.54, 120.06, 115.26, 115.07, 111.54, 77.33, 77.22, 77.01, 76.70, 67.06, 52.51, 51.50, 47.08, 36.28, 29.70, 28.39, 28.07.

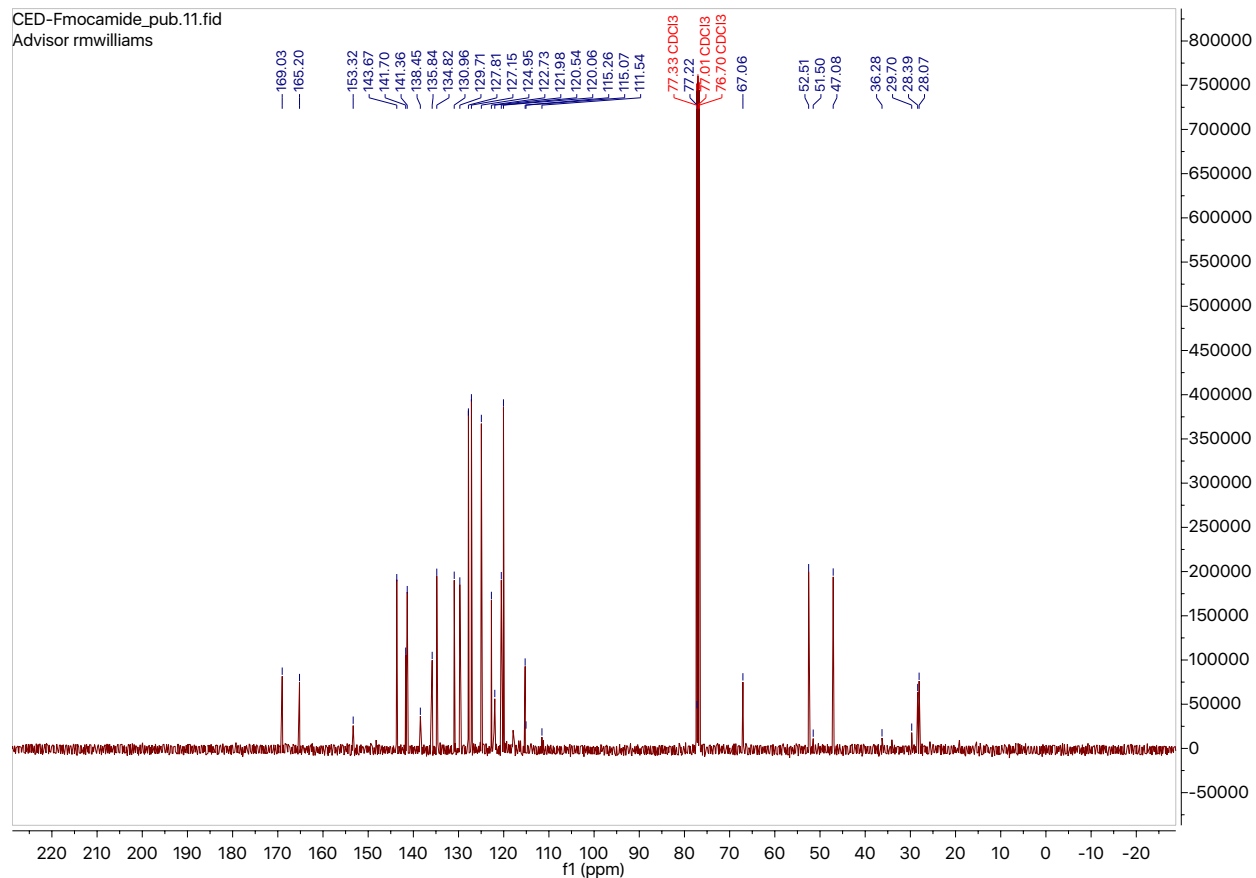
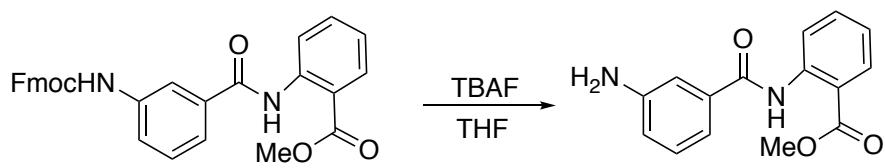
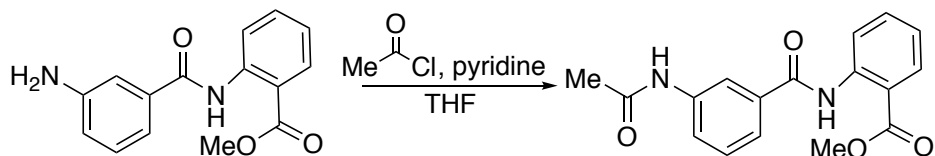


Figure 47. NMR of product



Scheme 140. Reaction conditions

Fmoc amide (0.127 mmoles, 62.6 mg) was taken up in 5 mL THF. TBAF (0.19 mmoles, 50 mg) was added to the solution at room temperature. The reaction was stirred overnight. Under an inert atmosphere. The reaction was concentrated and immediately carried on to acylation.



Scheme 141. Reaction conditions

Crude amine (0.127 mmol) was redissolved in THF. Pyridine (0.51 mmol, 40 mg) and acetyl chloride (0.38 mmol, 30 mg) were added and the solution was stirred for three hours. Diamide methyl ester was purified with column chromatography on silica gel (0% to 100% EtOAc in hexanes). Compound (22 mg) was isolated in a 55% yield.

^1H NMR (400 MHz, Chloroform-*d*) δ 12.02 (s, 1H), 8.91 (dd, $J = 8.6, 1.2$ Hz, 1H), 8.10 (dd, $J = 8.0, 1.7$ Hz, 1H), 8.03 (d, $J = 8.2$ Hz, 1H), 7.92 (s, 1H), 7.77 (d, $J = 7.8$ Hz, 1H), 7.67 – 7.56 (m, 1H), 7.49 (d, $J = 8.0$ Hz, 1H), 7.19 – 7.06 (m, 1H), 3.98 (s, 3H), 2.23 (s, 3H).

^{13}C NMR (101 MHz, CDCl_3) δ 168.95, 168.90, 165.43, 165.35, 141.55, 141.41, 138.84, 135.54, 135.49, 134.73, 131.00, 129.60, 123.51, 123.41, 122.82, 122.30, 120.51, 120.45, 118.85, 118.74, 115.37, 115.34, 77.35, 77.23, 77.03, 76.71, 52.53, 29.69, 24.58, 24.54.

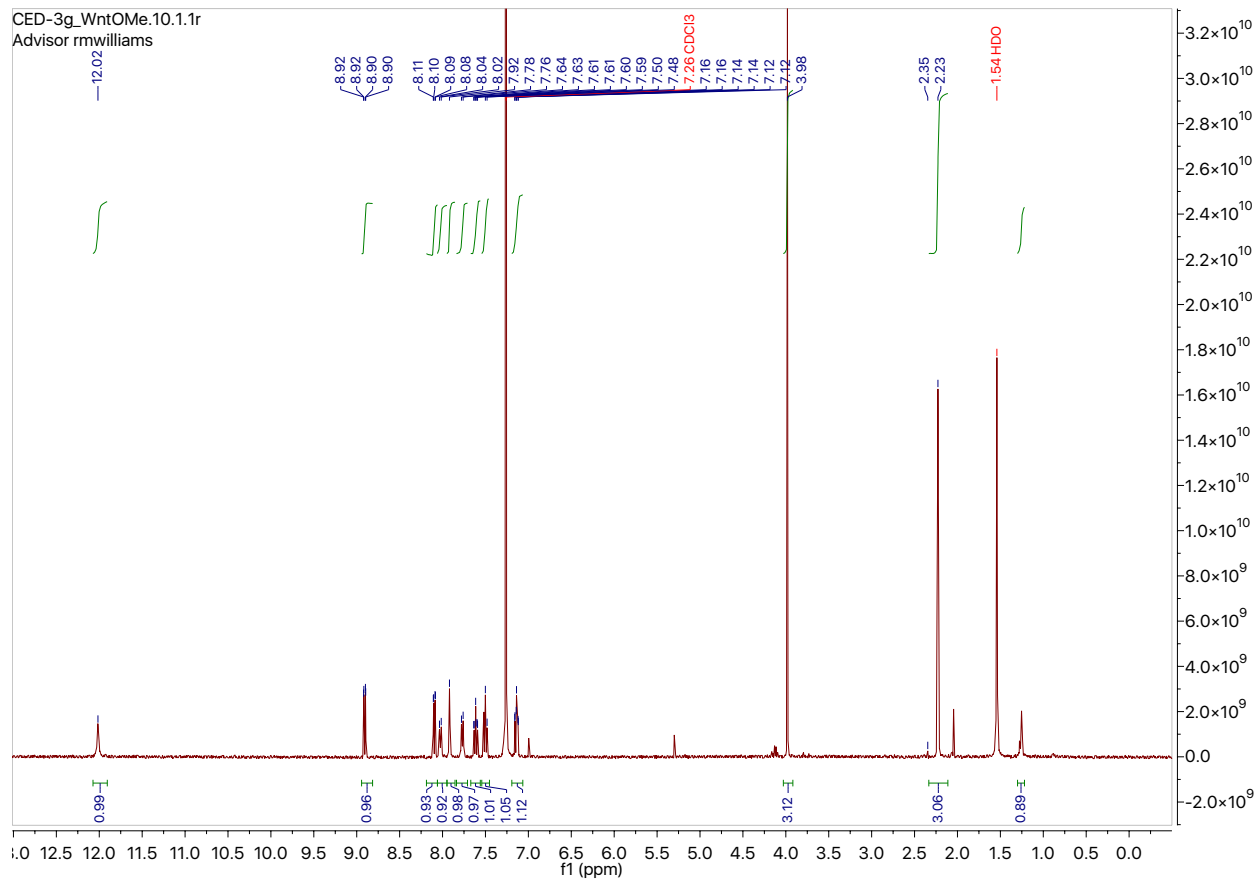


Figure 48. NMR of product

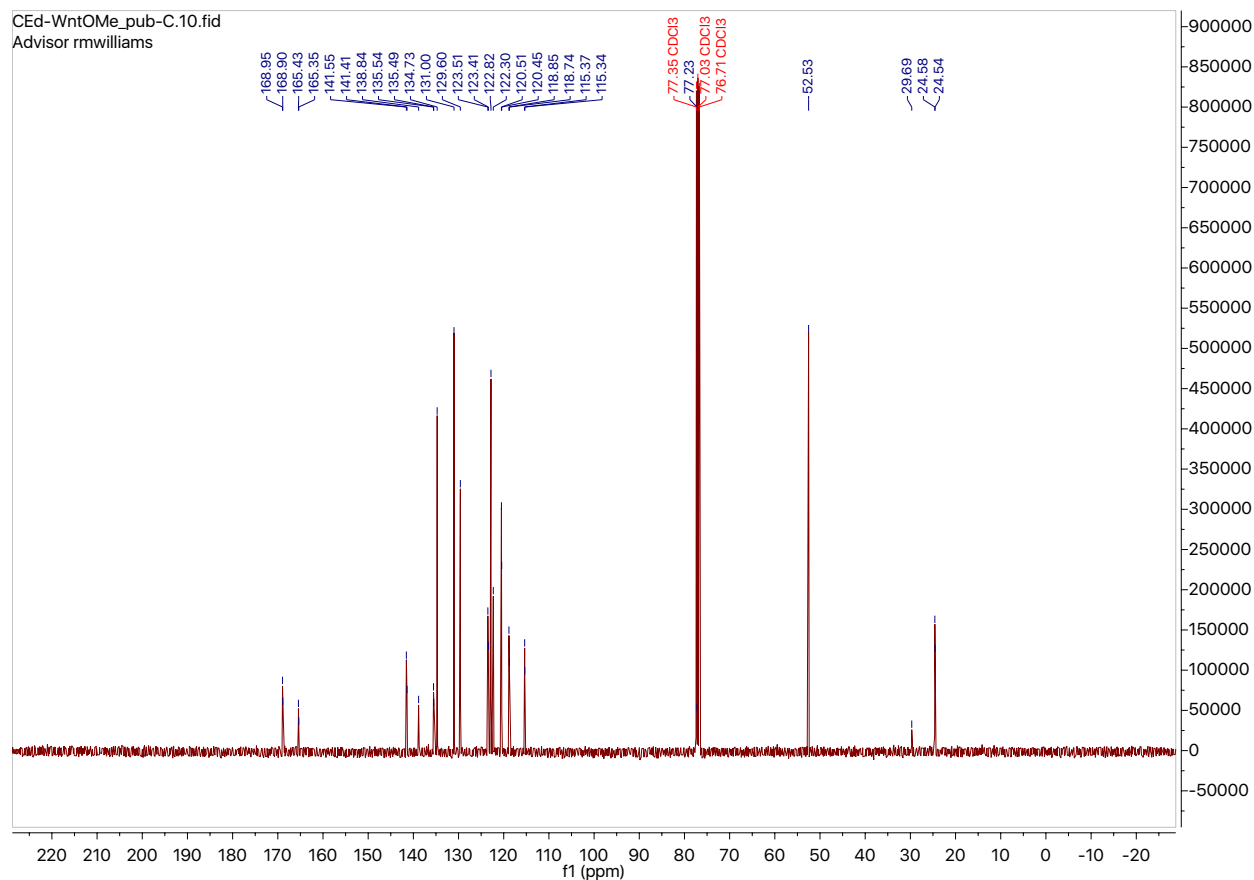
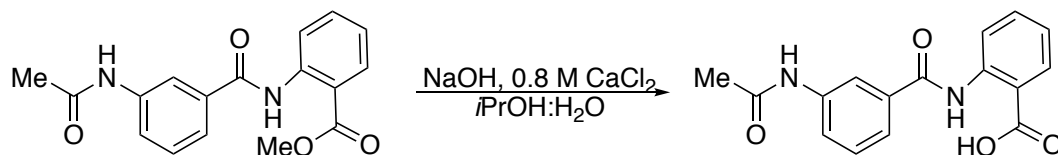


Figure 49. NMR of product



Scheme 142. Reaction conditions

Methyl ester (2.24 mmoles, 700 mg) was dissolved in 70 mL of a 0.8M solution of CaCl₂ in a 7:3 mixture of iPrOH:H₂O. NaOH (5.6 mmoles, 224 mg) was added to the solution and the reaction was stirred for four hours. The mixture was acidified with 1M HCl and extracted with EtOAc. The organic was washed with brine and dried over MgSO₄. The solution was concentrated and purified with flash column chromatography on silica gel (10% MeOH in DCM). 3289-5066 (274 mg) was isolated in a 41% yield.

^1H NMR (400 MHz, methanol- d_4) δ 11.97 (s, 1H), 8.85 (d, $J = 8.5$ Hz, 1H), 8.02 (ddd, $J = 18.9, 8.1, 1.9$ Hz, 2H), 7.91 (s, 1H), 7.71 (d, $J = 7.8$ Hz, 1H), 7.64 – 7.50 (m, 2H), 7.45 (d, $J = 8.0$ Hz, 0H), 7.22 (s, 1H), 7.09 (t, $J = 7.6$ Hz, 1H), 3.93 (d, $J = 1.5$ Hz, 3H), 2.16 (s, 3H). ^{13}C NMR (101 MHz, MeOD) δ 170.60, 170.30, 165.70, 141.27, 139.23, 135.26, 134.17, 131.34, 129.09, 123.34, 122.89, 122.05, 119.89, 118.74, 116.01, 48.43, 48.22, 48.00, 47.78, 47.58, 47.36, 47.15, 22.80.

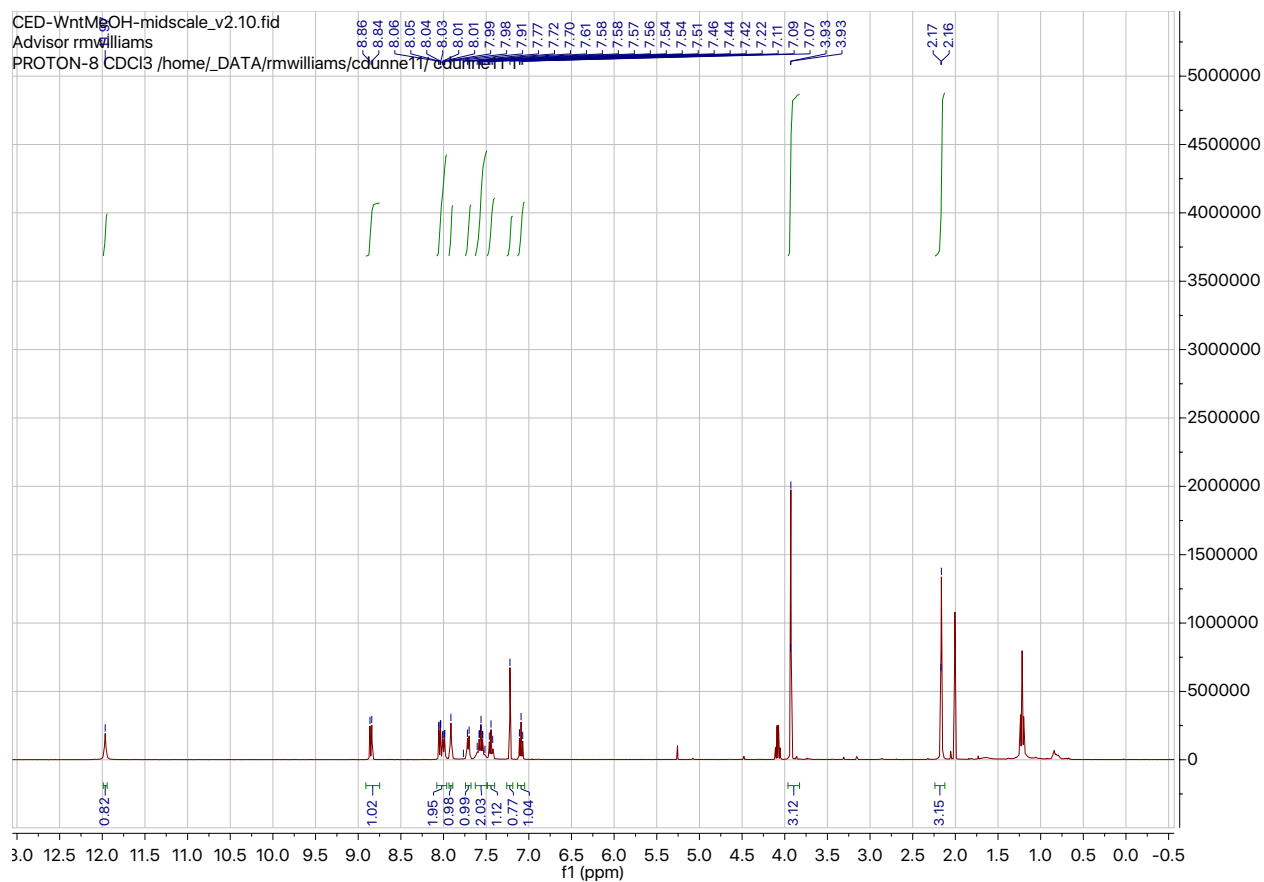


Figure 50. NMR of product

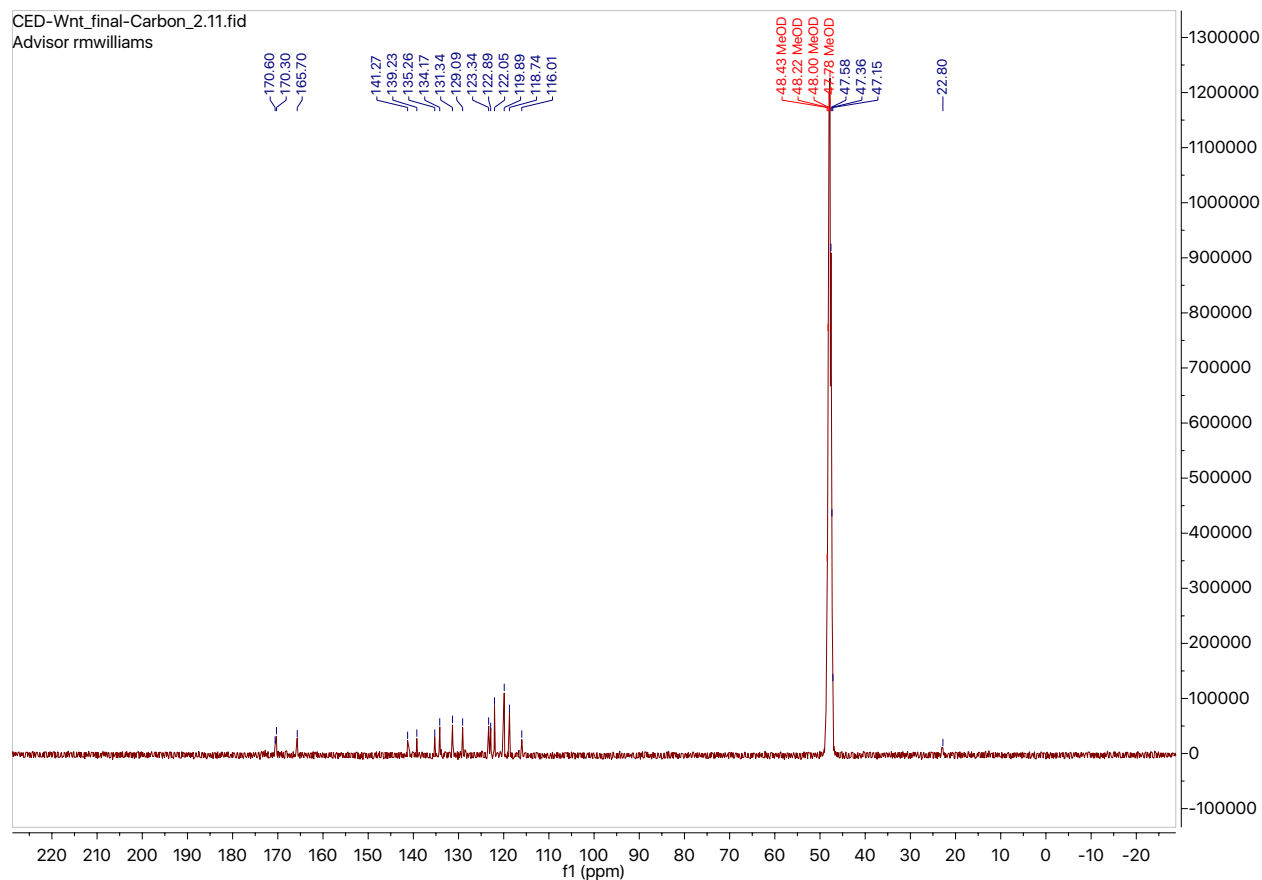
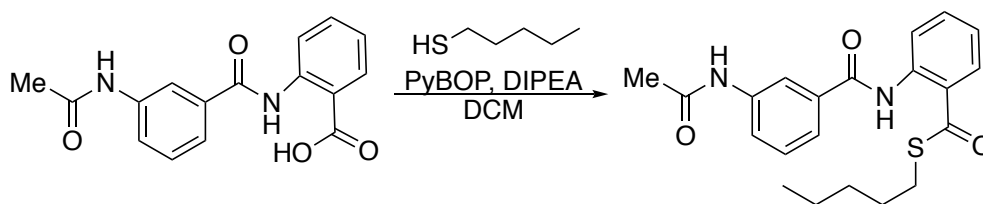


Figure 51. NMR of product



Scheme 143. Reaction conditions

3289-5066 (0.05 mmol, 15 mg) was dissolved in 2 mL DCM. DIPEA (0.065 mmol, 11.5 μ L) and PyBOP (0.065 mmol, 34 mg) were added to the solution. After one minute, pentane-1-thiol (0.065 mmol, 6 μ L) was added and the reaction was stirred at room temperature overnight. The solution was evaporated to provide crude product that was purified via preparatory TLC (5% MeOH in DCM).

^1H NMR (400 MHz, Chloroform-*d*) δ 11.81 (s, 1H), 8.85 (dd, $J = 8.5, 1.2$ Hz, 1H), 8.14 (dd, $J = 8.0, 1.5$ Hz, 1H), 8.09 – 8.01 (m, 1H), 7.92 (t, $J = 2.0$ Hz, 1H), 7.70 (t, $J = 6.4$ Hz, 1H), 7.62 – 7.46 (m, 3H), 7.15 (ddd, $J = 8.3, 7.3, 1.2$ Hz, 1H), 3.30 (dtd, $J = 6.6, 4.8, 2.5$ Hz, 2H), 3.07 (t, $J = 7.2$ Hz, 2H), 2.21 (s, 3H), 2.02 – 1.95 (m, 2H), 1.79 – 1.68 (m, 2H), 1.06 (t, $J = 7.4$ Hz, 3H).

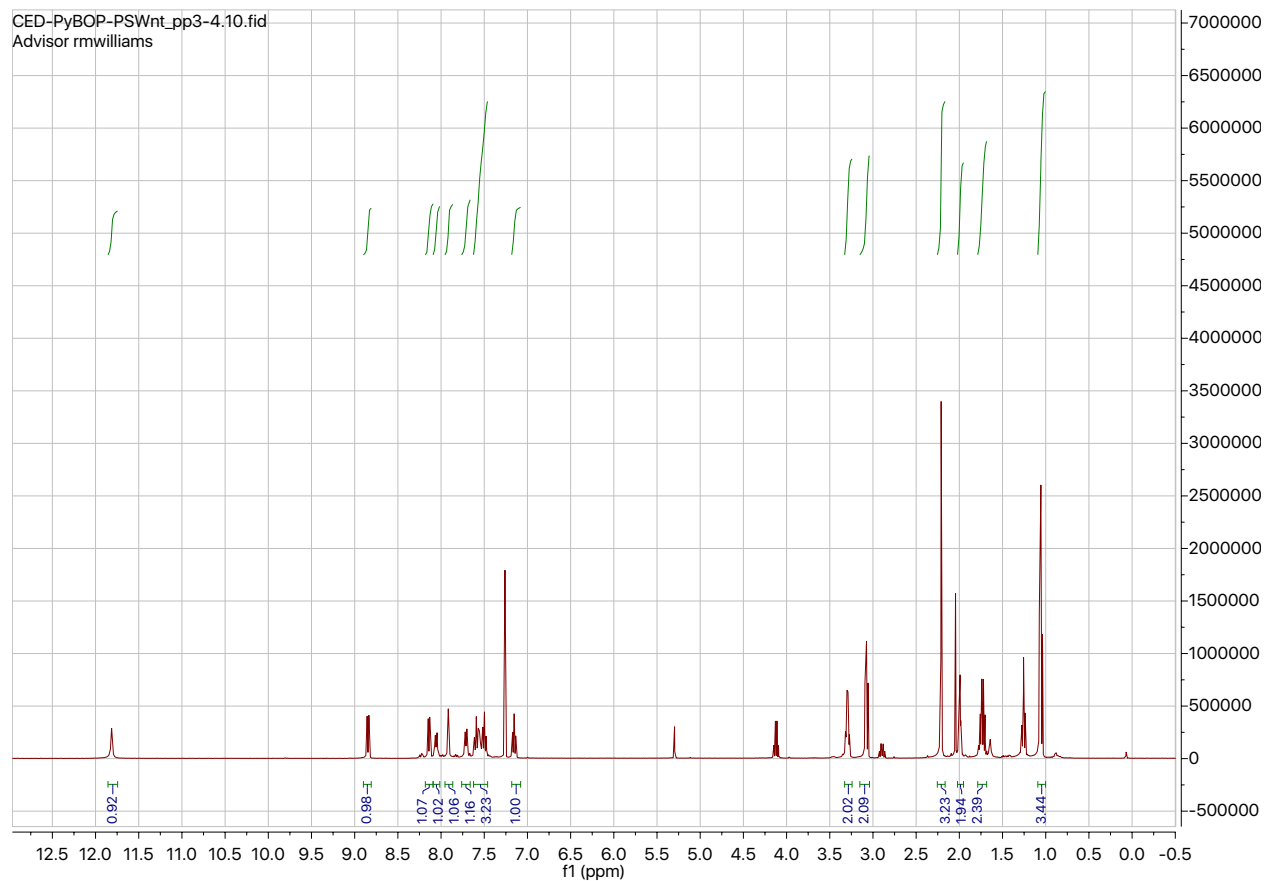
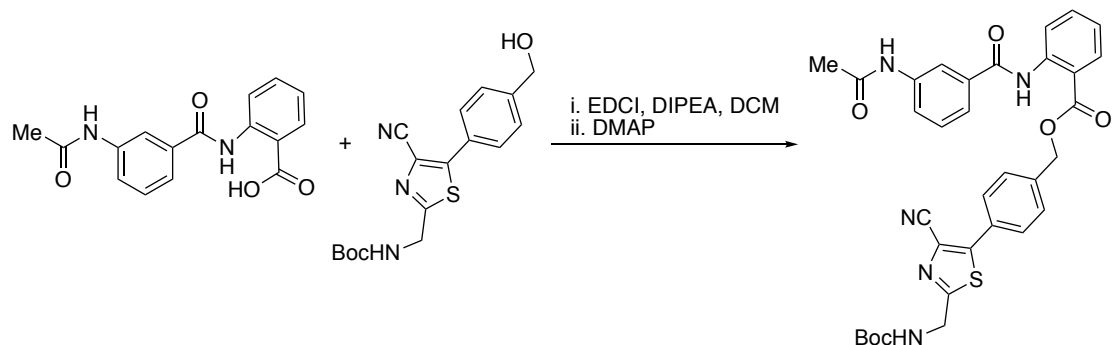


Figure 52. NMR of product



Scheme 144. Reaction conditions

3289-5066 (0.034 mmoles, 10 mg) was taken up in 2 mL DCM and brought to 0 °C. To the suspension, DIPEA (0.068 mmoles, 12 μ L), EDCI (0.041 mmoles, 8 mg) was added. The mixture was stirred for 2 hours at 0 °C. Alcohol (0.041 mmoles, 14 mg) and DMAP were added. The reaction was brought to room temperature and stirred for 30 hours. The solution was diluted with DCM:H₂O (1:1) and extracted with DCM (3x). The organic layer was dried over MgSO₄ and concentrated. The product was purified via preparatory TLC in 5% MeOH in DCM.

¹H NMR (400 MHz, Methanol-*d*₄) δ 8.73 (s, 1H), 8.26 – 8.14 (m, 2H), 7.80 (s, 3H), 7.76 – 7.62 (m, 4H), 7.49 (t, *J* = 8.0 Hz, 1H), 7.24 (ddd, *J* = 8.3, 7.3, 1.2 Hz, 1H), 4.51 (s, 2H), 2.18 (s, 3H), 1.48 (s, 9H).

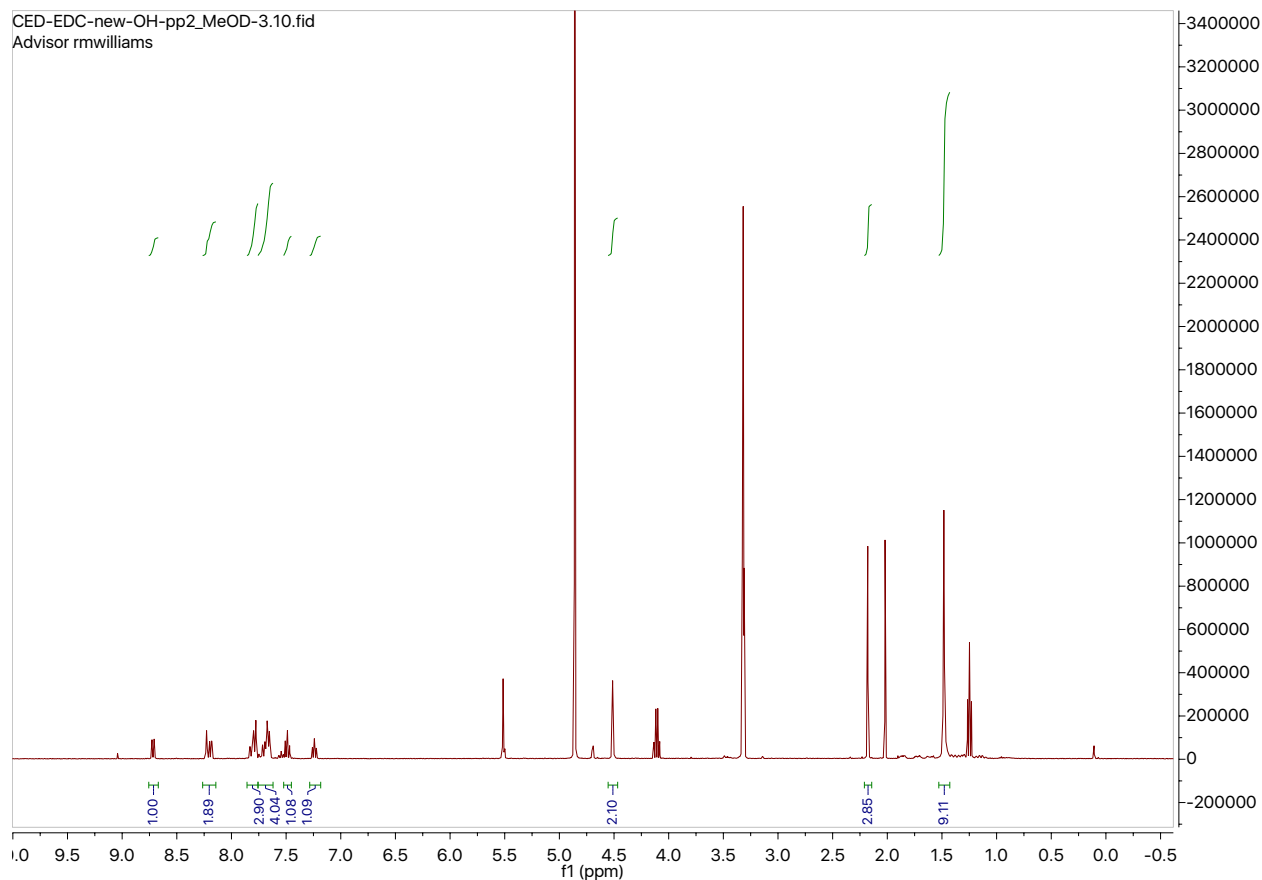


Figure 53. NMR of product



Scheme 145. Reaction conditions

3289-5066 (0.034 mmoles, 10 mg) and PyBOP (0.044 mmoles, 23 mg) were taken up in 2 mL DCM. DIPEA (0.044 mmoles, 6 mg) was added to the solution. Reaction was stirred overnight. The solution was concentrated and analyzed for cyclization product.

^1H NMR (400 MHz, Methanol- d_4) δ 8.48 (s, 1H), 8.20 (s, 1H), 8.02 (s, 1H), 7.91 (s, 1H), 7.84 (s, 1H), 7.70 (s, 1H), 7.59 (s, 1H), 7.51 (s, 1H), 2.17 (s, 3H).

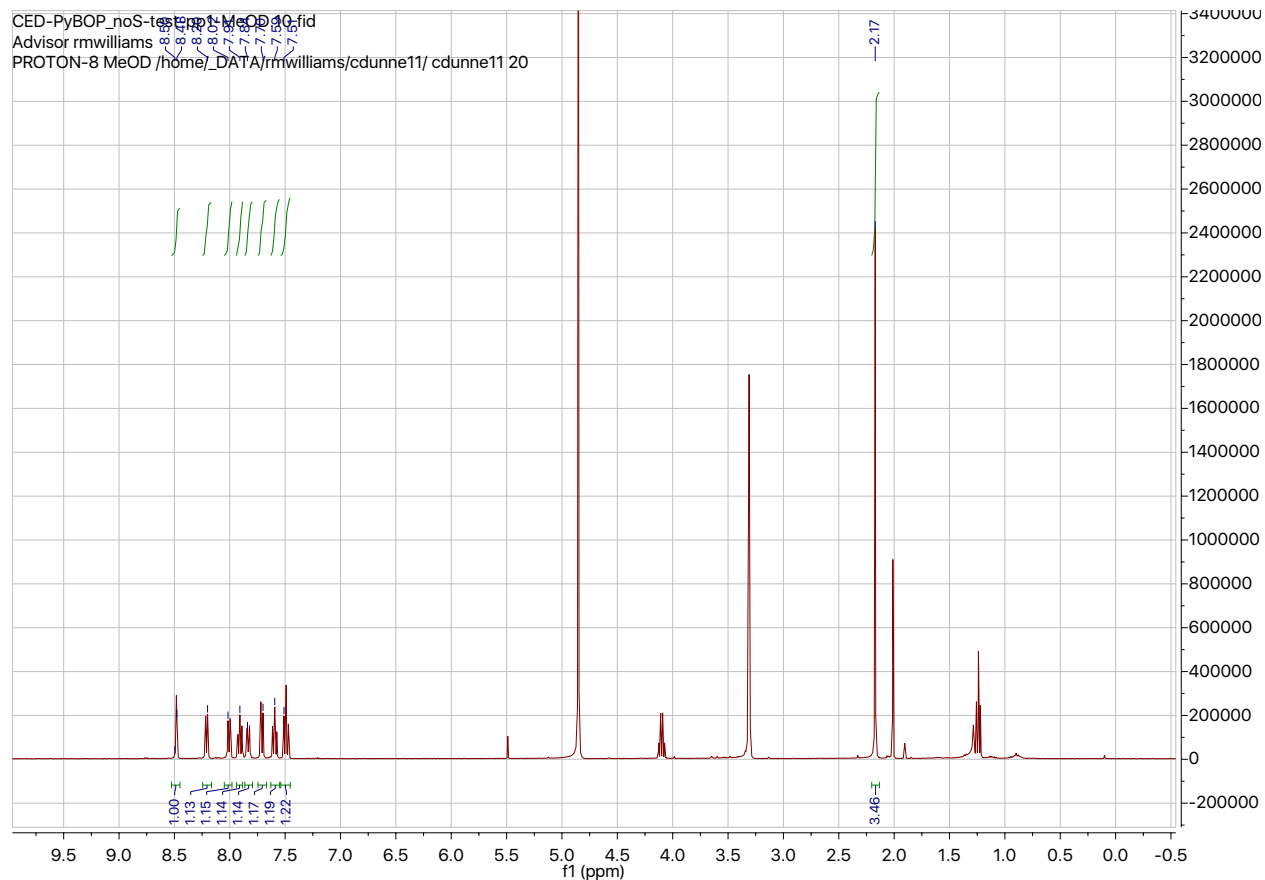
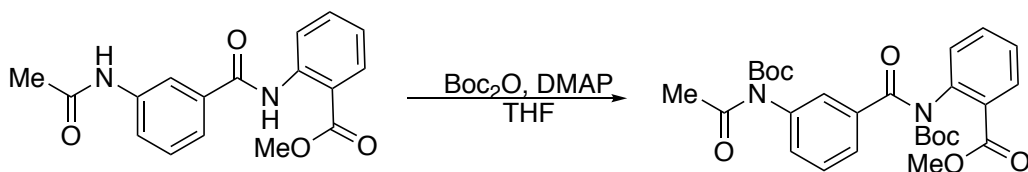


Figure 54. NMR of product



Scheme 146. Reaction conditions

To a solution of amide (0.064 mmoles, 20 mg) in 2 mL THF were added DMAP (0.083 mmoles, 10 mg) and Boc_2O (0.17 mmoles, 36 mg). The reaction was stirred at room temperature for 50 minutes. THF solution was diluted with EtOAc, washed with 1M HCl, st. aq. NaHCO_3 , brine, and dried over Na_2SO_4 . The organic layer was concentrated and purified with preparatory TLC (10% EtOAc in hexanes).

^1H NMR (400 MHz, Methanol- d_4) δ 8.08 (dd, $J = 7.8, 1.6$ Hz, 1H), 7.73 – 7.61 (m, 2H), 7.54 – 7.47 (m, 3H), 7.39 – 7.30 (m, 2H), 3.86 (s, 3H), 2.56 (s, 3H), 1.41 (s, 9H), 1.25 (d, $J = 5.5$ Hz, 9H).

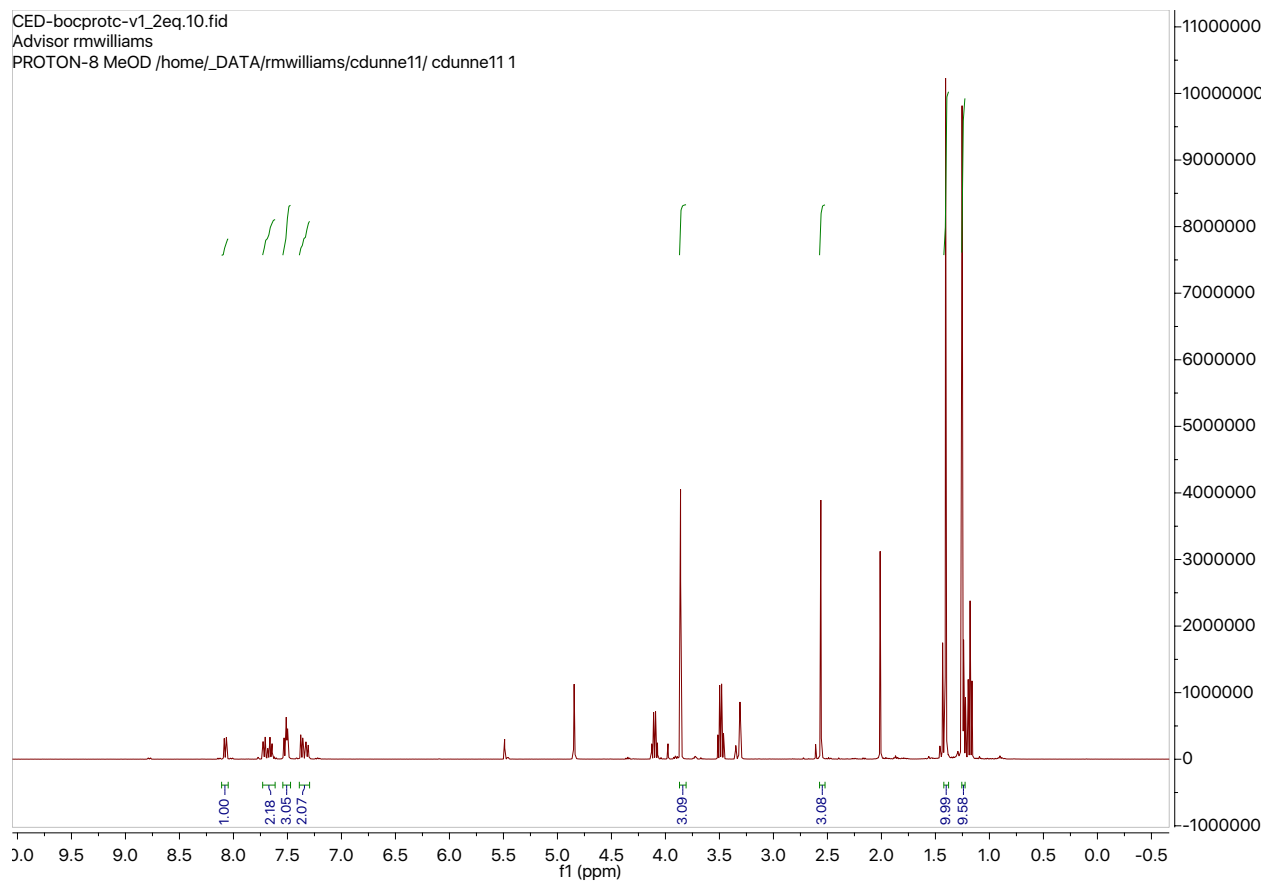
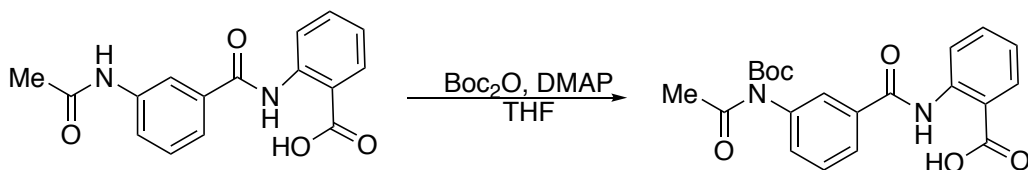


Figure 55. NMR of product



Scheme 147. Reaction conditions

To a solution of carboxylic acid (0.034 mmoles, 10 mg) in 2 mL THF were added DMAP (0.044 mmoles, 6 mg) and Boc_2O (0.088 mmoles, 20 mg). The reaction was stirred at room temperature for 50 minutes. THF solution was diluted with EtOAc, washed with 1M HCl, sat. aq.

NaHCO₃, brine, and dried over Na₂SO₄. The organic layer was concentrated and purified with preparatory TLC (10% EtOAc in hexanes).

¹H NMR (400 MHz, Methanol-*d*₄) δ 8.26 (dt, *J* = 8.0, 1.4 Hz, 1H), 8.19 (dd, *J* = 7.9, 1.5 Hz, 1H), 8.03 (t, *J* = 1.9 Hz, 1H), 7.89 (ddd, *J* = 8.2, 7.3, 1.5 Hz, 1H), 7.72 – 7.67 (m, 1H), 7.64 – 7.54 (m, 2H), 7.39 (ddd, *J* = 7.9, 2.2, 1.1 Hz, 1H), 2.60 (s, 3H), 1.39 (s, 11H).

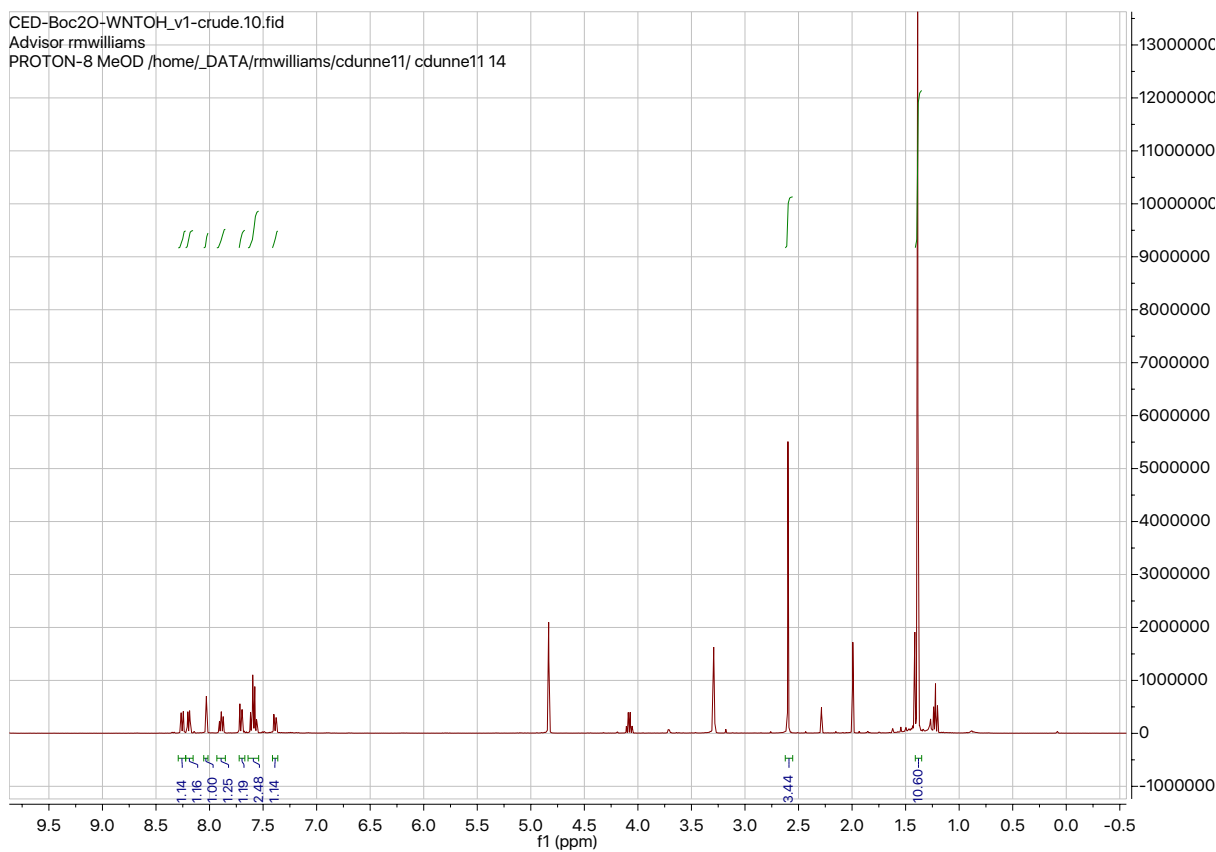
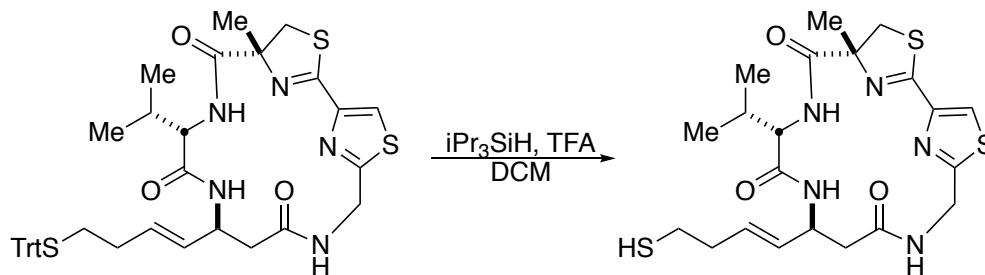


Figure 56. NMR of product



Scheme 148. Reaction conditions

Trityl thiol (0.009 mmoles, 6.6 mg) was taken up in 1 mL DCM at 0 °C. $i\text{Pr}_3\text{SiH}$ (0.018 mmoles, 4 μL) and 50 μL of TFA was added to the solution. The reaction was stirred for two hours and concentrated. Purification of Largazole peptide isostere thiol was complete via preparatory TLC (5% MeOH in DCM). It is important that isolate, loading, and development are completed under an inert atmosphere to avoid oxidation.

^1H NMR (400 MHz, Chloroform-*d*) δ 7.77 (d, $J = 5.4$ Hz, 1H), 6.23 (d, $J = 8.2$ Hz, 1H), 5.70 – 5.52 (m, 2H), 5.32 – 5.20 (m, 1H), 4.99 (s, 1H), 4.54 (dd, $J = 10.7, 3.5$ Hz, 1H), 4.33 (dd, $J = 17.6, 3.8$ Hz, 1H), 3.90 (dd, $J = 11.6, 5.3$ Hz, 1H), 3.38 (dd, $J = 11.7, 3.6$ Hz, 1H), 2.75 (d, $J = 4.1$ Hz, 1H), 2.57 (dd, $J = 11.0, 4.8$ Hz, 2H), 2.38 (ddd, $J = 30.0, 14.3, 7.0$ Hz, 3H), 1.88 (d, $J = 3.4$ Hz, 3H), 0.79 (d, $J = 7.0$ Hz, 2H), 0.40 (dd, $J = 12.3, 6.8$ Hz, 3H).

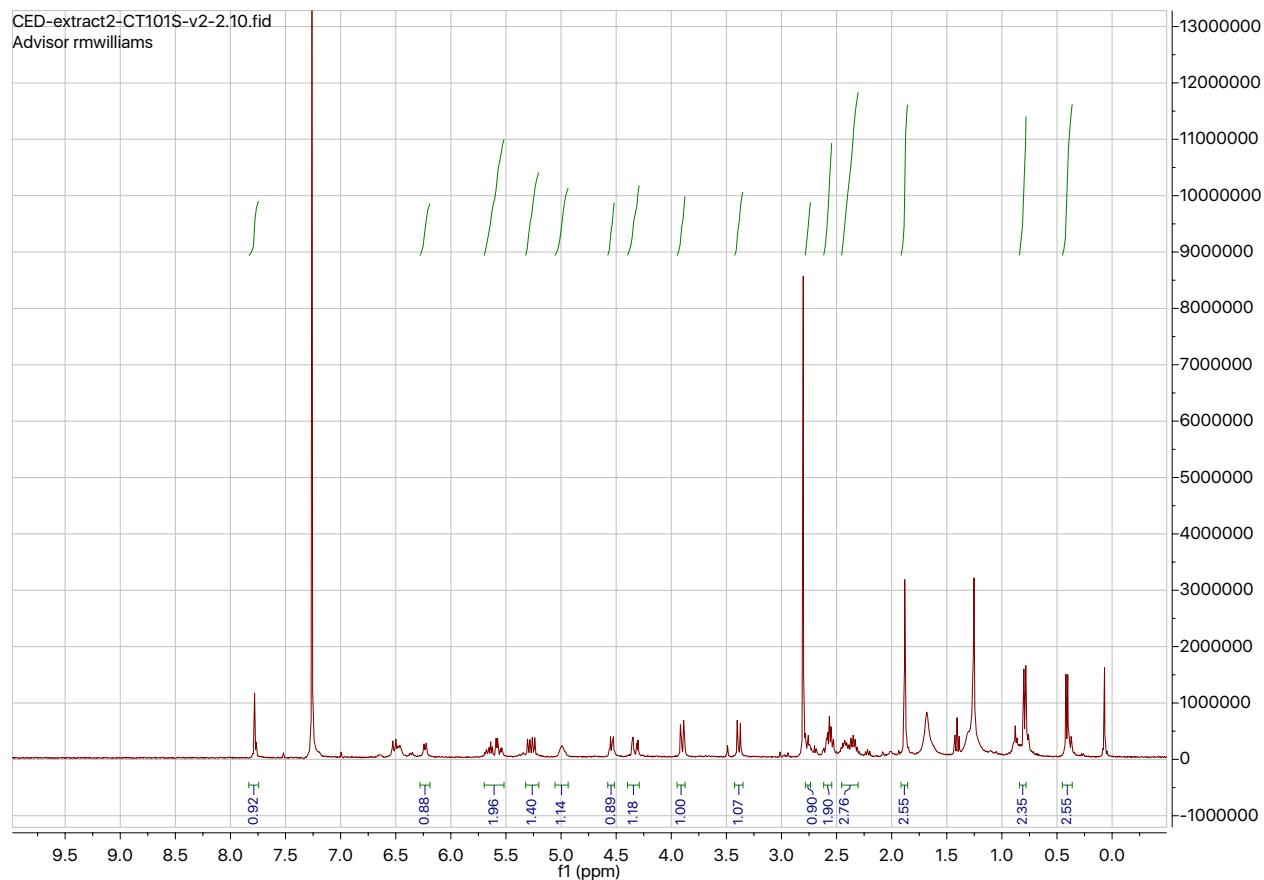
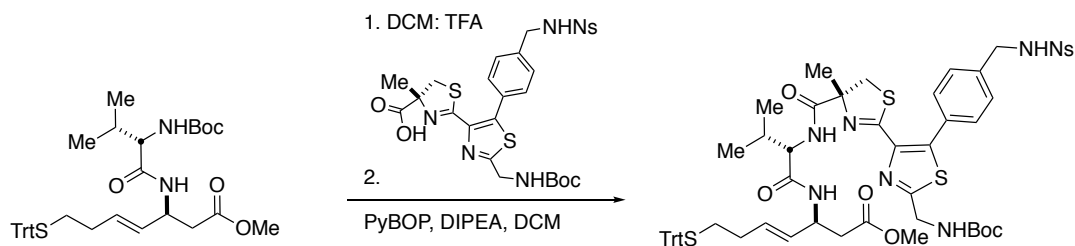


Figure 57. NMR of product



Scheme 149. Reaction conditions

^1H NMR (400 MHz, Methanol- d_4) δ 7.59 – 7.49 (m, 1H), 7.37 (ddd, J = 9.2, 4.9, 2.5 Hz, 4H), 7.31 – 7.21 (m, 4H), 7.19 (dq, J = 7.1, 4.5, 4.0 Hz, 2H), 5.51 (ddd, J = 13.3, 8.0, 5.3 Hz, 1H), 5.42 – 5.29 (m, 1H), 4.52 (d, J = 7.5 Hz, 1H), 3.72 (h, J = 6.6 Hz, 2H), 3.60 – 3.53 (m, 1H), 2.54 (ddt, J = 11.0, 8.9, 2.9 Hz, 1H), 2.17 (tq, J = 6.9, 4.0 Hz, 1H), 2.03 – 1.94 (m, 1H), 1.48 (s, 4H), 1.37 (dd, J = 7.1, 1.9 Hz, 12H), 1.27 (dq, J = 4.6, 2.9 Hz, 4H), 0.88 – 0.77 (m, 2H), 0.68 (dt, J = 17.9, 6.7 Hz, 1H).

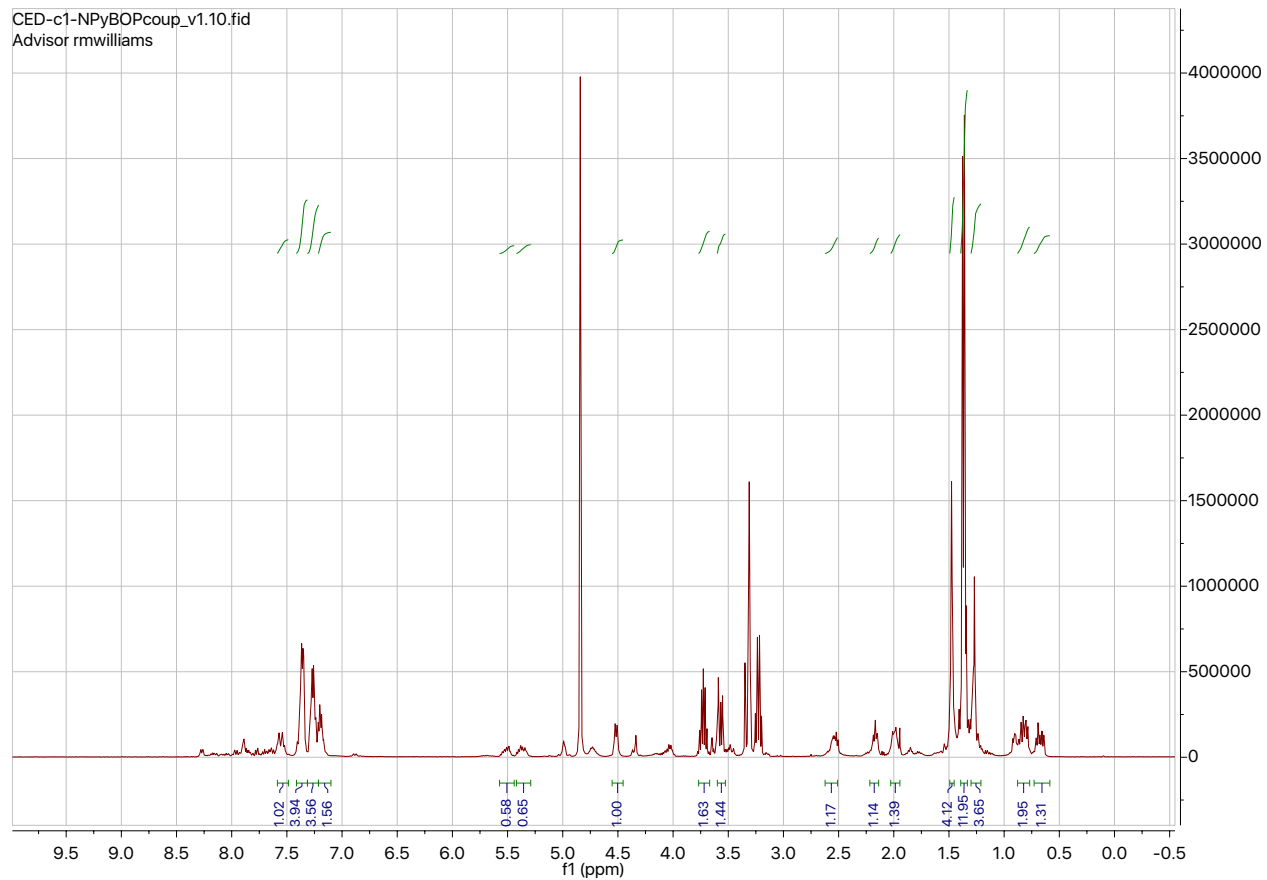


Figure 58. NMR of product